JSCSEN 88(12)1189–1382(2023)

ISSN 1820-7421(Online)

Journal of the Serbian Chemical Society

Electronic version

VOLUME 88

No 12

BELGRADE 2023

Available on line at

www.shd.org.rs/JSCS/

The full search of JSCS is available through

DOAJ DIRECTORY OF OPEN ACCESS JOURNALS

www.doaj.org

The **Journal of the Serbian Chemical Society** (formerly Glasnik Hemijskog društva Beograd), one volume (12 issues) per year, publishes articles from the fields of chemistry. The **Journal** is financially supported by the **Ministry of Education, Science and Technological Development of the Republic of Serbia.**

Articles published in the **Journal** are indexed in **Clarivate Analytics products: Science Citation Index-Expanded™** – accessed *via* **Web of Science®** and **Journal Citation Reports®**.

Impact Factor announced on 28 June, 2023: **1.000; 5-year Impact Factor**: **1.100**.

Articles appearing in the **Journal** are also abstracted by: **Scopus, Chemical Abstracts Plus (CAplus℠), Directory of Open Access Journals, Referativnii Zhurnal (VINITI), RSC Analytical Abstracts, EuroPub, Pro Quest** and **Asian Digital Library.**

Publisher:	**Serbian Chemical Society**, Karnegijeva 4/III, P. O. Box 36, 1120 Belgrade 35, Serbia tel./fax: +381–11–3370–467, E-mails: **Society** – shd@shd.org.rs; **Journal** – jscs@shd.org.rs Home Pages: **Society** – http://www.shd.org.rs/, **Journal** – http://www.shd.org.rs/JSCS/
Internet Service:	Contents, Abstracts and full papers (from Vol 64, No. 1, 1999) are available in the electronic form at the Web Site of the **Journal** (http://www.shd.org.rs/JSCS/).
Former Editors:	**Nikola A. Pušin** (1930–1947), **Aleksandar M. Leko** (1948–1954), **Panta S. Tutundžić** (1955–1961), **Miloš K. Mladenović** (1962–1964), **Đorđe M. Dimitrijević** (1965–1969), **Aleksandar R. Despić** (1969–1975), **Slobodan V. Ribnikar** (1975–1985), **Dragutin M. Dražić** (1986–2006).
Editor-in-Chief:	BRANISLAV Ž. **NIKOLIĆ**, Serbian Chemical Society (E-mail: jscs-ed@shd.org.rs)
Deputy Editor:	DUŠAN **SLADIĆ**, Faculty of Chemistry, University of Belgrade
Sub editors:	
Organic Chemistry	DEJAN **OPSENICA**, Institute of Chemistry, Technology and Metallurgy, University of Belgrade JÁNOS **CSANÁDI**, Faculty of Science, University of Novi Sad
Biochemistry and Biotechnology	OLGICA **NEDIĆ**, INEP – Institute for the Application of Nuclear Energy, University of Belgrade
Inorganic Chemistry	MILOŠ **ĐURAN**, Serbian Chemical Society
Theoretical Chemistry	IVAN **JURANIĆ**, Serbian Chemical Society
Physical Chemistry	LJILJANA **DAMJANOVIĆ-VASILIĆ**, Faculty of Physical Chemistry, University of Belgrade
Electrochemistry	SNEŽANA **GOJKOVIĆ**, Faculty of Technology and Metallurgy, University of Belgrade
Analytical Chemistry	RADA **BAOŠIĆ**, Faculty of Chemistry, University of Belgrade
Polymers	BRANKO **DUNJIĆ**, Faculty of Technology and Metallurgy, University of Belgrade
Thermodynamics	MIRJANA **KIJEVČANIN**, Faculty of Technology and Metallurgy, University of Belgrade
Chemical Engineering	TATJANA **KALUĐEROVIĆ RADOIČIĆ**, Faculty of Technology and Metallurgy, University of Belgrade
Materials	RADA **PETROVIĆ**, Faculty of Technology and Metallurgy, University of Belgrade
Metallic Materials and Metallurgy	ANA **KOSTOV**, Mining and Metallurgy Institute Bor, University of Belgrade
Environmental and Geochemistry	VESNA **ANTIĆ**, Faculty of Agriculture, University of Belgrade
History of and Education in Chemistry	DRAGICA **TRIVIĆ**, Faculty of Chemistry, University of Belgrade
English Language Editors:	LYNNE **KATSIKAS**, Serbian Chemical Society VLATKA **VAJS**, Serbian Chemical Society JASMINA **NIKOLIĆ**, Faculty of Technology and Metallurgy, University of Belgrade
Technical Editors:	VLADIMIR **PANIĆ**, Institute of Chemistry, Technology and Metallurgy, University of Belgrade, MARIO **ZLATOVIĆ**, Faculty of Chemistry, University of Belgrade
Journal Manager & Web Master:	MARIO **ZLATOVIĆ**, Faculty of Chemistry, University of Belgrade
Office:	VERA **ĆUŠIĆ**, Serbian Chemical Society

Editorial Board

From abroad: **R. Adžić**, Brookhaven National Laboratory (USA); **A. Casini**, University of Groningen (The Netherlands); **G. Cobb**, Baylor University (USA); **D. Douglas**, University of British Columbia (Canada); **G. Inzelt**, Etvos Lorand University (Hungary); **J. Kenny**, University of Perugia (Italy); **Ya. I. Korenman**, Voronezh Academy of Technology (Russian Federation); **M. D. Lechner**, University of Osnabrueck (Germany); **S. Macura**, Mayo Clinic (USA); **M. Spiteller**, INFU, Technical University Dortmund (Germany); **M. Stratakis**, University of Crete (Grecce); **M. Swart**, University de Girona (Cataluna, Spain); **G. Vunjak-Novaković**, Columbia University (USA); **P. Worsfold**, University of Plymouth (UK); **J. Zagal**, Universidad de Santiago de Chile (Chile).

From Serbia: **B. Abramović**, **V. Antić**, **R. Baošić**, **V. Beškoski**, **J. Csanadi**, **Lj. Damjanović-Vasilić**, **A. Dekanski**, **V. Dondur**, **B. Dunjić**, **M. Đuran, S. Gojković**, **I. Gutman**, **B. Jovančićević**, **I. Juranić**, **T. Kaluđerović Radoičić**, **L. Katsikas**, **M. Kijevčanin**, **A. Kostov**, **V. Leovac**, **S. Milonjić**, **V.B. Mišković-Stanković**, **O. Nedić**, **B. Nikolić**, **J. Nikolić**, **D. Opsenica**, **V. Panić**, **M. Petkovska**, **R. Petrović**, **I. Popović**, **B. Radak**, **S. Ražić**, **D. Sladić**, **S. Sovilj**, **S. Šerbanović**, **B. Šolaja**, **Ž. Tešić**, **D. Trivić**, **V. Vajs, M. Zlatović**.

Subscription: The annual subscription rate is **150.00 €** including postage (surface mail) and handling. For Society members from abroad rate is **50.00 €**. For the proforma invoice with the instruction for bank payment contact the Society Office (E-mail: shd@shd.org.rs) or see JSCS Web Site: http://www.shd.org.rs/JSCS/, option Subscription.

Godišnja pretplata: Za članove SHD: **2.500,00 RSD**, za penzionere i studente: **1000,00 RSD**, a za ostale: **3.500,00 RSD**:za organizacije i ustanove: **16.000,00 RSD**. Uplate se vrše na tekući račun Društva: **205-13815-62**, poziv na broj **320**, sa naznakom "pretplata za JSCS".

Nota: Radovi čiji su svi autori članovi SHD prioritetno se publikuju.

Odlukom Odbora za hemiju Republičkog fonda za nauku Srbije, br. 66788/1 od 22.11.1990. godine, koja je kasnije potvrđena odlukom Saveta Fonda, časopis je uvršten u kategoriju međunarodnih časopisa (**M-23**). Takođe, aktom Ministarstva za nauku i tehnologiju Republike Srbije, 413-00-247/2000-01 od 15.06.2000. godine, ovaj časopis je proglašen za publikaciju od posebnog interesa za nauku. **Impact Factor** časopisa objavljen 28. juna 2023. godine je **1,000**, a petogodišnji **Impact Factor 1,100**.

Journal of the Serbian Chemical Society
JSCS-info@shd.org.rs • www.shd.org.rs/JSCS

J. Serb. Chem. Soc. Vol. 88, No. 12 (2023)

CONTENTS*

Published by the Serbian Chemical Society
Karnegijeva 4/III, P. O. Box 36, 11120 Belgrade, Serbia
Printed by the Faculty of Technology and Metallurgy
Karnegijeva 4, P. O. Box 35-03, 11120 Belgrade, Serbia

* For colored figures in this issue please see electronic version at the Journal Home Page: http://www.shd.org.rs/JSCS/

This Special Issue is dedicated to Academician Vukadin M. Leovac on the occasion of his 80th birthday.

Publication of this issue is financially co-sponsored by

University of Novi Sad Faculty of Sciences
Department of Chemistry, Biochemistry and Environmental Protection

Professor Emeritus Association of University of Novi Sad

Autonomous Province of Vojvodina
Provincial Secretariate for Higher Education and Science

Journal of the Serbian Chemical Society
JSCS-info@shd.org.rs • www.shd.org.rs/JSCS

EDITORIAL

It is a tremendous honor and a delightful privilege to celebrate the accomplishments of Dr. Vukadin Leovac, Professor Emeritus at the University of Novi Sad and a distinguished member of the Academy of Sciences and Arts of Vojvodina. We are delighted to present this Special Issue of the *Journal of the Serbian Chemical Society*, which happens to be his preferred journal, in recognition of his 80th birthday. Dr. Leovac's profound influence on the advancement of chemical research and education is not limited to our university alone but extends to institutions throughout Serbia.

Vukadin Leovac was born on 14th March 1943 in the village of Glisnica near Pljevlja, Montenegro, in a large family of farmers. He finished Elementary School in Gradac, and High School in Pljevlja in 1962. It is interesting to say that he enrolled in studies at the Faculty of Law, at the University of Zagreb. Before the start of the first semester, at the end of September, due to the Autonomous Province of Vojvodina scholarship, he transferred to study chemistry at the Faculty of Philosophy at the University of Novi Sad. At the start of the third year of studies, he got a tempting scholarship from the Electronic Industry of Niš (EI--Niš). During that year, thanks to IAESTE he spent two months at practice in the Factory for plastic masses in Bydgoszcz, Poland. After graduation (1966) the committee suggested he apply for the position of teaching assistant for the course Inorganic Chemistry, but due to the obligations of the scholarship he was employed in EI-Niš, as the chief technologist for the production of loudspeaker membranes (Factory „Akustika" in Svrljig).

After the mandatory military service, in December 1969 he transferred to the newly formed Faculty of Sciences, University of Novi Sad as a teaching assistant for Inorganic Chemistry. At the same faculty, he defended the Master's Thesis titled „Synthesis and research on geometric isomerism of some chalogeno-cobalt(III) complexes" in 1975, which made him the founder of scientific research in the field of inorganic and coordination chemistry at his university.

During the academic 1975/76 and 1977/78 year, through the Provincial Committee for bonding with other countries, he spent 13 months at the Faculty of Chemistry in Kishinev (Moldova) under the supervision of the Academician N.

V. Gerbeleu. During this internship, he did the investigation of the coordination chemistry of the isothiosemicarbazide derivatives. These results were crucial for his PhD Thesis „Synthesis and investigation of coordination compounds of 3d--elements with S-methylisothiosemicarbazide and S-methylisothiosemicarbazones“ which he defended in 1978. At the Faculty of Sciences in Novi Sad he became Assistant Professor in 1979, Associate Professor in 1984 and Full Professor in 1989. In 2014 he earned the title of professor emeritus at the University of Novi Sad. After 44 years of work, on 30th September 2011, he retired.

Prof. Leovac has been very successful in his teaching work. He taught different courses in Inorganic and Coordination Chemistry at a modern level, often informing his students about the newest discoveries in chemistry. Except at the University of Novi Sad, he also taught courses at the University of Priština and the University of Montenegro. His laboratory has always been full of undergraduates, MSc and PhD students. Among them, there were also doctorands from other university centers, as well as from abroad, S. Čundak (Ukrain) and K. Cvrkalj (Canada), who are presently known, as university professors and scientific researchers. He belongs to that group of university professors and researchers who generously share his knowledge with students, coworkers, and interested colleagues, which has brought him high popularity and recognition. Thus, it is not surprising that he was the mentor of 12 PhD theses, 4 master theses and more than 80 diploma works, and that he has given enormous contributions and numerous ideas for many other theses and research. For the students in the first year of studies, he wrote a textbook titled “Structure of atoms and molecules” which enables them to establish a great foundation and deep understanding of basic chemical principles by resolving the problems given there. This involved many contemporary examples of the chemical phenomena, which were not easy to collect when the first version of this textbook was written, more than 30 years ago. One of the main advantages of this book is that it is still evolving, and expanding, and thus cannot be addressed as an old, out-of-date book. Nowadays, Professor’s closest co-workers gladly suggest this book as the literature for many courses, and even call it a holy book of general chemistry.

Also, he worked on the education of teachers, and students from high school, to which he held a great number of lectures, and he was included in the work of Research Center “Petnica”.

Prof. Leovac is a founder of the study of Inorganic/Coordination Chemistry at the University of Novi Sad and is the leading researcher in this field in the former Yugoslavia. His scientific interest is in the synthesis, physicochemical, structural and biological studies of complexes containing not only 3d-metals but also Mo, Pd, Pt, U, Cd, and Hg with different classes of O-, N-, S-, P- and Se--binding polydentate organic ligands. Among them prevail the ligands of the type of Schiff-base derivatives of different mono- and dicarbonyl compounds and

(chalcogen)semi/isothiosemicarbazides, oxamic hydrazide, Girard-T reagent, hydrazide of carboxylic acids, aminoguanidine, and others, as well as ligands based on pyrazole derivatives. Numerous of these complexes are synthesized by template reactions, an approach that enabled the formation of metal complexes with the ligands previously unknown in organic chemistry.

He published more than 200 scientific papers including two review papers, in international journals. He is the co-author of a scientific monograph of national significance devoted to the coordination chemistry of S-alkylisothiosemicarbazide derivatives. The great majority of compounds from the publications were the realization of the ideas of Prof. Leovac. His works have been cited 2054 times, excluding self-citations (*h* index 23). He supervised work on many multi-year research projects at both national and bilateral levels.

Of his works, the most important are undoubtedly those (more than 90 publications) concerning transition metal complexes with derivatives of thio- and S-alkylisothiosemicarbazides of different denticity (2 to 8) and sets of donor atoms, among most of which are various tridentate ligands. From this area, we point out the results that represent fundamental contributions to the coordination and structural chemistry of the mentioned ligands:

1. Syntheses of the first metal complexes of S-alkylisothiosemicarbazides which, for more than 40 years were thought not to be capable of forming metal complexes, and for which an NN coordination was found, which is in principle different from thiosemicarbazide (NS), for which a characteristic is a prototropic tautomerism of the isothioureido fragment.

2. Synthesis of complexes with the tetradentate (N_4) pentane-2,4-dione bis(S-alkylisothiosemicarbazones), which among others, give stable complexes also with Fe(IV) in the presence of iodide. K. Wieghardt characterized these results as “fascinating” and “inspiring” (K. Wieghardt et al. *J. Chem. Soc., Chem. Commun.* (1993) 726, *Angew. Chem.* **32** (1993) 1635).

3. Synthesis of dinuclear complexes of Ni(III) with the octadentate (N_8) *noninnocent* ligands, 3,4-diacetyl-2,5-hexanedione-tetrakis(S-alkylisothiosemicarbazones) with interesting structural, electronic, spectral, magnetic and electrochemical properties.

4. Syntheses of complexes with the tetradentate (ON_3 or ON_2P) N1-salicylidene/acetylacetoneimine-*N*-4-*α*-alkoxypicolyl/2-diphenylphosphinobenzyl-*S*-methyliso-thiosemicarbazide.

5. Unique and diverse (five different modes!) coordination of usually pentadentate (N_5) 2,6-diacetylpyridine bis(S-methylisothiosemicarbazone, H_2L) in mononuclear complexes of Mn(II), Ni(II) and Cu(II), and mixed-valence octanuclear Cu(II)-Cu(I) complex $[Cu^{II}_2(\mu\text{-}H_2L)_2Cu^{I}_6(\mu\text{-}Br_8)Br_2]$. This made the coordination chemistry of Novi Sad unique and recognizable in the scientific com-

munity. (V. B. Arion, *Coord. Chem. Rev.* **387** (2019) 348, S. Floquet *et al*. *Polyhedron* **80** (2014) 60).

Another important series of his papers (over 30) is related to complexes of different derivatives of pyrazole. In this field too, Prof. Leovac and his coworkers have made a valuable contribution to the coordination chemistry of this diverse class of ligands. They have found some interesting structures of the synthesized complexes, as well as degradation reactions during the complexation of some of these ligands. There is no doubt that the most important reaction discovered in his laboratory is the unexpected preparation of 3(5)-amino-4-acetyl-5(3)-methylpyrazole, which with the Co(II), Ni(II) and Cu(II) in the presence of triethyl orthoformate, gave complexes with the *in situ* formed tridentate ON_2, a new formamidine-type ligand, *N,N'*-bis(4-acetyl-5-methylpyrazol-3-yl) formamidine, with a unique coordination of the mentioned pyrazole derivative, enabling the synthesis of numerous complexes. In this place, it is important to stress the biological activity of the polymeric complex of Cu(II) with the tridentate ONS Schiff base, a derivative of pyrazolone and thiosemicarbazide and 1-adamantoylhydrazone di(2-pyridyl)ketone, with the cytotoxicity significantly higher than that of cisplatin. Concerning other results, it is worth mentioning the metal complexes with various coordination modes and forms of polydentate condensation product 2,6-diacetylpyridine and semioxamazide/Girard-T reagent, thus enriching the structural coordination chemistry of derivatives of the mentioned dicarbonyl compound. In addition, there are also dinuclear Co(II) complexes and di- and tetranuclear complexes of Cu(II) with the pendant octaazamacrocyclic *tpmc* ligand and with different bridging ligands of interesting geometrical structures of the complexes and of *tpmc* conformations. The research on the coordination properties of aminoguanidine Schiff bases, with pyridoxal, salicylaldehyde and 2--acetylpyridine also stands out. More than 40 complexes of 3d- and 4d-metals with these ligands were isolated in the form of single crystals and their physicochemical and structural properties were investigated in Prof. Leovac's laboratory. Several complexes have shown great photoluminescence, and thus are studied for application in the field of optical materials.

Furthermore, it has to be especially pointed out that a large number of ligands and their complexes were characterized by X-ray structural analysis, which made Prof. Leovac the one scientist credited for more than 50 % of crystal structures determined in Serbia. The synthesis of the majority of these compounds was the idea and the act of Prof. Leovac, who although retired, continues with undiminished enthusiasm, curiosity, and energy to create new ideas, and he is one of the rare researchers who at his age is doing laboratory experiments (syntheses) himself and thus inspires the young colleagues to behave similarly. He rejoices whenever a new result is obtained, especially when it is something

unexpected. His attitude is that “each unexpected (unplanned) result is, as a rule, more interesting and more significant than the expected one”.

It should also be mentioned that Prof. Leovac cooperates not only with scientists from the former Yugoslavia or recently from Serbia but also frequently from abroad. He has reviewed numerous papers for many international scientific journals, but also two doctoral theses from abroad (Pakistan and Moldavia).

Prof. Leovac has been Head of the Chair of Inorganic Chemistry, Director of the Department of Chemistry and President of the Education Council of the Faculty of Sciences. During his mandate as the Director of the Department the foundation of the famous “blue building” was made. Prof. Leovac is a very active member of the Serbian Chemical Society, in which he is currently a Merited Member. He was awarded the October Award of Novi Sad, the Golden Award of the Association of University Professors and Scientists for life’s work, as well as the First Award of the Ministry of Sciences and Environmental Protection of the Republic of Serbia and the Provincial Secretariat for Science and Technological Development. For a long time, he has been acting as a volunteer member of the Association of the Anticancer Societies of Vojvodina and thus has been awarded the Charter of this Association.

The prestigious journal Polyhedron published a special issue in honor of Prof. Leovac’s 70th birthday, demonstrating great respect for his remarkable scientific achievements. This recognition was of significant importance for bolstering the reputation and validation of chemical research at the University of Novi Sad.

Prof. Leovac always suggested that it is important to have a hobby, and his hobbies are daily one-hour-long walks by the kay in Novi Sad, as well as weekend routes throughout the forest of Fruška gora no matter the weather conditions. The latter reminds him of the mountains back in his hometown.

Since our Professor was always fond of publishing papers on special issues dedicated to fellows coordination chemists, we found this way as an appropriate to express our gratitude and admiration, and to wish him good health, many fruitful experiments, and many joyful moments for his 80th birthday.

***

After the formal part of the preface, I want to write a few words from a more personal point of view. Back in 2005, I was looking forward to applying for medical studies, and I decided to visit the famous “blue building” of the Faculty of Sciences, just to make a backup plan. Fate seemed to play a hand as the elevator unexpectedly paused between floors, with Prof. Leovac, my father, and me on board. Hailing from Montenegro, and thanks to Prof. Leovac’s warmth and the generosity typical of our people, we received an invitation to his office for a

cup of coffee. I am not sure if it was him talking about his science and teaching, the laboratory itself, the nice people I met there, or, most probably the perfect mixture of everything mentioned, I started to think of myself as a chemist. A few days later, I applied for the studies of chemistry.

During my first year, Prof. Leovac taught us General and Inorganic Chemistry, and some would say it is the basics. But he enabled us to go through our knowledge and rethink everything we think we know, to abstract what we are sure of, and to open our minds to new approaches, and new knowledge, to make corrections to the foundation we thought we had. To this day, I often find myself recalling his famous words: „The rule is that there are no rules!“. The Professor's manner of teaching was truly distinctive, and for me, who was always more of a problem-solver than a definition learner, it was perfect. Later, he led us into the captivating realm of coordination chemistry, the most enchanting offspring of this wondrous scientific discipline, often unjustly overlooked by many students but cherished by those who had the courage and the knowledge to explore it and let it become a part of their lives.

None of my fellow students were surprised when I chose to do my diploma work with Prof. Leovac's team of coordination chemists. Prof. Leovac deserves immense gratitude for shaping me into the chemist I am today and for fostering a harmonious team spirit in our laboratory. While working on my master's and doctoral thesis, even though he was not formally my co-mentor, he was the one who gave my work the essence. Not only did he offer ideas, but he also actively engaged in experiments, provided insights on results and wrote papers with me. We had a daily tradition of taking a break every day around noon, and that is when our Professor would tell us about some new, fascinating, or surprising scientific facts, so interesting that I had made a notebook called "Know-it-all" with the notes from those conversations. Just another reminder that real scientist has no working hours if they are the true ones, like our Professor. Also, even though he has an office, he is almost always in his laboratory, busy working on new ideas and conducting experiments. I truly valued his keen interest in upholding the proper use of our language, a matter that regrettably often goes overlooked, even within academic circles. When the work on the syntheses of single crystals was overwhelming, he was always there as a support, and with a few words like: "You cannot change the nature of the matter, but you could learn how to use it" he could make everything seem perfectly fine. It is an indescribable honor to have learned from the most renowned and respected coordination chemist from our region. He is an endless wellspring of incredible teaching and captivating scientific ideas, and the man who finds happiness in assisting others. Now, after all these years, I can hear my Professor's words echoing during my own lectures, I can see his sentences written by my hand, and witness his ideas sparking a sea of new ones in my mind.

My dearest Professor, ”Greetings for your birthday, and thank you for everything!” seems like too modest a phrase. Instead, I want to express that I will always be proud of being your apprentice and that I hope I was a merit of your trust and worthy to be called your academic heir.

Guest Editor
Prof. Mirjana Radanović
University of Novi Sad Faculty of Sciences

Of Prof. Leovac as a man, supervisor, and colleague his associates testify with words of gratitude, some of which are given here.

I find it hard to remember when I first heard about Professor Vukadin Leovac, but it must have been at the beginning of the eighties during the experimental work on my Ph.D. thesis at the University of Kragujevac. Searching for the literature for my Ph.D. thesis, I often had an opportunity to read his scientific papers published in the most reputable journals of Inorganic and Coordination Chemistry. During that period, the research group of Prof. Leovac from the University of Novi Sad was famous in the field of Coordination Chemistry not only at Serbian universities but many other universities in Europe, too. The scientific results that his research group achieved during that time have been a great motivation to us all working in Inorganic and Coordination Chemistry, especially young scientists. His papers often served as the supporting literature on which we relied for the purpose of structural characterization of coordination compounds by using spectroscopic and crystallographic methods. Later, after I had returned from my postdoctoral stay at the University of London, we established a closer cooperation. Prof. Leovac was a principal leader of numerous national projects funded by the Ministry of Science of the Republic of Serbia. Many scientists from different state universities in Serbia participated in these projects. Along with the University of Novi Sad, he significantly contributed to the development of Inorganic and Coordination Chemistry at the University of Belgrade and the University of Kragujevac. He was a committee member for the defense of many MSc and Ph.D. theses, thus largely contributing to the development of academic and research staff at the above-mentioned universities. Prof. Leovac is particularly and constantly dedicated to advancing the careers of young scientists. His knowledge of chemistry is so vast that it can be concluded that to him chemistry is the meaning of life rather than simply a field of science.

Academician Miloš I. Djuran
Serbian Academy of Sciences and Arts

Prof. Leovac is very esteemed and respected by his colleagues from the Faculty of Chemistry, University of Belgrade, especially from us from the Department of Inorganic Chemistry. His advice, ideas for the themes for the theses, and his thorough examination of different ligand systems coordinated to copper, zinc, nickel, cobalt, vanadium, iron, etc. helped many of us. He was the Doktorvater (mentor) to numerous candidates, some directly, some indirectly. Always ready to share, teach, show, and explain, with a big heart full of passion, especially for surprising results and structures. In both Novi Sad and Belgrade, he left a permanent stamp and influence through many complexes and crystal structures. This expands out of the Serbian border, to Montenegro, Moldavia, and Germany, because of all of us who have learned from him to accept the challenges and develop a love for coordination chemistry.

The results of Prof. Leovac with the unusual Fe(IV) complexes have fascinated and inspired well-known Prof. Karl Wieghardt, from the Ruhr University in Bochum, who mentioned it in two papers in prestigious journals – *Angew. Chem. In. Ed.* **32** (1993) 1635 and *J. Chem. Soc., Chem. Commun.* (1993) 726. The great accomplishment of Prof. Leovac is also the collaboration with Prof. Wieghardt that resulted in a mutual paper in *Inorg. Chem.* **36** (1997) 661.

As a crown of his work, many colleagues from Serbia and abroad have dedicated one Special Issue of one of his favorite journals, the prestigious Polyhedron, with 37 papers, to his 70th birthday.

Dear Prof. Leovac, I wish you many unexpected results and to inspire us further.

Prof. Goran Kaluđerović
University of Applied Sciences, Merseburg, Germany

It is both an honor and a privilege to contribute my personal note to this special issue celebrating Professor Leovac's 80th birthday and acknowledging his remarkable contributions to the field of coordination chemistry.

I first had the privilege of being a student in Professor Leovac's freshman class, and that experience marked the beginning of an incredible academic journey. Little did I know then that his guidance and mentorship would shape my entire scientific career. As my professor, he introduced me to the captivating world of coordination chemistry, laying the foundation for my academic pursuits. Professor Leovac’s lectures were not just lessons; they were an invitation into the realm of scientific endeavor. I was captivated by his teaching practices, particularly his method of using pieces of his own research to illustrate the concepts he was teaching. This unique approach made complex ideas accessible and ignited my curiosity. It was during those moments that my fascination with coordination

chemistry and X-ray crystallography was born. I especially recall when Professor Leovac shared the fascinating details of his synthesis, resulting in octadentate macrocyclic ligands, complexes with exotic oxidation states, and the myriad of unexpected ligand transformations that occurred during template syntheses. It left a profound and lasting influence on me as a student.

As I continued my academic journey through my master's and PhD studies, Professor Leovac transitioned from being my professor to my mentor. We spent countless hours working together in the laboratory, discussing results, and planning our next steps. One of the most enjoyable aspects of working with him was finalizing our research through the process of writing publications. Professor Leovac's mastery of crafting precise statements and sentences is truly remarkable, and it has always been my aspiration to reach the same level of writing skills.

Professor Leovac often emphasized, “It is good when things get complicated,” signifying his belief that there is much more to learn from unraveling intricate synthetic routes and deciphering complex crystal structures. He also had a fondness for celebrating “unexpected results”, not only for their surprising nature but also as a source of inspiration for exploring new and innovative approaches.

Dear Professor Leovac, as you celebrate your 80th birthday, I join the scientific community in wishing you continued good health and happiness. Your wisdom, your contributions, and your presence in our community are truly invaluable. It is an honor to have learned from you and to continue to be inspired by your work.

Prof. Marko Rodić
Faculty of Sciences, Novi Sad

Professor with the capital P, emeritus with the capital E, man–giant, role model, support, and many more represent my dear Prof. Leovac. He is not just my dear professor but the dearest one, thanks to whom, I came to love Novi Sad and all the wonderful people around him. Prof. Leovac had a great impact and has left a valuable mark on the careers of all of them, but also many others throughout the country. Luckily, he is still doing it.

His huge reputation in the field of inorganic chemistry was obvious wherever he went. As a respected and loved professor, he expanded his positive influence on colleagues. I am and always was, proud to have the privilege and the pleasure of working with a man, professor, and scientist like him.

As a crystallographer, I must mention the great contribution of Prof. Leovac to chemical crystallography in Serbia. Like a magician, he made many single

crystals, and he is the one scientist credited for more than 50 % of crystal structures determined in Serbia.

When I look back, the support of Professor Leovac was a decisive influence on my career. He is directly or indirectly the most responsible for my motivation, achieved results, and will for work. I always tried my best to repay him with diligence and effort to meet his expectations.

Dr Goran Bogdanović, principal research fellow
„Vinča“ Institute of Nuclear Sciences, Belgrade

It is a great privilege to have the opportunity to learn from professional and affirmed mentors, respected in a large scientific community. The willingness of the mentor to teach and transfer their knowledge to others is a great advantage, but the special fortune is when that person has sincere kindness and shows interest in your advancement. Prof. Leovac belongs to this rare group of complete scientists, professors, and mentors. He was the mentor to my master's and doctoral thesis, and besides my colleagues from Vinča Institute, he had a substantial impact on my research.

The professionalism of Prof. Leovac is undeniable, but what fascinates the most is his enthusiasm, energy, commitment, devotion, and enjoyment of work, which could be seen in the laboratory. It seemed that he could spend endless hours in ligand modification, and syntheses of the complexes, with constant aim to try novel approaches, and to gain new knowledge. From this point of view, I am the most intrigued by the fact that, after so many years of work, he preserved the curiosity of a scientist at the beginning of their career. This inspires all of us who had the opportunity to work with him.

The results of Prof. Leovac's work are reflected in the impressive bibliography, which confirms his outstanding contributions to the development of coordination chemistry in the region. It really makes me proud that most of these results are documented by crystal structures. We could always count on exceptional crystals that come from his laboratory, some of which were used for the calibration of our diffractometer, instead of the standard crystal. This could not be explained only as the nature of the compounds, but maybe a reasonable mixture of knowledge, skill, and intuitiveness. Besides the outstanding knowledge, Prof. Leovac taught all of us that research is much more than ambition and intelligence. That is why the special place in his achievements represents the number of his hardworking co-workers, and great professionals, my dear colleagues from the Faculty of Sciences in Novi Sad, that he gathered and made what they are now.

I owe Prof. Leovac gratitude for his involvement in my research, and all the knowledge he led me to. It is an honor to know and work with one great maestro of coordination chemistry, a remarkable mentor, and friend.

Dr Slađana Novaković, principal research fellow
„Vinča“ Institute of Nuclear Sciences, Belgrade

I have known Professor Vukadin Leovac for almost half of a century, from my early student days when he was my assistant and professor, and later a colleague. His pedagogical work in the development of young scientists and the quality of scientific research is evident from the numbers and data in his fruitful biography and bibliography presented here. Although I did not closely collaborate with him in teaching and research, I have been a witness to his exceptional scientific potential and significance for our faculty and department throughout these years. Prof. Leovac is more than a colleague; he is a friend, always well-intentioned to help and ready to find the best solution for his collaborators and colleagues in any situation. As the dean of the faculty at the time when Prof. Leovac was promoted to the position of professor emeritus at the University of Novi Sad, it was my special honor to introduce Prof. Leovac to the wider scientific audience and to emphasize his contributions to our university. In those moments, I felt a sense of pride and great satisfaction because I had the privilege of introducing an outstanding scientist and professor who, by all criteria, was far ahead of all other candidates. Prof. Vukadin Leovac was a pioneer in research in inorganic chemistry, especially coordination chemistry, not only at the University of Novi Sad but also on a much broader scale. The extent of his importance is best illustrated by the fact that one of the most prestigious journals in this field, Polyhedron, published a special issue dedicated to his seventieth birthday. With great pleasure, I have written these lines dedicated to Prof. Leovac, who truly deserves to have his eightieth birthday celebrated in this way.

Prof. Emeritus Neda Mimica-Dukić
University of Novi Sad

The most beautiful possessions in life are good friends, colleagues, places, and memories that those moments give.

I have known colleague Vukadin Leovac for more than 40 years, from the early days when he came from Niš to Novi Sad and was elected as an assistant at the Institute of Chemistry at the Faculty of Natural Sciences, while I was an assistant at the Faculty of Technology. In those early years, we led laboratory

exercises on the subject of General and Inorganic Chemistry for students of the Faculty of Technology at the same time. We spent breaks together, discussing and conducting dialogs about research, science, philosophy, life, and ideas on how to best organize exercises for first-year students. Those were wonderful times when experiences, knowledge, and vision of science could be exchanged. I recognized Prof. Vukadin has high potential, love, and passion for coordination chemistry and experimental work. The chemical passion and dedication last his entire career and are still remarkable. It was an extraordinary pleasure to listen to Prof. Leovac's excitement when, as a result of the experiment, he obtained a completely new compound, with a magical color of the complex substance that he hadn't even planned. I remember this period; those were the last years of the 1970s. Memories also take me back to our joint study stay in Halle, East Germany, in the laboratories of the Faculty of Natural Sciences. There, colleague Leovac demonstrated his distinctive dedication to experimental work, commitment, and selflessness toward broad horizons of chemical research.

Prof. Emeritus Mirjana Vojinović Miloradov
University of Novi Sad

I was very fortunate to be introduced to higher spheres of chemistry by Prof. Leovac. His informal style freed from rigidity and narrowness, full of passion for science and knowledge has attracted many of us. One of the main characteristics of good lecturers is the reference to contemporary scientific achievements, which inspire students and make science more interesting. During his lectures, I was breathless when I heard about the existence of quadruple bonds, the ghosts like solvated electrons and alkalide ions, or superacids that could protonate even alkanes. This trip through the periodic table led us to the very edge of human knowledge and it seemed that it has no ending – crowns, cryptands, catenate complexes, phenomena like back-donation, Jan-Theller effect, *etc*. His statement that „only God and a chemist can make a new molecule“ had the most effect on me as a student, and I find it inspiring even today. Not because we chemists want to become gods, but because this sentence elevated my favorite science to the level of a religion.

Prof. Leovac introduced me to the world of chemistry and he was my guide at one of the most exciting travels in my life – those across the endless expanse of the periodic table of elements. The last station on this journey was my diploma work which I have finished under the supervision of Prof. Leovac. I was honored to have contributed to the synthesis of a new molecule, a new complex of copper with hydrazone derivative. Also, at that young age, I was privileged to feel the fulfillment and happiness of taking part in the birth of a new molecule, but also to

be part of a research team, and to feel the delight of working with esteemed Prof. Leovac.

As a university professor myself, I could say that I have learned from one of the best professors and scientists at our University and I am glad to have the opportunity to cite his words during my lectures. In that way, I hope to be an inspiration to my students like he was for many, many generations.

Prof. Boris Popović
Faculty of Agriculture, Novi Sad

Professor Vukadin Leovac is my favorite professor, esteemed colleague, and true friend. His great scientific opus and the will to move and erase boundaries in coordination chemistry, as well as the expanded network of collaborators in academic institutions in Serbia and abroad, made him well-known and dominant in his field. For many decades, he was an associate of the members of the Department of General and Inorganic Chemistry of the Faculty of Chemistry in Belgrade on many scientific projects, in which he was the principal investigator. This resulted in the publication of numerous papers, many master's and Ph.D. theses, and his involvement in the procedures of elections of new professors and teaching assistants at our faculty.

Prof. Leovac teaches with patience and persistence, good energy, and enthusiasm. His charisma, charm, and wit, as well as the professional and friendly relationships, enabled Prof. Leovac to find a direct way to guide every one of his co-workers to new ideas, thorough work practice, and wish to gain new knowledge.

Dear Prof. Leovac, thank you for all your scientific contributions, for every thought and word, advice, and patience. You made us the scientists we are today.

Prof. Sofija Sovilj
Faculty of Chemistry, Belgrade

Prof. Leovac and I have known each other for 25 years, first as a mentor and Ph.D. student and then as friends. Even now, I am sure that my journey would be different if not for his advice and limitless help. But I was not the only one he helped to. Many ideas realized in the papers of Serbian researchers in the field of coordination are his. He was generous not only with ideas, but with the prepared ligands, or precursors, without any demand for co-authorship. I am sure that those unselfish moments of sharing and transferring his knowledge to everyone who

asked for help made him not only satisfied but sincerely happy. Many experienced researchers in Serbian laboratories, but also abroad are his doctoral students.

His knowledge of complex compounds is fascinating, now even intuitive, and his energy as a researcher is wonderful. He is one of the very rare scientists who loves to do his experiments after all these years. Sometimes I think with jealousy that he does not even try the reactions, but „makes deals with the ligands and the central metal ions how to form single crystals“. His word „maybe“ is a path to successful synthesis.

I finish these lines with the citation of the thank you note from my dissertation: „I owe enormous gratitude to Prof. Leovac from whom I plan on keep learning, not only about chemistry but also the pleasure of finding, generous giving and guiding youngers to real values. Without his help, I am sure, this dissertation would not come to an end, and I would, possibly, have been lost away from the scientific roads I chose for my career.“

Prof. Ilija Brčeski
Faculty of Chemistry, Belgrade

Prof. Leovac was the one who brought my associates and me to the wonderful world of the coordination chemistry of hydrazide and hydrazone ligands. This wide field of research enabled us to publish numerous papers in the most eminent international journals and to collaborate with many outstanding professors and researchers both in Serbia, and abroad. For this, we must be thankful to our Prof. Leovac.

I hope that the future will bring more professors like him, but I am sure that we, his contemporaries, will remember his devotion to his research and teaching forever. Besides the teaching mission, our dear Vukadin was a real friend, full of understanding. I find the memories of our conferences, informal gatherings, and trips very dear. So, after 40 years at the University, I have the right to teach the younger generations who prepare for this type of work always to learn from the best. And one of those is surely Prof. Vukadin Leovac.

Prof. Katarina Anđelković
Faculty of Chemistry, Belgrade

Many years ago, when I was at the crossroads of my life and professional roads, dilemmas and doubts, by accident, I met Prof. Vukadin Leovac, who became my friend and my colleague – Vule. The warmth of his wards and his scientific enthusiasm led me to become part of his group of researchers. Now, with this time distance, I am free to say that those years were the most fruitful

period of my research work. Due to Prof. Leovac, I gained the self-confidence, and sometimes fanatic appetite for novel scientific achievement, and by analyzing his approach to science with his advice and suggestions I became what I am today.

If life is supposed to be a game, and science is and always was the core of his life, then science is woven into his game of life which he plays with incredible ease. That is the only way of completing so demanding tasks of making hundreds of crystal structures, by merging the perfect ratio of scientific knowledge, experience, creative intuition, and artistic expression. The amount of different structures of ligands and their metal complexes one must consider art. I was always fascinated by his intuition which manifests the highest level of intelligence, as one of the key requirements for success in scientific research.

I am proud to have a friend like he is – real and honest, unselfish, and always prepared to help, understand, and respect in those moments many would not. Our friendship is solid, mutual, and invincible. I owe him respect and gratitude for many noble lessons from life and science.

Prof. Milan Joksović
Faculty of Sciences, Kragujevac

During the work on my master's thesis, I met Prof. Leovac, who was, later, my mentor for my Ph.D. thesis. His advice during our work together was not just expert, nor distant and strict, but full of the kindness and warmth of a friend. That was something that guided me towards our goal. Prof. Leovac always knew all the details of every experiment I was doing, even though he had numerous candidates under his supervision. He followed and got involved in all the problems and dilemmas of his co-workers with true commitment. At the Chair of General and Inorganic Chemistry and the Faculty for Metallurgy and Technology, University of Montenegro, he kept teaching, until we were able to take over that assignment. His visits to Podgorica brought joy, not only for chemists but other scientists as well. With his cheerful spirit, friendliness, and humanistic approach, he has built many bridges of friendship.

Prof. Zorica Leka
Faculty for Metallurgy and Technology, Podgorica, Montenegro

As a colleague and former Ph.D. student of Prof. Leovac, I must stress it is, and always was my honor and privilege to have the opportunity to meet him and work with him. He made that stressful period of working on my Ph.D. thesis,

which involved regular work hours in Podgorica, while trying to find time to go to Novi Sad and do experiments, full of dear memories. Always there to help as an expert, a professor, with advice and new ideas, but above all as a human, a friend, sincerely, he was the best support I could have asked for. He made me express real joy whenever we get a new single crystal, good result, or idea and that is what, nowadays, I obliged myself to teach the new generations.

The collaboration with Prof. Leovac and his colleagues, my dear friends from Novi Sad, is still successful and fruitful, and we plan to keep it on the nice path our Professor has pointed us to.

Prof. Željko Jaćimović
Faculty for Metallurgy and Technology, Podgorica, Montenegro

***

Concluding Editorial remarks

It is great pleseaure for me to underline that the decision of the Serbian Chemical Society to publish the issue dedicated to the occasion of the jubilee of Prof. Vukadin Leovac 80th birthday is a real recognition to his achievements to Chemistry, especially to Inorganic Chemistry, and also to the recognition of his friendly and warm relations to collegues, students and people in general.

On behalf of your coleagues and friends, thank you Vule for all our relations! We wish you all the best for the years to come.

Prof. Branislav Nikolić
Journal of the Serbian Chemical Society Editor in Chief
Honorary President of the Serbian Chemical Society

Journal of the Serbian Chemical Society
JSCS@tmf.bg.ac.rs • www.shd.org.rs/JSCS
J. Serb. Chem. Soc. *88* (12) 1205–1222 (2023)
JSCS–5690
Original scientific paper
Published 19 December 2023

Iron(III) complexes with ditopic macrocycles bearing crown-ether and bis(salicylidene) isothiosemicarbazide moieties

VLADIMIR B. ARION[1]*, OLEG PALAMARCIUC[2], SERGIU SHOVA[3], GHENADIE NOVITCHI[4] and PETER RAPTA[5]

[1]University of Vienna, Institute of Inorganic Chemistry, Währinger Strasse 42, A-1090 Vienna, Austria, [2]Moldova State University, A. Mateevici Street 60, MD-2009 Chisinau, Republic of Moldova, [3]Inorganic Polymers Department, "Petru Poni" Institute of Macromolecular Chemistry, Aleea Gr. Ghica Voda 41 A, Iasi 700487, Romania, [4]CNRS-LNCMI, 38042 Grenoble Cedex, France and [5]Institute of Physical Chemistry and Chemical Physics, Faculty of Chemical and Food Technology, Slovak University of Technology in Bratislava, Radlinského 9, SK-81237 Bratislava, Slovakia

(Received 7 June, revised 4 July, accepted 8 September 2023)

Abstract: The main aims of this work were the synthesis and characterization of iron(III) complexes with a ditopic ligand H_2L consisting of a bis(salicylidene)isothiosemicarbazide moiety with a N_2O_2 binding site and a crown-ether (O_6) moiety. A series of high-spin iron(III) complexes, *i.e.*, $[Fe^{III}LClBa(CH_3OH)(H_2O)_{0.5}(ZnCl_4)]$ (**1**), $[Fe^{III}LCl]$ (**2**), $[Fe^{III}L(N_3)]$ (**3**) and $[(Fe^{III}L)_2O]$ (**4**), were synthesized. The complexes were characterized by mass spectrometry, IR and UV–Vis spectroscopy, variable temperature (VT) magnetic susceptibility measurements, Mössbauer spectroscopy, single crystal X-ray diffraction and cyclic voltammetry.

Keywords: iron(III); bi-compartmental ligand; Mössbauer; magnetism.

INTRODUCTION

Bi-compartmental ligands with both a salen moiety for "soft" metal cations and a crown ether moiety for "hard" metal cations were reported 35 years ago by Reinhoudt *et al.*[1,2] Nickel(II), copper(II) and zinc(II) complexes, with both metal-free crown ether cavity and alkali- and alkaline-earth cations located in crown ether moiety in close proximity to first-row transition metal, were synthesized and comprehensively characterized by spectroscopic, electrochemical and X-ray diffraction methods. The relative simplicity of the general approach for their assembly[3,4] has permitted the building up of a large number of such systems, systematically modifying the structure of each binding site. The nature of

* Corresponding author. E-mail: vladimir.arion@univie.ac.at
https://doi.org/10.2298/JSC230607065A

the metal-binding sites in these systems is so different that hard alkali, alkaline-earth or lanthanide metal cations and softer transition metal ions can be bound simultaneously and located in close proximity to each other within the same macrocycle. Generally, these bi-compartmental ligands are assembled in the presence of a metal ion template. Barium(II) proved to be the most suitable template for the synthesis of macrocyclic salen- and salophen-crown ethers from the appropriate building blocks.[5–7] This behavior is not surprising as Ba^{2+} has been successfully used in the synthesis of a number of crown ethers.[8] The template role of barium(II) is predominantly conformational. By coordination of the polyoxyethylene-containing building blocks to barium(II) the terminal 2-hydroxybenzaldehyde groups are held in close proximity. Under such conditions the cyclization of the 1+1 open-chain condensation product occurs inevitably at the next step of the template process. This pathway is favored over the intermolecular one that leads to polymerization. Another important reason for using Ba^{2+} as template is the possibility to remove it easily from the final template product by treatment with SO_4^{2-}. Even though first attempts to use K^+, Rb^+ or Cs^+ as templates failed,[1] later it was shown that K^+, which has very close ionic radius to that of Ba^{2+}, can also serve as a template for assembly of heterometallic systems.[9]

By using Ba^{2+} as template ditopic macrocycles based on bis(salicylidene)-isothiosemicarbazide or acetamidrazone unit and crown-ether moiety were assembled and isolated as Ni(II)–Ba(II), Cu(II)–Ba(II), Zn(II)–Ba(II), VO(II)–Ba(II) and Cu(II)–Gd(III) heterodinuclear complexes[10–14] as shown in Scheme 1.

The "complex formation" behavior of nickel(II) complexes with alkali and alkaline earth metal ions was investigated by UV–Vis spectroscopy and calorimetric techniques and revealed building of 1:2 metal-nickel(II) macrocycle associates.[15] In addition, electrochemical recognition properties of first raw transition metal macrocycles vs alkali and alkaline earth metal cations, ammonium cation and protonated dopamine were studied.[16]

Herein we report the synthesis of iron(III) complexes with a bi-compartmental macrocyclic system H_2L, namely $[Fe^{III}LClBa(CH_3OH)(H_2O)_{0.5}(ZnCl_4)]$ (**1**), $[Fe^{III}LCl]$ (**2**), $[Fe^{III}L(N_3)]$ (**3**) and $[(Fe^{III}L)_2O]$ (**4**) as shown in Scheme 2, their characterization by single crystal X-ray diffraction, spectroscopic techniques (UV−Vis, IR), ESI mass spectrometry, magnetochemistry, Mössbauer spectroscopy and cyclic voltammetry. As the interstitial solvent or its amount in the isolated bulk samples and single crystals investigated by X-ray crystallography (vide infra) differ, the numbering of the complexes in the following discussion will not include the co-crystallized solvent.

EXPERIMENTAL

All starting materials and solvents were purchased from Aldrich and used without further purification.

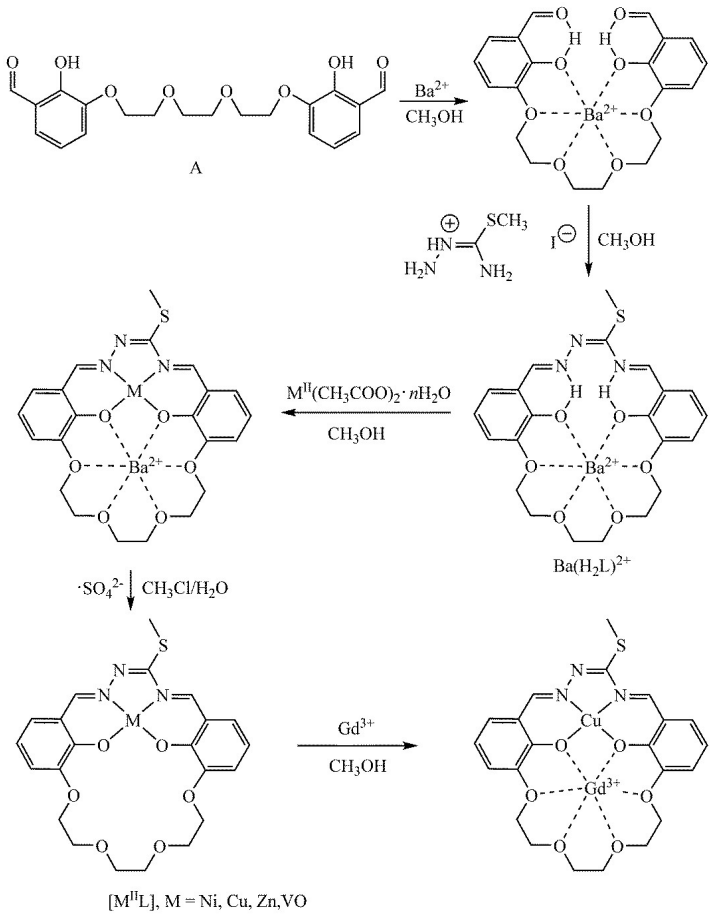

Scheme 1. Synthetic pathway to the heteronuclear bis(salicylidene)isothiosemicarbazide--crown ether macrocycle H_2L. The last transformation was reported for M = Cu.[14]

Synthesis of $[Fe^{III}LClBa(CH_3OH)(H_2O)_{0.5}(ZnCl_4)]\cdot CH_3OH$ (**1**$\cdot CH_3OH$)

To $[ZnLIBa(CF_3SO_3)CH_3OH]_2\cdot 0.5H_2O$[11] (0.7 g, 0.36 mmol) in CH_3OH (20 ml) was added $FeCl_3\cdot 6H_2O$ (0.9 g, 3.3 mmol) in methanol (15 ml). The black crystals formed were isolated by filtration, washed with cold methanol and diethyl ether and dried in air. Yield: 0.45 g (64 %).

Synthesis of $[Fe^{III}LCl]\cdot CH_2Cl_2\ 0.5H_2O$ (**2**$\cdot CH_2Cl_2\ 0.5H_2O$)

A suspension of $[Fe^{III}LClBa(CH_3OH)(H_2O)_{0.5}(ZnCl_4)]\cdot CH_3OH$ (1.0 g, 1.1 mmol) in CH_2Cl_2 (250 ml) was stirred with a solution of guanidinium sulfate (3.0 g) in water (150 ml) for 30 min. The resulting colored organic layer was separated off and dried over $MgSO_4$. The solvent was removed to ~20 ml by evaporation under a reduced pressure and the product

precipitated with pentane. X-ray diffraction quality single crystals were grown from CH_2Cl_2. Yield: 0.55 g (82 %).

*Synthesis of [$Fe^{III}L(N_3)$] (**3**)*

A mixture of [Fe^{III}LCl]·CH_2Cl_2·0.5H_2O (0.55 g, 0.86 mmol) and NaN_3 (0.51 g, 22.2 mmol) in CH_3OH was stirred for 1 h. The solvent was then evaporated under reduced pressure, the residue re-dissolved in CH_2Cl_2 (50 ml) and the solution formed filtered. The solvent was removed under reduced pressure up to *ca*. 10 ml and the product precipitated with pentane. Yield: 0.44 g (94 %).

*Synthesis of [($Fe^{III}L)_2O$]·H_2O (**4**·H_2O)*

Method a. To green-brown solution of [Fe^{III}LCl]·CH_2Cl_2·0.5H_2O (0.5 g, 0.78 mmol) in methanol (170 ml) at 60 °C was added triethylamine (0.22 ml, 1.56 mmol). The red solution generated was allowed to stand at room temperature for 48 h. The product was isolated by filtration, washed with methanol and dried in vacuo. Yield: 0.30 g (79 %). X-ray diffraction quality single crystals were grown by slow diffusion of pentane into solution of the product (14 mg) in chloroform (15 ml).

Method b. To a red-brown solution of [Fe^{III}LCl]·CH_2Cl_2·0.5H_2O (0.2 g, 0.31 mmol) in CH_2Cl_2 (35 ml) was added a solution of KOH (0.02 g, 0.37 mmol) in water (35 ml). The mixture was stirred at room temperature for 105 min. After separation of the two phases the organic one was dried over $MgSO_4$. Slow addition of pentane to the solution produced a small amount of red microcrystals, which were separated by filtration, washed with pentane and dried in air. Yield: 0.02 g (13 %). The IR spectrum of the isolated product was identical with that synthesized by method a.

Analytical and spectral data are given in Supplementary material to this paper.

Crystallographic structure determination

The measurements were performed on Siemens SMART (**1**·H_2O) and **2**·CH_2Cl_2·0.5H_2O) and Bruker D8 Venture (**4**·$CHCl_3$) diffractometers. Crystal data, data collection parameters, and structure refinement details are given in Table S-I of the Supplementary material. The structures were solved by direct methods and refined by full matrix least-squares techniques. Non-hydrogen atoms were refined with anisotropic displacement parameters. The positional parameters of the atoms belonging to disordered fragments were modeled by using PART, DFIX and SADI tools of SHELXL-2014 program. The *S*-methylisothiosemicarbazide fragment was found to be disordered over two positions with the refined occupancy factors 0.59:0.41, 0.58:0.42 (0.66:0.33) and 0.74:0.26 (0.75:0.25) for **1**·H_2O, **2**·CH_2Cl_2·0.5H_2O and **4**·$CHCl_3$, respectively. In the crystal of **1**·H_2O, $ZnCl_4^{2-}$ is also disordered, wherein two chlorido coligands occupy unique positions, while the other two are equally distributed between the two orientations. The disorder was modeled similarly in the crown-ether moieties in **2**·CH_2Cl_2·0.5H_2O and **4**·$CHCl_3$. It turned out, that one of two independent crown-ether moieties is fully disordered (for **2**·CH_2Cl_2·0.5H_2O) or partially disordered (**4**·$CHCl_3$) over two positions with 0.5:0.5 occupancy. H atoms were inserted in calculated positions and refined with a riding model. The following computer programs and hardware were used: structure solution, SHELXS-2014 and refinement, SHELXL-2014;[17] molecular diagrams, ORTEP;[18] computer, IntelCoreDuo. CCDC: 2263681, 2263682 and 2263683 for **1**·H_2O, **2**·CH_2Cl_2·0.5H_2O and **4**·$CHCl_3$, respectively.

Magnetic measurements

Dc magnetic susceptibility data (2–300 K) were collected on powdered samples using a SQUID magnetometer (Quantum Design MPMS-XL), applying a magnetic field of 0.1 T. All data were corrected for the contribution of the sample holder and the diamagnetism of the samples estimated from Pascal's constants.[19,20] The Mössbauer spectra were recorded on an alternating constant-acceleration spectrometer. The sample temperature was maintained constant in an Oxford Variox cryostat. The ^{57}Co/Rh source (1.8 GBq) was positioned at room temperature inside the gap of the magnet system at a zero-field position. Isomer shifts are referenced relative to iron metal at 295 K.

Electrochemistry

Cyclic voltammetric experiments with 0.5 mM solutions of investigated samples in 0.1 M *n*-Bu_4NPF_6 (p.a. quality from Fluka) supporting electrolyte in acetonitrile (p.a. quality from Sigma–Aldrich) were performed under argon atmosphere using a three-electrode arrangement with a platinum disk working electrode (from Ionode, Australia), platinum wire as a counter electrode, and silver wire as a pseudo reference electrode. All potentials in voltammetric studies were quoted vs ferricenium/ferrocene (Fc^+/Fc) redox couple. A Heka PG310USB (Lambrecht, Germany) potentiostat with a PotMaster 2.73 software package served for the potential control in voltammetric studies.

RESULTS AND DISCUSSION

Synthesis

Transmetallation reaction (Scheme 2) of $[ZnLIBa(CF_3SO_3)(CH_3OH)]_2\cdot 0.5H_2O$[11] with excess $FeCl_3\cdot 6H_2O$ in boiling methanol afforded the complex $[Fe^{III}LClBa(CH_3OH)(H_2O)_{0.5}\ (ZnCl_4)]\cdot$(**1**) crystallized as brown-black crystals of X-ray diffraction quality upon slow cooling of the reaction mixture in 64 % yield. Treatment of solution of **1** in CH_2Cl_2 with an aqueous solution of guanidinium sulfate resulted in the complex $[Fe^{III}LCl]$ (**2**) in 82 % yield. Metathesis reaction of 2 with excess NaN_3 in methanol afforded $[Fe^{III}L(N_3)]$ (**3**) in 94 % yield. The red solution obtained from the reaction of green-brown solution of **2** in methanol with air oxygen in the presence of triethylamine produced the μ_3-oxido-dimeric complex $[(Fe^{III}L)_2O]$ (**4**) in 79 % yield. The same complex **4** was synthesized from **2** when treated with KOH in water/$CHCl_3$.

*Characterization of **1**–**4***

Positive ion ESI mass spectrum of **1** showed a peak with *m*/*z* 513, which was assigned to $[Fe^{III}L]^+$, while the negative ion spectrum revealed a peak with *m/z* 169 attributed to $[ZnCl_3]^-$. The FAB mass spectrum displayed three peaks in the positive ion mode with *m/z* 720, 685 and 571. Their isotopic patterns were in agreement with theoretical isotopic distributions for $[Fe^{III}LBaCl_2–H]^+$, $[Fe^{III}LBaCl–H^+]^+$ and $[Fe^{III}LCl+Na^+]^+$, respectively. Like **1**, complexes **2** and **3** revealed in the ESI mass spectra a peak with *m*/*z* 513 due to $[Fe^{III}L]^+$ ion. A

strong stretching vibration at 2034 cm^{-1} in the IR spectrum of $[FeL(N_3)]$ indicated the presence of azide co-ligand in the complex.

In the positive ion ESI mass spectrum of **4** peaks at *m*/z 1081, 1065 and 1043 were assigned to $[(FeL)_2O+K^+]^+$, $[(FeL)_2O+Na^+]^+$ and $[(FeL)_2O+H^+]^+$, respectively. The band at 840 cm^{-1} in IR spectrum is due to asymmetric Fe–O–Fe stretching vibration.

$[ZnLIBa(CF_3SO_3)CH_3OH]$

↓(i)

$[Fe^{III}LClBa(CH_3OH)(H_2O)_{0.5}(ZnCl_4)]$ (**1**)

↓(ii)

$[Fe^{III}LCl]$ (**2**) —(iv)→ $[(Fe^{III}L)_2O]$ (**4**)

↓(iii)

$[Fe^{III}L(N_3)]$ (**3**)

Scheme 2. Synthesis of complexes **1**–**4**; Reaction conditions: i) $FeCl_3 \cdot 6H_2O$, CH_3OH; ii) guanidinium sulfate, CH_2Cl_2/H_2O 3:2; iii) NaN_3 (excess), CH_3OH; iv) Et_3N, CH_3OH or KOH, CH_2Cl_2/H_2O.

X-ray crystallography

The results of X-ray diffraction studies of complexes **1**, **2** and **4** are shown in Figs. 1–3 with pertinent metrical parameters in Table S-I. The iron(III) in **1** is five-coordinate with square-pyramidal coordination geometry. The ligand coordinates to iron(III) through two nitrogen atoms N1 and N3 of the isothiosemicarbazide moiety and two phenolato oxygen atoms O1 and O2 in the basal plane, while chlorido co-ligand Cl1 occupies the apical position. The iron(III) comes

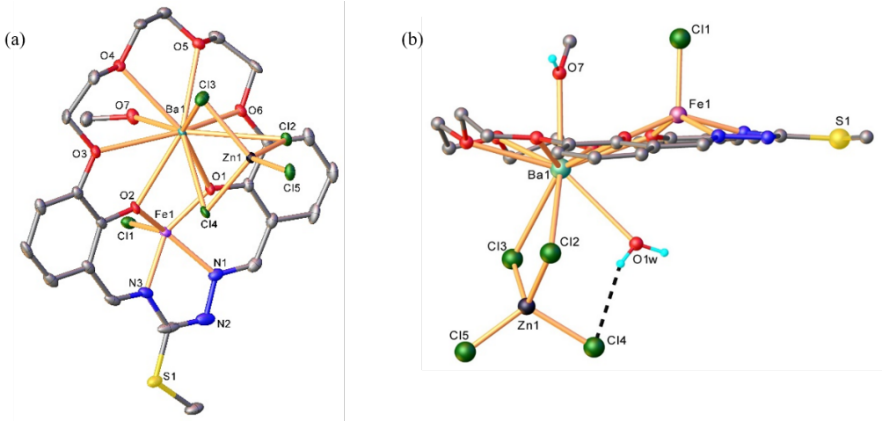

Fig. 1. a) ORTEP view of $[Fe^{III}LClBa(CH_3OH)(ZnCl_4)]$ with thermal ellipsoids at 50 % probability level and b) ball-and-stick representation of the second resolved counterpart of $[Fe^{III}LClBa(CH_3OH)(H_2O)_{0.5}(ZnCl_4)]$ in the crystal of $\mathbf{1} \cdot H_2O$. Interstitial solvent was removed for clarity.

out from the basal plane towards Cl1 by 0.612(2) Å. The metrical parameters are very close to those reported for iron(III) complex with bis(salicylidene)isothiosemicarbazide.[21] The Ba atom is 10-coordinate, with all six oxygen atoms of the macrocycle linked to the barium(II). The tetrahedral $[ZnCl_4]^{2-}$, which is disordered over two positions, forms three (Fig. 1a) and two bonding contacts to barium(II) through the chloride ions (Fig. 1b). When only two chlorido co-ligands are coordinated to the barium atom, an additional coordination of H_2O molecule is found (Fig. 1b). The molecule of CH_3OH is coordinated to the barium(II) on the other side of the macrocycle. The Ba^{2+} is displaced from the mean plane formed by the oxygen atoms of the crown ether moiety in opposite direction with that of iron(III) by 0.819(1) Å due to stronger interactions with $ZnCl_4^{2-}$ than with methanol molecule as shown in Fig. 1.

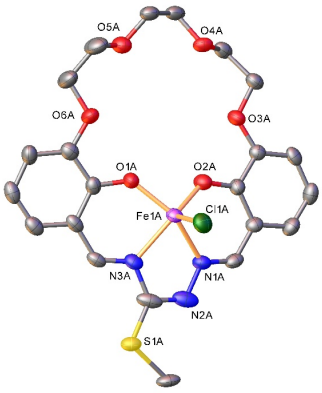

Fig. 2. ORTEP view of one of the two crystallographically independent molecules of $[Fe^{III}LCl]$ (**2**) with thermal ellipsoids at 50 % probability level. Interstitial solvent is not shown for clarity.

As expected square-pyramidal coordination geometry around Fe(III) was disclosed in complex **2**. The bi-compartmental ligand is bound to iron(III) through two nitrogen atoms N1 and N3 of the isothiosemicarbazide moiety and two phenolato oxygen atoms O1 and O2 in the basal plane, while the chlorido co-ligand Cl1 occupies the apical position. The iron(III) comes out from the basal plane towards Cl1 by 0.547(2) and 0.559(2) Å for the two crystallographically independent molecules A and B, respectively. The bond lengths around Fe(III) are very close to those in complex **1** and complex **5** (Table II).

The SC-XRD structure of **4** revealed that the two iron(III) ions with a square-pyramidal coordination environment N_2O_3 are associated into a dimer *via* a bridging oxido anion, O^{2-}. The angle Fe1−O1−Fe2 of 154.57(12)° is determined by steric repulsions between the two bi-compartmental ligands and is much higher than the angle of 139° reported as minimal for documented in the literature μ-oxido-bridged iron(III) complexes.[22]

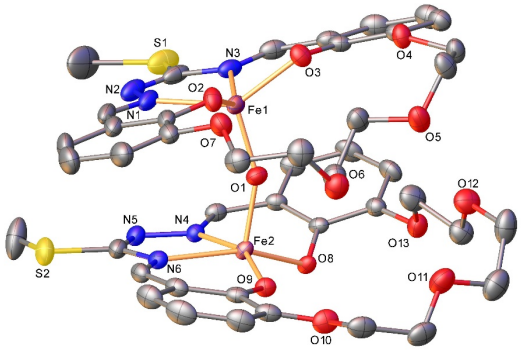

Fig. 3. ORTEP view of the μ_3-oxido-dimeric iron(III) complex $[(Fe^{III}L)_2O]$ **(4)**. Interstitial solvent was omitted for clarity.

TABLE II. Selected bond distances (Å) in the coordination polyhedron of Fe(III) in complexes **1**, **2** and **5**

Bond	Compound			
	1	**2**		**5**[a]
		Molecule A	Molecule B	
Fe–Cl1	2.1981(15)	2.2280(15)	2.2215(15)	2.212(2)
Fe–N1	2.085(5)	2.091(4)	2.086(4)	2.084(5)
Fe–N3	2.065(5)	2.075(4)	2.082(4)	2.101(4)
Fe–O1	1.899(4)	1.880(3)	1.882(4)	1.875(4)
Fe–O2	1.915(4)	1.879(3)	1.875(4)	1.894(4)

[a]Iron(III) complex with *S*-methyl-bis(salicylidene)isothiosemicarbazide (**5**) is reported in ref. 21

The dimeric complexes $[(Fe^{III}L)_2O]$ form centrosymmetric tetranuclear associates bridged *via* μ-phenolato oxygen atoms O8 and O8^i as shown in Fig. 4 with bond distances Fe2–O8 of 1.9463(17) Å and Fe2–O8^i of 2.4713(18) Å, ∠O8–Fe2–O8^i = 75.56(7)° and ∠Fe2–O8^i–Fe2^i = 104.44(7)° (symmetry code i: $1 - x$, $2 - y$, $1 - z$).

The optical spectra of **1**–**4** in methanol are shown in Fig. 5. The spectra are dominated by charge-transfer and intra-ligand transitions.

Magnetism and Mössbauer spectra

The variable temperature (*VT*) magnetic susceptibility measurement for complex **1** is shown in Fig. 6 as plots of χ_M vs. T and μ_{eff} *vs.* T, while the Mössbauer spectrum at 80 K is displayed in Fig. 7.

The magnetic susceptibility values for **1** at room temperature are of the order expected for the high-spin Fe(III) (S = 5/2) (5.98 μ_B or 4.465 cm^3 K mol^{-1}) at 300 K assuming g = 2.0, theoretical $\chi_M T$ value of 4.377 cm^3 K mol^{-1}.[20] The values of the magnetic susceptibility remain almost constant up to 50 K, after

which a progressive decrease of the magnetic susceptibility up to 2 K was seen, where the magnetic susceptibility value of 3.544 μ_B is reached.

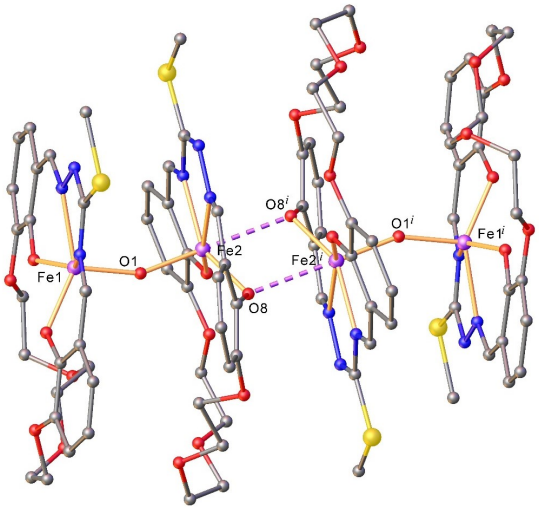

Fig. 4. Pairwise association of μ_3-oxido dimeric iron(III) complexes **4**.

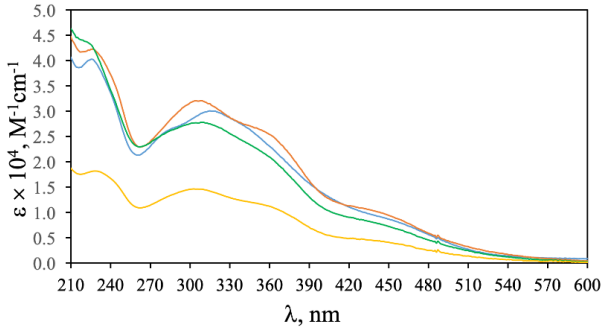

Fig. 5. The electronic spectra of methanolic solutions of **1** (red trace), **2** (blue trace), **3** (green trace) and **4** (yellow trace).

For an octahedral mononuclear high-spin iron(III) complex the ground state is $^6A_{1g}$ and the expected spin-only magnetic moment is 5.92 μ_B, which is temperature independent. However, if the symmetry is lowered, the $^6A_{1g}$ term can split to a small extent by mixing in, *via* spin-orbit coupling, the components of a higher-lying $^6T_1$ term.[23] Under symmetry lowering, some departure of the magnetic moment from the spin-only value and from Curie law behavior might be expected. Also, if there were any significant antiferromagnetic exchange interaction between the iron atoms in the crystal, the magnetic moment would be exp-

ected to decrease below the spin-only value and also to show an appreciable temperature dependence.[24]

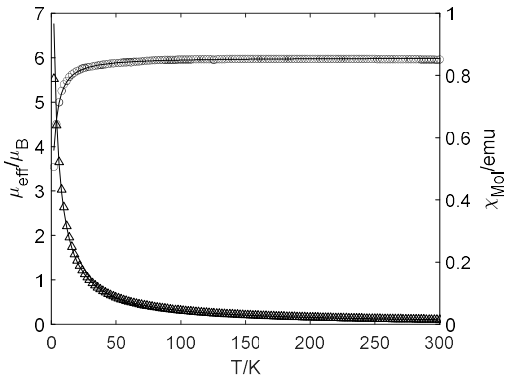

Fig. 6. The temperature dependence of the effective magnetic moment μ_{eff} and molar magnetic susceptibility for **1**.

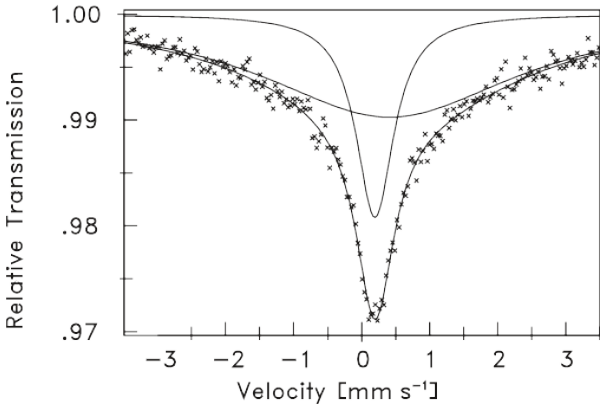

Fig. 7. Mössbauer spectrum of complex **1** at 80 K.

A series of Fe(salen)X complexes with magnetic moments in the range 5.7––6.0 μ_B at room temperature obeyed the Curie–Weiss law with small values of θ. The *VT* magnetic susceptibilities indicated that there was no significant magnetic exchange present. This result strongly suggested that those complexes were five-coordinate. In the case of nitromethane adduct of Fe(salen)Cl, X-ray diffraction analysis[25,26] revealed essentially square-pyramidal Fe(salen)Cl molecules, with the nitromethane molecule as interstitial solvent. At room temperature that compound had a magnetic moment close to the spin-only value for five unpaired electrons and the crystals also showed considerable magnetic anisotropy. This anisotropy arose from a zero-field splitting (ZFS) of the free-ion ^6S term, due to at least in part the low symmetry of the complex. Coordination of iron(III) com-

plex with a salen-crown bi-compartmental macrocycle to Ba^{2+} was reported previously and did not cause a change in the spin state of iron(III) in the solid state.[27]

Based on the structural data, the magnetic behavior of **1** was explained by the presence of anisotropy caused by ZFS, which will be also discussed in the Mössbauer study, as well as by a small intermolecular interaction (*zJ*). The following Hamiltonian was applied to model the magnetic susceptibility of **1**:[20]

$$\hat{H} = D\left(\vec{\hat{S}}_{z_i}^{\,2} - S(S+1)/3\right) + E\left(\vec{\hat{S}}_x^{\,2} - \vec{\hat{S}}_y^{\,2}\right) \quad (1)$$

Fitting the experimental data afforded the ZFS parameters: $D = 4.5(1)$ cm^{-1}; $E = 0.01(1)$ cm^{-1} and $g = 2.029(3)$ with intermolecular interaction $zJ = -0.11(1)$ cm^{-1}. Such values of the ZFS parameters were expected for square-pyramidal coordination geometry and are consistent with reported in the literature data for similar compounds.[28,29]

The Mössbauer spectrum of **1** (Fig. 7) was calculated as two broad singlets with isomeric shift (*I.S.*) *I.S.* 0.19 and 0.41 mm s^{-1} and full width at half maximum (*FWHM*) of 0.67 and 4.64 mm s^{-1}, respectively. The isomeric shifts are in agreement with high-spin iron(III) as also suggested from *VT* magnetic susceptibility measurements. Lack of quadrupole splitting indicates spherical symmetry of the iron(III) charge cloud in **1**.

The *I.S.* and quadrupole splitting (ΔE_Q) for complex **2** at 80 K (Fig. 8) are 0.43 and 0.94 mm/s and *FWHM* for both lines of the doublet line is 0.66 mm/s. These Mössbauer parameters are well comparable to that of iron complex with *S*-methyl-bis(salicylidene)isothiosemicarbazide[30] with *I.S.* of 0.50 mm/s and $\Delta E_Q = 0.95$ mm/s and $(FWHM)_L$ 0.64 mm s^{-1} and $(FWHM)_R$ 1.16±0.03 mm s^{-1} referred to iron foil and indicate high-spin Fe(III) ($S = 5/2$). The main feature of the Mössbauer spectrum of **2** and those of $Fe^{III}QCl$, where H_2Q = *S*-methyl-bis-(salicylidene)isothiosemicarbazide is their asymmetry, which was found temperature-dependent for iron(III) complex with *S*-methyl-bis(salicylidene)isothiosemicarbazide. The intensity of the two absorption peaks of the Mössbauer spectra of this latter complex was shown to be equalized at 4.2 K. The observed asymmetry of the Mössbauer spectra is likely due to spin-orbit coupling, which removes Zeeman degeneracy of the ground state ^6S into three Kramer's doublets, and different spin relaxation rates for the level ±1/2 and for ±3/2 and ±5/2.[25,31] This degeneration can be characterized in the first approximation with terms of ZFS (*D* and *E*) based on the Hamiltonian used for the description of magnetism. Similar spectroscopic behavior was also reported for iron(III) complexes with porphyrins.[28]

Somewhat different ΔE_Q values to those for high-spin octahedral and five-coordinate iron(III) complexes with thiosemicarbazones[32,33] are likely due to difference in population of d_{x2-y2}, d_{xy}-orbitals from one side, and d_{z2}, d_{xz}, d_{yz}-orb-

itals from the other side, because of different ligand identity and coordination geometry of iron(III). The total s-electron density on the nucleus remained unchanged, while the quadrupole splitting markedly differed.

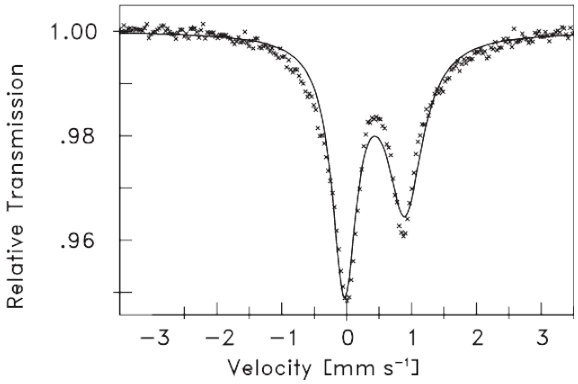

Fig. 8. Mössbauer spectrum of complex **2** at 80 K.

The Mössbauer spectrum of complex **3** (Fig. 9) revealed a doublet with almost equal intensity of both lines already at 80 K. The *I.S.* and ΔE_Q of 0.42 and 0.74 mm s^{-1} respectively, and *FWHM* of 0.35 mm s^{-1} are close to the Mössbauer parameters for complex **2** and in agreement with high-spin configuration of Fe(III).

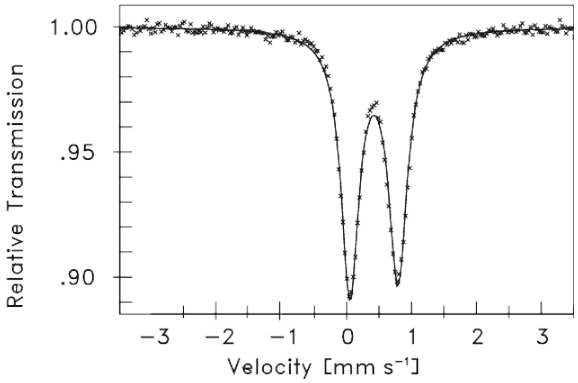

Fig. 9. Mössbauer spectrum of **3** at 80 K.

The departure of the iron(III) charge cloud from spherical symmetry of the free iron(III) ion is higher in complex **2** with chlorido apical ligand (ΔE_Q = 0.94 mm s^{-1}) than in complex **3** with azide as co-ligand (ΔE_Q = 0.74 mm s^{-1}). The same picture was disclosed previously for iron(III) porphyrin complexes.[28]

The magnetic measurement for complex **4** showed an expected, for dimeric μ-oxido-bridged iron(III) complexes, temperature dependence (Fig. 10). The

effective magnetic moment was of 2.65 μ_B (0.875 cm^3 K mol^{-1}) at 300 K and decreased steadily up to 0.6 μ_B at 2 K. This behavior indicated a strong antiferromagnetic interaction between the two high-spin iron(III) centers. From this interaction resulted a spin ground state $S_T = 0$. The low temperature curve indicated the presence of temperature independent paramagnetism (TIP). The fitting procedure gave a coupling constant $J = -113.1$ cm^{-1} ($H = -2JS_1 \cdot S_2$, $g = 2.0$ fixed parameter) and *TIP* of 496×10^{-6} cm^3 mol^{-1} per dimer.

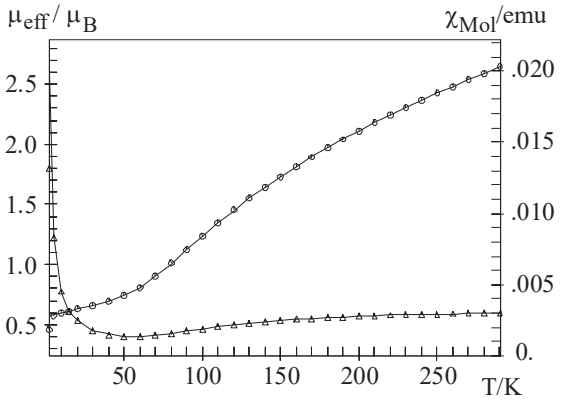

Fig. 10. The *VT* effective magnetic moment μ_{eff} and *VT* molar magnetic susceptibility for di-iron(III) complex **4**.

The strong antiferromagnetic Fe–Fe interaction with a similar magnitude of –115.3 cm^{-1} was reported for μ-oxido di-Fe(III) complex with 1,2-bis((3-methoxysalicylidene)amino)ethane[34] and other μ-oxido-bridged diiron(III) complexes and falls in the range of those calculated from empirical correlation equations considering the average Fe–O bond within the μ-oxido bridge.[35]

Electrochemical studies

The electrochemical behavior of **1**–**4** in MeCN was studied by cyclic voltammetry. The cyclic voltammogram of [Fe^{III}LCl] (**2**) in MeCN/*n*-Bu_4NPF_6 at Pt working electrode at scan rate of 100 mV s^{-1} showed in the cathodic region a quasireversible reduction with cathodic half-wave potential $E_{1/2} = -0.64$ V *vs*. Fc^+/Fc^0 (Fig. 11a). This event was attributed to the one-electron reversible reduction of Fe(III) to Fe(II). At more negative potentials new redox processes were identified in the range from –1.2 to –1.4 V *vs*. Fc^+/Fc^0, which were likely due to the ligand reduction. Coordination of iron(III) complex *via* its crown ether moiety to Ba^{2+} led to a shift of the first reduction step for **1** to the less negative value of –0.41 V *vs*. Fc^+/Fc^0 when compared to **2** indicating a quite strong effect of Ba^{2+} binding to the macrocycle on the redox behavior of Fe(III) (Fig. 11b). The second nearly irreversible reduction step took place at $E_{pc} = -1.68$ V *vs*.

Fc^+/Fc^0. Replacement of the chlorido co-ligand by azide (N_3^-) co-ligand afforded a slight shift of the cathodic half-wave potential for **3** ($E_{1/2}$ = –0.67 V *vs*. Fc^+/Fc^0) when compared to **2**. The second nearly irreversible cathodic peak for **3** was seen at E_{pc} = –1.1 V *vs*. Fc^+/Fc^0. For the dimeric μ-oxido bridged iron(III) complex [$(Fe^{III}L)_2O$] (**4**) a more complex redox behavior in the cathodic part was observed (Fig. 12).

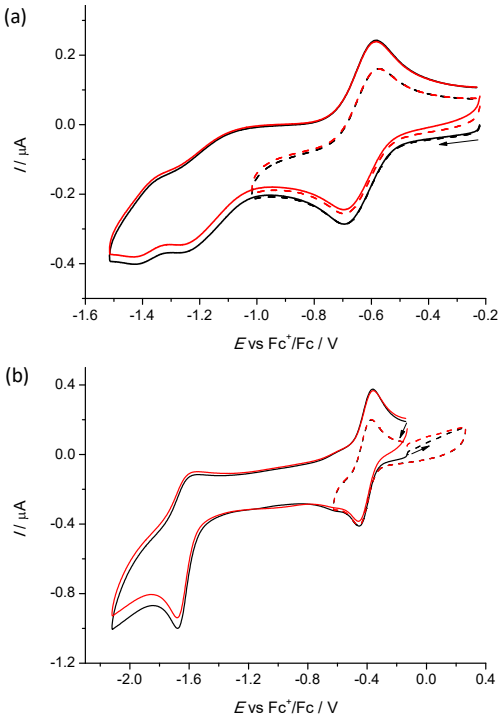

Fig. 11. Cyclic voltammetry of: a) [$Fe^{III}LCl$] (**2**) and b) complex **1** in MeCN/*n*-Bu_4NPF_6 at Pt working electrode (scan rate 100 mV s^{-1}, black trace – the first scan, red trace – the second scan, dashed lines – reduction to the first redox event).

The corresponding cyclic voltammogram showed the first reduction peak at E_{pc} = –1.29 V *vs.* Fc^+/Fc^0 with a strongly shifted reoxidation peak at –0.54 V exhibiting typical features of either a slow electron process or electrochemical square scheme. We suggest that a strongly shifted reoxidation peak upon reverse scan was due to a significant rearrangement of the dimeric complex after one electron reduction of one Fe(III) center in the dimer to Fe(II). Note that no oxidation process was observed in the range from –0.1 to 0.3 V just going to the anodic region before starting the reduction. The second reduction peak at E_{pc} = = –1.50 V *vs.* Fc^+/Fc^0 showed reversible behavior and was tentatively ascribed to the reduction of the second Fe(III) in the dimer at a slightly more negative potential compared to the first reduction event. Additionally, a further quasirev-

ersible, likely ligand-based, reduction at more negative potential (E_{pc} = –2.0 V *vs*. Fc^+/Fc^0) was found. Generally the dimeric μ-oxido-bridged iron(III) complex exhibited more negative redox potentials compared to those of the monomeric counterparts. No oxidation processes were observed in the range from –0.4 to +0.4 V vs Fc^+/Fc^0 when going to the anodic region.

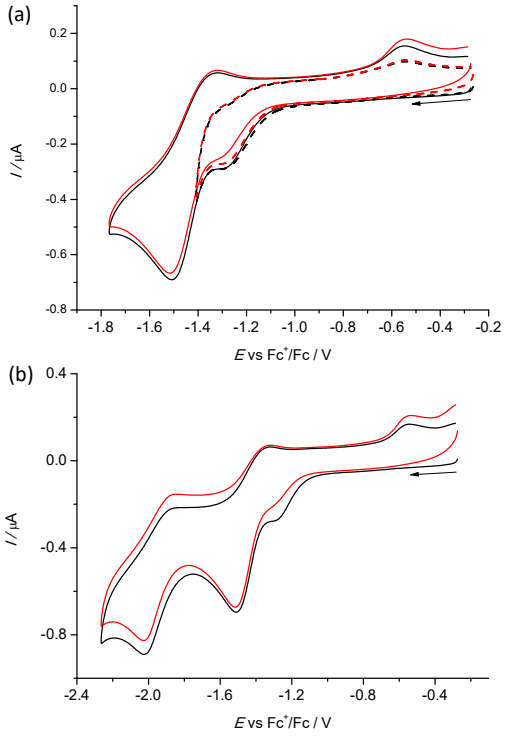

Fig. 12. a) Cyclic voltammetry of dimeric μ-oxido-bridged iron(III) complex $[(Fe^{III}L)]_2O]$ (**4**) in MeCN/*n*-Bu_4NPF_6 at Pt working electrode (scan rate 100 mV s^{-1}, black traces – the first scan, red traces – the second scan, dashed lines – reduction to the first redox event); b) cathodic reduction of **4** when going to the more negative potentials.

CONCLUSION

Transmetallation reaction of $[ZnLIBa(CF_3SO_3)(CH_3OH)]_2$ with excess $FeCl_3 \cdot 6H_2O$ in methanol afforded the high-spin iron(III)–barium(II)–zinc(II) complex **1**. Accommodation of barium(II) in the crown-ether moiety and coordination of tetrahedral dication $[ZnCl_4]^{2-}$ *via* three chlorido co-ligands (face) or via two chlorido ligands (edge) resulted in spherical symmetry of the iron(III) charge cloud as implied from the lack of quadrupole splitting in Mössbauer spectrum. Demetallation of crown-ether moiety by treatment of **1** with guanidinium sulfate afforded the mononuclear high-spin iron(III) complex $[Fe^{III}LCl]$ (**2**), which was further converted by metathesis reaction into $[Fe^{III}L(N_3)]$ (**3**). Like in **1**, the iron(III) in **2** and **3** adopts high-spin electronic configuration and square-pyramidal coordination geometry. In contrast to **1**, complexes **2** and **3** show a

quadrupole doublet in Mössbauer spectra at 80 K. The doublet asymmetry, which was more obvious in the spectrum of **2**, was likely due to spin-orbit coupling of the ground state ^6S into three Kramer's doublets and different spin relaxation rates for the level ±1/2 and for ±3/2 and ±5/2 as was also observed in five-coordinate iron(III) complexes with porphyrins. Complexes **2** and **3** in the presence of a strong base were found to form the μ-oxido-dimeric iron(III) complex $[(Fe^{III}L)_2O]$ (**4**). The *VT* magnetic measurements for **4** indicated strong antiferromagnetic interaction between two high-spin iron(III) centers and a spin ground state $S_T = 0$. Cyclic voltammograms showed that complexes **1**–**3** can be quasireversible reduced by one-electron at iron center. The $E_{1/2}$ reduction potential follows the order: **1 > 2 > 3**. The μ-oxido diiron(III) complex can be reduced stepwise at more negative potentials (–1.29 and –1.50 V) compared to those for mononuclear compounds (–0.41 V for **1**, –0.64 V for **2** and –0.67 V for **3**) indicating marked electrochemical communication between the two iron centers in **4**.

SUPPLEMENTARY MATERIAL

Additional data and information are available electronically at the pages of journal website: https://www.shd-pub.org.rs/index.php/JSCS/article/view/9813, or from the corresponding author on request. CIFs are available from the corresponding author on request.

Acknowledgements. VBA thanks the Austrian Science Fund for the support of the present work via grant no. I4729. We thank Dr. Richard Goddard for collection of X-ray diffraction data. PR thanks the Slovak Grant Agency APVV (grant APVV-19-0024) and the Operational Program Integrated Infrastructure for the project: "Support of research activities of Excellence laboratories STU in Bratislava", Project no. 313021BXZ1, co-financed by the European Regional Development Fund, for the financial support. OP thanks National Agency for Research and Development of the Republic of Moldova, grant 20.80009.5007.12. We thank Manuela Gross for the synthesis of X-ray diffraction quality single crystals of complex **4**.

ИЗВОД

КОМПЛЕКСИ ГВОЖЂА(III) СА ДИТОПИЈСКИМ МАКРОЦИКЛИКЛИМА КОЈИ САДРЖЕ КРУНА-ЕСТАРСКИ И БИС(САЛИЦИЛИДЕН)-ИЗОТИОСЕМИКАРБАЗИДНИ ОСТАТАК

VLADIMIR B. ARION[1], OLEG PALAMARCIUC[2], SERGIU SHOVA[3], GHENADIE NOVITCHI[4] и PETER RAPTA[5]

[1]University of Vienna, Institute of Inorganic Chemistry, Währinger Strasse 42, A-1090 Vienna, Austria, [2]Moldova State University, A. Mateevici Street 60, MD-2009 Chisinau, Republic of Moldova, [3]Inorganic Polymers Department, "Petru Poni" Institute of Macromolecular Chemistry, Aleea Gr. Ghica Voda 41 A, Iasi 700487, Romania, [4]CNRS-LNCMI, 38042 Grenoble Cedex, France и [5]Institute of Physical Chemistry and Chemical Physics, Faculty of Chemical and Food Technology, Slovak University of Technology in Bratislava, Radlinského 9, SK-81237 Bratislava, Slovakia

Главни циљеви рада били су синтеза и карактеризација комплекса гвожђа(III) са дитопијским лигандом H_2L који се састоји од бис(салицилиден)изотиосемикарбазидног остатка са N_2O_2 донорским сетом и круна-етарског остатка са O_6 донорским сетом атома. Синтетисана су четири високоспинска комплекса гвожђа(III) формула $[Fe^{III}LClBa(CH_3OH)(H_2O)_{0.5}(ZnCl_4)]$ (**1**), $[Fe^{III}LCl]$ (**2**), $[Fe^{III}L(N_3)]$ (**3**) и $[(Fe^{III}L)_2O]$ (**4**). Комплекси су окарактерисани масеном спектрометријом, IR и UV–Vis спектроско-

пијом, мерењима магнетне сусцептибилности при варијабилној температури, Mössbauer спектроскопијом, дифракцијом рендгенских зрака на монокристалу и цикличном волтаметријом.

(Примљено 7. јуна, ревидирано 4. јула, прихваћено 8. септембра 2023)

REFERENCES

1. C. J. Van Staveren, J. Van Eerden, F. C. J. M. Van Veggel, S. Harkema, D. N. Reinhoudt, *J. Am. Chem. Soc.* **110** (1988) 4994 (https://doi.org/10.1021/ja00223a017)
2. F. C. J. M. Van Veggel, S. Harkema, M. Bos, W. Verboom, C. J. Van Staveren, G. J. Gerritsma, D. N. Reinhoudt, *Inorg. Chem.* **28** (1989) 1133 (https://doi.org/10.1021/ic00305a025)
3. F. C. J. M. van Veggel, W. Verboom, D. N. Reinhoudt, *Chem. Rev.* **94** (1994) 279 (https://doi.org/10.1021/cr00026a001)
4. D. N. Reinhoudt, A. R. Van Doorn, W. Verboom, *J. Coord. Chem.* **27** (1992) 91 (https://doi.org/10.1080/00958979209407946)
5. C. J. Van Staveren, D. E. Fenton, D. N. Reinhoudt, J. Van Eerden, S. Harkema, *J. Am. Chem. Soc.* **109** (1987) 3456 (https://doi.org/10.1021/ja00245a045)
6. C. J. van Staveren, D. N. Reinhoudt, J. van Eerden, S. Harkema, *J. Chem. Soc., Chem. Commun.* (1987) 974 (https://doi.org/10.1039/c39870000974)
7. D. M. Rudkevich, W. P. R. V. Stauthamer, W. Verboom, J. F. J. Engbersen, S. Harkema, D. N. Reinhoudt, *J. Am. Chem. Soc.* **114** (1992) 9671 (https://doi.org/10.1021/ja00050a064)
8. J. Halfpenny, R. W. H. Small, *J. Chem. Soc., Chem. Commun.* (1979) 879 (https://doi.org/10.1039/c39790000879)
9. V. B. Arion, V. C. Kravtsov, J. I. Gradinaru, Yu. A. Simonov, N. V. Gerbeleu, J. Lipkowski, J.-P. Wignacourt, H. Vezin, O. Mentré, *Inorg. Chim. Acta* **328** (2002) 123 (https://doi.org/10.1016/S0020-1693(01)00717-4)
10. M. T. Reetz, V. B. Arion, R. Goddard, Y. A. Simonov, V. Ch. Kravtsov, J. Lipkowski, *Inorg. Chim. Acta* **238** (1995) 23 (https://doi.org/10.1016/0020-1693(95)04661-R)
11. V. B. Arion, E. Bill, M. T. Reetz, R. Goddard, D. Stöckigt, M. Massau, V. Levitsky, *Inorg. Chim. Acta* **282** (1998) 61 (https://doi.org/10.1016/S0020-1693(98)00198-4)
12. V. B. Arion, J. P. Wignacourt, P. Conflant, M. Drache, M. Lagrenee, O. Cousin, H. Vezin, G. Ricart, W. Joppek, H.-W. Klein, *Inorg. Chim. Acta* **303** (2000) 228 (https://doi.org/10.1016/S0020-1693(00)00038-4)
13. V. B. Arion, V. C. Kravtsov, R. Goddard, E. Bill, J. I. Gradinaru, N. V. Gerbeleu, V. Levitschi, H. Vezin, Y. A. Simonov, J. Lipkowski, V. K. Bel'skii, *Inorg. Chim. Acta* **317** (2001) 33 (https://doi.org/10.1016/S0164-1212(00)00107-2)
14. J. Costes, F. Dahan, G. Novitchi, V. Arion, S. Shova, J. Lipkowski, *Eur. J. Inorg. Chem.* (2004) 1530 (https://doi.org/10.1002/ejic.200300486)
15. M. T. Reetz, V. B. Arion, R. Trültzsch, H. Buschmann, E. Cleve, *Chem. Ber.* **128** (1995) 1089 (https://doi.org/10.1002/cber.19951281106)
16. J.-C. Moutet, E. Saint-Aman, E.-M. Ungureanu, V. Arion, N. Gerbeleu, M. Revenco, *Electrochim. Acta* **46** (2001) 2733 (https://doi.org/10.1016/S0013-4686(01)00482-0)
17. G. M. Sheldrick, *Acta Crystallogr., A* **64** (2008) 112 (https://doi.org/10.1107/S0108767307043930)
18. M. N. Burnett,C. K. Johnson, *ORTEP-III: Oak Ridge Thermal Ellipsoid Plot Program for Crystal Structure Illustrations*, Oak Ridge National Laboratory, Oak Ridge, TN, 1996 (https://doi.org/10.2172/369685)

19. G. A. Bain, J. F. Berry, *J. Chem. Educ.* **85** (2008) 532 (https://doi.org/10.1021/ed085p532)
20. O. Kahn, *Molecular Magnetism*, Wiley-VCH, New York, 1993 (ISBN 0471188787, 9780471188384)
21. M. A. Yampol'skaya, S. G. Shova, N. V. Gerbeleu, V. K. Bel'skii, Yu. A. Simonov, *Zh. Neorg. Khim.* **27** (1982) 2551
22. K. S. Murray, *Coord. Chem. Rev.* **12** (1974) 1 (https://doi.org/10.1016/S0010-8545(00)80384-7)
23. J. S. Griffith, *Mol. Phys.* **8** (1964) 213 (https://doi.org/10.1080/00268976400100251)
24. M. Gerloch, J. Lewis, F. E. Mabbs, A. Richards, *J. Chem. Soc. A* (1968) 112 (https://doi.org/10.1039/J19680000112)
25. M. Gerloch, J. Lewis, F. E. Mabbs, A. Richards, *Nature* **212** (1966) 809 (https://doi.org/10.1038/212809a0)
26. M. Gerloch, F. E. Mabbs, *J. Chem. Soc., A* (1967) 1598 (https://doi.org/10.1039/J19670001598)
27. S. Hayami, S. Nomiyama, S. Hirose, Y. Yano, S. Osaki, Y. Maeda, *J. Radioanal. Nucl. Chem*. **239** (1999) 273 (https://doi.org/10.1007/BF02349496)
28. T. H. Moss, A. J. Bearden, W. S. Caughey, *J. Chem. Phys.* **51** (1969) 2624 (https://doi.org/10.1063/1.1672387)
29. G. Feher, P. L. Richards, in *Magnetic Resonance in Biological Systems*, Elsevier, Amsterdam, 1967, pp. 141−144 (https://doi.org/10.1016/B978-1-4832-1333-0.50019-7)
30. S. G. Shova, M. A. Yampol'skaya, B. G. Zemskov, N. V. Gerbeleu, K. I. Turta, I. N. Ivleva, *Zh. Neorg. Khim.* **30** (1985) 2309
31. M. Blume, *Phys. Rev. Lett.* **18** (1967) 305 (https://doi.org/10.1103/PhysRevLett.18.305)
32. A. V. Ablov, V. I. Gol'danskii, K. I. Turta, R. A. Stukan, V. V. Zelentsov, E. V. Ivanov, N. V. Gerbeleu, *Dokl. Akad. Nauk SSSR* **196** (1971) 1101
33. N. V. Gerbeleu, K. I. Turta, V. M. Canic, V. M. Leovac, V. B. Arion, *Koord. Khim.* **6** (1980) 446
34. J.-P. Costes, F. Dahan, F. Dumestre, J. Modesto Clemente-Juan, J. Garcia-Tojal, J.-P. Tuchagues, *Dalton Trans.* (2003) 464 (https://doi.org/10.1039/b210950f)
35. S. M. Gorun, S. J. Lippard, *Inorg. Chem.* **30** (1991) 1625 (https://doi.org/10.1021/ic00007a038).

Journal of the Serbian Chemical Society
JSCS@tmf.bg.ac.rs • www.shd.org.rs/JSCS
J. Serb. Chem. Soc. *88* (12) S346–S347 (2023) *Supplementary material*

SUPPLEMENTARY MATERIAL TO

Iron(III) complexes with ditopic macrocycles bearing crown-ether and bis(salicylidene) isothiosemicarbazide moieties

VLADIMIR B. ARION[1]*, OLEG PALAMARCIUC[2], SERGIU SHOVA[3], GHENADIE NOVITCHI[4] and PETER RAPTA[5]

[1]University of Vienna, Institute of Inorganic Chemistry, Währinger Strasse 42, A-1090 Vienna, Austria, [2]Moldova State University, A. Mateevici Street 60, MD-2009 Chisinau, Republic of Moldova, [3]Inorganic Polymers Department, "Petru Poni" Institute of Macromolecular Chemistry, Aleea Gr. Ghica Voda 41 A, Iasi 700487, Romania, [4]CNRS-LNCMI, 38042 Grenoble Cedex, France and [5]Institute of Physical Chemistry and Chemical Physics, Faculty of Chemical and Food Technology, Slovak University of Technology in Bratislava, Radlinského 9, SK-81237 Bratislava, Slovakia

J. Serb. Chem. Soc. *88* (12) (2023) 1205–1222

ANALYTICAL AND SPECTRAL DATA

*$[Fe^{III}LClBa(CH_3OH)(H_2O)_{0.5}(ZnCl_4)]\cdot CH_3OH$ (**1·CH_3OH**)*

Anal. Found, %: C, 29.91; H, 3.29; N, 4.05. Calcd for $C_{24.5}H_{33}BaCl_5FeN_3O_{8.5}SZn$ (M_r 973.43), %: C, 30.23; H, 3.42; N, 4.32. ESI positive: *m/z* 513 $[FeL]^+$; ESI negative: *m/z* 169 $[ZnCl_3]^-$; FAB: *m/z* 685 (100%), *m/z* 720 (50%), *m/z* 571 (47%).

*$[Fe^{III}LCl]\cdot CH_2Cl_2$ 0.5H_2O (**2·CH_2Cl_2 0.5H_2O**)*

Anal. Found, %: C, 43.11; H, 3.99; N, 7.01. Calcd for $C_{23}H_{26}FeN_3O_{6.5}SCl_3$ (M_r 642.73), %: C, 42.98; H, 4.08; N, 6.54. IR spectra, selected bands, ν, cm^{-1}: 2984(w), 2921(w), 1599(s) (C=N), 1577(m), 1244(m), 738(m).

*$[Fe^{III}L(N_3)]$ (**3**)*

Anal. Found, %: C, 47.31; H, 3.99; N, 15.05. Calcd for $C_{22}H_{23}FeN_6O_6S$ (M_r 555.37), %: C, 47.58; H, 4.17; N, 15.13. IR spectra, selected bands, ν, cm^{-1}: 2924(w), 2034(m) (N_3^-), 1578(s) (C=N), 1246(m) (C–N), 736(m).

*$[(Fe^{III}L)_2O]\cdot H_2O$ (**4·H_2O**)*

Anal. Found, %: C, 49.91; H, 4.54; N, 7.79; S, 5.81. Calcd for $C_{44}H_{48}Fe_2N_6O_{14}S_2$ (M_r 1060.71), %: C, 49.82; H, 4.56; N, 7.92; S, 6.05. IR spectra, selected bands, ν, cm^{-1}: 2919(w), 2982(w), 1600(s), 1578(s), 1248(m) (C–N), 840(m) (FeOFe), 731(s).

* Corresponding author. E-mail: vladimir.arion@univie.ac.at

Table S-I. Crystal Data and Details of Data Collection for $[Fe^{III}LClBa(CH_3OH)(H_2O)_{0.5}(ZnCl_4)]\cdot H_2O$ (**1·H$_2$O**), $[Fe^{III}LCl]\cdot CH_2Cl_2\cdot 0.5H_2O$ (**2·CH$_2$Cl$_2$·0.5H$_2$O**) and $[(Fe^{III}L)_2O]\cdot CHCl_3$ (**4·CHCl$_3$**)

Compound	**1·H$_2$O**	**2·CH$_2$Cl$_2$·0.5H$_2$O**	**4·CHCl$_3$**
empirical formula	$C_{23}H_{30}BaCl_5FeN3O_{8.5}SZn$	$C_{23}H_{26}Cl_3FeN_3O_{6.5}S$	$C_{45}H_{47}Cl_3Fe_2N_6O_{13}S_2$
fw	952.37	642.73	1162.05
space group	*P*-1	$P2_1/c$	*P*-1
a / Å	10.1054(2)	19.8072(9)	12.926(2)
b / Å	10.2497(2)	18.0736(8)	13.460(2)
c / Å	18.7003(4)	16.8200(8)	14.438(2)
α / °	90.031(1)		93.451(9)
β / °	93.822(1)	113.778(2)	96.088(9)
γ / °	119.201(1)		94.944(10)
V / Å^3	1685.79(6)	5510.2(4)	2482.4(7)
Z	2	4	2
λ / Å	0.71073	0.71073	0.71073
ρ_{calcd} / g cm^{-3}	1.876	1.550	1.555
cryst size / mm^3	0.70 × 0.35 × 0.14	0.33 × 0.18 × 0.07	0.50 × 0.25 × 0.25
T / K	100(2)	100(2)	100(2)
μ / mm^{-1}	2.793	0.959	0.900
R_1[a]	0.0502	0.0644	0.0430
wR_2[b]	0.1372	0.1753	0.1129
GOF[c]	1.069	1.071	1.048

[a] $R_1 = \Sigma||F_o| - |F_c||/\Sigma|F_o|$. [b] $wR_2 = \{\Sigma[w(F_o^2 - F_c^2)^2]/\Sigma[w(F_o^2)^2]\}^{1/2}$.

[c] GOF = $\{\Sigma[w(F_o^2 - F_c^2)^2]/(n - p)\}^{1/2}$, where n is the number of reflections and p is the total number of parameters refined.

Journal of the Serbian Chemical Society
JSCS@tmf.bg.ac.rs • www.shd.org.rs/JSCS
J. Serb. Chem. Soc. *88* (12) 1223–1236 (2023)
JSCS–5691
Original scientific paper
Published 19 December 2023

Ligands containing 7-azaindole functionality for inner-sphere hydrogen bonding: Structural and photophysical investigations

ALEC B. COLES, OSKAR G. WOOD and CHRIS S. HAWES*

School of Chemical and Physical Sciences, Keele University, Keele ST5 5BG, United Kingdom

(Received 23 June, revised 10 July, accepted 8 September 2023)

Abstract: The synthesis, structural analysis and spectroscopic characterisation of three new 7-azaindole ligands is reported, alongside a novel 7-azaindole derived coordination polymer, with the aim of identifying new bridging ligands containing inner-sphere hydrogen bond donor functionality. Structural characterisation shows that the 7-azaindole hydrogen bond donor ability is significantly stronger in the hydrazone and imine species **1** and **2** compared to the amine **3**, with the opposite trend evident in their hydrogen bond acceptor character. These findings are mirrored by the fluorescence spectroscopy results which show bimodal emission, characteristic of multiple emissive species related by proton transfer, is only evident in the amine species and not the more acidic imines. The polymeric copper(II) complex of the hydrazone ligand **1** shows the anticipated inner-sphere hydrogen bonding with a similar donor strength to that observed in the free ligand, which leads to deformation in the remainder of the coordination sphere. These results show the untapped versatility of the 7-azaindole functional group as a building block for ligands in coordination polymers and other multinuclear assemblies, with the potential for both stabilisation through hydrogen bonding and interesting photophysical properties.

Keywords: coordination chemistry; X-ray crystallography; Schiff bases; fluorescence spectroscopy.

INTRODUCTION

In the development of new functional coordination compounds, careful and deliberate ligand design is essential for balancing geometry and functionality.[1] In this regard, synthetic routes which allow access to a broad range of ligand functionalities are useful for fine-tuning properties of the resulting coordination compounds.[2,3] The Schiff base functionality is useful for these purposes, as simple aldehyde and amine precursors can be used to self-assemble ligands (or libraries of ligands) and coordinate to metal ions *in situ*.[4,5] Schiff base complexes, and

* Corresponding author. E-mail: c.s.hawes@keele.ac.uk
https://doi.org/10.2298/JSC230623061C

those of related hydrazone and semicarbazide functionalities,[6,7] have been widely explored for catalysis, medicine, molecular magnetism and sensing applications, among others.[8–12] These complexes often suffer from relatively low stability in the presence of water and other nucleophiles, however, which despite providing interesting possibilities for reversible self-assembly[13] can also limit their use in aqueous environments. As such, the inclusion of extra stabilising interactions around the coordination sphere may be a viable strategy for the generation of new stable Schiff base complexes.

Our interest in this area has concerned nitrogen heterocyclic ligands with hydrogen bond donors near the metal ion.[14] Such species may strengthen the coordination sphere against chemical degradation, both through the enthalpic contribution of extra bonding interactions but also by restricting molecular rotation or rearrangement.[15,16] The *1H*-pyrazole moiety is the quintessential example of such a ligand, and many instances of hydrogen-bonded assemblies in pyrazole--containing complexes are known.[17–19] However, expansion of this approach to larger or fused heterocycles is less common.[20] The 7-azaindole (7AI) fragment shows similar structural characteristics to *1H*-pyrazole in this regard. As shown in Fig. 1, 7AI contains a heterocyclic N–H hydrogen bond donor (with similar acidity to pyrazole) separated by one carbon to an imine-like nitrogen atom, and with a carbon backbone readily capable of derivatisation to add additional metal coordination sites. The photophysics of the parent heterocycle have been widely studied based on the tendency for solvent-dependent excited state proton transfer in the dimer and solvent adducts,[21–23] and as a simplified structural analogue for DNA base pairs.[24] Despite the interest in these compounds, surprisingly there have been relatively few investigations into the coordination chemistry of 7AI ligands in polymeric species, mostly focused on N-substituted derivatives.[25–27] Here we describe our attempts to develop heterotopic 7AI ligands, investigations into their photophysical behaviour, and report an unusual structurally characterised example of a 7AI-based coordination polymer.

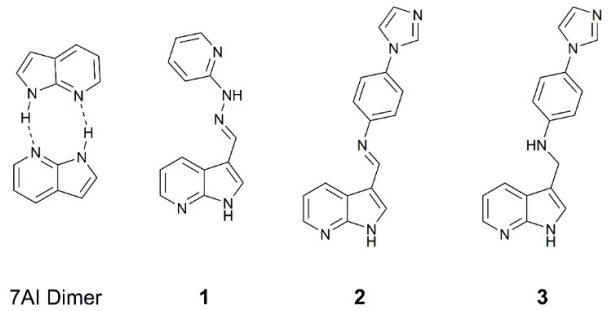

Fig. 1. Compounds of interest to this study; the 7-azaindole hydrogen-bonded dimer represented as the ground-state tautomer (7AI Dimer), and the structures of compounds **1**–**3**.

EXPERIMENTAL

Materials and methods

All starting materials and reagents were purchased from Merck or Fluorochem. NMR spectra were collected using a Bruker Avance III HD spectrometer using DMSO-d_6 and referenced to the residual solvent peak. Infrared spectra were recorded on a Thermo Fisher Nicolet iS10 spectrometer with an ATR sampling attachment. Elemental analysis was performed on a Thermo Flash 2000 CHNS elemental analyser. Photophysical measurements were collected using an Agilent Cary 60 Bio spectrophotometer and an Agilent Cary Eclipse fluorimeter using Starna quartz cuvettes of 1 cm path length. X-ray powder diffraction patterns were collected using a Bruker D8 Advance diffractometer with CuKα (λ = 1.5406 Å) radiation. Samples were mounted on a zero background silicon sample holder, and measured in the range 5–55° (2θ). Single crystal X-ray diffraction methods, as well as analytical and spectral data, are given in the Supplementary material to this paper. Hydrogen bonding parameters are given in Table I.

TABLE I. Hydrogen bonding parameters for all structures; symmetry codes: [1]1–*x*,–1/2+*y*,3/2–*z*; [2]2–*x*,–1/2+*y*,1/2–*z*; [3]–1–*x*,1–*y*,1–*z*; [4]1–*x*,1–*y*,–*z*; [5]+*x*,+*y*,–1+*z*; [6]1/2–*x*,1–*y*,1/2+*z*; [7]3/2–*x*,1–*y*,1/2+*z*

D–H···A	*d*(D–H) / Å	*d*(H–A) / Å	*d*(D–A) / Å	D–H–A / °
Compound **1**				
N2–H2···N5[1]	0.897(17)	1.977(18)	2.868(3)	173(3)
N7–H7···N10[2]	0.902(17)	1.946(18)	2.840(3)	171(3)
Compound **2**				
N2–H2···N1[3]	0.914(18)	1.958(19)	2.865(4)	171(3)
Compound **3**				
N2–H2···N1[4]	0.895(15)	2.054(16)	2.933(2)	167(2)
N3–H3···N5[5]	0.889(16)	2.104(16)	2.990(2)	174(2)
Poly-[Cu(**1**)Cl_2]				
N2–H2···Cl2[6]	0.88(2)	2.39(3)	3.225(4)	157(4)
N4–H4···Cl1[7]	0.89(2)	2.56(3)	3.380(3)	154(4)

*Synthesis of 7-azaindole-3-carboxaldehyde 2-pyridylhydrazone (**1**)*

To a suspension of 7-azaindole-3-carboxaldehyde (243 mg, 1.66 mmol) in 25 mL of methanol was added 2-hydrazinopyridine (183 mg, 1.67 mmol), and the mixture was heated under reflux for 24 hr. On cooling to room temperature an orange precipitate formed which was isolated by filtration, washed with methanol and dried in air. Yield 210 mg (53 %).

*Synthesis of 7-azaindole-3-carboxaldehyde 4-(*N*-imidazolyl)phenyl imine (**2**)*

To a suspension of 7-azaindole-3-carboxaldehyde (549 mg, 3.76 mmol) in MeOH (25 mL) was added 4-(*N*-imidazolyl)aniline (597 mg, 3.74 mmol), and the mixture was heated under reflux for 24 h. On cooling to room temperature, the resulting off-white precipitate was filtered, washed with cold methanol and air dried. Yield 559 mg (52 %).

*Synthesis of 3-(4-(*N*-imidazolyl)phenyl)aminomethyl-7-azaindole (**3**)*

To a suspension of compound **2** (540 mg, 1.88 mmol) in MeOH (50 mL) was added $NaBH_4$ (160 mg, 4.22 mmol) portion-wise over 30 min. Following this addition, the mixture was stirred at room temperature overnight. After 24 h, the solution was poured onto ice water

(15 mL) and the white precipitate was isolated by filtration, washed with a 1:1 MeOH:H_2O mixture, and dried in air. Yield 486 mg (89 %).

*Synthesis of poly-[Cu(**1**)Cl_2]*

A suspension of **1** (11 mg, 46 μmol) in methanol (5 mL) was combined with a solution of copper(II) chloride dihydrate (7.0 mg, 41 μmol) in methanol (5 mL). The resulting dark brown solution was dispersed by sonication for 10 min before being filtered, and the filtrate was subjected to diffusion of diethyl ether vapour. Dark brown crystals were formed within 24 h, isolated by filtration and washed with a small amount of cold methanol. Yield 8.5 mg (56 %).

RESULTS AND DISCUSSION

The synthesis of the 7AI derivatives **1** and **2** was achieved in a single step condensation reaction from 7-azaindole-3-carboxaldehyde and 2-hydrazinopyridine or *N*-(4-aminophenyl)imidazole, respectively. Reduction of **2** with sodium borohydride afforded the amine derivative **3** in good yield. These ligands, shown in Fig. 1, were chosen for a study into the effect of backbone substitution on the coordination chemistry and photophysics of 7AI derivatives, based on their potential for bridging coordination through the additional heterocyclic groups. Single crystals of all three ligands were first analysed by single crystal X-ray diffraction to determine their geometric parameters and tendencies for hydrogen bonding in the absence of metal ions.

Single crystals of **1** were prepared by recrystallization from ethanol, and the diffraction data were solved and refined in the monoclinic space group $P2_1/c$ with $Z' = 2$. The two residues in the asymmetric unit vary only slightly in their molecular geometry. Both residues adopt the expected *E* configuration at the hydrazone and essentially coplanar *anti* conformations for the terminal pyridine rings, with N_{PY}–C–N(H)–N torsion angles of 178.7(2) and 169.5(2)° for residues **1** and **2**, respectively, as shown in Fig. 2. A slight difference is also observed in the azaindole···pyridine interplanar angles for the two residues, of 10.6 *vs.* 12.8°, respectively.

The *anti* conformation of the pyridylhydrazone in **1** results in both this group and the 7AI moiety adopting equivalent hydrogen bond donor/acceptor capabilities. Interestingly, the hydrogen bonding mode observed for both residues is a head-to-tail interaction between one 7AI group and one pyridylhydrazone group, rather than the more symmetric head-to-head/tail-to-tail pairing. Generally, formation of the strongest donor/acceptor pair is expected, followed by the next strongest, although this can be complicated by many structural factors.[28] While unsubstituted 7AI has a higher ground state pKa than typical pyridylhydrazones (12.1 *vs.* 10–11, respectively),[29,30] we would anticipate the electron withdrawing substituent at the 7AI 3-position to bring these two values closer to unity. However, the difference in geometry for the resulting $R_2^2(8)$ rings[31] presumably disfavours the symmetric dimer which is observed in simpler 7AI systems.[32] Here, the idealised N–H vector is 18° removed from the acceptor lone pair in 7AI,

compared to these vectors being parallel in the pyridylhydrazone (as with other hydrogen bond dimers, such as carboxylic acids).[33] The difference in hydrogen bond donor strength is evident from the difference in donor···acceptor distances, which fall at 2.869(3) and 2.840(3) Å for the 7AI donors and 3.048(3) and 3.195(3) Å for the hydrazone donors. These hydrogen bonds between molecules lead to two crystallographically independent, parallel hydrogen bonding chains oriented parallel to the *b* axis. These chains further interact through π···π contacts which, as expected, take a head-to-tail form to favour contact between the relatively electron rich and poor regions of the two aromatic systems.

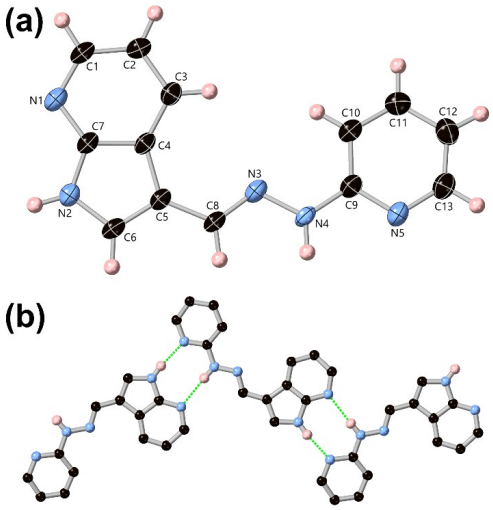

Fig. 2. a) Structure of compound **1** with atom labelling scheme. ADPs are rendered at the 50 % probability level, and the second fragment is omitted for clarity. b) The hydrogen bonding behaviour of compound **1**. Selected hydrogen atoms are omitted for clarity.

Single crystals of compound **2** were isolated from ethanol, and the diffraction data were solved and refined in the monoclinic space group $P2_1/n$ with $Z' = = 1$. The structural model confirms the expected structure as shown in Fig. 3, showing the *E* configuration of the imine and an essentially coplanar shape, with the central phenyl ring exhibiting mean interplanar angles of 6.3 and 23.8° relative to the 7AI and imidazole groups, respectively. With only one classical hydrogen bond donor, the centrosymmetric 7AI dimer motif is observed with an N···N distance of 2.865(4) Å equivalent to the 7AI-donated interactions seen in **1**, and N–H···N angle of 171(3).° Neither the imine nor imidazole nitrogen atoms participate in any significant directional interactions with other hydrogen atoms. The dominant modes of intermolecular interaction beyond hydrogen bonding are edge-to-face C-H···π contacts between the imidazole and 7AI groups. The shortest interatomic distances of 3.532(5) and 3.544(5) Å for C17···C3 and C6···C15, respectively, are consistent with typical magnitudes for such interactions.[34]

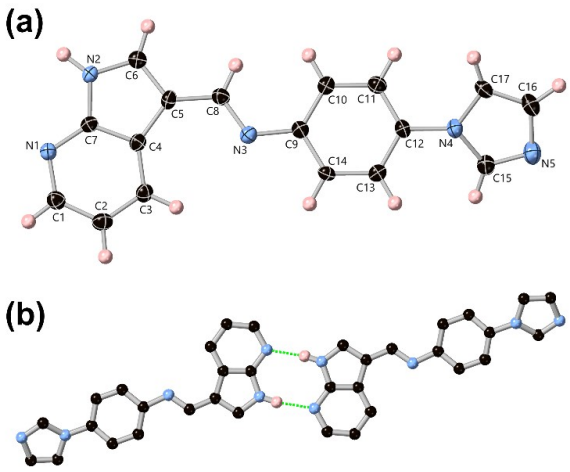

Fig. 3. a) Structure of compound **2** with atom labelling scheme. ADPs are rendered at the 50 % probability level. b) Hydrogen bonding behaviour in the structure of **2** consisting of a centrosymmetric 7AI dimer-type motif. Selected hydrogen atoms are omitted for clarity.

For comparison with additional hydrogen bond donation capability, and to provide a spectroscopic comparison with a more electron rich 7AI derivative, compound **2** was reduced to the amine **3**, which was crystallised from ethanol. The diffraction data for **3** were solved and refined in the monoclinic space group $P2_1/n$, with $Z' = 1$. Reduction to the amine is evident from the longer C–N bond (1.446(3) Å, *cf.* 1.285(4) Å in **2**) and a significantly less planar geometry, with the 7AI···phenyl interplanar angle increasing to 66.9°, while the imidazole–phenyl interplanar angle remains similar at 34.4°. The centrosymmetric 7AI dimer hydrogen bonding motif is again evident, as shown in Fig. 4, although reduction to the amine leads to a much longer N···N distance of 2.933(2) Å, while the N–H···N angle is unchanged at 167(2)°. The longer donor···acceptor distance in this interaction likely relates to lower acidity of the N–H group following loss of the electron withdrawing imine. This is supported by the infrared spectra for the three ligands. Compounds **1** and **2** show similar broad absorbances at 3205 and 3210 cm^{-1}, respectively, consistent with the NH stretch in a hydrogen-bonded 7AI species.[35] In **3**, this band is shifted to a higher frequency of 3247 cm^{-1} indicative of a decrease in hydrogen bond donor strength for this species in the solid state.

In addition to the 7AI dimer, further hydrogen bonding is evident between the amine N–H group and the imidazole nitrogen atom of adjacent molecules, at a similar donor···acceptor distance of 2.990(2) Å and N–H···N angle of 174(2)°. The combination of both interactions leads to the formation of a one-dimensional hydrogen bonded ribbon oriented parallel to the *c* axis. Adjacent ribbons interact

through a series of diffuse π···π and C–H···π contacts, although these are less prominent than those in **2** due to the lesser degree of conjugation in **3**.

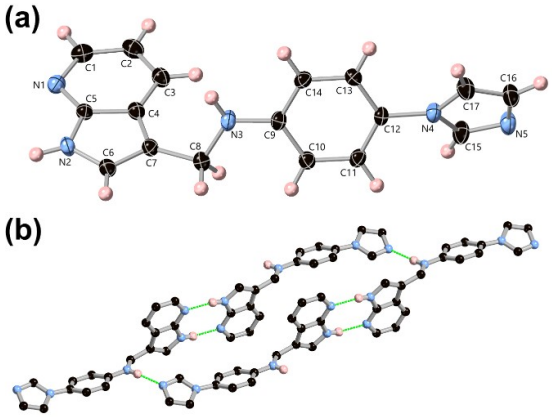

Fig. 4. a) Structure of compound **3** with atom labelling scheme. ADPs are rendered at the 50 % probability level. b) The hydrogen bonding environment in the structure of **3**. Selected hydrogen atoms are omitted for clarity.

With the structures and key interaction modes of **1**–**3** confirmed, we turned our attention to their use as ligands for coordination compounds. Despite our efforts over a range of conditions (near-ambient to high temperature hydro/solvothermal), we were unable to isolate any coordination compounds containing ligands **2** or **3**, instead generally recovering either unreacted starting materials or unidentified decomposition products. We ascribe these to the poor solubility of these species and vulnerability to either hydrolysis (**2**) or acid catalysed amine elimination (**3**)[36] reactions at high temperatures, alongside low stability constants for the pure monodentate coordination modes. However, the chelating ligand **1** readily reacted with copper(II) chloride dihydrate at room temperature, to form a dark brown solution giving crystals on standing overnight or under diffusion of diethyl ether vapour, which analysed for a complex of the formula poly-[Cu(**1**)Cl_2], a one-dimensional coordination polymer. The diffraction data for poly-[Cu(**1**)Cl_2] were solved and refined in the orthorhombic space group $P2_12_12_1$ with $Z' = 1$. The copper ion adopts a distorted square pyramidal coordination geometry (τ_5 = = 0.22),[37] where the basal plane is occupied by two *cis*-oriented chlorido ligands and the chelating pyridylhydrazone moiety, while the axial position is occupied by the 7AI nitrogen atom, as shown in Fig. 5. The axial Cu–N distance of 2.293(4) Å is significantly longer than those corresponding to the pyridine or hydrazone nitrogen atoms (2.008(3) and 2.037(3) Å, respectively, a consequence of the typical axial bond elongation in square pyramidal d^9 complexes rather than being indicative of any particular difference in donor strength. The copper ion

acts as a corner in the expanded structure, relating each ligand segment to the next by a mean interplanar angle of 86.6° as the overall zig-zag polymer aligns parallel to the *c* axis.

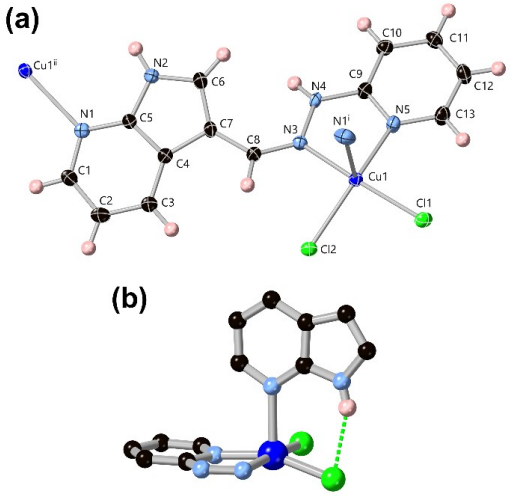

Fig. 5. a) Structure of poly-[Cu(**1**)Cl_2] with atom labelling scheme. ADPs are rendered at the 50 % probability level. Symmetry codes used to generate equivalent atoms: (*i*) ½–*x*, 1–*y*, 1/2+*z*; (*ii*) ½–*x*, 1–*y*, –1/2–*z*. b) The inner-sphere hydrogen bond in the structure of poly-[Cu(**1**)Cl_2] showing the deflection of the chlorido ligand. Selected atoms are omitted for clarity.

The complex poly-[Cu(**1**)Cl_2] contains two classical hydrogen bond donors, and each engages in the expected N–H···Cl hydrogen bonding, given all other acceptors are involved in coordination to the metal ion. As we had intended, the 7AI hydrogen bond donor engages in hydrogen bonding within the coordination sphere to the adjacent chlorido ligand Cl2, at an N···Cl distance of 3.225(4) Å and a relatively small N–H···Cl angle of 157(4)°. The donor···acceptor distance for this interaction is comparable to that typically observed for N–H···Cl contacts (3.2–3.3 Å),[38] and accounting for the *ca.* 0.35 Å difference in atomic radii for N and Cl, are consistent with the donor strength of this group observed in the structure of the free ligand. Notably, the chlorido ligand involved in this interaction is also bent out of the basal plane, evident by the angle N5–Cu1–Cl2 of 159.22(9) (Fig. 5b), compared to the N3–Cu1–Cl1 angle of 172.47(9). The hydrazone N–H group is oriented away from the coordination sphere, and instead donates a hydrogen bond to the chlorido ligand Cl1 of an adjacent chain, as shown in Fig. 6. The longer N···Cl distance of 3.380(4) and N–H···Cl angle of 154(4)° are consistent with the previous observation of a weaker hydrazone N–H donor com-

pared to 7AI. The inter-strand hydrogen bonding also facilitates additional π···π interactions between hydrogen bonded strands, where 7AI and pyridylhydrazone groups interact with a minimum interatomic distance of 3.223(6) Å for C1···C6 and a mean interplanar angle of 18.4°.

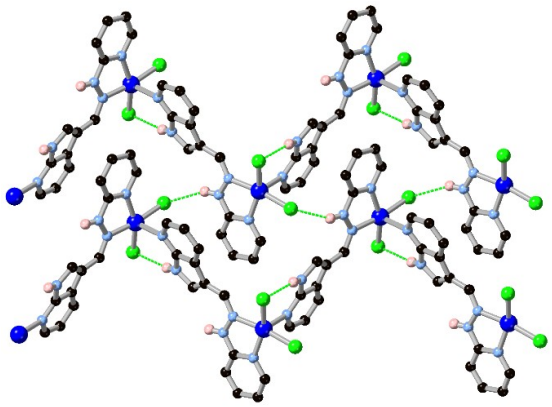

Fig. 6. The extended structure of the coordination polymer *poly*-[Cu(**1**)Cl_2] showing the hydrogen bonding behaviour between strands. Selected hydrogen atoms are omitted for clarity.

The structural data for compounds **1**–**3** suggest reduction of the imine at the 3 position leads to a decrease in hydrogen bond donor strength for the 7AI proton. Given the tendency for the photophysical properties of 7AIs to be impacted by proton transfer, we investigated the absorption and emission behaviour of compounds **1–3** to probe this influence. In DMSO, all three compounds show absorption bands with maxima in the range 22–26×10^3 L mol^{-1} cm^{-1} from n→π* and/or π→π* transitions, as shown in Fig. 7. The more conjugated species **1** and **2** show lower energy absorbances at 325 and 331 nm, respectively, both with higher energy shoulders. The absorbance for **3** has a maximum at 277 nm, with any structuring at the high energy edge falling outside of the solvent window. Excitation leads to emission in the near-UV to visible region of the spectrum; compound **1** shows a single emission band with maximum at 457 nm, while the emission from compound **2** is substantially blue-shifted to 378 nm. Given the similar absorbance profiles and structures of the two compounds, this difference in Stokes shift (8900 *vs*. 3800 cm^{-1}) is surprising, and may indicate the emissive states in the two species arise from different tautomers or hydrogen-bonded environments.

Compound **3**, on the other hand, shows a structured emission profile in DMSO comprised of two bands, the larger at 470 nm with a distinct second band visible as a shoulder at 365 nm. These band positions are similar to those observed for 7-azaindole itself in protic solvents, where the “normal” emission at

370 nm is accompanied by a tautomer band at 510 nm.[39] In contrast to the emission profile here, the normal emission is usually more intense than the tautomer band, although this trend can be reversed in solutions of more acidic alcohols where emission from either the solvated tautomer or protonated cation can be favoured.[40]

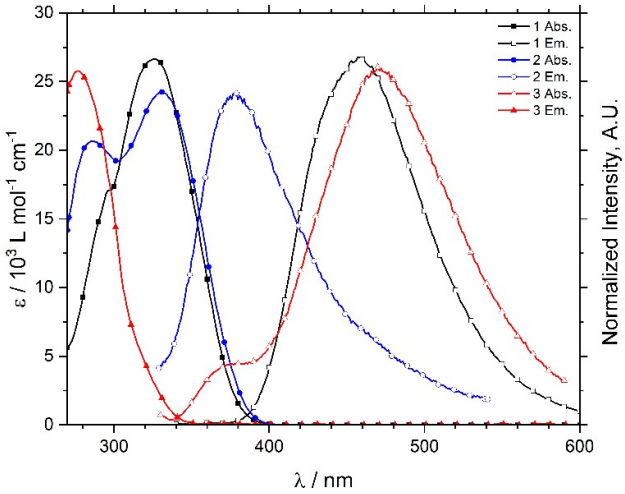

Fig. 7. Combined absorption (solid markers) and normalized emission (hollow markers) spectra for compounds **1** (black, 27 μM, λ_{ex} = 318 nm), **2** (blue, 22 μM, λ_{ex} = 286 nm) and **3** (red, 26 μM, λ_{ex} = 300 nm) in DMSO.

To further explore the discrepancy in emission behaviour of the three 7AI species, each was diluted into acetonitrile, as a weaker hydrogen bond acceptor less likely to mediate proton transfer, and methanol, expected to alter any proton transfer pathways by the formation of hydrogen-bonded solvent adducts. In acetonitrile, all three compounds display essentially equivalent behaviour to that in DMSO with only minor blue-shifting of the emission of all three compounds, indicating slightly negative solvatochromism (Supporting Information). In methanol, however, while compounds **1** and **2** exhibit the same behaviour (albeit at much lower intensity, presumably due to extra vibrational relaxation with solvent protons), the two emission bands in **3** are swapped in intensity, with emission from the normal band at 368 nm much brighter than emission from the tautomer band at 525 nm, as shown in Fig. 8. These findings suggest that only **3,** lacking conjugation at the 3 position, follows the typical excited state proton transfer pathway of the parent 7-azaindole, while the fully conjugated **1** and **2** show emission behaviour which is mostly invariant to the local hydrogen bonding environment. This effect may relate to competition in electronic demand from the imine/

/hydrazone substituent raising the energy of the proton transfer processes, or additional decay pathways involving the backbone, such as photoinduced electron transfer (PET) depopulating the emissive states.

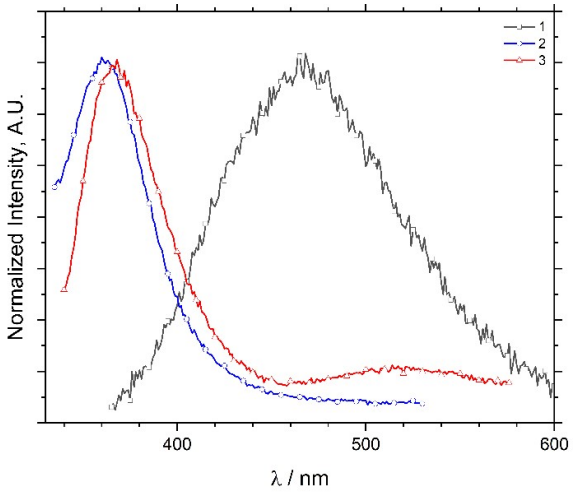

Fig. 8. Normalized emission spectra for compounds 1 (black, 27 μM, λ_{ex} = 318 nm), **2** (blue, 22 μM, λ_{ex} = 280 nm) and **3** (red, 26 μM, λ_{ex} = 300 nm) in MeOH.

CONCLUSION

Three new 7-azaindole derived ligands have been prepared and characterised, and used to generate a crystalline coordination polymer containing a 7-azaindole ligand. Structural analysis of the ligands shows the typical 7AI dimer motif can be overridden in the presence of a more basic acceptor of similar donor–acceptor geometry, while reduction from the imine to the amine significantly reduces the donor capability of the N–H group. On reaction with copper(II), the chelating hydrazone derivative **1** forms a linear coordination polymer containing an inner-sphere hydrogen bonding motif, although likely due to the geometric mismatch of donor and acceptor in this system this interaction was associated with a deformation of the square pyramidal coordination sphere in this system. Investigation of the photophysical properties of these ligands revealed that only the reduced species **3** gave the solvent-dependent bimodal emission indicative of proton transfer-related emission pathways in the excited state, while the more acidic hydrazone **1** and Schiff base **2** exhibited more straightforward emission behaviour which was independent of solvent. These results outline a new path to a diverse family of functional heterotopic ligands for coordination polymers and MOFs, with 7AI-containing systems expected to offer useful inner-sphere

hydrogen bonding capabilities alongside a potential fluorescent signalling mechanism which may be linked to the electronic environment of the adjacent proton.

SUPPLEMENTARY MATERIAL

Additional data and information are available electronically at the pages of journal website: https://www.shd-pub.org.rs/index.php/JSCS/article/view/12451, or from the corresponding author on request. CCDC 2269543-2269546.

Acknowledgements. The authors gratefully acknowledge the Royal Society of Chemistry (Research Enablement Grant E21-4110373157) and the School of Chemical and Physical Sciences at Keele University for funding support. C.S.H. also acknowledges the X-ray diffraction group at the University of Novi Sad for fruitful discussions in Schiff base chemistry, facilitated by the Erasmus+ and Science Fund of the Republic of Serbia PROMIS schemes.

ИЗВОД

ЛИГАНДИ СА 7-АЗАИНДОЛНОМ ФУНКЦИОНАЛНОМ ГРУПОМ ЗА ФОРМИРАЊЕ ВОДОНИЧНИХ ВЕЗА У УНУТРАШЊОЈ СФЕРИ: СТРУКТУРНА И ФОТОФИЗИЧКА ИСПИТИВАЊА

ALEC B. COLES, OSKAR G. WOOD и CHRIS S. HAWES

School of Chemical and Physical Sciences, Keele University, Keele ST5 5BG, United Kingdom

У овом раду описана је синтеза, структурна анализа и спектроскопска карактеризација три нова 7-азаиндолна лиганда, као и новог координационог полимера са једним од ових лиганада, а са циљем идентификације нових мостовних лиганада са водоник-донорним групама у унутрашњој сфери. Структурна карактеризација је показала да 7-азаиндоли имају бољу водоник-донорну способност у хидразонској и иминској форми (једињења **1** и **2**), у поређењу са аминском (**3**). Насупрот томе, обрнути тренд је опажен када је испитивана водоник-акцепторска способност ових једињења. Ова сазнања се рефлектују и у резултатима флуоресцентне спектроскопије, који показују бимодалну емисију карактеристичну за присуство више хемијских врста које учествују у трансферу протона. Овај ефекат је присутан код амина, али не и код киселијих имина. У структури полимерног комплекса бакра(II) са хидразинским лигандом **1** уочено је очекивано формирање водоничних веза у унутрашњој сфери са сличном јачином као у слободном лиганду, што доводи до деформације координационе сфере. Ови резултати показују раније неиспитивану разноликост 7-азаиндолне функционалне групе као блока за изградњу лиганада у координационим полимерима и другим полинуклеарним врстама, са потенцијалом за стабилизацију путем водоничног везивања и интересантним фотофизичким својствима.

(Примљено 23. јуна; ревидирано 10. јула; прихваћено 8. септембра 2023)

REFERENCES

1. Z. Yin, Y.-L. Zhou, M.-H. Zeng, M. Kurmoo, *Dalton Trans.* **44** (2015) 5258 (https://doi.org/10.1039/C4DT04030A)
2. B. G. Diamond, L. I. Payne, C. H. Hendon, *Commun. Chem.* **6** (2023) 67 (https://doi.org/10.1038/s42004-023-00863-z)
3. M. Eddaoudi, J. Kim, N. Rosi, D. Vodak, J. Wachter, M. O'Keeffe, O. M. Yaghi, *Science* **295** (2002) 469 (https://doi.org/10.1126/science.1067208)

4. M. M. Radanović, S. B. Novaković, M. V. Rodić, L. S. Vojinović-Ješić, C. Janiak, V. M. Leovac, *J. Serb. Chem. Soc.* **87** (2022) 1259 (https://doi.org/10.2298/JSC220613072R)
5. P. D. Frischmann, V. Kunz, F. Würthner, *Angew. Chem. Int. Ed.* **54** (2015) 7285 (https://doi.org/10.1002/anie.201501670)
6. J. G. Betancourth, J. A. Castaño, R. Visbal, M. N. Chaur, *Eur. J. Org. Chem.* **2022** (2022) e202200228 (https://doi.org/10.1002/ejoc.202200228)
7. V. M. Leovac, V. S. Jevtović, L. S. Jovanović, G. A. Bogdanović, *J. Serb. Chem. Soc.* **70** (2005) 393 (https://doi.org/10.2298/JSC0503393L)
8. A. Erxleben, *Inorg. Chim. Acta* **472** (2018) 40 (https://doi.org/10.1016/j.ica.2017.06.060)
9. J.-F. Ayme, J. E. Beves, C. J. Campbell, D. A. Leigh, *J. Am. Chem. Soc.* **141** (2019) 3605 (https://doi.org/10.1021/jacs.8b12800)
10. S. Shaw, J. D. White, *Chem. Rev.* **119** (2019) 9381 (https://doi.org/10.1021/acs.chemrev.9b00074)
11. V. M. Leovac, M. V. Rodić, L. S. Jovanović, M. D. Joksović, T. Stanojković, M. Vujčić, D. Sladić, V. Marković, L. S. Vojinović-Ješić, *Eur. J. Inorg. Chem.* **2015** (2015) 882 (https://doi.org/10.1002/ejic.201403050)
12. A. Ferguson, M. A. Squire, D. Siretanu, D. Mitcov, C. Mathonière, R. Clérac, P. E. Kruger, *Chem. Commun.* **49** (2013) 1597 (https://doi.org/10.1039/C3CC00012E)
13. L. Fabbrizzi, *J. Org. Chem.* **85** (2020) 12212 (https://doi.org/10.1021/acs.joc.0c01420)
14. C. S. Hawes, *Dalton Trans.* **50** (2021) 6034 (https://doi.org/10.1039/D1DT00675D)
15. X.-L. Lv, S. Yuan, L.-H. Xie, H. F. Darke, Y. Chen, T. He, C. Dong, B. Wang, Y.-Z. Zhang, J.-R. Li, H.-C. Zhou, *J. Am. Chem. Soc.* **141** (2019) 10283 (https://doi.org/10.1021/jacs.9b02947)
16. K. Wang, Q. Wang, X. Wang, M. Wang, Q. Wang, H.-M. Shen, Y,-F. Yang, Y. She, *Inorg. Chem. Front.* **7** (2020) 3548 (https://doi.org/10.1039/D0QI00772B)
17. T. Basu, H. A. Sparkes, M. K. Bhunia, R. Mondal, *Cryst. Growth Des.* **9** (2009) 3488 (https://doi.org/10.1021/cg900195f)
18. C. S. Hawes, B. Moubaraki, K. S. Murray, P. E. Kruger, D. R. Turner, S. R. Batten, *Cryst. Growth Des.* **14** (2014) 5749 (https://doi.org/10.1021/cg501004u)
19. M. R. Healy, J. W. Roebuck, E. D. Doidge, L. C. Emeleus, P. J. Bailey, J. Campbell, A. J. Fischmann, J. B. Love, C. A. Morrison, T. Sassi, D. J. White, P. A. Tasker, *Dalton Trans.* **45** (2016) 3055 (https://doi.org/10.1039/C5DT04055H)
20. O. G. Wood, C. S. Hawes, *CrystEngComm* **24** (2022) 8197 (https://doi.org/10.1039/D2CE01475K)
21. R. S. Moog, M. Maroncelli, *J. Phys. Chem.* **95** (1991) 10359 (https://doi.org/10.1021/j100178a023)
22. X.-F. Yu, S. Yamazaki, T. Taketsugu, *J. Chem. Theory Comput.* **7** (2011) 1006 (https://doi.org/10.1021/ct200022a)
23. D. E. Folmer, E. S. Wisniewski, S. M. Hurley, A. W. Castleman Jr. *Proc. Natl. Acad. Sci. U.S.A.* **96** (1999) 12980 (https://doi.org/10.1073/pnas.96.23.12980)
24. A. V. Smirnov, D. S. English, R. L. Rich, J. Lane, L. Teyton, A. W. Schwabacher, S. Luo, R. W. Thornburg, J. W. Petrich, *J. Phys. Chem., B* **101** (1997) 2758 (https://doi.org/10.1021/jp9630232)
25. E. Wong, J. Li, C. Seward, S. Wang, *Dalton Trans.* (2009) 1776 (https://doi.org/10.1039/B814393E)
26. A. Domínguez-Martín, M. P. Brandi-Blanco, A. Matilla-Hernández, H. El Bakkali, V. M. Nurchi, J. M. González-Pérez, A. Castiñeiras, J. Niclós-Gutiérrez, *Coord. Chem. Rev.* **257** (2013) 2814 (https://doi.org/10.1016/j.ccr.2013.03.029)

27. B. Morzyk-Ociepa, K. Szmigiel, R. Petrus, I. Turowska-Tyrk, D. Michalska, *J. Mol. Struct.* **1144** (2017) 338 (https://doi.org/10.1016/j.molstruc.2017.05.059)
28. T. Steiner, *Acta Crystallogr., B* **57** (2001) 103 (https://doi.org/10.1107/S0108768100014348)
29. Y. Chen., R. L. Rich, F. Gai, J. W. Petrich, *J. Phys. Chem.* **97** (1993) 1770 (https://doi.org/10.1021/j100111a011)
30. P. Doungdee, S. Sarel, N. Wongvisetsirikul, S. Avramovici-Grisaru, *J. Chem. Soc., Perkin Trans. 2* (1995) 319 (https://doi.org/10.1039/P29950000319)
31. M. C. Etter, J. C. MacDonald, J. Bernstein, *Acta Crytallogr., B* **46** (1990) 256 (https://doi.org/10.1107/S0108768189012929)
32. B. Morzyk-Ociepa, K. Dysz, I. Turowska-Tyrk, D. Michalska, *J. Mol. Struct.* **1101** (2015) 91 (https://doi.org/10.1016/j.molstruc.2015.08.003)
33. T. Beyer, S. L. Price, *J. Phys. Chem., B* **104** (2000) 2647 (https://doi.org/10.1021/jp9941413)
34. M. Nishio, *CrystEngComm* **6** (2004) 130 (https://doi.org/10.1039/B313104A)
35. H. Yokoyama, H. Watanabe, T. Omi, S. Ishiuchi, M. Fujii, *J. Phys. Chem., A* **105** (2001) 9366 (https://doi.org/10.1021/jp011245g)
36. H. Masui, S. Kanda, S. Fuse, *Commun. Chem.* **6** (2023) 47 (https://doi.org/10.1038/s42004-023-00837-1)
37. A. W. Addison, T. N. Rao, J. Reedijk, J. van Rijn, G. C. Verschoor, *J. Chem. Soc., Dalton Trans.* (1984) 1349 (https://doi.org/10.1039/DT9840001349)
38. G. Bartlett, I. Langmuir, *J. Am. Chem. Soc.* **43** (1921) 84 (https://doi.org/10.1021/ja01434a010)
39. C. A. Taylor, M. A. El-Bayoumi, M. Kasha, *Proc. Natl. Acad. Sci. U.S.A.* **63** (1969) 253 (https://doi.org/10.1073/pnas.63.2.253)
40. J. Konijnenberg, A. H. Huizer, C. A. G. O. Varma, *J. Chem. Soc., Faraday Trans. 2* **84** (1988) 1163 (https://doi.org/10.1039/F29888401163).

Journal of the Serbian Chemical Society
JSCS@tmf.bg.ac.rs • www.shd.org.rs/JSCS
J. Serb. Chem. Soc. *88* (12) S348–S355 (2023) *Supplementary material*

SUPPLEMENTARY MATERIAL TO

Ligands containing 7-azaindole functionality for inner-sphere hydrogen bonding: Structural and photophysical investigations

ALEC B. COLES, OSKAR G. WOOD and CHRIS S. HAWES*

School of Chemical and Physical Sciences, Keele University, Keele ST5 5BG, United Kingdom

J. Serb. Chem. Soc. *88* (12) (2023) 1223–1236

ANALYTICAL AND SPECTRAL DATA

7-Azaindole-3-carboxaldehyde 2-pyridylhydrazone ***(1)****.* Mp 260 °C (decomp.); δ_H (400 MHz; DMSO-d_6) 11.90 (s, 1H, H11), 10.54 (s, 1H, H6), 8.54 (d, 1H, *J* = 7.9 Hz, H1), 8.30 (d, 1H, *J* = 4.8 Hz, H3), 8.21 (s, 1H, H4), 8.08 (d, 1H, *J* = 4.9 Hz, H10), 7.80 (s, 1H, H5), 7.65 (t, 1H, *J* = 7.8 Hz, H8), 7.34 – 7.12 (m, 2H, H2 + H7), 6.70 (dd, 1H, *J* = 7.0, 4.9 Hz, H9), δ_C (100 MHz; DMSO-d_6) 157.4, 149.3, 147.8, 143.7, 137.9, 136.4, 129.8, 128.2, 116.6, 116.5, 114.0, 111.4, 105.7; ν_{max} (ATR, cm^{-1}) 3205m br, 3068m, 2979m, 2784w, 2627w, 1598s, 1578s, 1541m, 1499w, 1456m sh, 1439s, 1413m, 1317m, 1286s, 1241m, 1126s, 1083s, 991s, 920m, 812w, 792w, 760s, 726m, 623s; λ_{max}(DMSO) /nm (ε /L mol^{-1} cm^{-1}) 326 (26700). Single crystals for SCXRD were prepared by recrystallization from ethanol.

*7-Azaindole-3-carboxaldehyde 4-(*N*-imidazolyl)phenyl imine* ***(2)****.* Mp 270 °C (decomp.); δ_H (400 MHz; DMSO-d_6) 12.34 (1H, br s, H11), 8.75 (s, 1H, H5), 8.67 (d, 1H, *J* = 7.8 Hz, H1), 8.35 (d, 1H, *J* = 4.7 Hz, H3), 8.26 (s, 1H, H4), 8.17 (s, 1H, H8), 7.75 (s, 1H, H10), 7.67 (d, 2H, *J* = 8.3 Hz, H6), 7.38 (d, 2H, *J* = 8.2 Hz, H7), 7.26 (dd, 1H, *J* = 7.8, 4.7 Hz, H2), 7.11 (s, 1H, H9) δ_C (100 MHz; DMSO-d_6) 155.7, 151.3, 149.5, 144.3, 135.5, 134.0, 133.9, 130.1, 129.8, 122.0, 121.2, 118.1, 117.4, 117.1, 113.7; ν_{max} (ATR, cm^{-1}) 3210w br, 3111m, 3070m, 3019m, 2808m, 2597w, 1620m, 1607m, 1575s, 1505m, 1465m, 1416s, 1280s, 1243s, 1134s, 1116s, 1054s, 960w, 896m, 842s, 804s, 766s, 657s, 626s; λ_{max} (DMSO) /nm (ε /L mol^{-1} cm^{-1}) 331 (24100). Single crystals for SCXRD were prepared by recrystallization from ethanol.

*3-(4-(*N*-Imidazolyl)phenyl)aminomethyl-7-azaindole* ***(3)****.* Mp 234-238 °C; δ_H (400 MHz; DMSO-d_6) 11.44 (s, 1H, H12), 8.19 (d, 1H, *J* = 4.2 Hz, H1), 8.06 (d, 1H, *J* = 7.8 Hz, H3), 7.95 (s, 1H, H9), 7.50 – 7.44 (m, 2H, H4 + H11), 7.25 (d, 2H, *J* = 8.5 Hz, H8), 7.04 (dd, 1H, *J* = 7.8, 4.6 Hz, H2), 7.00 (s, 1H, H10), 6.75 (d, 2H, *J* = 8.7 Hz, H7), 6.25 (t, 1H, *J* = 5.5 Hz, H6), 4.40 (d, 2H, *J* = 5.6 Hz, H5) δ_C (100 MHz; DMSO-d_6) 148.7, 148.0, 142.6, 135.4, 129.1, 127.1, 126.2, 124.2, 121.9, 118.9, 118.4, 115.0, 112.6, 111.4, 38.7; ν_{max} (ATR, cm^{-1}) 3247 m br, 3122m, 3092w, 3031m, 2886w, 1610s, 1582m, 1534s, 1519s, 1496m, 1457m, 1418s, 1359w, 1330s, 1306m, 1292m, 1275w, 1244m, 1180w, 1119s, 1058s, 982w, 961w, 911w, 842w, 817s, 765s, 659s; λ_{max} (DMSO) /nm (ε /L mol^{-1} cm^{-1}) 277 (25600). Single crystals for SCXRD were prepared by recrystallization from ethanol.

* Corresponding author. E-mail: c.s.hawes@keele.ac.uk

*Poly-[Cu(**1**)Cl$_2$]*. Mp 196-198 °C (decomp.); Found C, 41.62; H, 3.04; N, 18.21; Calculated for [Cu(**1**)Cl$_2$] ($C_{13}H_{11}N_5CuCl_2$) C, 42.01; H, 2.98; N, 18.84%; ν_{max} (ATR, cm^{-1}) 3450 w br, 3229m br, 3104m, 1616s, 1569m, 1520m, 1502s, 1484s, 1427s, 1409s, 1337w, 1306m, 1248m, 1152w, 1119s, 1091s, 1059s, 1039m, 1014m, 937w, 869w, 826w, 793w, 767s sh, 692m, 622s. Phase purity was confirmed with X-ray powder diffraction.

X-RAY CRYSTALLOGRAPHY

All crystal and diffraction data are given in Table S-I. Single crystal X-ray diffraction data were recorded using a Bruker D8 Quest ECO diffractometer equipped with graphite-monochromated MoKα radiation (λ = 0.71073 Å) and a Photon II C14 pixel array detector. Temperature control was provided with an Oxford Cryosystems Cryostream 800. Crystals were mounted on Mitegen micromounts in NVH immersion oil, and datasets were collected using ϕ and ω scans. Data collection and reduction was controlled with the Bruker APEX-3 suite of programs,[1] and multi-scan absorption corrections were applied using SADABS.[2] The corrected intensity data were solved using the intrinsic phasing routine in SHELXT,[3] and structural models were refined on F^2 with full matrix least-squares procedures in SHELXL,[4] operating within the OLEX-2 GUI.[5] All non-hydrogen atoms were refined anisotropically, while hydrogen atoms were modelled as isotropic and placed in calculated positions, except for those involved in hydrogen bonding which were located from Fourier residuals and refined with distance restraints and U_{iso} dependencies 1.2 or 1.5 times those their carrier atoms. CCDC 2269543-2269546.

Table 1 Crystal and refinement parameters for all structures

Identification code	1	2	3	*poly*-[Cu(**1**)Cl_2]
Empirical formula	$C_{13}H_{11}N_5$	$C_{17}H_{13}N_5$	$C_{17}H_{15}N_5$	$C_{13}H_{11}Cl_2CuN_5$
Formula weight	237.27	287.32	289.34	371.71
Temperature/K	166	150	150	150
Crystal system	monoclinic	monoclinic	monoclinic	orthorhombic
Space group	$P2_1/c$	$P2_1/n$	$P2_1/n$	$P2_12_12_1$
a/Å	17.0143(11)	5.8887(7)	6.1005(3)	7.8301(4)
b/Å	17.1117(10)	8.0233(10)	25.2741(12)	13.5294(6)
c/Å	7.9866(6)	28.779(3)	9.7148(5)	13.7427(6)
α/°	90	90	90	90
β/°	93.538(2)	94.406(3)	104.095(2)	90
γ/°	90	90	90	90
Volume/Å^3	2320.8(3)	1355.7(3)	1452.78(12)	1455.85(12)
Z	8	4	4	4
ρ_{calc}g/cm^3	1.358	1.408	1.323	1.696
2Θ range /°	5.638 to 51.996	5.678 to 51.436	4.614 to 52.946	5.928 to 54.99
Index ranges	$-20 \le h \le 20$, $-20 \le k \le 21$, $-9 \le l \le 9$	$-7 \le h \le 7$, $-9 \le k \le 9$, $-35 \le l \le 35$	$-7 \le h \le 7$, $-31 \le k \le 31$, $-12 \le l \le 10$	$-10 \le h \le 10$, $-17 \le k \le 17$, $-17 \le l \le 14$
Reflections collected	30794	17657	17760	19212
Independent reflections	4542 [R_{int} = 0.0761, R_{sigma} = 0.0513]	2579 [R_{int} = 0.1358, R_{sigma} = 0.0951]	2994 [R_{int} = 0.0574, R_{sigma} = 0.0454]	3346 [R_{int} = 0.0575, R_{sigma} = 0.0467]
Data/restraints/parameters	4542/4/337	2579/1/202	2994/2/205	3346/2/196
Goodness-of-fit on F^2	1.037	1.047	1.06	1.036
Final R indexes [I>=2σ (I)]	R_1 = 0.0572, wR_2 = 0.1309	R_1 = 0.0752, wR_2 = 0.1306	R_1 = 0.0494, wR_2 = 0.0973	R_1 = 0.0327, wR_2 = 0.0663
Final R indexes [all data]	R_1 = 0.0981, wR_2 = 0.1524	R_1 = 0.1424, wR_2 = 0.1529	R_1 = 0.0812, wR_2 = 0.1095	R_1 = 0.0453, wR_2 = 0.0705
Largest peak/hole / e Å^{-3}	0.27/-0.25	0.22/-0.30	0.18/-0.24	0.53/-0.32
Flack Parameter	n/a	n/a	n/a	0.015(9)

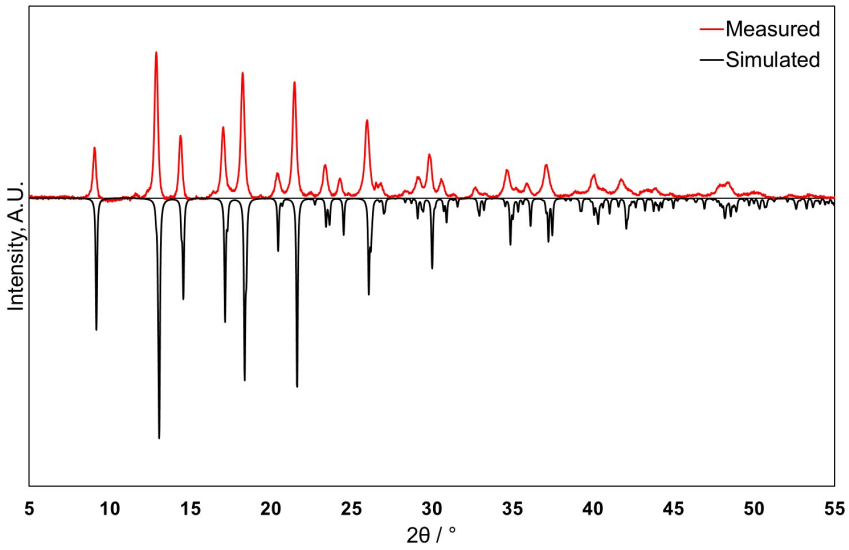

Figure S-1. X-ray powder diffraction pattern for *poly*-[Cu(**1**)Cl_2] comparing the measured data at room temperature (red) to the pattern simulated from the single crystal dataset (black, 150 K).

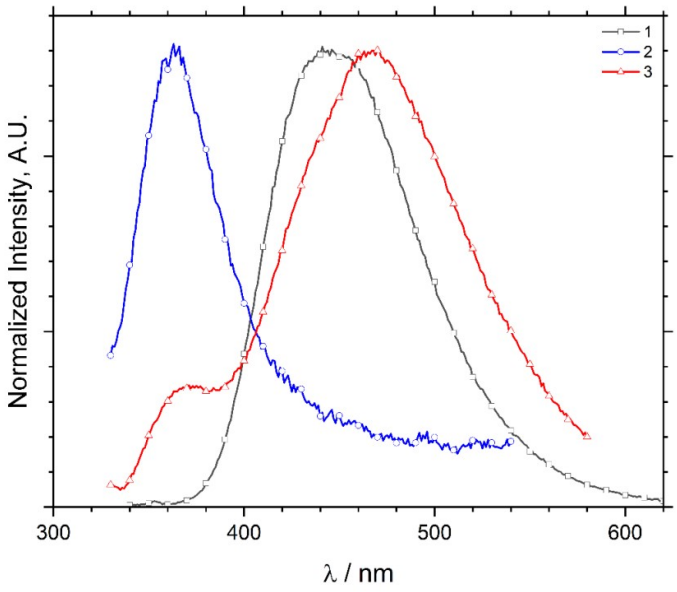

Figure S-2. Normalized emission spectra for compounds **1** (black, 27 μM, λ_{ex} = 318 nm), **2** (blue, 22 μM, λ_{ex} = 286 nm) and **3** (red, 26 μM, λ_{ex} = 300 nm) in MeCN.

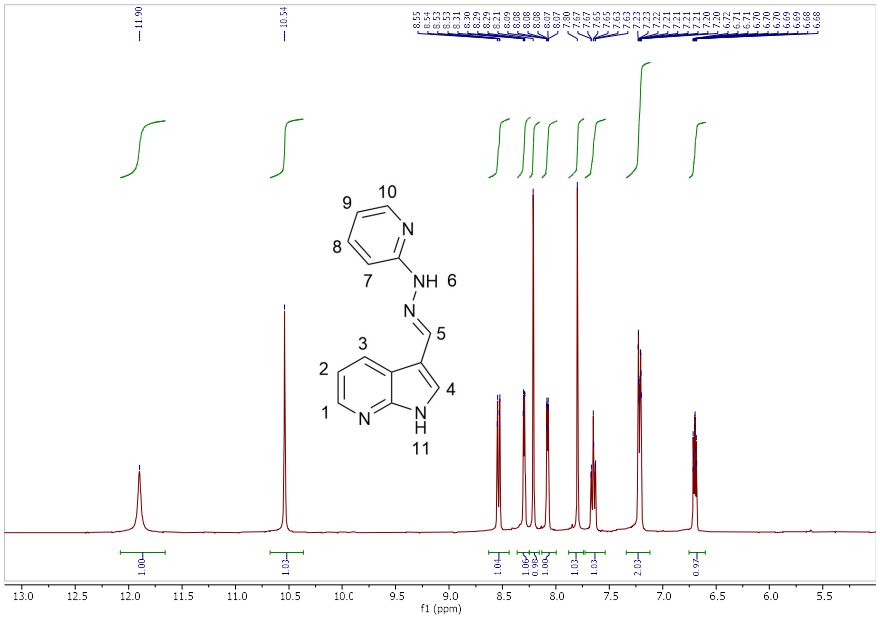

Figure S-3. ^{1}H NMR spectrum (d_6-DMSO, 400 MHz) for compound **1** with proton numbering scheme.

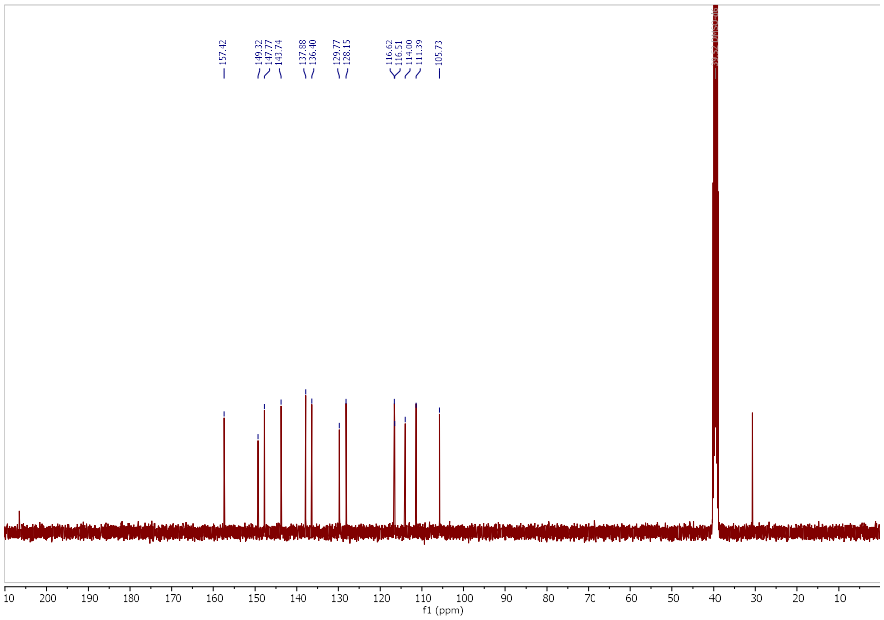

Figure S-4. ^{13}C NMR spectrum (d_6-DMSO, 100 MHz) for compound **1**.

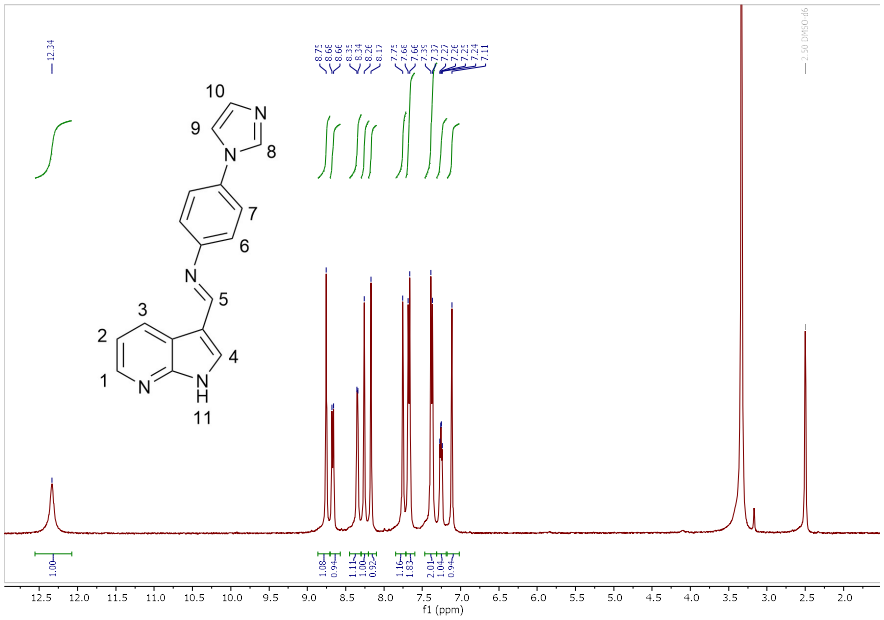

Figure S-5. ^{1}H NMR spectrum (d_6-DMSO, 400 MHz) for compound **2** with proton numbering scheme.

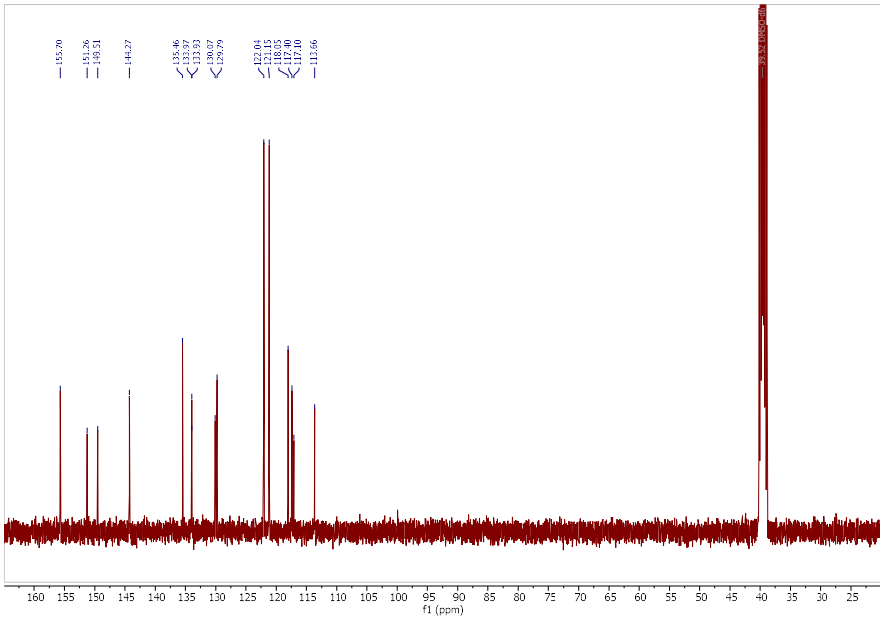

Figure S-6. ^{13}C NMR spectrum (d_6-DMSO, 100 MHz) for compound **2**.

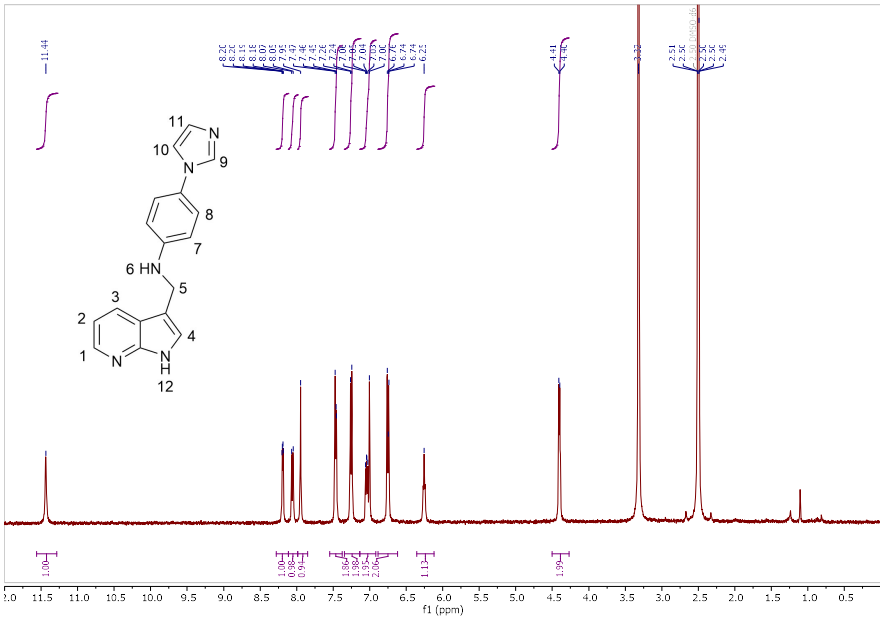

Figure S-7. ^{1}H NMR spectrum (d_6-DMSO, 400 MHz) for compound **3** with proton numbering scheme.

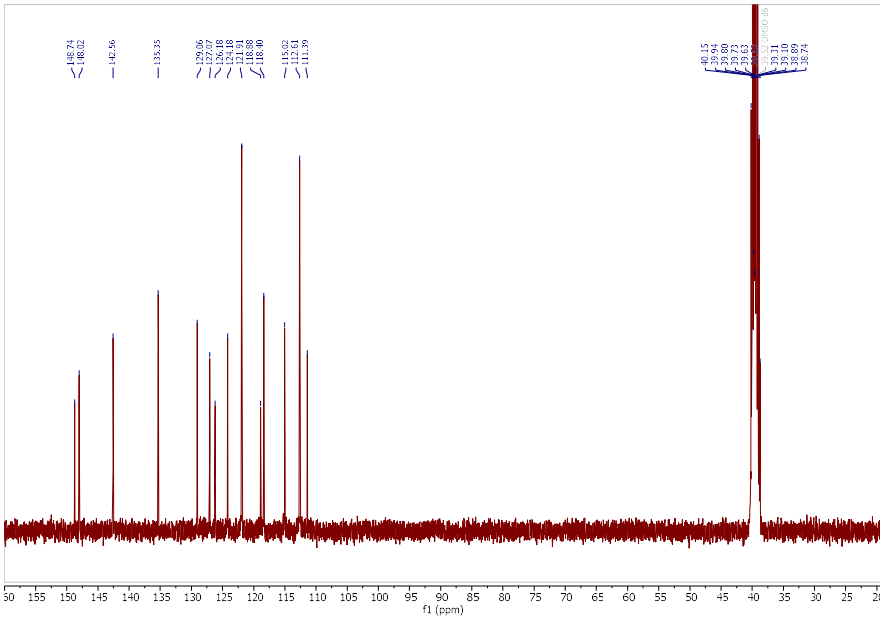

Figure S-8. ^{13}C NMR spectrum (d_6-DMSO, 100 MHz) for compound **3**.

REFERENCES

1. Bruker-AXS *APEX-3,* Bruker-AXS Inc., Madison, WI, 2018
2. Bruker-AXS *SADABS 2016/2,* Bruker-AXS Inc., Madison, WI, 2016
3. G. M. Sheldrick, *Acta. Crystallogr., A* **71** (2015) 3 (https://doi.org/10.1107/S2053273314026370)
4. G. M. Sheldrick, *Acta. Crystallogr., C* **71** (2015) 3 (https://doi.org/10.1107/S2053229614024218)
5. O. V. Dolomanov, L. J. Bourhis, R. J. Gildea, J. A. K. Howard, H. Puschmann, *J. Appl. Crystallogr.* **42** (2009) 339 (https://doi.org/10.1107/S0021889808042726).

Journal of the Serbian Chemical Society
JSCS@tmf.bg.ac.rs • www.shd.org.rs/JSCS
J. Serb. Chem. Soc. *88* (12) 1237–1252 (2023)
JSCS–5692
Original scientific paper
Published 19 December 2023

Spectroscopic and structural characterization of hexaamminecobalt(III) dibromide permanganate

BERTA BARTA HOLLÓ[1#], NILOOFAR BAYAT[2,3], LAURA BERECZKI[2,4], VLADIMIR M. PETRUŠEVSKI[5], KENDE ATTILA BÉRES[2,6], ATTILA FARKAS[7], IMRE MIKLÓS SZILÁGYI[2] and LÁSZLÓ KÓTAI[2,8]*

[1]*Department of Chemistry, Biochemistry and Environmental Protection, Faculty of Sciences, University of Novi Sad, Trg Dositeja Obradovića 3, 21000 Novi Sad, Serbia,* [2]*Institute of Materials and Environmental Chemistry, Research Centre for Natural Sciences, Magyar Tudósok krt. 2., H-1117 Budapest, Hungary,* [3]*Department of Inorganic and Analytical Chemistry, Budapest University of Technology and Economics, Műegyetem rakpart 3, H-1111 Budapest, Hungary,* [4]*Centre for Structural Science, Research Centre for Natural Sciences, Magyar Tudósok krt. 2., H-1117 Budapest, Hungary,* [5]*Faculty of Natural Sciences and Mathematics, Ss. Cyril and Methodius University, Skopje, MK-1000, North Macedonia,* [6]*György Hevesy PhD School of Chemistry, Institute of Chemistry, ELTE Eötvös Loránd University, Pázmány Péter s. 1/A, H-1117 Budapest, Hungary,* [7]*Department of Organic Chemistry and Technology, Budapest University of Technology and Economics, Műegyetem rkp. 3., H-1111, Budapest, Hungary and* [8]*Deuton-X Ltd., Selmeci u. 89, H-2030, Érd, Hungary*

(Received 2 July, revised 11 July, accepted 8 September 2023)

Abstract: Structural and spectroscopic characterization (SXRD, IR, liq. N_2 temperature Raman, UV) of hexaamminecobalt(III) dibromide permanganate, $[Co(NH_3)_6]Br_2(MnO_4)$ (compound **1**), are described. There is a 3D hydrogen bond network including N–H···O–Mn and N–H···Br interactions, which could serve as potential reaction centres for solid-phase redox reactions between the ammonia ligands and/or bromide ions as reductants and permanganate ions as oxidant agents. The effect of the nature of halogen ions on the structural and spectroscopic properties of $[Co(NH_3)_6]Br_2(MnO_4)$ and the analogous chloride compound, $[Co(NH_3)_6]Cl_2(MnO_4)$ (compound **2**), are discussed in detail.

Keywords: permanganate; ammine; cobalt(III); IR and Raman spectroscopy; solid-phase quasi-intramolecular redox reaction.

INTRODUCTION

The preparation and thermal decomposition of transition metal complexes with reducing ligands and oxygen-containing anions are intensively studied areas

* Corresponding author. E-mail: kotai.laszlo@ttk.hu
# Serbian Chemical Society member.
https://doi.org/10.2298/JSC230702062B

of coordination chemistry,[1–5] especially due to the possible quasi-intramolecular redox reactions observed between their reducing ligands and oxidizing anions,[6–10] which result in various simple and mixed nanosized metal oxides, nitrides or alloys.[11–21]

The controlled-temperature thermal decomposition reaction of ammine complexes with permanganate counter ion generally resulted in regular $M^{II}Mn_2O_4$ spinels (M = Cu, Zn, Cd) from divalent and mixed spinels ($M^{II}M^{III}{}_2O_4$, M = = $Co^{II/III}$, $Mn^{II/III}$) from trivalent metals, depending on the decomposition conditions.[6–10] The permanganate salts of the ammonia complexes of cobalt(III) have enormous importance (compound **1**–**3**, Table I) because the mixed Co–Mn oxides formed during their thermal decomposition (*e.g.*, compounds **2**–**4**) were proved to be efficient catalysts in Fischer–Tropsch synthesis and in the photochemical decomposition of toxic dyes (compounds **2** and **4**).[11,12] The Co:Mn mole ratios in the prepared oxides can be adjusted with the Co:permanganate ion ratios in the precursors, *e.g.*, with the use of other counter ions such as carbonate or halides. The presence of halide ions, depending on the chemical form (coordinated or counter-ion) can drastically change the nature of the decomposition products.[12,17] In order to predict the possibility of quasi-intramolecular solid--phase redox reactions, knowing the structural and spectroscopic features of the potential precursors is essential, thus continuing our previous efforts to synthesise, characterise and decompose various halogenide ion-containing ammine complexes of cobalt(III) permanganate,[4,11,12,15,17,21] we have synthesized the poorly characterized hexaamminecobalt(III) dibromide permanganate[22] and discussed its structural and spectroscopic features. The list of compounds used in the evaluation of the properties of compound **1** is given in Table I.

TABLE I. Labels of compounds prepared or evaluated

Compound	Label	Co:Mn ratio	Reference
$[Co(NH_3)_6]Br_2(MnO_4)$	1	1	Present work
$[Co(NH_3)_6]Cl_2(MnO_4)$	2	1	12
$[Co(NH_3)_4CO_3]MnO_4$	3	1	11
$[Co(NH_3)_6](MnO_4)_3$	4	3	12
$[Co(NH_3)_6]Br_3$	5	–	23

EXPERIMENTAL

Chemical-grade cobalt(II) bromide, ammonium bromide, hexachloridoplatinic acid ($H_2PtCl_6{\cdot}6H_2O$), silver nitrate, sodium chromate, or 40, 25 and 37 % aq. sodium permanganate, ammonia and hydrobromic acid solutions, respectively, were supplied by Deuton-X Ltd. (Érd, Hungary).

*Synthesis of compound **1***

Compound **1** was prepared following Klobb's method[22] by a direct combination of 1.00 g of $[Co(NH_4)_3](MnO_4)_3$ and 4.13 g of $[Co(NH_3)_6]Br_3$ in 70 mL of water at 60.0 °C. The mix-

ture was stirred for 15 min and cooled in a refrigerator, where blocks of small strips of crystals were formed at about 1 °C. Then the formed crystals were filtered off and dried in a desiccator at room temperature.

*Preparation of $[Co(NH_3)_6](MnO_4)_3$ (compound **4**) and $[Co(NH_3)_6]Br_3$ (compound **5**)*

$[Co(NH_3)_6]Br_3$ was prepared according to the method of Jörgensen,[23] whereas compound **4** was prepared according to our method.[12]

Analytical methods

The classical analytical and basic instrumental measurements were performed using methods and instruments described in detail in our earlier papers.[1-5] The essential conditions of the measurement methods are listed below.

Elemental analysis. The Co and Mn content of compound **1** was determined by ICP-OES (atomic emission spectroscopy) with a Spectro Genesis ICP-OES instrument (Spectro Analytical Instruments GmbH, Kleve, Germany). A multielement standard (Merck Chemicals GmbH, Darmstadt, Germany) was used for calibration. Bromide content was determined by argentometric titration. The ammonia content was determined by gravimetry in the form of $(NH_4)_2PtCl_6$.

Vibrational spectroscopy. The FT-IR and far-IR spectra of compound **1** were recorded between 4000–400 and 600–100 cm^{-1} ranges in attenuated total reflection (ATR) mode using a BioRad-Digilab FTS-30-FIR and a Bruker Alpha IR spectrometer, respectively.

Raman spectra were measured between 4000 and 200 cm^{-1} on a Horiba Jobin-Yvon LabRAM microspectrometer. An external 532 nm Nd:YAG laser source was used with ~40 mW power and an Olympus BX-40 optical microscope, with an objective of 20× for laser beam focusing. A D2 intensity filter was used to decrease the laser power to 1 %, a confocal hole of 1000 μm, and a monochromator with 1800 groove mm^{-1} (gratings were used for light dispersion). The resolution was 3 cm^{-1}, and the exposure times was 60 s. Due to its sensitivity, the Raman measurement was conducted at 123 K (–150 °C) using a Linkam THMS600 temperature control stage cooled by liquid N_2.

UV–Vis spectroscopy. The room temperature UV–Vis diffuse reflectance spectrum of compound **1** was measured with a Jasco V-670 UV–Vis instrument equipped with an NV-470 integrating sphere ($BaSO_4$ was used as standard).

Powder X-ray diffractometry. Powder X-ray tests were performed with a Philips PW--1050 Bragg–Brentano parafocusing goniometer equipped with a copper cathode (40 kV, 35 mA, secondary beam graphite monochromator, proportional counter). Scans were recorded in the step mode and the diffraction patterns were evaluated with a full profile fitting technique.

Single-crystal X-ray diffraction. A clear red prism-like crystal of $[Co(NH_3)_6]Br_2(MnO_4)$ was mounted on a loop. Cell parameters were determined by the method of least squares using 29943 ($3.080 \leq \theta \leq 30.510$) reflections. Intensity data were collected on a Rigaku R-Axis Rapid diffractometer (monochromator; MoK_α radiation, $\lambda = 0.71073$Å) at 103(2) K. A total of 39290 reflections were collected of which 3727 were unique (R(int) = 0.1132, $R(\sigma) = 0.0438$); intensities of 3309 reflections were greater than $2\sigma(I)$. Completeness to $\theta = 1.000°$. A numerical absorption correction was applied to the data (the minimum and maximum transmission factors were 0.482 and 0.889).

The structure was solved by iterative methods (and subsequent difference syntheses).

Anisotropic full-matrix least-squares refinement on F2 for all non-hydrogen atoms yielded $R_1 = 0.0438$ and $wR_2 = 0.0759$ for 3309 ($I > 2\sigma(I)$) and $R_1 = 0.0531$ and $wR_2 = 0.0783$ for all (3727) intensity data, (number of parameters = 136, goodness-of-fit = 1.188, the max-

imum and mean shift/esd are 0.001 and 0.000, respectively). The maximum and minimum residual electron densities in the final difference map were 0.67 and –0.68 eÅ^{-3}, respectively. The weighting scheme applied was $w=1/(\sigma^2(F_o^2) + (0.0133P)^2 + 3.4263P)$, where $P = (F_o^2 + 2F_c^2)/3$.

Hydrogen atomic positions were calculated from assumed geometries. Hydrogen atoms were included in the structure factor calculation but they were not refined. The isotropic displacement parameters of the hydrogen atoms were approximated from the *U*(eq) value of the atom they were bonded to. CSD Deposition Number is 2277240.

Thermal studies

The DSC curves were recorded between −140 and 25 °C with a Perkin Elmer DSC 7 instrument, with a sample mass of 3–5 mg and a heating rate of 5 °C/min under a continuous nitrogen or oxygen flow (20 cm^3 min^{-1}) in an unsealed aluminium pan.

RESULTS AND DISCUSSION

*Synthesis and properties of compound **1***

Hexaamminecobalt(III) dibromide permanganate (compound **1**) was isolated by Klobb[22] in the reaction (1) of $[Co(NH_3)_6](MnO_4)_3$ (compound **4**) and $[Co(NH_3)_6]Br_3$ (compound **5**) in water at 50 °C in a mole ratio of 1:2:

$$[Co(NH_3)_6](MnO_4)_3 + 2[Co(NH_3)_6]Br_3 \rightarrow 3[Co(NH_3)_6]Br_2(MnO_4) \quad (1)$$

The brilliant purple prisms of compound **1** contrary to the chloride complex (compound **2**) dissolve congruently in water. Repeating the Klobb's experiment, but with concentrated $NaMnO_4$ solution instead of $KMnO_4$ solution, the yield was found to be 84.3 %. The chloride complex (compound **2**) was prepared with 17.6 % yield[12] under similar conditions. The satisfactory yield of compound **1** might be attributed to the higher permanganate concentration in the solution of $NaMnO_4$ than in the concentrated solutions of $KMnO_4$[24] and to the lower solubility of compound **1** (0.32 g/100 mL water) than compound **2** (7.89 g/100 mL of water).[12] Some alternative reaction routes to prepare the permanganate salts[25–28] were also tested but these methods resulted in mixtures of products due to by--reactions of the bromides.

Compound **1** is not soluble in common organic solvents like hexane, benzene, toluene, CCl_4, chloroform, dichloromethane or acetone. $[Co(NH_3)_6]Br_2(MnO_4)$ decomposes at refluxing under xylene (b.p. 140 °C). During the DSC measurement, there was no sign of structural transformation between –140 and 25 °C (Fig. S-1 of the Supplementary material to this paper).

*Structure of compound **1***

Red prismatic single crystals of compound **1** were grown upon slow evaporation of the saturated aqueous solution at room temperature. Some selected crystallographic data of compound **1** based on the refinement results are compared with the data of compound **2** in Table S-I of the Supplementary material.

The structural features of compound **1** are given in Figs. 1–3. The bond distances and angles including the parameters of the hydrogen bond system in compound **1** are given in Tables S-II–S-IV of the Supplementary material. Compound **1** crystallises in the monoclinic system with space group $P2_1/c$ (Nr. 14). The asymmetric unit contains two (different) halves of hexaamminecobalt(III) cation (Fig. 1), and three anions (two bromides and one permanganate). The unit cell contains 4 hexaamminecobalt(III) dibromide permanganate ($Z = 4$).

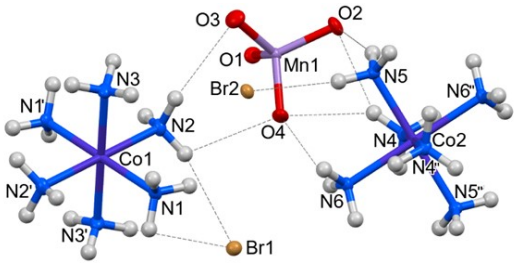

Fig. 1. Structure and labelling of hexaamminecobalt(III) dibromide permanganate, hydrogen bonds are drawn with grey dashed lines (thermal ellipsoids are drawn at the 50 % probability level, symmetry codes to generate equivalent atoms: ': $-x+1,-y+1,-z+1$, ": $-x,-y+1,-z$).

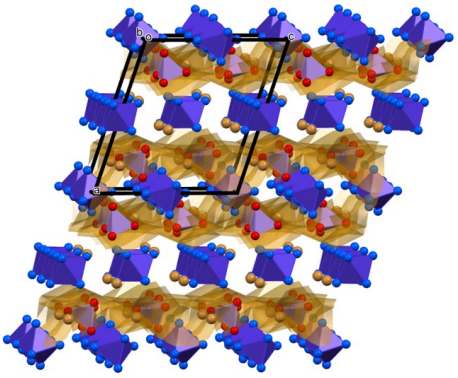

Fig. 2. The unit cell of: $[Co(NH_3)_6]Br_2(MnO_4)$, (polyhedral representation, hydrogen atoms are omitted for clarity, anionic layers are marked with orange shading).

The two different complex cations (labelled as A and B) in compound **1** have distorted octahedral geometries (bond angles ranging between 89.0 and 91.1°, very close to those in compound **2** (89.1 and 91.9°, Fig. 1). Each cation component has three kinds of ammonia ligands. The ammonia ligands in the opposite (axial) positions are equal within both cations A (N1,N1'; N2,N2'; N3,N3') and B (N4,N4"; N5,N5"; N6,N6"). The cations Co–N and anions Mn–O bond distances in compound **1** were found to be 1.957(3)–1.982(3) Å and 1.608–1.627 Å, which values are a little bit shorter than those found in compound **2** (1.949–1.975 Å and 1.605–1.622 Å), respectively.

Direct metal–metal interactions are not present in the structure of compound **1**. The shortest Co–Co, Mn–Mn, and Co–Mn distances are 7.223, 6.922 and 5.032 Å, respectively. The values of 7.198(1), 6.895(1) and 5.011(1) Å were found in compound **2**. The packing arrangement of compound **1** is shown in Fig. 2. The structure is built up of two types of 2D cationic layers in the *bc* plane alternating with anionic layers.

In the first cationic layer, hexaamminecobalt(III) cation A is placed together with Br1 anions whereas the second cationic layer is built up of cation B only (without bromides). The Br2 ions are pushed into the anionic permanganate layers. The anionic permanganate–Br2 layers are in close contact with the cationic B layers. In the layers of cation A, the charge is reduced due to the presence of Br1 anion, and the cation A stays further from the permanganate layers.

A total of 24 hydrogen bonds with various strengths exist between the two kinds of complex cations and the bromideS and permanganates. The ammonia molecules of cation A form three to four and in cation B three to five hydrogen bonds, with the permanganates and bromides. Each bromide has six hydrogen bonds: all the Br1 atom hydrogen bonds are attached to cation A, in addition, two Br1 and four Br2 hydrogen bonds are attached to cation B, too. The Br1 has a bidentate (hydrogen) bonding mode with two ammonia ligands. The cations A and B have 3 and 9 N–H···O (2.937(4)–3.273(4) Å and 2.922(4)–3.243(4) Å) and 8 and 4 N–H···Br (3.402(3)–3.702(3) Å and 3.417(3)–3.704(2) Å) hydrogen bonds, respectively. The summarized number of hydrogen bonds in the cations A and B are equal, 12 in each. The summarized number of hydrogen bonds in the cations A and B are equal, 12 in each. The permanganate oxygens have one bidentate and three tridentate coordination modes. All ammonia ligands of cations A and B are involved in the permanganate hydrogen bonds. The cation A forms altogether 6 hydrogen bonds and the cation B forms 18 hydrogen bonds with the permanganate ions.

The Hirshfeld surface analysis of the two different complex cations supports the structural features characterizing the crystal lattice. The Hirshfeld surface partitions the space between regions where the electron density summed for the atoms of a given molecule surpasses the summed electron density for the remainder of the crystal. 2D fingerprint plots demonstrate best the differences between the two cations. Fingerprint plots were generated for the total interactions of a complex cation and separately for the N–H···O and the N–H···Br interactions. In all cases, the differences are well-marked.

For the cation B, which is embedded in a permanganate anion layer, a spike of N–H···O interactions, marked by the low d_e and d_i values, is visible on the fingerprint plots (Fig. 3d and e) while the spike for the N–H···O interactions for the cation A is missing (Fig. 3b). This shows that while cation *B* has strong interaction with the permanganate anions, cation A is placed further from the

permanganates (the same can also be observed at the H-bond interaction lengths in Table S-III). At the same time, the number of N–H···Br interactions of the cation A is very high (red spike in Fig. 3c). The interaction distances to the bromides, however, are not really different for the two types of cations.

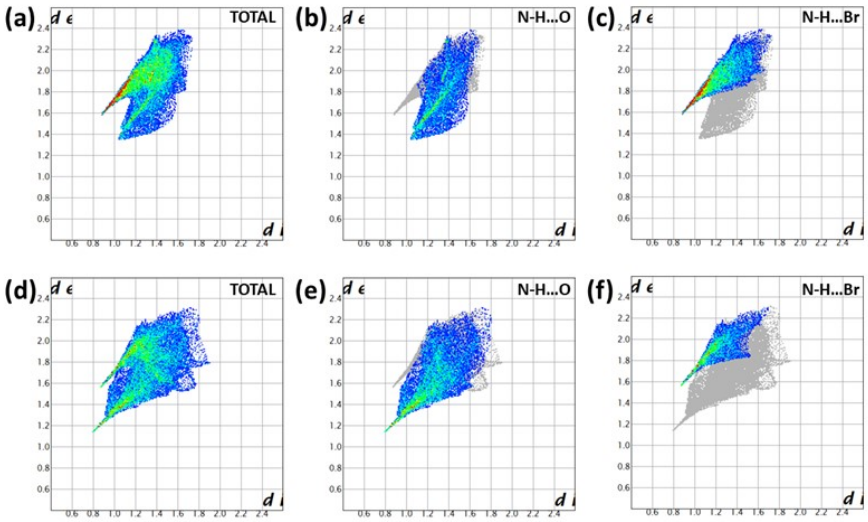

Fig. 3. Fingerprint plots for the two hexaamminecobalt(III) cations: a) total interaction of cation A, b) N–H···O hydrogen bond interactions of cation A, c) N–H···Br hydrogen bonds of cation A, d) intermolecular interactions of cation B, e) NH···O interactions of cation B, f) N–H···Br interactions of cation B; d_i: distance from the Hirshfeld surface to the nearest atom internal to the surface; d_e: distance from the Hirshfeld surface to the nearest atom external to the surface.

*Spectroscopic properties of compound **1***

The factor group analysis results (Figs. 4 and 5), IR and Raman spectra and data (Fig. 6 and Tables II–IV) of compound **1** together with the available spectroscopic data of compound **2** and $[Co(NH_3)_6]^{3+}$have been evaluated in detail.[29–33] The structure of compound **1** in the asymmetric cell was considered to be composed of a central Co^{III} (C_i) cation, two bromides (C_1), six NH_3 molecules (C_1), and one permanganate (C_1). Six (2×3) crystallographically different NH_3 molecules are ligated to the cobalt(III) ion of the two crystallographically different half-cations. Compound **1** is monoclinic ($P2_1/c$) with $Z = 4$, thus a total of 36 internal vibrational modes of the permanganate, 9 of each symmetry species is expected (ν_1 (ν_s) (A) mode, ν_2 (δ_s) (E) mode, and ν_{as} and δ_{as} modes (F_2), respectively, up to 18 bands (9 A_u and 9 B_u) in the IR and the same number (9 A_g and 9 B_g) in the Raman spectra (Fig. 4). The appearance of 12 hindered rotational, and

further 12 hindered translational modes both in the IR (6 A_u and 6 B_u) and Raman (6 A_g and 6 B_g) spectra (Fig. 4) can be expected in the low-frequency part of the spectra.

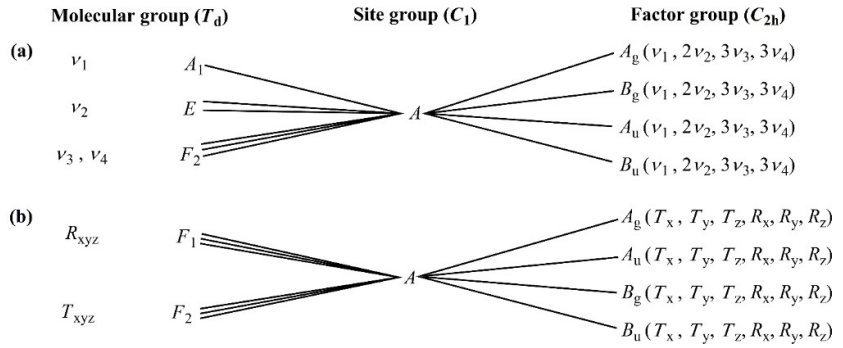

Fig. 4. Internal (a) and external (b) vibrational modes of permanganate ion in compound **1**. ν_1–symmetric stretch.; ν_2–symmetric bend.; ν_3–antisymmetric stretch; ν_4–antisymmetric bend.

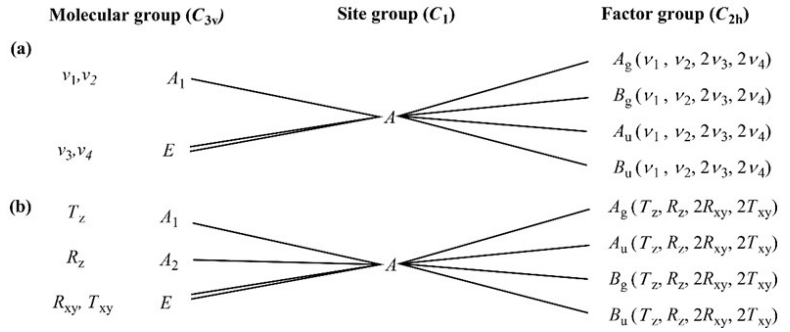

Fig. 5. Internal (a) and external (b) ammonia vibrational modes in compound **1**. ν_1–symmetric stretch.; ν_2–symmetric bend.; ν_3–antisymmetric stretch; ν_4–antisymmetric bend.

Due to the presence of two crystallographically different kinds of Co atoms in compound **1**, the number of translational modes is doubled (2×3 in A_u, and 2×3 in B_u, Fig. S-2).

As the two crystallographically different types of Br ions are at positions of trivial symmetry, the number of modes is also doubled (2×12), thus 6 hindered translations are expected of each symmetry (12 bands in the IR and in the Raman spectra each, Fig. S-3). The six crystallographically different NH_3 molecules are located at positions of trivial symmetry, C_1, thus 12 modes are expected in both the IR (6 A_u and 6 B_u) and the Raman spectra (6 A_g and 6 B_g) (1 ν_1 (ν_s), 1 ν_2 (δ_s) and 2 ν_3 (ν_{as}) and 2 ν_4 (δ_{as}) each) for each crystallographic type of ammonia. The total number of internal vibrations is 6×24 = 144 (Fig. 5). Translations and rotat-

ions along and around an axis, respectively, are given by the lower indices of the axis/axes in question. Due to the six crystallographically different NH_3 molecules, the number of expected modes has to be multiplied by 6, *i.e.*, 6×12 = 72 hindered rotations and 72 hindered translations are expected.

TABLE II. The IR and liq. N_2 temperature Raman spectral data of permanganates in compounds **1** and **2**

Band/assignation	Compound **1**		Compound **2**[12]	
	IR wavenumber, cm^{-1}	Raman shift (532 nm excitation, 130 K) cm^{-1}	IR wavenumber, cm^{-1}	Raman shift (785 nm excitation, 123 K) cm^{-1}
$\nu_1(MnO_4)$, $\nu_s(A)$	834	833	852	843
$\nu_2(MnO_4)$, $\delta_s(E)$	318	348	350	350
$\nu_3(MnO_4)$, $\nu_{as}(F_2)$	922, 896	921,903	924*sh*, 910, 894	927,922,917,912*sh*, 896
$\nu_4(MnO_4)$, $\delta_{as}(F_2)$	388	383	388	398*sh*,393

TABLE III. The IR and liq. N_2 Raman spectral data of the ammonia ligand in compounds **1** and **2**

Band/Assignment	Compound **1**		Compound **2**[12]	
	IR wavenumber, cm^{-1}	Raman shift (532 nm excitation, 130 K) cm^{-1}	IR wavenumber, cm^{-1}	Raman shift (785 nm excitation, 123 K) cm^{-1}
$\rho(NH_3)$	834*	833[a]	813	800
$\delta_s(NH_3)$	1345	325,1310	1340, 1327*sh*	1330, 1323, 1305
$\delta_{as}(NH_3)$	1591	–	1608	–
$\nu_s(NH_3)$	3156	Not measured	3174	Not measured
$\nu_{as}(NH_3)$	3242	Not measured	3256	Not measured

[a]Mixed with $\nu_1(MnO_4)$

TABLE IV. The IR and Raman spectral data of the CoN_6 skeleton in compounds **1** and **2** at 298 K

Band/Assignment	Compound **1**		Compound **2**[12]	
	IR wavenumber, cm^{-1}	Raman shift (532 nm excitation), cm^{-1}	IR wavenumber, cm^{-1}	Raman shift (785 nm excitation), cm^{-1}
$\nu_1(CoN_6)$ ν_s	569, 554, 532*sh*	494	547 (*m*)	507,499
$\nu_2(CoN_6)$ ν_{as}	473,459	-	–	460, 453, 446
$\nu_3(CoN_6)$ ν_s	516, 507, 497,490*sh*	494*	485 (*vw*)	490
$\nu_4(CoN_6)$ δ_{as}	317	323*sh*	317 (*vs*)	320
$\nu_5(CoN_6)$ δ_s		304		311,306
$\nu_6(CoN_6)$ δ	254*sh*	-	254*sh*	–

There are 32 atoms in the formula unit, $Z = 4$, thus it must be multiplied by 4 and by 3 ($3N$, where $N = 32 \times Z = 128$), therefore the total number of rotational

degrees of freedom is altogether 84 (hindered rotations). The total number of internal vibrations and hindered translations in compound **1** is 180 and 120 (72 and 48 for the ammonia ligands and the other parts of the complex), respectively. Three of them are acoustic modes, but the rest (117) are vibrations of translational origin. These give a total number of 384 degrees of freedom.

*Vibrational modes of the permanganate in compound **1***

The IR and Raman spectra of compound **1** are given in Fig. 6 and the band assignments together with those of compound **2** can be seen in Tables II–IV. A singlet symmetric stretching (ν_1), triplet antisymmetric stretching (ν_3) and bending (ν_4) and doublet symmetric deformation (ν_2) modes of permanganates are expected to appear in the IR and Raman spectra. The IR forbidden ν_1 and ν_2 modes are also expected to appear with weak intensities due to the distortion of tetrahedral permanganate ion geometry (Fig. 6).

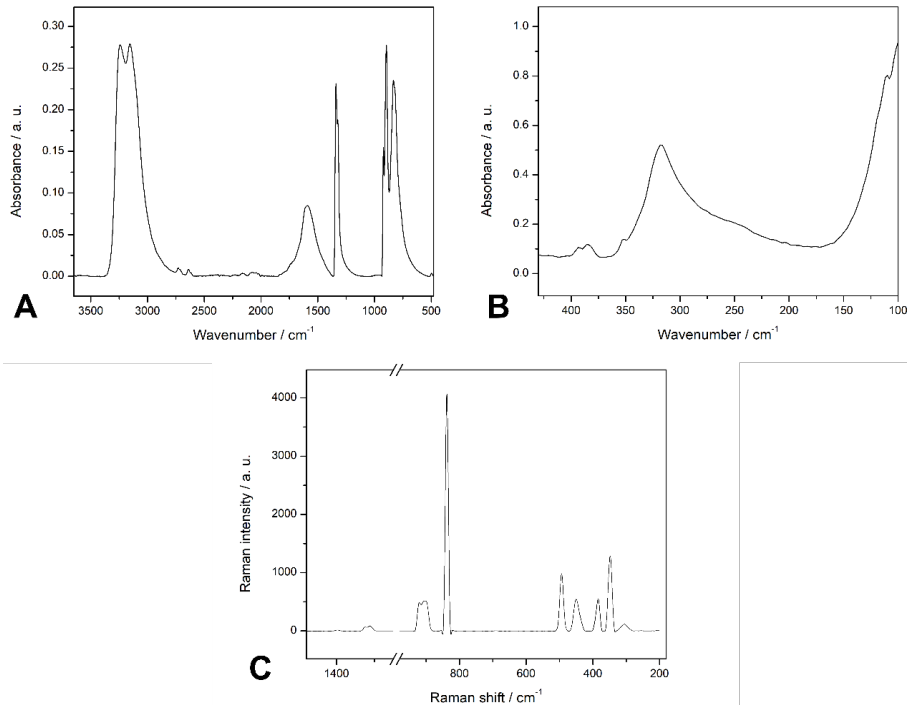

Fig. 6. IR (A), far IR (B) and Raman spectra (C) of compound **1**.

The stretching modes of the permanganate ion in compound **1** appear as a weak singlet at 834 cm^{-1} (ν_s) and as a doublet at 922 and 896 cm^{-1} (ν_{as}), Fig. 6A. The intensity of the band at 834 cm^{-1} shows that the band belongs to the

$\nu_1(MnO_4)$ which is expected to be weak in the IR spectrum and is coinciding with $\rho(NH_3)$. The position of ν_1 is confirmed by the very intense $\nu_1(MnO_4)$ band in the Raman spectrum of compound **1** at 833 cm^{-1} (Fig. 6C) because the $\rho(NH_3)$ is generally weak in the Raman spectra of ammine complexes.[34]

The antisymmetric stretching mode gives the strongest Mn–O band as a doublet in the IR (922, 896 cm^{-1}), and a weak doublet (921, 903 cm^{-1}) in the Raman spectrum of compound **1** (Fig. 6A and C). The two deformation modes of the permanganate ion were found in the far-IR range, δ_s(Mn–O) is a weak band at 318 cm^{-1}, whereas the δ_{as} appeared as a wide band around 388 cm^{-1} (Fig. 6B and C). The IR and Raman bands of permanganate vibrational modes in the IR and Raman spectra of compound **1** are very similar in their positions and intensity to those of the IR and Raman spectra of compound **2**[12] (Table II).

*Vibrational modes of the hexaamminecobalt(III) cation in compound **1***

The correlation analysis of the hexaamminecobalt(III) cation in compound **1** showed two sets of ligand vibrational modes (2×2×3 different ammonia molecules in the two octahedral CoN_6 skeletons). The band assignations of the hexaamminecobalt(III) cation in compound **1** based on normal coordinate analysis, quantum chemical considerations,[29–33] and the recent results on compound **2** are given in Tables III and IV.

The 2×3 crystallographically different NH_3 ligands in each cation type (A and B) resulted in complex band systems for each N–H mode. The band belonging to the symmetric deformation mode appears around 1345 cm^{-1}, thus the relative Co–N bond strength parameter (ε) for the ammonia molecules defined by Grinberg[34] is the same as in compound **2**. Among the vibrational modes belonging to the ammonia ligand, only the rocking mode $\rho(NH_3)$ is sensitive enough to characterise the strength of hydrogen bonds in ammonia complexes.[31] This shows that the average strength of the hydrogen bonds in compound **1** is closer in its strength to $[Co(NH_3)_6]Cl_3$ ($\rho(NH_3)$ = 830 cm^{-1})[31] than that to $[Co(NH_3)_6]Br_3$ ($\rho(NH_3)$ = 830 cm^{-1})[31] or $[Co(NH_3)_6](MnO_4)_3$ ($\rho(NH_3)$ = 803 cm^{-1}).[35]

The CoN_6 octahedron (O_h) has six normal modes, among them three [$\nu_1(\nu(CoN), A_g]$, $\nu_2(\nu_{as}, E_g)$ and $\nu_5(\delta_s, F_{2g})$ are only Raman and two ($\nu_3(\nu_s, F_{1u})$ and $\nu_4(\delta_{as}, F_{1u})$) are only IR active modes. The $\nu_6(\delta(NCoN), F_{2u})$ mode is silent in both IR and Raman spectra. The band positions were determined based on the normal coordinate analysis[29,30,33,36] and the spectroscopic results of compound **2**.[12] The ν_1 mode is singlet, thus the two bands and a shoulder show the separation of $\nu(CoN_6)$ modes in the two different CoN_6 moieties. The well-separated $\nu_3(CoN_6)$ (ν_s) and a singlet of $\nu_4(CoN_6)$ (δ_{as}) appear in the IR spectrum, whereas only three bands, the ν_3–ν_5 modes were found in the Raman spectra. The geometry distortion results in the appearance of the forbidden ν_6 ($\delta(CoN_6)$) band as

well as a shoulder in the IR spectrum around 254 cm^{-1} observed in the IR spectrum of compound **2** as well.[12]

UV–Vis Spectroscopy

The solid phase UV–Vis spectrum of compound **1** can be seen in Fig. S-4. The strongly overlapping absorption bands of four possible d–d transitions of the $[Co(NH_3)_6]^{3+}$ and the CT bands of the permanganate can be observed.[17,37] Co(III) in compound **1** is a low spin cation, the ground state of $[Co(NH_3)_6]^{3+}$ is t_{2g}^6 ($^1A_{1g}$). The excited electron ($t_{2g}^5e_g$) spans with $^3T_{1g}$+$^1T_{1g}$+$^1T_{2g}$+$^3T_{2g}$ terms. The triplet states have lower energies than the singlet ones. As usual, the intensity of spin-allowed transitions (singlet terms) is expected to give weak bands.[38–42] The presence of hydrogen bonds can result in trigonal distortion of the octahedral structure and accordingly to the appearance of new bands.[38] The experimentally found UV–Vis bands' data are given in Table V.

TABLE V. Electronic transitions (in nm) of the hexaamminecobalt(III) cation in compounds **1** and **2** and in octahedral and trigonally distorted (compressed) octahedral structures

Assignment in O symmetry	Assignment in D_3 symmetry	Compound **1**	Compound **2**[12]	$[Co(NH_3)_6]Cl_3$[38]	Calculated DFT (LC-BLYP/6-31G)[38]
$^1A_1 \rightarrow {}^3T_1$	$^1A_1 \rightarrow {}^3E$	805	830	833	806
	$^1A_1 \rightarrow {}^3A_2$				775
$^1A_1 \rightarrow {}^5T_2$	$^1A_1 \rightarrow {}^5E$	676	727	730	740
	$^1A_1 \rightarrow {}^5A_1$				724
$^1A_1 \rightarrow {}^3T_2$	$^1A_1 \rightarrow {}^3E$	600	–	617	613
	$^1A_1 \rightarrow {}^3A_1$	567	575sh	581	585
$^1A_1 \rightarrow {}^1T_1$	$^1A_1 \rightarrow {}^1E$	485	490	486	465
	$^1A_1 \rightarrow {}^1A_2$	419	450	444	459
$^1A_1 \rightarrow {}^1T_2$	$^1A_1 \rightarrow {}^1E$	391	375	367	367
	$^1A_1 \rightarrow {}^1A_1$	352*sh*, 337	343, 330*sh*	324	327

The $^1A_1 \rightarrow {}^1T_1$ and $^1A_1 \rightarrow {}^1T_2$ transitions of the octahedral $Co(NH_3)_6^{3+}$ are spin-allowed, and the hydrogen bonds can cause trigonal distortion (compression) as it was found experimentally in the aq. $[Co(NH_3)_6]Cl_3$ solutions and obtained by the DFT calculations in water–$[Co(NH_3)_6]^{3+}$ systems.[38] The band observed at 253 cm^{-1} as in the case of compound **2** (250 cm^{-1}) may be assigned to the CT band of the cation or to the $^1A_1$–$^1T_2$ ($3t_2$–2e) transition of the permanganate (259 nm for $KMnO_4$). The band at 225 nm (220 nm in the spectrum of compound **2**) may be assigned to the $^1A_1$–$^1T_2$ (t_1–$4t_2$) transition of a permanganate (227 nm for $KMnO_4$).[17] The visible region of the spectrum of compound **1** contains the bands at 510 and 530 nm that might belong to the permanganate $^1A_1$–$^1T_2$ (t_1–2e) transition. The bands at 490 and 551 nm may belong to the permanganate ion. Similar bands were found in the spectrum of $KMnO_4$ at 500 and

562 nm.[17] The band found at 725 nm in the spectrum of compound **2** is shifted to 676 nm, and it probably consists of the $^1A_1$–$^1T_1(t_1$–$2e)$ transition of the permanganate and a component of the $^1A_1 \rightarrow {}^5T_2$ transition of the hexaamminecobalt(III) cation.[12,17] The $^1A_1$–$^1T_1(t_1$–$2e)$ transition of the permanganate was found at 720 nm for $KMnO_4$ and 710 nm for $[Agpy_2]MnO_4$.[2]

In the visible region of spectra, the bands at 510 and 530 nm belong to the permanganate $^1A_1$–$^1T_2$ (t_1–$2e$) transition, whereas the bands at 490 and 551 nm may belong to the permanganate and cation transitions (Table S-VII) as well. A similar band system was found in the UV–Vis spectrum of $KMnO_4$ between 500 and 562 nm.[17] The band at 725 nm is the strongest and probably consists of the $^1A_1$–$^1T_1(t_1$–$2e)$ transition of the permanganate ion and a weak component of the $^1A_1 \rightarrow {}^5T_2$ transition of the complex cation. The $^1A_1$–$^1T_1(t_1$–$2e)$ transition of the permanganate was found at 720 nm for $KMnO_4$ and 710 nm for $[Agpy_2]MnO_4$.[2]

CONCLUSION

We synthesised hexaamminecobalt(III) dibromide permanganate, $[Co(NH_3)_6]Br_2(MnO_4)$ (compound **1**) in the reaction of $[Co(NH_3)_6]Cl_3$ and $[Co(NH_3)_6](MnO_4)_3$. Compound **1** was characterised spectroscopically (FT-IR, far-IR, Raman and UV). Its structure was determined by single-crystal X-ray diffraction. The 3D hydrogen bond network (N–H···O–Mn and N–H···Br interactions) are potential centres of a solid-phase redox reaction between the permanganate and the ammonia ligand. $[Co(NH_3)_6]Br_2(MnO_4)$ decomposes at refluxing under xylene (b.p. 140 °C), thus as a hydrogen bond-containing compound with a low decomposition point is a potential candidate to perform further studies on the existence and reaction products of solid phase heat-induced redox reactions between the cationic and anionic components.

SUPPLEMENTARY MATERIAL

Additional data and information are available electronically at the pages of journal website: https://www.shd-pub.org.rs/index.php/JSCS/article/view/12464, or from the corresponding author on request.

Acknowledgements. The research was supported by the European Union and the State of Hungary, co-financed by the European Regional Development Fund (VEKOP-2.3.2-16-2017--00013) (LK) and the ÚNKP-21-3 and 22-3 New National Excellence Program of the Ministry of Culture and Innovation from the source of the National Research, Development and Innovation Fund (KAB) and the National Research Development and Innovation Office through OTKA grant K124544. BBH thanks the Ministry of Education, Science and Technological Development of the Republic of Serbia (Grant No. 451-03-68/2023-14/200125) for funding.

ИЗВОД

СПЕКТРОСКОПСКА И СТРУКТУРНА КАРАКТЕРИЗАЦИЈА [ХЕКСААММИНКОБАЛТ(III)]-БРОМИД-ПЕРМАНГАНАТА

BERTA BARTA HOLLÓ,[1] NILOOFAR BAYAT,[2,3] LAURA BERECZKI[2,4], VLADIMIR M. PETRUŠEVSKI[5], KENDE ATTILA BÉRES[2,6], ATTILA FARKAS[7], IMRE MIKLÓS SZILÁGYI[2] и LÁSZLÓ KÓTAI[2,8]

[1]Департман за хемију, биохемију и заштиту животне средине, Природно-математички факултет, Универзитет у Новом Сад, Трг Доситеја Обрадовића 3, 21000 Нови Сад, Србија, [2]Institute of Materials and Environmental Chemistry, Research Centre for Natural Sciences, Magyar Tudósok krt. 2., H-1117 Budapest, Hungary, [3]Department of Inorganic and Analytical Chemistry, Budapest University of Technology and Economics, Műegyetem rakpart 3, H-1111 Budapest, Hungary, [4] Centre for Structural Science, Research Centre for Natural Sciences, Magyar Tudósok krt. 2., H-1117 Budapest, Hungary, [5]Faculty of Natural Sciences and Mathematics, Ss. Cyril and Methodius University, Skopje, MK-1000, North Macedonia, [6]György Hevesy PhD School of Chemistry, Institute of Chemistry, ELTE Eötvös Loránd University, Pázmány Péter s. 1/A, H-1117 Budapest, Hungary, [7]Department of Organic Chemistry and Technology, Budapest University of Technology and Economics, Műegyetem rkp. 3., H-1111, Budapest, Hungary, [8]Deuton-X Ltd., Selmeci u. 89, H-2030, Érd, Hungary

У овом раду је описана структурна и спектроскопска карактеризација (дифракција X-зрака на монокристалу, инфрацрвена и Раман спектроскопија на температури течног азота) хексаамминкобалт(III)-бромид-перманганата $[Co(NH_3)_6]Br_2(MnO_4)$ (једињење **1**). Тродимензионална мрежа водоничних веза у једињењу **1** која укључује N–H···O–Mn и N–H···Br интеракције представља потенцијални центар чврстофазне редокс реакције координованог амонијака или бромидних јона као редукујућих и перманганата као оксидујућег агенса. Ефекат природе халогенидног јона на структурна и спектроскопска својства једињења **1**, као и аналогни хлоридни комплекс (једињење **2**) је детаљно дискутован у раду.

(Примљено 2. јула, ревидирано 11. јула, прихваћено 8. септембра 2023)

REFERENCES

1. B. Barta Holló, V. M. Petruševski,G. B. Kovács, F. P. Franguelli, A. Farkas, A. Menyhárd, G. Lendvay, I. E. Sajó, L. Bereczki, R. P. Pawar, E. Bódis, I. M. Szilágyi, L. Kótai, *J. Therm. Anal. Calorim.* **138** (2019)1193 (https://doi.org/10.1007/s10973-019-08663-1)
2. G. B. Kovács, N. V. May, P. A. Bombicz, S. Klébert, P. Németh, A. Menyhárd, G. Novodárszki, V. Petruševski, F. P. Franguelli, J. Magyari, K. Béres, I. M. Szilágyi, L. Kótai, *RSC Adv.* **9** (2019) 28387 (https://doi.org/10.1039/C9RA03230D)
3. K.A. Béres, Z. Homonnay, L. Kvitek, Zs. Dürvanger, M. Kubikova, V. Harmat, F. Szilágyi, Zs. Czégény, P. Németh, L. Bereczki, V.M. Petrusevski, M. Pápai, A. Farkas, L. Kótai, *Inorg. Chem.* **61** (2022) 14403 (https://doi.org/10.1021/acs.inorgchem.2c02265)
4. L. Bereczki, L. A. Fogaca, Zs. Durvanger, V. Harmat, K. Kamarás, G. Németh, B. Barta Holló, V. Petruševski, E. Bódis, A. Farkas, I. M. Szilágyi, L. Kótai, *J. Coord. Chem.* **74** (2021) 2144 (https://doi.org/10.1080/00958972.2021.1953489)
5. V. M. Petruševski, K. A. Béres, P. Bombicz, A. Farkas, L. Kótai, L. Bereczki, *Maced. J. Chem. Chem. Eng.* **41** (2022) 37 (https://doi.org/10.20450/mjcce.2022.2490)
6. F.F. Tao, *Chem. Soc. Rev.* **41** (2012) 7977 (https://doi.org/10.1039/C2CS90093A)
7. L. Kótai, K. K. Banerji, I. Sajó, J. Kristof, B. Sreedhar, S. Holly, G. Keresztury, A. Rockenbauer, *Helv. Chim. Acta* **85** (2002) 2316 (https://doi.org/10.1002/1522-2675(200208)85:8<2316::AID-HLCA2316>3.0.CO;2-A)
8. V. I. Saloutin, Y. O. Edilova, Y. S. Kudyakova, Y. V. Burgart, D. N. Bazhin, *Molecules* **27** (2022) 7894 (https://doi.org/10.3390/molecules27227894)

9. L. Kótai, I. E. Sajó, E. Jakab, G. Keresztury, Cs. Németh, I. Gács, A. Menyhárd, J. Kristóf, L. Hajba, V. Petruševski, V. Ivanovski, D. Timpu, P. L. Sharma, *Z. Anorg. All. Chem.* **638** (2012) 177 (https://doi.org/10.1002/zaac.201100467)
10. I. E. Sajó, L. Kótai, G. Keresztury, I. Gács, Gy. Pokol, J. Kristóf, B. Soptrayanov, V. Petruševski, D. Timpu, P.K. Sharma, *Helv. Chim. Acta* **91** (2008) 1646 (https://doi.org/10.1002/hlca.200890180)
11. M. Mansouri, H. Atashi, F. F. Tabrizi, A. A. Mirzaei, G. Mansouri, *J. Ind. Eng. Chem.* **19** (2013) 1177 (https://doi.org/10.1016/j.jiec.2012.12.015)
12. L. Bereczki, V. M. Petruševski, F. P. Franguelli, K. A. Béres, A. Farkas, B. Barta Holló, Zs. Czégény, I. M. Szilágyi, L. Kótai, *Inorganics* **10** (2022) 252 (https://doi.org/10.3390/inorganics10120252)
13. R. N. Mehrotra, *Inorganics* **11**(2023), 308 (https://doi.org/10.3390/inorganics11070308)
14. L. A. Fogaça, L. Bereczki, V. M. Petruševski, B. Barta Holló, F. P. Franguelli, M. Mohai, K. A. Béres, I. E. Sajó, I. M. Szilágyi, L. Kotai, *Inorganics* **9** (2021) 38 (https://doi.org/10.3390/inorganics9050038)
15. F. P. Franguelli, B. Barta Holló, V. M. Petruševski, I. E. Sajó, S. Klébert, A. Farkas, E. Bódis, I. M. Szilágyi, R. P. Pawar, L. Kótai, *J. Therm. Anal. Calorim.* **145** (2021) 2907 (https://doi.org/10.1007/s10973-020-09991-3)
16. K. A. Béres, I. E. Sajó, G. Lendvay, L. Trif, V. M. Petruševski, B. Barta Holló, L. Korecz, F. P. Franguelli, K. László, I. M. Szilágyi, L. Kótai, *Molecules* **26** (2021) 4022 (https://doi.org/10.3390/molecules26134022)
17. F. P. Franguelli, É. Kováts, Zs. Czégény, L. Bereczki, V. M. Petruševski, B. Barta Holló, K. A. Béres, A. Farkas, I. M. Szilágyi, L. Kótai, *Inorganics* **10** (2022) 18 (https://doi.org/10.3390/inorganics10020018)
18. L. A. Fogaca, É. Kováts, G. Németh, K. Kamarás, K. A. Béres, P. Németh, V. Petruševski, L. Bereczki, B. Barta Holló, I. E. Sajó, I. M. Szilágyi, L. Kótai, *Inorg. Chem.* **60** (2021) 3749 (https://doi.org/10.1021/acs.inorgchem.0c03498)
19. H. E. Solt, P. Németh, M. Mohai, I. E. Sajó, S. Klébert, F. P. Franguelli, L. A. Fogaca, R. P. Pawar, L. Kótai, *ACS Omega* **6** (2021) 1523 (https://doi.org/10.1021/acsomega.0c05301)
20. K. A. Béres, Z. Homonnay, B. Barta Holló, M. Gracheva, V. M. Petruševski, A. Farkas, Zs. Dürvanger, L. Kótai, *J. Mater. Res.* **38** (2023) 1102 (https://doi.org/10.1557/s43578-022-00794-w)
21. K. A. Béres, F. Szilágyi, Z. Homonnay, Zs. Dürvanger, L. Bereczki, L. Trif, V. M. Petruševski, A. Farkas, N. Bayat, L. Kótai, *Inorganics* **11** (2023) 68 (https://doi.org/10.3390/inorganics11020068)
22. T. Klobb, *Bull. Soc. Chim.* **47** (1887) 240
23. S. M. Jörgensen, *J. Prakt. Chem.* **35** (1887) 417
24. L. Kótai, L. Gács, I. E. Sajó, P. K. Sharma, K. K. Banerji, *Trends. Inorg. Chem.* **11** (2011) 25 (10.1002/chin.201113233)
25. L. Kótai, I. E. Sajó, I. Gács, K. S. Pradeep, K. K. Banerji, *Z. Anorg. All. Chem.* **633** (2007) 1257 (https://doi.org/10.1002/zaac.200700142)
26. L. Kótai, K. K. Banerji, *Synth. React. Inorg. Met. Org. Chem.* **31** (2001) 491 (https://doi.org/10.1081/SIM-100002234)
27. L. Kótai, A. Keszler, J. Pató, S. Holly, K. K. Banerji, *Ind. J. Chem., A* **38** (1998) 966 (https://nopr.niscpr.res.in/handle/123456789/15865)
28. T. Klobb, *Bull. Soc. Chim. Paris* **25** (1901) 1022 (https://www.persee.fr/doc/bulmi_0366-3248_1901_num_24_5_2591)

29. Y. Chen, D. H. Christensen, G. O. Sorensen, O. F. Nielsen, E. B. Pedersen, *J. Mol. Struct.* **299** (1993) 61 (https://doi.org/10.1016/0022-2860(93)80283-2)
30. C. Téllez, *Semin., Ciênc. Exatas Tecnol.* **3** (1982) 185 (http://dx.doi.org/10.5433/1679-0367.1982v3n11p185)
31. K. H. Schmidt, A. Müller, *J. Mol Struct.* **22** (1974) 343 (https://doi.org/10.1016/0022-2860(74)85004-0)
32. B. L. Sacconi, A. Sabatini, P. Cans, *Inorg. Chem*. **3** (1964) 1772 (https://doi.org/10.1021/ic50022a026)
33. H. Block, *Trans. Faraday Soc.* **55** (1959) 867 (https://doi.org/10.1039/TF9595500867)
34. A. A. Grinberg, Y. S. Varshavskii, *Primen. Molekul. Spektr. Khim.* **0** (1966) 104
35. E. J. Baran, P. J. Aymonino, *Z. Anorg. Allg. Chem.* **362** (1968) 215 (https://doi.org/10.1002/zaac.19683620312)
36. W. Kiefer, H. J. Bernstein, *Mol. Phys.* **23** (1972) 835 (https://doi.org/10.1080/00268977200100841)
37. P. Hendry, A. Ludi, *Adv. Inorg. Chem.* **35** (1990) 117 (https://doi.org/10.1016/S0898-8838(08)60162-2)
38. H. Sakiyama, Y. Ishiyama, H. Sugawara, *Spectrosc. Lett.* **50** (2017) 111 (https://doi.org/10.1080/00387010.2017.1295272)
39. R. Benedix, H. Hennig, C. Nieke, *Inorg. Chim. Acta* **172** (1990) 109 (https://doi.org/10.1016/S0020-1693(00)80458-2)
40. Y. Mitsutsuka, I. Kondo, M. Nakahara, *Bull. Chem. Soc. Japan* **59** (1986) 2767 (http://pascal-francis.inist.fr/vibad/index.php?action=getRecordDetail&idt=8207253)
41. R. B. Wilson, E. I. Solomon, *J. Am. Chem. Soc.* **102** (1980) 4085 (https://doi.org/10.1021/ja00532a018)
42. R. B. Wilson, E. I. Solomon, *Inorg. Chem.* **17** (1978) 1729 (https://doi.org/10.1021/ja0286371).

Journal of the Serbian Chemical Society
JSCS@tmf.bg.ac.rs • www.shd.org.rs/JSCS
J. Serb. Chem. Soc. *88* (12) S356–S360 (2023) *Supplementary material*

SUPPLEMENTARY MATERIAL TO

Spectroscopic and structural characterization of hexaamminecobalt(III) dibromide permanganate

BERTA BARTA HOLLÓ[1#], NILOOFAR BAYAT[2,3], LAURA BERECZKI[2,4], VLADIMIR M. PETRUŠEVSKI[5], KENDE ATTILA BÉRES[2,6], ATTILA FARKAS[7], IMRE MIKLÓS SZILÁGYI[2] and LÁSZLÓ KÓTAI[2,8]*

[1]Department of Chemistry, Biochemistry and Environmental Protection, Faculty of Sciences, University of Novi Sad, Trg Dositeja Obradovića 3, 21000 Novi Sad, Serbia, [2]Institute of Materials and Environmental Chemistry, Research Centre for Natural Sciences, Magyar Tudósok krt. 2., H-1117 Budapest, Hungary, [3]Department of Inorganic and Analytical Chemistry, Budapest University of Technology and Economics, Műegyetem rakpart 3, H-1111 Budapest, Hungary, [4]Centre for Structural Science, Research Centre for Natural Sciences, Magyar Tudósok krt. 2., H-1117 Budapest, Hungary, [5]Faculty of Natural Sciences and Mathematics, Ss. Cyril and Methodius University, Skopje, MK-1000, North Macedonia, [6]György Hevesy PhD School of Chemistry, Institute of Chemistry, ELTE Eötvös Loránd University, Pázmány Péter s. 1/A, H-1117 Budapest, Hungary, [7]Department of Organic Chemistry and Technology, Budapest University of Technology and Economics, Műegyetem rkp. 3., H-1111, Budapest, Hungary and [8]Deuton-X Ltd., Selmeci u. 89, H-2030, Érd, Hungary

J. Serb. Chem. Soc. *88* (12) (2023) 1237–1252

Table S-I. Crystal data and structure refinement

	$[Co(NH_3)_6]Br_2(MnO_4)$	$[Co(NH_3)_6]Cl_2(MnO_4)$[12]
Empirical formula	$Br_2H_{18}CoMnN_6O_4$	$Cl_2H_{18}CoMnN_6O_4$
Formula weight	439.89	350.97
Temperature	103(2)	163(2)
Radiation and wavelength	Mo-Kα, λ=0.71073Å	Mo-Kα, λ=0.71075Å
Crystal system	monoclinic	Monoclinic
Space group	$P2_1/c$	$P2_1/c$
Unit cell dimensions	a =13.9533(6)Å	a =13.6133(7)Å
	b =7.4499(4)Å	b =7.3658(5)Å
	c =12.3766(7)Å	c =12.3682(6)Å
	α = 90°	α = 90°
	β = 108.453(8)°	β = 108.547(8)°
	γ = 90°	γ = 90°
Volume	1220.41(12)Å^3	1175.78(13)Å^3
Z	4	4
Density (calculated)	2.394 Mg/m^3	1.983 Mg/m^3

* Corresponding author. E-mail: kotai.laszlo@ttk.hu

Absorption coefficient, μ	8.944 mm^{-1}	2.941 mm^{-1}
F(000)	856	712
Crystal color	red	Red
Crystal description	prism	Platelet
Crystal size	0.45 x 0.43 x 0.11 mm	0.56 x 0.41 x 0.11 mm
Absorption correction	numerical	Numerical
Max. and min. transmission	0.4820.889	0.8680.987
θ - range for data collection	$3.078 \le \theta \le 30.504°$	$3.157 \le \theta \le 27.473°$
Index ranges	$-19 \le h \le 19;-10 \le k \le 10;-17 \le l \le 17$	$-17 \le h \le 17;-9 \le k \le 9;-16 \le l \le 15$
Reflections collected	39290	18320
Completeness to 2θ	1.000	1.000
Independent reflections	3727 [*R*(int) =0.1132]	2684 [*R*(int) =0.0588]
Reflections $I>2\sigma(I)$	3309	2351
Refinement method	full-matrix least-squares on F^2	full-matrix least-squares on *F*2
Data/restraints/parameters	3727 /0 /136	2684 /0 /136
Goodness-of-fit on F^2	1.188	1.152
Final *R* indices [$I>2\sigma(I)$]	R_1 =0.0438, wR_2 =0.0759	R_1 =0.0422, wR_2 =0.0854
R indices (all data)	R_1 =0.0531, wR_2 =0.0783	R_1 =0.0528, wR_2 =0.0892

Table S-II. Bond lengths [Å] of compound **1**.

Mn1-O1	1.608(3)		Mn1-O4	1.614(3)
Mn1-O3	1.620(3)		Mn1-O2	1.627(3)
Co1-N1#1	1.958(3)		Co1-N1	1.958(3)
Co1-N2#1	1.960(3)		Co1-N2	1.960(3)
Co1-N3#1	1.965(3)		Co1-N3	1.965(3)
Co2-N4#2	1.957(3)		Co2-N4	1.957(3)
Co2-N5#2	1.962(3)		Co2-N5	1.962(3)
Co2-N6	1.982(3)		Co2-N6#2	1.982(3)

Table S-III. Bond angles [°] of compound **1.**

O1-Mn1-O4	109.3(1)		O1-Mn1-O3	110.3(1)
O4-Mn1-O3	109.9(1)		O1-Mn1-O2	110.1(1)
O4-Mn1-O2	108.5(1)		O3-Mn1-O2	108.8(2)
N1#1-Co1-N1	180.0		N1#1-Co1-N2#1	89.6(1)
N1-Co1-N2#1	90.4(1)		N1#1-Co1-N2	90.4(1)
N1-Co1-N2	89.6(1)		N2#1-Co1-N2	180.0
N1#1-Co1-N3#1	90.3(1)		N1-Co1-N3#1	89.7(1)
N2#1-Co1-N3#1	89.0(1)		N2-Co1-N3#1	91.0(1)
N1#1-Co1-N3	89.7(1)		N1-Co1-N3	90.3(1)
N2#1-Co1-N3	91.0(1)		N2-Co1-N3	89.0(1)
N3#1-Co1-N3	180.0(2)		N4#2-Co2-N4	180.0(2)
N4#2-Co2-N5#2	89.9(1)		N4-Co2-N5#2	90.1(1)
N4#2-Co2-N5	90.1(1)		N4-Co2-N5	89.9(1)
N5#2-Co2-N5	180.0(2)		N4#2-Co2-N6	89.2(1)
N4-Co2-N6	90.8(1)		N5#2-Co2-N6	88.9(1)
N5-Co2-N6	91.1(1)		N4#2-Co2-N6#2	90.8(1)
N4-Co2-N6#2	89.2(1)		N5#2-Co2-N6#2	91.1(1)
N5-Co2-N6#2	88.9(1)		N6-Co2-N6#2	180.00(9)

Symmetry codes to generate equivalent atoms:
1. -x+1,-y+1,-z+1
2. -x,-y+1,-z

Table S-IV. Analysis of Potential Hydrogen Bonds and Schemes with d(D...A) < R(D)+R(A)+0.50, d(H...A) < R(H)+R(A)-0.12 Ang., D-H...A > 100.0 Deg in compound **1.**

Nr	Donor --- H....Acceptor	Symm. op.	D - H	H...A	D...A	D - H...A
1	N1 --H1A ..Br2	x,y,z	0.91	2.87	3.402(3)	119
2	N1 --H1A ..O1	x,1+y,z	0.91	2.45	2.937(4)	113
3	N1 --H1B ..Br1	1-x,1/2+y,1/2-z	0.91	2.57	3.460(3)	165
4	N1 --H1C ..Br1	x,3/2-y,1/2+z	0.91	2.70	3.518(3)	149
5	N2 --H2A ..Br1	x,y,z	0.91	2.66	3.539(3)	164
6	N2 --H2B ..O3	x,y,z	0.91	2.59	3.273(4)	132
7	N2 --H2C ..Br1	1-x,-1/2+y,1/2-z	0.91	2.70	3.513(3)	149
8	N3 --H3A ..Br2	x,y,z	0.91	2.86	3.555(3)	134
9	N3 --H3A ..O1	x,1/2-y,1/2+z	0.91	2.49	2.930(4)	110
10	N3 --H3B ..Br1	1-x,1-y,1-z	0.91	2.62	3.484(3)	159
11	N3 --H3C ..Br1	x,1/2-y,1/2+z	0.91	2.88	3.703(3)	152
12	N4 --H4A ..O2	-x,1-y,-z	0.91	2.37	3.179(4)	149
13	N4 --H4A ..O4	-x,1-y,-z	0.91	2.30	3.070(4)	142
14	N4 --H4B ..O2	x,1+y,z	0.91	2.03	2.922(4)	166
15	N4 --H4C ..O3	-x,1/2+y,1/2-z	0.91	2.14	3.028(4)	165

16	N5	--H5A	..O2	x,y,z	0.91	2.34	3.181(4)	154
17	N5	--H5A	..Br2	-x,-1/2+y,1/2-z	0.91	2.89	3.417(3)	118
18	N5	--H5B	..O2	-x,1/2+y,1/2-z	0.91	2.45	3.120(4)	131
19	N5	--H5B	..O3	-x,1/2+y,1/2-z	0.91	2.38	3.243(4)	159
20	N5	--H5C	..Br2	x,y,z	0.91	2.53	3.423(3)	167
21	N6	--H6A	..Br2	x,3/2-y,-1/2+z	0.91	2.72	3.619(3)	169
22	N6	--H6B	..O4	x,y,z	0.91	2.47	3.163(4)	133
23	N6	--H6C	..Br2	x,y,z	0.91	2.86	3.704(2)	155
24	N6	--H6C	..O1	x,1+y,z	0.91	2.58	3.063(4)	114

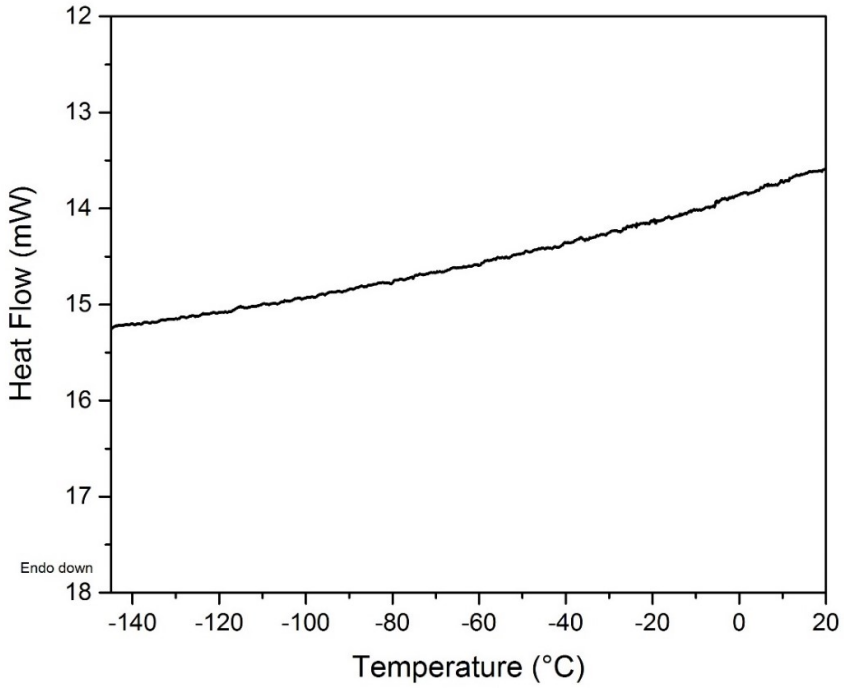

Fig. S-1. The low temperature (between -140 — 25 °C) DSC curve of compound **1**.

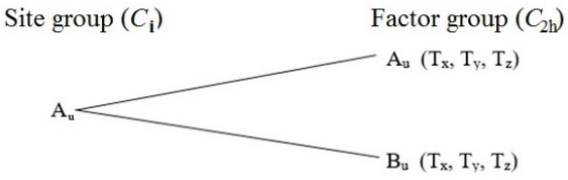

Fig. S-2. The correlation analysis for Co^{III} ions in compound **1**.

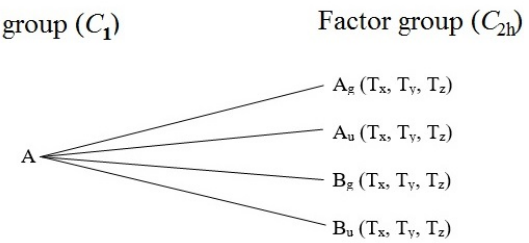

Fig. S-3. The correlation analysis for Br ions in compound **1**.

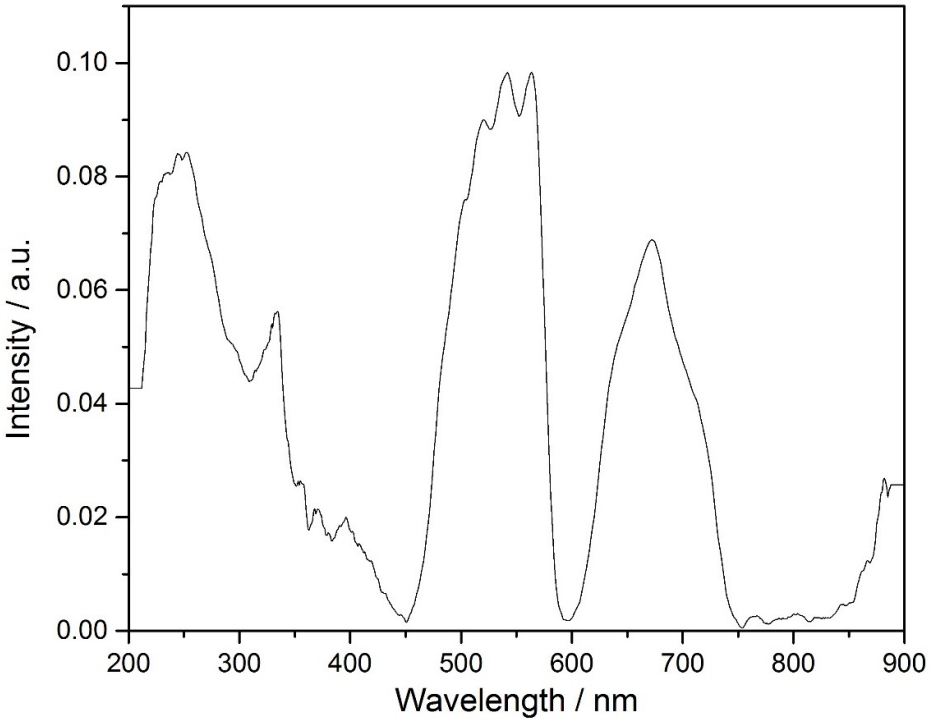

Fig. S-4. The UV-VIS spectra of compound **1**.

Journal of the Serbian Chemical Society
JSCS@tmf.bg.ac.rs • www.shd.org.rs/JSCS
J. Serb. Chem. Soc. *88* (12) 1253–1264 (2023)
JSCS–5693
Original scientific paper
Published 19 December 2023

Synthesis and structural analysis of tetranuclear Zn(II) complex with 2,3-dihydroxybenzaldehyde-aminoguanidine

MARIJANA S. KOSTIĆ[#], MARKO V. RODIĆ*[#], LJILJANA S. VOJINOVIĆ-JEŠIĆ[#] and MIRJANA M. RADANOVIĆ[#]

University of Novi Sad, Faculty of Sciences, Trg Dositeja Obradovića 3, 21000, Novi Sad

(Received 8 August, revised 22 August, accepted 8 September 2023)

Abstract: Here we report a new Schiff base of aminoguanidine and 2,3-dihydroxybenzaldehyde (H_2L) and its physicochemical characterization, along with an investigation into its coordination affinities towards zinc. By reacting zinc acetate with the chloride salt of the ligand in the MeCN–H_2O solution, yellow single-crystals of tetranuclear, centrosymmetric complex, with the formula $[Zn_2(\mu\text{-}L)(\mu\text{-}OAc)_2]_2 \cdot 2MeCN$, were obtained. The complex was characterized by IR spectroscopy, conductometry, elemental analysis, and single-crystal X-ray diffraction analysis. Notably, both nitrogen atoms of the aminoguanidine residue coordinate to the same zinc atom, while both deprotonated phenyl oxygen atoms achieve bridging coordination. Furthermore, two acetate anions bridge adjacent zinc atoms in addition to the Schiff base anion. Meaningful insights into the hierarchy and significance of intermolecular interactions within the crystal structure were gained by estimating the energies using the CrystalExplorer model. The calculations revealed that the crystal structure can be classified as a layer type, with notably stronger interactions occurring along the [001] and [011] directions.

Keywords: Schiff base; guanylhydrazones; acetate coordination; crystal structure.

INTRODUCTION

Schiff bases and their metal complexes represent a large class of compounds interesting from both fundamental and practical points of view,[1] due to their easy synthesis, versatile structural features, and coordination modes, but also the enormous application potential in many different fields. Some of these compounds are good analytical and electroanalytical reagents, precursors in organic synthesis, catalysts, polymer stabilators, *etc*.[2] On the other hand, the others show promising anti-tuberculosis, antimicrobial, anti-inflammatory, and antitumor activities.[3] Additionally, an interest in Schiff bases and their metal complexes and

* Corresponding author. E-mail: marko.rodic@dh.uns.ac.rs
https://doi.org/10.2298/JSC230808067K

their use as organic layers in OLED materials and other emissive organic devices,[4] as well as photosensitizers in dye-sensitized solar cells,[5] has arisen. The steric, electronic and biological potential of the mentioned compounds is tunable by choosing the appropriate amine and carbonyl precursors. One of the always interesting areas of coordination chemistry is the design of novel Schiff bases, especially those with multiple donor sites.[6] Having that in mind, the Schiff bases of 2,3-dihydroxybenzaldehyde seem to be a worthwhile candidate for further research.[7,8]

Zinc is well known for its biocompatibility and versatile importance for the organism.[6] However, the interest in phenoxido-bridged complexes of metals of group 12 was not great, mainly due to the absence of magnetic interactions.[9] Nevertheless, the fact that group 12 metal complexes usually show high photoluminescence, made them interesting for research in the field of optoelectronic devices.[10,11]

Based on the aforementioned, the presented research was designed to gain better insight into the coordination properties of the Schiff bases of aminoguanidine, obtain a phenoxido-bridged complex and characterize it. The Schiff base of aminoguanidine and 2,3-dihydroxybenzaldehyde and its first complex, *viz.* $[Zn_2(\mu\text{-L})(\mu\text{-OAc})_2]_2 \cdot 2MeCN$ are synthesized and physicochemically characterized. The structure of this tetranuclear centrosymmetric complex was determined by SC-XRD, and thoroughly discussed.

EXPERIMENTAL

Reagents

All chemicals used for syntheses and characterization were reagent-grade and used as received from commercial sources, without further purification.

Preparation of the ligand L·HCl – 2,3-dihydroxybenzaldehyde-aminoguanidine hydrogenchloride

2,3-Dihydroxybenzaldehide (25 mmol, 3.45 g) was dissolved in 75 mL H_2O, and 25 mmol (2.75 g) of aminoguanidine hydrogenchloride was added. The resulting mixture was refluxed for 1.5 h during which it completely dissolves. The resulting yellow solution was left at room temperature. After seven days, the yellow product was filtered and washed with H_2O. Yield: 3.50 g (67 %).

Preparation of $[Zn_2(\mu\text{-L})(\mu\text{-OAc})_2]_2 \cdot 2MeCN$

A mixture of 0.5 mmol (0.128 g) of the obtained ligand and 0.5 mmol (0.092 g) $Zn(OAc)_2 \cdot 2H_2O$ was poured over with 6 mL of CH_3CN–H_2O mixture (1:1), heated slightly until dissolved, and the resulting yellow solution was left at room temperature. After two days, yellow prismatic single crystals were filtered and washed with CH_3CN. Yield: 0.088 g (30 %).

Analytical methods

The air-dried compounds were subjected to elemental analyses (C, H, N) using standard micro-methods. Molar conductivity measurements of freshly prepared solutions (c = 1 mmol L^{-1}) were performed on a Jenway 4010 conductivity meter. The IR spectra were recorded on a

Nicolet Nexus 670 FTIR (Thermo Scientific) spectrophotometer in the 400–4000 cm^{-1} range by the KBr pellet technique. Melting points were determined using a Nagema melting point microscope Rapido.

Analytical and spectral data of the synthesized compounds are given in Supplementary material to this paper.

Crystal structure determination

X-ray diffraction data were obtained from a suitable single crystal using an Oxford Diffraction Gemini S diffractometer. The probe used was a graphite-monochromated MoKα X-radiation from a sealed tube. Reflections were recorded on a Sapphire CCD area detector at room temperature. CrysAlisPro was employed for instrument control and raw frames processing.[12] The crystal structure was solved using SHELXT[13] and refined with SHELXL.[14] For graphical user interface, ShelXle was utilized.[15]

During refinement, all non-hydrogen atoms were assigned anisotropic displacement parameters. Carbon-bonded hydrogen atoms were positioned ideally according to parent atom stereochemistry and refined using a riding model with their displacement parameters assumed to be a suitable multiple of the carrier atom's U_{eq}. Nitrogen-bonded hydrogen atoms were identified through residual density maps in the final iterations of the refinement. Their positions were refined with distance restraints, and their displacement parameters were treated similarly to those of hydrogen atoms bonded to carbons. Details are listed in Table S-I of the Supplementary material.

The crystal structure was internally validated using Platon[16] and externally validated against structures with similar fragments in the Cambridge Structural Database (CSD)[17] through the Mogul algorithm[18] implemented in the Mercury CSD.[19]

Interaction energies calculations

Intermolecular energy calculations were employed to examine the crystal packing using CrystalExplorer.[20] Quantum chemistry calculations were performed using TONTO[21] as the backend. A Hirshfeld surface was computed for the complex molecule, and all nearby molecules were taken into account for the pairwise energy calculations. CE-HF model energies were employed.[22]

RESULTS AND DISCUSSION

Syntheses and characterization

Yellow microcrystals of the ligand were obtained in the reaction of an aqueous solution 2,3-dihydroxybenzaldehyde and aminoguanidine hydrogenchloride in a mole ratio of 1:1 under reflux conditions. Subsequently, the obtained ligand was reacted with zinc(II) acetate, in a 1:1 mole ratio in a MeCN–H_2O solution, resulting in the formation of prismatic yellow single crystals of neutral Zn(II) complex of the formula $[Zn_2(\mu\text{-L})(\mu\text{-OAc})_2]_2 \cdot 2MeCN$.

Obtained ligand is well soluble in water, methanol, ethanol, acetonitrile, and dimethylformamide. The complex is well soluble in dimethylformamide, moderately soluble in acetone and methanol, and only sparingly soluble in water, ethanol and acetonitrile. The molar conductivity value of the complex dissolved in DMF (8 S cm^2 mol^{-1}) confirms its non-electrolyte nature.

The ligand is coordinated in its dianionic form as N_2O_2 tetradentate, involving coordination through azomethine and imino nitrogen atoms, and phenolic oxygen atoms. This is primarily assumed by the comparison of the IR spectrum of the complexes with that of the ligand. In the spectrum of the complex, the bands related to the ν(C–N) vibrations in the guanido fragment, as well as the band originating from the azomethine function, display a negative shift of approximately 50 cm^{-1}. Furthermore, the ν(Ar–O) band, present at 1264 cm^{-1} in the ligand's spectrum, experiences a shift to 1250 cm^{-1} in the spectrum of the complex, suggesting coordination of the phenolic oxygen atom.[23] Bands in the region 3600–3000 cm^{-1}, originating from O–H vibrations in the spectrum of the ligand, are absent in the complex' spectrum, indicative of ligand deprotonation. Additionally, bands in the 1460–1400 cm^{-1} region are potentially attributed to ν(O–Ac) vibrations of coordinated acetate ions,[24] although this assignment is challenging due to the presence of numerous other bands in this spectral region in the IR spectrum of the uncomplexed ligand.

Crystal structure description

The molecular structure of the obtained tetranuclear Zn(II) complex is presented in Fig. 1 and key structural data are presented in Table I. The asymmetric unit contains the dianion of the chelate ligand, which is coordinated as ONN tridentate to one zinc atom (Zn1) and monodentate *via* the oxygen atom of the deprotonated hydroxyl group from position 3 to the second zinc atom (Zn2). Additionally, two acetate ions bridge two adjacent units, and a solvent molecule is also present.

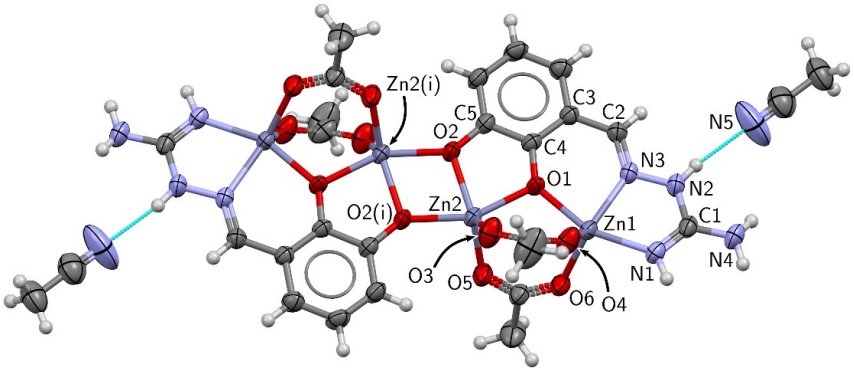

Fig. 1. Molecular structure of the complex formula $[Zn_2(\mu\text{-L})(\mu\text{-OAc})_2]_2 \cdot 2MeCN$. Symmetry operation: (*i*) $-x+1, -y+1, -z$.

The coordination mode of the chelating ligand in this centrosymmetric complex is intriguing and multifaceted. The chelating ligand employs four donor

atoms for coordination (N_2O_2), namely, azomethine and imino nitrogen atoms, and two phenolic oxygen atoms as donors. Both oxygen atoms have a bridging role connecting two zinc atoms. The tridentate ONN coordination of the chelating ligand was achieved through the oxygen atom of the deprotonated hydroxyl group from position 2, and nitrogen atoms from azomethine and imino group from aminoguanidine residue. Except through acetate bridges, neighboring units are connected by bridging coordination of oxygen atoms O1 and O2. The resulting intermetallic distances are 3.3008(4) and 3.1926(4) Å for Zn1···Zn2 and Zn2···Zn2^i, respectively (symmetry operation: (i) $-x+1, -y+1, -z$).

TABLE I. Selected bond lengths and valence angles; symmetry operation: (i) $-x+1, -y+1, -z$

Bond	Bond length, Å	Bonds	Bond angle, °
Zn1–N1	2.024(2)	N1–Zn1–N3	76.12(7)
Zn1–N3	2.183(2)	N1–Zn1–O1	157.36(7)
Zn1–O1	1.993(2)	N3–Zn1–O1	81.36(7)
Zn1–O4	2.013(2)	N3–Zn1–O4	130.30(7)
Zn1-O6	2.033(2)	N3–Zn1–O6	124.41(7)
Zn2–O1	2.053(2)	O1–Zn2–O2	153.86(6)
Zn2–O2	2.007(2)	O1–Zn2–O3	96.99(7)
Zn2–O2^i	2.007(2)	O1–Zn2–O5	94.82(7)
Zn2–O3	1.983(2)	O2–Zn2–O2^i	75.72(6)
Zn2–O5	2.001(1)	O2–Zn2–O3	100.24(7)
Zn1···Zn2	3.3008(4)	O2^i–Zn2–O3	123.28(7)
Zn2···Zn2^i	3.1926(4)	O2–Zn2–O5	98.48(7)
N1–C1	1.293(3)	O2^i–Zn2–O5	129.04(7)
N2–C1	1.357(3)	O3–Zn2–O5	107.64(7)
N3–C2	1.281(3)	N1–C1–N2	118.4(2)
N4–C1	1.350(3)	N1–C1–N4	126.9(2)
C2–C3	1.440(3)	O3–C10–O4	126.6(2)
O1–C4	1.329(2)	O5–C11–O6	126.1(2)
O2–C5	1.333(3)	Bonds	Torsion angle, °
O3–C10	1.248(3)	N1–C1–N2–N3	0.3(3)
O4–C10	1.244(3)	N4–C1–N2–N3	−178.5(2)
O5–C11	1.245(3)	C1–N2–N3–C2	176.4(2)
O6–C11	1.257(3)	N2–N3–C2–C3	−179.4(4)

This coordination of the chelate ligand and acetate ions as coligands to four zinc atoms resulted in the formation of a diverse array of versatile metallocycles. These include four five-membered and two six-membered chelate rings with one metal atom, along with one four-membered, four six-membered, and two eight--membered metallocycles with two metal atoms. All rings containing one metal atom are essentially flat. Of those with two metal atoms, the four-membered ring is planar due to symmetry restriction, while others are significantly puckered.

In this complex, Zn(II) ions, denoted as Zn1 and Zn2, adopt highly deformed N_2O_3 and O_5 environments, respectively. The results obtained from Addison's method[25] and Holmes' method[26–28] show differences in assessing whether the polyhedra centered at Zn1 and Zn2 are closer to the ideal square pyramid with a trans basal angle of 150° (SPY-5) or the ideal trigonal bipyramid (TBPY-5).

In particular, based on the τ_5 values (τ_5 = 0.45 for Zn1 and τ_5 = 0.41 for Zn2), both polyhedra are determined to be closer to SPY-5 than TBPY-5. However, Holmes' method places both polyhedra at 36 % along the Berry pseudorotation coordinate $D_{3h}\rightarrow C_{2v}\rightarrow C_{4v}$. This suggests a closer proximity to TBPY-5, but it also indicates significant deviations from the ideal Berry pseudorotation in both cases.

This later outcome is consistent with the calculations of continuous shape measures,[29] which assign both polyhedrons a closer alignment to TBPY-5 (*S*(TBPY-5) = 2.147 for Zn1; *S*(TBPY-5) = 2.301 for Zn2) than to SPY-5 (*S*(SPY-5) = 3.444 for Zn1; *S*(SPY-5) = 3.255 for Zn2). However, both deformation paths diverge by 42 % from the ideal Berry pseudorotation coordinate which represents minimal distortion pathway in this polyhedral rearrangement.[30]

The coordination environment of Zn1 formally adopts a trigonal-bipyramidal configuration, with the axial positions being occupied by the N1 and O1 atoms of the Schiff base ligand. This arrangement is supplemented by the presence of N3 from the Schiff base ligand, in addition to two oxygen atoms (O4 and O6) derived from bridging acetate ions, collectively constituting the equatorial plane. On the other hand, Zn2 also adopts a trigonal-bipyramidal coordination. In this context, the equatorial plane is formed by the participation of two oxygen atoms (O3 and O5) originating from acetate bridges, along with an O2 moiety sourced from a 2,3-dihydroxybenzaldehyde fragment located in an adjacent subunit. Meanwhile, the axial positions are occupied by the hydroxyl groups of 2,3-dihydroxybenzaldehyde, namely O2 and O1, the latter stemming from the neighboring subunit.

Atom Zn1 forms the longest bond with the N3 donor atom of the azomethine group, and the shortest one with the O1 ligator from the hydroxyl group of 2,3--dihydroxybenzaldehyde. On the other hand, Zn2 forms the longest Zn2–ligand bond with the bridging O1 atom, while the shortest bond is between Zn2 and O3 from the carboxyl group of the acetato ligand. The second oxygen atom from this carboxyl group (O4) forms a slightly longer bond with the first zinc atom, Zn1.

In the aminoguanidine fragment of the ligand, the C2–N3 and C1–N1 bond lengths indicate the presence of localized double bonds, whereas the other bonds in this fragment exhibit intermediate lengths, which can be attributed to electron delocalization, a common feature for this class of compounds.[31] In the 2,3-dihydroxybenzaldehyde part of the chelating ligand, the longest bond observed is C2–C3, which is the bond between the carbon atom of the benzene ring and the carbon

atom of the azomethine group. Remarkably, this C2–C3 bond stands as the longest bond within the entire ligand structure.

Another intriguing feature of this structure is the exo-bidentate coordination of two acetate ligands. The survey of CSD[17] was made to gain further insight into the prevalence of this coordination mode and similar ones involving acetate ligands. The survey revealed that the bridging mode of coordination of two acetate ions in zinc(II) complexes was found in 240 structures. In most instances, these complexes are binuclear, featuring (bis)condensed carbonyl compounds or monodentate ligands. The occurrence of polynuclear complexes with this specific coordination mode of acetate ions is relatively less frequent.

Although the coordination mode presented here is complex, it is not unexpected. It showcases an interesting attribute of the 2,3-dihydroxybenzaldehyde fragment when acetate serves as a bridging coligand, as exemplified in the structure of the tetranuclear complex described in the work.[32]

Upon inspection of the Hirshfeld surface of the complex molecule, 22 nearest neighbors (11 independent pairs) can be identified within the crystal structure. The results of pairwise intermolecular interaction energies calculation are given in Table II. Among these neighbors, 16 are complex molecules, forming 8 independent pairs. Notably, the crystal packing energy landscape is dominated by two pairs, with interaction energies exceeding 100 kJ mol^{-1}. Furthermore, only two more pairs were found to have energy contributions surpassing 15 kJ mol^{-1}.

TABLE II. Summary of important intermolecular interaction energies in the crystal structure of $[Zn_2(\mu\text{-L})(\mu\text{-OAc})_2]_2\cdot 2MeCN$; R is the distance between molecular centroids. $E_{tot} = k_{ele}E_{ele} + k_{pol}E_{pol} + k_{dis}E_{dis} + k_{rep}E_{rep}$, where scale factors for benchmarked CE-HF energy model are $k_{ele} = 1.019$, $k_{pol} = 0.651$, $k_{dis} = 0.901$, and $k_{rep} = 0.811$, as taken from the paper of Thomas *et al.*[33] Symmetry operation correspond to the second molecule in the pair

Label	N	Symmetry operation	R / Å	E / kJ mol^{-1}				
				E_{ele}	E_{pol}	E_{dis}	E_{rep}	E_{tot}
Complex⋯ Complex								
I	2	Translation	15.50	−115.8	−36.9	−41.0	0.0	−178.9
II	2	Translation	11.44	−80.5	−32.2	−82.3	28.6	−153.9
III	2	Translation	9.99	1.6	−14.0	−56.2	27.0	−36.2
IV	2	Translation	8.82	7.4	−10.4	−45.7	18.9	−25.2
V	2	Translation	16.62	−12.4	−2.8	−5.0	0.0	−18.9
VI	2	Translation	14.65	−3.2	−0.8	−5.1	0.0	−8.4
VII	2	Translation	14.61	3.8	−0.6	−5.6	0.0	−1.6
VIII	2	Translation	11.91	10.1	−1.3	−10.5	2.3	1.8
Complex⋯MeCN								
IX	2	Translation	10.68	−59.5	−16.8	−8.6	44.7	−43.1
X	2	Inversion	6.53	−24.4	−4.8	−25.6	10.6	−42.5
XI	2	Inversion	3.60	−12.2	−10.5	−35.2	17.2	−37.0

The strongest intermolecular interaction observed in the crystal structure (–179 kJ mol^{-1}) occurs between complex molecules related by translation (for symmetry codes see Table II). This interaction is predominantly driven by electrostatic forces, which can be attributed to the excellent complementarity in molecular electrostatic potential on the patches of the Hirshfeld surfaces of neighboring molecules (Fig. 2a). The interaction is mediated through N4–H4B···O6(i) hydrogen bond (d(N4–H4B) = 0.853(16) Å, d(H4B···O6(i)) = = 2.154(17) Å, d(N4··· O6(i)) = 2.981(2) Å and α(N4–H4B···O6(i)) = 163(2)°; symmetry operation: (*i*) x, y+1, z+1). Due to centrosymmetric nature of the complex molecule, these interactions occur in pairs, combining to create a 24-membered ring with graph set descriptor $R_2^2(24)$.[34] These interactions then form a chain, that propagates in the [011] direction.

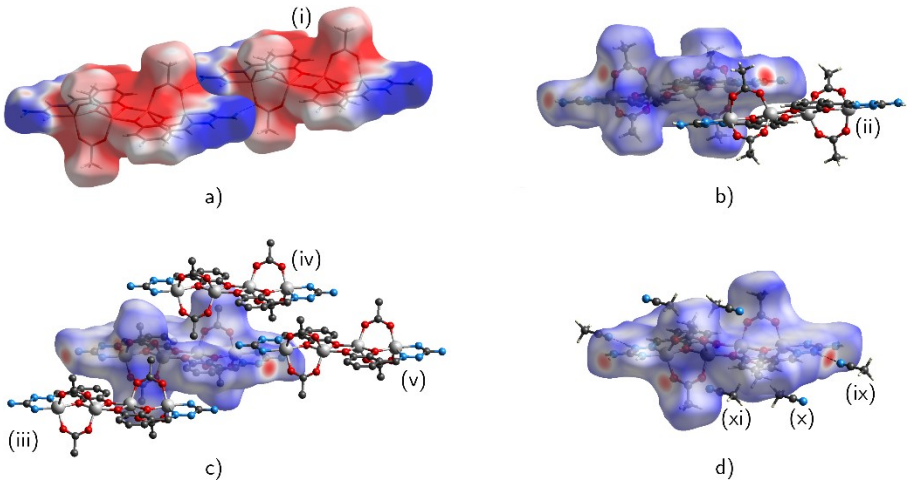

Fig. 2. a) Hirshfeld surfaces of the molecular pair of $[Zn_2(\mu\text{-L})(\mu\text{-OAc})_2]_2$ with strongest interaction, decorated with molecular electrostatic potential in the range from −0.05 a.u. (red) to +0.05 a.u. (blue); b)–d) selected molecules surrounding a central one of $[Zn_2(\mu\text{-L})(\mu\text{-OAc})_2]_2$ with its Hirshfeld surface decorated with d_{norm}. Molecules are labeled as in Table II.

The second strongest interaction (−153 kJ mol^{-1}) has equal contribution of dispersion and electrostatic components, as well as a non-negligible contribution from polarization effects. Notably, no significant atom–atom short contacts can be identified (Fig. 2b), and the detection of this interaction is a direct consequence of the whole-molecule approach to the crystal packing analysis, rather than focusing solely on atom–atom features. These interactions form a chain that propagates along the crystallographic axis *c*.

Only three more interactions are noteworthy (Fig. 2c), as the weakest two make minor contributions to the lattice energy. Specifically, two independent pairs exhibit interaction energies of −36 and −25 kJ mol^{-1}, dominated solely by dispersion forces, with a minor contribution from polarization terms. Interestingly, electrostatic contribution is slightly destabilizing for these interactions. The third pair represents the final one with a notable interaction energy (−19 kJ mol^{-1}), which is predominantly governed by electrostatics. However, due to the considerable separation between the molecules (Cg···Cg distance of 16.6 Å), the interaction is relatively weak. Notably, all three mentioned cases exhibit no significant atom–atom short contacts between the molecules involved.

Surrounding each complex molecule are six MeCN molecules, forming three independent pairs. Only one pair is involved in a hydrogen bond N2–H2···N5 (d(N2–H2) = 0.84(2)Å, d(H2···N5) = 2.04(2)Å, d(N2···N5) = 2.872(5) Å, α(N2–H2···N5) = 169(2)°) with an interaction energy of −43 kJ mol^{-1}, predominantly governed by electrostatic forces. The other two independent pairs have comparable interaction energies (−43 and −37 kJ mol^{-1}), with a significant contribution from dispersion forces and no notable atom–atom short contacts (Fig. 2d).

Overall, from the perspective of energy of the intermolecular interactions, crystal structure can be classified as a layer type, as depicted by an energy framework shown in Fig. 3. Notably, significantly stronger interactions occur along the [001] and [011] directions, with a higher proportion of electrostatic contributions, leading to the observed anisotropy in their distribution.

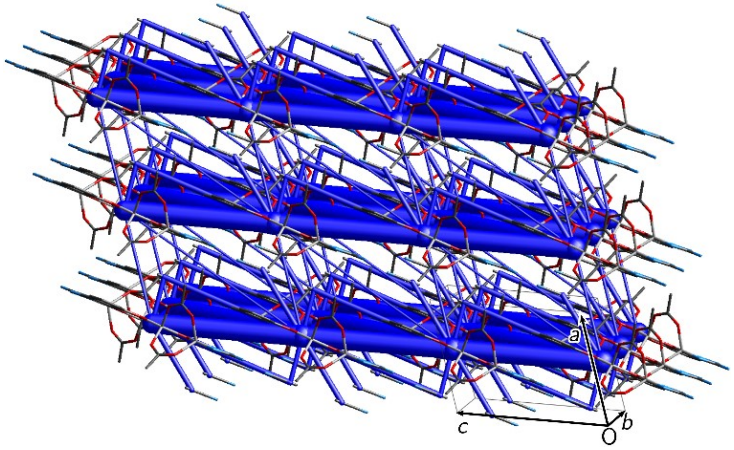

Fig. 3. Energy framework for the crystal structure of [Zn_2(μ-L)(μ-OAc)$_2$]$_2$·2MeCN, represented in a 3×3×3 cells cluster. Total interaction energy is proportional to blue tubes diameter. Only interactions with $-E$ < 15 kJ mol^{-1} are displayed.

CONCLUSION

The yellow microcrystals of the ligand were obtained in the reaction of an aqueous solution 2,3-dihydroxybenzaldehyde and aminoguanidine hydrogenchloride in a mole ratio of 1:1 under reflux conditions, and characterized by IR spectroscopy and elemental analysis. The reaction of the obtained ligand and zinc acetate yielded the formation of yellow single crystals of the tetranuclear complex $[Zn_2(\mu\text{-L})(\mu\text{-OAc})_2]_2\cdot 2MeCN$. This is the first complex with the obtained Schiff base, as well as the first tetranuclear complex with aminoguanidine derivatives. The SC-XRD revealed an interesting coordination mode with two nitrogen and two oxygen atoms of the chelating ligand involved in coordination, with the latter being the bridging ligators, as well. Besides, bidentate bridging coordination of four acetate ions was found. The hierarchy and significance of intermolecular interactions within the crystal structure were calculated and those results showed the crystal structure could be classified as a layer type, with notably stronger interactions occurring along the [001] and [011] directions. The detailed knowledge of the crystal structure and intermolecular interactions present is vital for the design of further research, which is currently being done concerning the optical characteristics, as well as the antioxidant activity of these compounds.

SUPPLEMENTARY MATERIAL

Additional data and information are available electronically at the pages of journal website: https://www.shd-pub.org.rs/index.php/JSCS/article/view/12533, or from the corresponding author on request. CCDC 2285370 contains the supplementary crystallographic data for this paper. These data can be obtained free of charge from The Cambridge Crystallographic Data Centre (https://www.ccdc.cam.ac.uk/structures).

Acknowledgement. The authors gratefully acknowledge the financial support of the Ministry of Science, Technological Development and Innovation of the Republic of Serbia (Grant No. 451-03-47/2023-01/200125).

ИЗВОД

СИНТЕЗА И СТРУКТУРНА АНАЛИЗА ТЕТРАНУКЛЕАРНОГ КОМПЛЕКСА Zn(II) СА 2,3-ДИХИРОКСИБЕНЗАЛДЕХИД-АМИНОГВАНИДИНОМ

МАРИЈАНА С. КОСТИЋ, МАРКО В. РОДИЋ, ЉИЉАНА С. ВОЈИНОВИЋ ЈЕШИЋ и МИРЈАНА М. РАДАНОВИЋ

Универзитет у Новом Саду, Природно-математички факултет, Трг Доситеја Обрадовића 3, 21000 Нови Сад

У овом раду приказана је синтеза и физичкохемијска карактеризација нове Шифове базе аминогванидина и 2,3-дихидроксибензалдехида, као и испитивање координационих својстава добијеног једињења. У реакцији цинк-ацетата и хлоридне соли лиганда у смеши растварача ацетонитрил-вода добијени су жути монокристали тетрануклеарног, центросиметричног комплекса формуле $[Zn_2(\mu\text{-L})(\mu\text{-OAc})_2]_2\cdot 2MeCN$. Комплекс је окарактерисан ИС спектроскопијом, кондуктометријом, елементалном анализом и рендгенском структурном анализом. У добијеном комплексу, оба донорна атома азота аминогванидинског фрагмента координовани су за исти атом цинка, док оба атома кисеоника депротонованих фенолних група имају улогу моста. Осим тога, ацетатни јони

такође остварују мостовну координацију. Испитивање значајних међумолекулских интеракција извршено је проценом енергија уз коришћење CrystalExplorer модела. На основу ових прорачуна може се закључити да се кристална структура може сматрати слојевитом, са значајно јачим интеракцијама дуж [001] и [011] праваца.

(Примљено 8. августа, ревидирано 22. августа, прихваћено 18. септембра 2023)

REFERENCES

1. D. Aggoun, Z. Messasma, B. Bouzerafa, R. Berenguer, E. Morallon, Y. Ouennoughi, A. Ourari, *J. Mol. Struct.* **1231** (2021) 129923 (https://doi.org/10.1016/J.MOLSTRUC.2021.129923)
2. A. Kajal, S. Bala, S. Kamboj, N. Sharma, V. Saini, *Journal of Catalysts* **2013** (2013) 1 (https://doi.org/10.1155/2013/893512)
3. Saswati, M. Mohanty, A. Banerjee, S. Biswal, A. Horn, G. Schenk, K. Brzezinski, E. Sinn, H. Reuter, R. Dinda, *J. Inorg. Biochem.* **203** (2020) 110908 (https://doi.org/10.1016/J.JINORGBIO.2019.110908)
4. M. Barwiolek, D. Jankowska, M. Chorobinski, A. Kaczmarek-Kędziera, I. Łakomska, S. Wojtulewski, T. M. Muzioł, *RSC Adv.* **11** (2021) 24515 (https://doi.org/10.1039/D1RA03096E)
5. P. Mahadevi, S. Sumathi, *Synth. Commun.* **50** (2020) 2237 (https://doi.org/10.1080/00397911.2020.1748200)
6. H. Kargar, M. Fallah-Mehrjardi, R. Behjatmanesh-Ardakani, H. A. Rudbari, A. A. Ardakani, S. Sedighi-Khavidak, K. S. Munawar, M. Ashfaq, M. N. Tahir, *Inorg. Chim. Acta* **530** (2022) 120677 (https://doi.org/10.1016/J.ICA.2021.120677)
7. M. Martínez Belmonte, E. C. Escudero-Adán, E. Martin, A. W. Kleij, *Dalton Transactions* **41** (2012) 5193 (https://doi.org/10.1039/C2DT30201B)
8. B. B. Tang, H. Ma, G. Z. Li, Y. B. Wang, G. Anwar, R. Shi, H. Li, *CrystEngComm* **15** (2013) 8069 (https://doi.org/10.1039/C3CE41034J)
9. R. Biswas, C. Diaz, A. Ghosh, *Polyhedron* **56** (2013) 172 (https://doi.org/10.1016/J.POLY.2013.03.046)
10. J. Adhikary, P. Chakraborty, S. Samanta, E. Zangrando, S. Ghosh, D. Das, *Spectrochim. Acta A Mol Biomol Spectrosc* **178** (2017) 114 (https://doi.org/10.1016/j.saa.2017.01.041)
11. B. Babic, M. Romcevic, M. Gilic, J. Trajic, M. M. Radanović, L. S. Vojinović-Ješić, M. V. Rodić, N. Romcevic, *Opt. Mater. (Amst)* **136** (2023) 113445 (https://doi.org/10.1016/J.OPTMAT.2023.113445)
12. Rigaku Oxford Diffraction, *CrysAlisPro Software system*, Rigaku Corporation, Oxford, 2022
13. G. M. Sheldrick, *Acta Cryst., A* **71** (2015) 3 (https://doi.org/10.1107/S2053273314026370)
14. G. M. Sheldrick, *Acta Cryst. C Struct. Chem.* **71** (2015) 3 (https://doi.org/10.1107/S2053229614024218)
15. C. B. Hübschle, G. M. Sheldrick, B. Dittrich, *J. Appl. Cryst.* **44** (2011) 1281 (https://doi.org/10.1107/S0021889811043202)
16. A. L. Spek, *Acta Cryst. D Biol Cryst.* **65** (2009) 148 (https://doi.org/10.1107/S090744490804362X)
17. C. R. Groom, I. J. Bruno, M. P. Lightfoot, S. C. Ward, *Acta Cryst., B* **72** (2016) 171 (https://doi.org/10.1107/S2052520616003954)

18. I. J. Bruno, J. C. Cole, M. Kessler, J. Luo, W. D. S. Momerwell, L. H. Purkis, B. R. Smith, R. Taylor, R. I. Cooper, S. E. Harris, A. G. Orpen, *J. Chem. Inf. Comp. Sci.* **44** (2004) 2133 (https://doi.org/10.1021/CI049780B)
19. C. F. MacRae, I. Sovago, S. J. Cottrell, P. T. A. Galek, P. McCabe, E. Pidcock, M. Platings, G. P. Shields, J. S. Stevens, M. Towler, P. A. Wood, *J. Appl. Cryst.* **53** (2020) 226 (https://doi.org/10.1107/S1600576719014092)
20. P. R. Spackman, M. J. Turner, J. J. McKinnon, S. K. Wolff, D. J. Grimwood, D. Jayatilaka, M. A. Spackman, *J. Appl. Cryst.* **54** (2021) 1006 (https://doi.org/10.1107/S1600576721002910)
21. D. Jayatilaka, D. J. Grimwood, in *Computational Science — ICCS 2003. ICCS 2003. Lecture Notes in Computer Science*, P. M. A. Sloot, D. Abramson, A. V. Bogdanov, Y. E. Gorbachev, J. J. Z. A. Y. Dongarra, Eds., Springer, Berlin, 2003
22. S. P. Thomas, P. R. Spackman, D. Jayatilaka, M. A. Spackman, *J. Chem. Theor. Comput.* **14** (2018) 1614 (https://doi.org/https://doi.org/10.1021/acs.jctc.7b01200)
23. W. K. Dong, J. Zhang, Y. Zhang, N. Li, *Inorg. Chim. Acta* **444** (2016) 95 (https://doi.org/10.1016/J.ICA.2016.01.034)
24. K. Nakamoto, *Infrared and Raman spectra of inorganic and coordination compounds. Part B, Applications in coordination, organometallic, and bioinorganic chemistry*, Wiley, New York, 2009
25. A. W. Addison, T. N. Rao, J. Reedijk, J. van Rijn, G. C. Verschoor, *J. Chem. Soc., Dalton Trans.* (1984) 1349 (https://doi.org/10.1039/DT9840001349)
26. R. R. Holmes, J. A. Deiters, *J. Am. Chem. Soc.* **99** (1977) 3318 (https://doi.org/10.1021/ja00452a021)
27. R. R. Holmes, *Acc. Chem. Res.* **12** (1979) 257 (https://doi.org/10.1021/ar50139a006)
28. R. R. Holmes, in *Progress in Inorganic Chemistry*, S. J. Lippard, Ed., Wiley, New York, 2007, pp. 119–235 (https://doi.org/10.1002/9780470166338.ch2)
29. M. Pinsky, D. Avnir, *Inorg. Chem.* **37** (1998) 5575 (https://doi.org/doi.org/10.1021/ic9804925)
30. D. Casanova, J. Cirera, M. Llunell, P. Alemany, D. Avnir, S. Alvarez, *J. Am. Chem. Soc.* **126** (2004) 1755 (https://doi.org/10.1021/ja036479n)
31. Lj. S. Vojinović-Ješić, M. M. Radanović, *Coordination chemistry of aminoguanidine and its Schiff bases*, Faculty of Sciences, Novi Sad, 2017 (https://www.pmf.uns.ac.rs/wp-content/uploads/2016/04/vojinovicjesic_radanovic_koordinaciona_hemija_aminogvanidina.pdf) (in Serbian)
32. M. M. Belmonte, E. C. Escudero-Adán, E. Martin, A. W. Kleij, *Dalton Trans.* **41** (2012) 5193 (https://doi.org/10.1039/C2DT30201B)
33. S. P. Thomas, P. R. Spackman, D. Jayatilaka, M. A. Spackman, *J. Chem. Theory Comput.* **14** (2018) 1614 (https://doi.org/10.1021/ACS.JCTC.7B01200)
34. M. C. Etter, J. C. MacDonald, J. Bernstein, *Acta Cryst. B Struct. Sci. Cryst. Eng. Mater.* **46** (1990) 256 (https://doi.org/10.1107/S0108768189012929).

Journal of the Serbian Chemical Society
JSCS@tmf.bg.ac.rs • www.shd.org.rs/JSCS
J. Serb. Chem. Soc. 88 (12) S361–S362 (2023) *Supplementary material*

SUPPLEMENTARY MATERIAL TO

Synthesis and structural analysis of tetranuclear Zn(II) complex with 2,3-dihydroxybenzaldehyde-aminoguanidine

MARIJANA S. KOSTIĆ, MARKO V. RODIĆ*, LJILJANA S. VOJINOVIĆ-JEŠIĆ and MIRJANA M. RADANOVIĆ

University of Novi Sad, Faculty of Sciences, Trg Dositeja Obradovića 3, 21000, Novi Sad

J. Serb. Chem. Soc. 88 (12) (2023) 1253–1264

ANALYTICAL AND SPECTRAL DATA

***L**·HCl – 2,3-dihydroxybenzaldehyde-aminoguanidine hydrogenchloride*

Anal. Calcd. for $C_8H_{11}N_4O_2Cl$: C, 41.67; H, 4.81; N, 24.29 %. Found: C, 41.90; H, 4.81; N, 24.29 %. Mp = 228 °C Selected IR bands [wavenumber, cm^{-1}]: 3308 (s), 3185 (s), 2884 (s), 2802 (s), 1670 (vs), 1624 (vs), 1580 (m), 1491 (m), 1456 (m), 1361 (m), 1264 (s), 1165 (w), 1074 (w), 956 (w), 846 (w).

*$[Zn_2(\mu$-**L**$)(\mu$-OAc$)_2]_2$·2MeCN*

Anal. Calcd. for $C_{28}H_{34}N_{10}O_{12}Zn_4$: C, 34.88; H, 3.53; N, 14.53 %. Found: C, 35.10; H, 3.66; N, 14.32 %. Conductivity, Λ = 8 S cm^2 mol^{-1} (in DMF). Mp > 250 °C. Selected IR bands [wavenumber, cm^{-1}]: 1626 (s), 1573 (vs), 1456 (s), 1427 (s), 1539 (w), 1250 (m), 1216 (m), 1138 (m), 1084 (m), 1030 (w), 953 (w), 865 (w).

Abbreviations used for IR spectra: vs, very strong; s, strong; m, medium; w, weak.

* Corresponding author. E-mail: marko.rodic@dh.uns.ac.rs

TABLE S-I. Crystallographic and refinement details for $[Zn_2(\mu\text{-}L)(\mu\text{-}OAc)_2]_2 \cdot 2MeCN$

Chemical formula	$C_{28}H_{34}N_{10}O_{12}Zn_4$
CCDC No.	2285370
Temperature, K	295(2)
Formula weight, g mol^{-1}	964.21
Crystal system	triclinic
Space group	$P\bar{1}$
a / Å	8.8225(3)
b / Å	9.9872(3)
c / Å	11.4437(4)
α / °	87.645(3)
β / °	70.488(3)
γ / °	78.268(3)
V / Å^3	930.18(5)
Crystal size, mm^3	0.67×0.34×0.16
Reflections collected	15341
Unique reflections	3805
Observed reflections [$I > 2\sigma(I)$]	3426
R_{int}	0.019
R [$I > 2\sigma(I)$]	0.022
R (all data)	0.061
Goodness-of-fit, S	1.071
$\Delta\rho_{max}$, $\Delta\rho_{min}$, e Å^{-3}	0.28 / −0.22

Journal of the Serbian Chemical Society
JSCS@tmf.bg.ac.rs • www.shd.org.rs/JSCS
J. Serb. Chem. Soc. *88* (12) 1265–1278 (2023)
JSCS–5694
Original scientific paper
Published 19 December 2023

Reactions of 2-acetylpyridine-aminoguanidine with Cu(II) under different reaction conditions

MARIJANA S. KOSTIĆ*#, NIKOLA D. RADNOVIĆ#, MARKO V. RODIĆ#, BERTA BARTA HOLLÓ#, LJILJANA S. VOJINOVIĆ-JEŠIĆ# and MIRJANA M. RADANOVIĆ#

University of Novi Sad, Faculty of Sciences, Trg Dositeja Obradovića 3, 21000 Novi Sad, Serbia

(Received 7 July, revised 28 July, accepted 8 September 2023)

Abstract: Aminoguanidine derivatives are the focus of research because of their various biological activities, such as antiviral, antibacterial, analgesic, antioxidant and anticancer. Their complexes with different metals are also examined and many of them show significant biological activity, too. Besides, some of the complexes show good photoluminescent properties and are used for the preparation of photoelectronic devices. Therefore, the synthesis, physicochemical, structural and thermal characterization of the complexes of 2-acetylpyridine-aminoguanidine (L) with copper (II) are described here. Under different reaction conditions, Cu(II) with L gives three complexes of different compositions. By varying the strength of basicity of the deprotonating agent used, it was proven here that the Schiff base given here could be coordinated in neutral or monoanionic form. In the presence of pyridine, a coordination polymer is obtained, while in the presence of ammonia/lithium acetate two different monomeric complexes were crystallised. Their physicochemical and thermal properties, as well as molecular and crystal structure, are determined.

Keywords: Schiff base; Cu complex; synthesis; crystal structure; thermal decomposition; structural characterization.

INTRODUCTION

Aminoguanidine was used as a drug for the treatment of diabetic complications, *i.e.* kidney disease, due to its ability to lower the level of advanced glycation end products.[1] However, some serious side effects were present, thus its Schiff bases were suggested as more suitable for the application.[2,3] Since the chelation, *i.e.*, the metal centre could have a positive effect on the biological activities of Schiff bases,[4] it is not surprising that the metal complexes with these ligands are widely studied.[5,6] Some of them were found to express various bio-

* Corresponding author. E-mail: marijana.kostic@dh.uns.ac.rs
# Serbian Chemical Society member.
https://doi.org/10.2298/JSC230707060K

logical effects, such as antiviral, antibacterial, analgesic, antioxidant, and even anticancer activity.[7] On the other hand, some of the complexes showed high photoluminescence and were used for the preparation of optoelectronic devices.[8]

The examination of the crystal structure of metal complexes with aminoguanidine Schiff bases started with the work of Leovac et al.[9] and since then numerous complexes were synthesised, characterised, and their possible applications investigated.[10–13]

Among the mentioned Schiff bases, 2-acetylpyridine-aminoguanidine (L) stands out, due to its ability to achieve different coordination modes in the complexes. Namely, depending on the synthetic conditions, this Schiff base could be coordinated or have a role of the counterion.[14] Nonetheless, if coordinated it could act as a tridentate ligand if in its neutral form,[13] or the bidentate ligand if in its monoprotonated form.[12] Since the well-known alkaline nature of the aminoguanidine residue, as well as the fact that the guanidinium group is found in proteins and at physiological pH is protonated, it is of interest to examine the conditions for its deprotonation and the influence of the different substituents attached to it.

Hence, in this paper, three new complexes of copper(II), of which one polymeric cationic $\{[Cu(L)(\mu\text{-}Cl)]NO_3\cdot 0.25H_2O\}_n$ (**1**), and two neutral complexes [Cu(L–H)Cl] (**2**) and $[Cu(L)ClNO_3]\cdot H_2O$ (**3**) were synthetized, and their physicochemical and thermal properties, as well as molecular and crystal structure were determined.

EXPERIMENTAL

Reagents

All chemicals used for synthesis and characterization were reagent-grade and used as received from commercial sources, without further purification, except for the ligand 2-acetylpyridine-aminoguanidine dihydrogendichloride, $[H_2L]Cl_2$, which was prepared according to the previously published procedure.[10]

Preparation of the complex $\{[Cu(L)(\mu\text{-}Cl)]NO_3\cdot 0.25H_2O\}_n$ (1)

To the warm solution of 0.25 mmol (0.063 g) $[H_2L]Cl_2$ in 5 mL H_2O, 0.25 mmol (0.06 g) $Cu(NO_3)_2\cdot 3H_2O$ and 0.5 mL pyridine were added. The mixture was slightly heated until dissolution. The resulting green solution was left at room temperature and after 7 days, green single crystals were filtered and washed with H_2O and EtOH. Yield: 0.064 g (70 %). The same complex was obtained in the reaction of the metal salt (0.25 mmol) dissolved in H_2O (3 mL), and the ligand (0.25 mmol) was dissolved in MeOH (5 mL).

Preparation of the complex [Cu(L–H)Cl] (2)

The warm solution of 0.25 mmol (0.06 g) $Cu(NO_3)_2\cdot 3H_2O$ in 3 mL MeOH was added to a warm solution of 0.25 mmol (0.063 g) $[H_2L]Cl_2$ in 5 mL MeOH, in the presence of the few drops of ammonia. The mixture was mildly heated until dissolution. The resulting solution was left at room temperature and after 7 days brown single crystals were filtered and washed with MeOH. Yield: 0.051 g (71 %).

*Preparation of the complex [Cu(L)ClNO$_3$]·H$_2$O (**3**)*

The warm solution of 0.25 mmol (0.06 g) Cu(NO$_3$)$_2$·3H$_2$O in 2 mL H$_2$O was added to the warm solution of 0.25 mmol (0.063 g) [H$_2$L]Cl$_2$ in 5 mL MeOH, in the presence of the lithium acetate (0.5 mmol, 0.05g). The mixture was slightly heated until dissolution. The resulting dark green solution was left at room temperature and after 7 days blue crystals were filtered and washed with MeOH. Yield: 0.056 g (63 %).

Analytical methods

Elemental analyses (C, H, N) of air-dried compounds were carried out by standard micro-methods. Molar conductivity measurements of freshly prepared solutions (c = 1 mmol L^{-1}) were performed on a Jenway 4010 conductivity meter. IR spectra were recorded on a Thermo Nicolet iS20 FTIR spectrophotometer (Thermo Fisher Scientific) with Smart iTR™ ATR sampling accessories, in a range of 4000–400 cm^{-1}. Thermal data were collected using TA Instruments SDT Q600 thermal analyser coupled to Hiden Analytical HPR20/QIC mass spectrometer. The decomposition was followed from room temperature to 700 °C at a 10 °C min^{-1} heating rate in the argon carrier gas (flow rate = 50 cm^3 min^{-1}). Sample holder/reference: alumina crucible/empty alumina crucible. Sample mass 2.5–3 mg. Selected ions between m/z 1 and 93 through the TG–MS measurements were monitored in multiple ion detection mode (MID).

Single crystal X-ray diffraction

Crystallographic and refinement details are listed in Table S-I of the Supplementary material. All data were collected at room temperature. Crystal structures were solved using the iterative dual-space routine within SHELXT[15] and refined with SHELXL[16]. All non-hydrogen atoms were refined anisotropically, while hydrogen atoms were placed in idealized positions and refined using a riding model.

The presence of water molecule in **1** was confirmed by TGA which matches with the occupancy factor of oxygen that was constrained to 0.25. Hydrogen atoms bonded to O4 in **1** could not be located in the residual density map due to low occupancy.

The final structures underwent internal validation using Platon[17] and external validation using the Cambridge Structural Database (CSD)[18] *via* the Mogul[19] knowledge bases accessible through Mercury CSD.[20]

Analytical and spectral data of the synthesized compounds are given in Supplementary material to this paper.

RESULTS AND DISCUSSION

Syntheses and characterization

The Cu(II) complexes **1**–**3** were obtained in the reaction of the warm solutions of the chloride salt of the ligand and copper(II) nitrate, in a mole ratio of 1:1 in the presence of the deprotonating agent (Scheme 1). The latter was pyridine in the case of complex **1**, ammonia for **2** and lithium acetate for **3**, and was used to deprotonate the Schiff base and enable its coordination. Depending on the strength of the base used as a deprotonating agent, three new complexes with two different degrees of deprotonation of the chelating ligand were isolated. Namely, when pyridine and lithium-acetate were used, the ligand was coordinated in its neutral, and, so far, the most common form.[12] On the contrary, when ammonia

was used, the monoanion of the ligand was coordinated. Since ammonia is a stronger base than pyridine and acetate ions, this is not surprising. The synthesis of complex **1** could be also carried out from the mixture of MeOH and H_2O. It is interesting to mention that the compound in which the monoanion of the ligand is coordinated (**2**) was also obtained during syntheses from methanolic solutions of copper (II) nitrate and chloride salt of the ligand, in the presence of Na_2CO_3 and KOH as diprotonation agents (proven by the results of elemental analysis and IR spectra), which was expected considering the strength of their basicity.

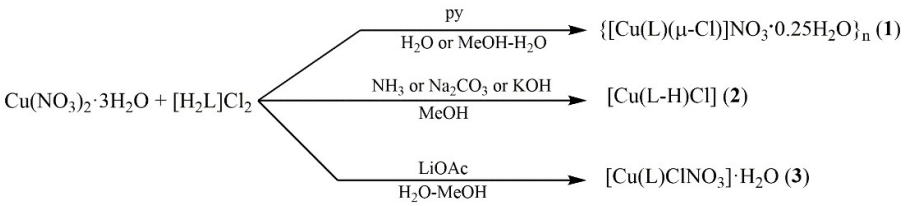

Scheme 1. Synthesis of the complexes.

All three compounds are well soluble in DMF. Complexes **1** and **3** are well soluble in water, as well, while complex **2** is insoluble in this solvent. Methanol dissolves complex **1** well, and the other two complexes moderately, and all three compounds dissolve poorly in ethanol. The molar conductivity values indicate that complex **1** is a 1:1 type electrolyte, thus the polymeric structure is lost. The value of molar conductivity of complex **3** is between 1:1 and 2:1 type electrolytes, which indicates the partial substitution of anionic ligands with solvent molecules. The molar conductivity measurements confirm the non-electrolytic nature of complex **2**.

The ligand coordinates as NNN-tridentate, *via* pyridine, azomethine and the imine nitrogen atom of the aminoguanidine residue, which is primarily assumed by the comparison of IR spectra of the complexes with the spectrum of the ligand. Due to the coordination, ν(CN) band originating from the azomethine group (found at 1684 cm^{-1} in the ligand spectrum) suffers a negative shift of *ca*. 35–40 cm^{-1}. Similarly, the band ascribed to the imine group of the aminoguanidine fragment was shifted from 1624 cm^{-1} (in the ligand spectrum) to 1595–1603 cm^{-1} (in the spectra of the complexes). A band of weak intensity that can be observed in the spectra of complexes, at 647 (**1**), 640 (**2**) and 645 cm^{-1} (**3**), may be assigned as the vibrations of the pyridine ring and confirm its coordination through the nitrogen atom.[10] Also, in the spectrum of **1**, another significant band at 1385 cm^{-1}, recognizable by its very strong intensity, originates from the uncoordinated NO_3^-. On the contrary, in complex **3**, the band occurring at 1299 cm^{-1} originates from the monodentate coordinated nitrate.[21]

Crystal structure description

The molecular structures of all three complexes are presented in Fig. 1, while the selected structural data are summarized in Table I. In all three structures the usual, tridentate coordination mode of the Schiff base, *i.e.*, through pyridine N5, azomethine N3 and imine N1 nitrogen atom of the aminoguanidine residue was found. This coordination mode resulted in the formation of two five--membered chelate rings, one of 2-acetylpyridine and one of aminoguanidine moiety (Fig. 1). In compounds **1** and **3** the ligand is present in its neutral form, and in compound **2** the ligand is present in its monodeprotonated form (deprotonation of the chelate ligand occurs on the hydrazine nitrogen atom N2).

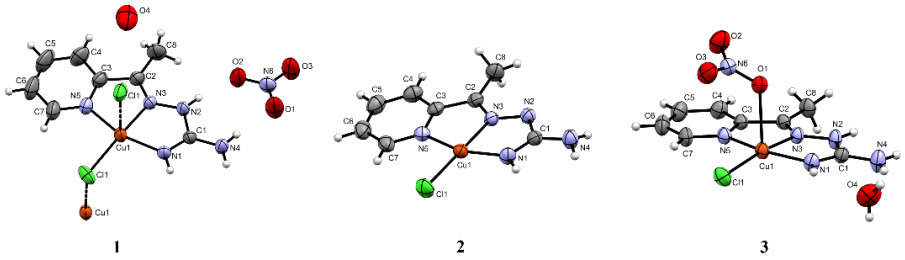

Fig. 1. Molecular structures of complexes **1**–**3**.

In complex **1**, copper (II) is situated in the square-pyramidal environment of the NNN-coordinated chelate ligand, and one chlorido bridge in the basal plane, and another chlorido bridge in the apical position. Deviation from the ideal square-pyramidal geometry, *i.e.*, the deformation towards trigonal-bypiramide, can be described by τ_5 parameter,[22] which for this compound has a value of 0.22 (the square-pyramidal environment of the copper(II) is moderately deformed). The copper (II) ion is shifted from the equatorial plane towards the apical ligand by 0.1159(9) Å. Of the two chlorido ligands, the equatorial one, forms the shorter bond with copper (II), while the apical one is much further away (by even more than 0.6 Å). It is important to mention that complex **1** is the first coordination polymer with this ligand. The monomer units are bridged by chlorido ligands and the Cu···Cu atom separation is 3.742(2) Å. The angle that the copper(II) atom from one subunit subtends with the copper(II) atom from another unit *via* the chlorido ion as a bridge between these subunits (Cl1–Cu1–Cl1^i, Table I) has the value of 97.28(3)°.

In complex **2**, the ligand is coordinated as a monoanion. Copper(II) is placed in the square-planar environment of three nitrogen donor atoms of the ligand and one chlorido ligand. Deviation of this geometry towards tetrahedral is described by τ_4 parameter,[23] which for complex **2** equals 0.16. As in structure **1**, the coor-

dination of Schiff base resulted in the formation of two five-membered chelate rings.

TABLE I. Selected bond lengths and bond angles; Symmetry operation: (*i*) *x*, −*y*+3/2, *z*+1/2

Bond	**1**	**2**	**3**
	Bond length, Å		
Cu1–N1	1.9340(19)	1.9130(17)	1.9393(12)
Cu1–N3	1.9713(19)	1.9523(14)	1.9665(11)
Cu1–N5	2.015(2)	2.0092(16)	2.0177(12)
Cu1–Cl1	2.2372(7)	2.2227(5)	2.2165(4)
Cu1–Cl1^{i}	2.8525(7)	-	-
Cu1–O1	-	-	2.4604(12)
N1–C1	1.298(3)	1.317(2)	1.2954(19)
N4–C1	1.322(3)	1.348(2)	1.3315(19)
N2–C1	1.375(3)	1.364(2)	1.3757(19)
N2–N3	1.352(3)	1.356(2)	1.3573(16)
C2–N3	1.279(3)	1.293(2)	1.2808(17)
Bonds		Bond angle, °	
Cl1–Cu1–N3	172.33(6)	178.64(5)	171.20(4)
N1–Cu1–N5	158.25(9)	159.80(6)	158.37(5)
N1–Cu1–N3	79.87(8)	79.47(6)	79.83(5)
N3–Cu1–N5	78.73(8)	80.34(6)	78.78(5)
N3–Cu1–O1	–	–	92.17(4)
N3–N2–C1	113.31(18)	107.77(14)	113.32(11)
N1–C1–N4	126.6(2)	123.33(17)	126.46(14)
N2–C1–N1	117.1(2)	121.41(17)	117.14(12)
C3–N5–C7	119.2(2)	119.05(17)	119.16(13)

The square-pyramidal copper (II) environment with a τ_5 parameter of 0.21 is found in complex **3**. The basal plane of this pyramid consists of the donor atoms of the chelate ligand and the chlorido ligand, while the apex of the pyramid is occupied by the oxygen atom O2 from the nitrato ligand. Copper (II) is shifted towards the apical oxygen by 0.1221(6) Å. Expectedly, of the three nitrate oxygen atoms, the coordinating one, O1, is at the greatest distance from nitrogen N6 (1.2642(17) Å), while the remaining two, O2 and O3 are at distances shorter by ca. 0.04 and 0.02 Å, respectively. In the polymeric complex **1**, nitrate has a role of a counterion, and the distance of its oxygen atoms from N6 is in the range of 1.221(3)–1.245(3) Å.

The entire ligand system in all three complexes shows a high level of planarity, which is evidenced by the values of the dihedral angles at which the pyridine ring is subtended with the 2-acetylpyridine and aminoguanidine metallocycles (5.9(13) and 3.5(15)° for **1**, 3.82(5) and 1.85(4)° for **2**, and 1.01(10) and 2.78(3)° for **3**, respectively).

In all these complexes, the distances between the Cu atom and chelating ligand donor atoms are in the range 1.9130(17) – 2.0177(12) Å, with Cu–pyridine nitrogen atom bond lengths being the longest, and those with the imine nitrogen atom being the shortest, making the nitrogen N1 a better electron donor than nitrogen N3. In the square-pyramidal structures of **1** and **3**, Cu-coligand bond lengths have also the expected values, with the equatorial ligand are closer to the metal centre and the apical ligand is further from it. In these two complexes, the length of the C1–N1 bond corresponds to the value of the localised double bond, and after coordination, this bond is shortened, compared to its length in the free ligand. The exceptions in the change of some geometric parameters after coordination in **2** and in the other two compounds can be explained by the coordination of the ligand in its monoanionic form (**2**), while in the other complexes, it is coordinated in its neutral form (**1** and **3**).

In **2**, deprotonation of the aminoguanidine residue leads to elongation of the C1–N2 and C1–N4, and shortening of N2–N3 bonds, but this trend is also observed in the structures of the other two complexes, which indicates that the formation of coordination covalent bond has a greater impact on bond lengths than deprotonation. Also, the ligand coordination leads to angular changes in aminoguanidine moiety, visualized through the shrinking of the N3–N2–C1 and N2––C1–N1 angles and widening of the N1–C1–N4 angle in these two complex compounds. The angle N1–C1–N4 has a larger value after coordination in **1** and **3**, but the smallest value in **2**, while the angles N3–N2–C1 and N2–C1–N1 have the same value as before deprotonation.

Besides the electrostatic interactions, the crystal structure of **1** is additionally stabilised by the intermolecular hydrogen bonds (Fig. S-1 of the Supplementary material), which engage all N–H donors of the cation and all three nitrate oxygens as acceptors (Table II). This way of hydrogen bonding affects forming of the layer in the crystallographic *bc* plane, where the nitrate ion connects two chains of monoperiodic cations through the previously mentioned hydrogen bonds (Fig. S-2 of the Supplementary material).

The crystal structures of **2** and **3** are also stabilised by hydrogen bonding. The intermolecular hydrogen bonds were observed in **2** which engages the N4 atom as a donor of two hydrogen bonds and N2 and Cl1 as acceptors. This way of bonding leads to the formation of a chain that extends along the crystallographic [01 $\bar{1}$] direction (Fig. S-3 of the Supplementary material). Crystal water molecules in **3** have a crucial role in connecting three neighbouring complex units. Besides the water molecule, in the same structure, the N–H donors are atoms N1, N2 and N4 while the acceptors are all three oxygen atoms of nitrato coligand. (Fig. S-4 of the Supplementary material). Two neutral complexes are connected *via* N2–H2···O1 and N4–H4B···O2 hydrogen bonds (Table II) forming the centrosymmetric dimers, while water molecules interconnect these dimers

via O4–H4D···Cl1 hydrogen bonds forming the chain of dimers shown in Fig. S-5a of the Supplementary material, where one dimer present pair of the green and blue model. These chains of dimers are interconnected also by the same water molecules, through O4–H4C···O2 and by ligand and nitrato coligand through N2–H2···O3 hydrogen bond (Fig. S-5b). On the other hand, there is a network of the same interconnected chains which is centrosymmetric in relation to the previously described one where there is stacking of pyridine aromatic ring and metallocycle Cu1–N1–C1–N2–N3 (Fig. S-6 of the Supplementary material), but with no hydrogen bonding between those two (Fig. S-5c).

TABLE II. Geometrical parameters for hydrogen bonds

D–H···A	*d*(H···A) / Å	*d*(D···A) / Å	∠(D–H···A) / °	Symmetry operation for A
		1		
N1–H1···O3	2.11(2)	2.941(3)	175(3)	$-x+1, y+1/2, -z+3/2$
N2–H2···O2	2.06(2)	2.893(3)	172(2)	x, y, z
N4–H4A···O2	2.14(2)	2.973(3)	175(3)	$-x+1, y+1/2, -z+3/2$
N4–H4B···O1	2.06(2)	2.892(3)	176(3)	x, y, z
		2		
N4–H4B···N2	2.21(2)	3.057(2)	169(2)	$-x+1, -y+1, -z+2$
N4–H4A···Cl1	2.57(2)	3.3618(19)	166(2)	$-x+1, -y+2, -z+1$
		3		
O4–H4C···O2	2.28(2)	3.004(2)	158(3)	$x-1, y-1, z$
O4–H4D···Cl1	2.49(2)	3.3017(18)	170(3)	$-x+1, -y, -z$
N4–H4A···O4	2.04	2.826(2)	152.2	x, y, z
N4–H4B···O2	2.08	2.934(2)	171.9	$-x+1, -y+1, -z$
N1–H1···O4	2.49	3.1408(19)	133.2	x, y, z
N2–H2···O3	2.57	3.0933(19)	120.1	$x-1, y, z$
N2–H2···O1	2.10	2.8750(16)	149.3	$-x+1, -y+1, -z$

*Thermal properties of complexes **1**–**3***

All three compounds were analysed by simultaneous TG-DTG and online coupled TG–MS measurements in argon. Complex **1** begins to lose mass somewhat above room temperature, which causes a broad low-intensity mass change of 0.9 % up to ~130 °C (Fig. 2). This mass loss is most probably the result of the lattice water evaporation. The measured mass loss is somewhat less than the water content calculated based on crystallographic data (1.3 %) due to the spontaneous evaporation at room temperature during storage. The spontaneous water loss is in accordance with the tight empty space which H_2O can occupy in the crystal structure of the monoperiodic cation of **1**. The thermal decomposition of anhydrous **1** begins at 215 °C, onset. A sharp mass loss step of 31.0 % is characteristic of the decomposition. Following, the nitrate can be marked as the most reactive component of complex **1**, and in this step, it most probably decomposes also causing the oxidative decomposition of the organic ligand. Due to such

redox processes, the crystal lattice very likely crushes, too at this step. Above ~230 °C the decomposition continues at a steady rate without any stable intermediate formation, and it is not finished up to 700 °C.

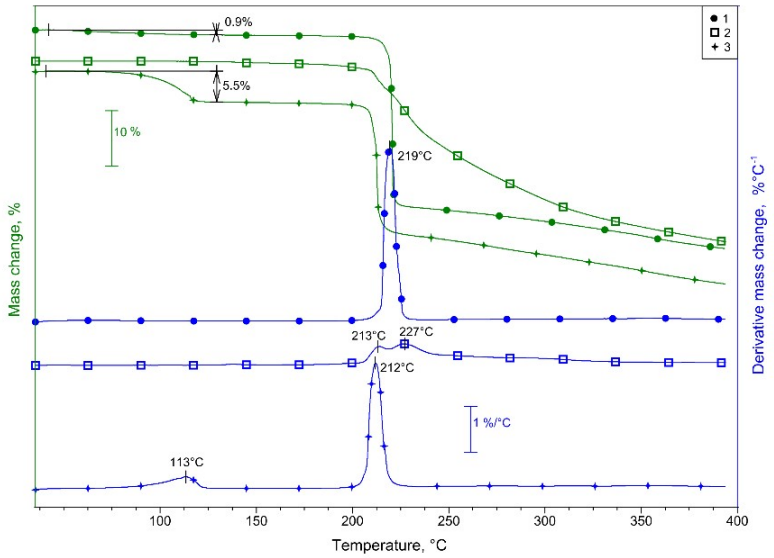

Fig. 2. TG and DTG curves of complexes **1**–**3** in argon.

Complex [Cu(L–H)Cl] (**2**) is stable up to 130 °C, onset. At this temperature, its mass is decreasing by 0.3 %. Considering that this complex does not contain lattice water, the mass loss in this step is most probably the result of the evaporation of water traces from the slightly hygroscopic compound. Above 190 °C complex **2** decomposes in several highly overlapped steps continuously without the formation of any stable intermediate. Its decomposition above 190 °C is not sharp as the decomposition of complexes **1** and **3**, because of the absence of nitrate and for the same reason its slighter decomposition process was expected, too.

The complex $[Cu(L)ClNO_3]\cdot H_2O$ (**3**) contains lattice water, which evaporates during the first mass loss step with DTG maximum at 113 °C. This was also proved by coupled TG–MS measurements. The measured mass loss of 5.5 % is a little bit higher than the mass percent of lattice water (5.06 %). Since compound **2** shows a slight hygroscopicity, the difference between the measured and calculated water content may originate from the absorbed humidity in this case too. The anhydrous **3** is stable up to 204 °C, onset. Above this temperature, the decomposition begins with a sharp mass loss step with the DTG maximum at 212 °C. The intensive mass loss is the result of the rapid decomposition of nitrate from **3**, like in the case of complex **1**. Above 219 °C the decomposition continues

at a steady rate without the formation of any stable intermediate, and it is not finished up to 700 °C.

The DSC data of the compounds are in accordance with their composition. The evaporation processes are endothermic, while the decomposition of the complexes is in all three cases exothermic. The exothermic effect of the thermal degradation of **1** and **3** was expected because of the presence of the nitrate group. Differently, in the case of **2**, the exothermicity of the decomposition process was not in prospect because it does not contain oxidative groups. However, due to the presence of nitrate, the exothermic effect, which follows the decomposition of complexes **1** and **3** is more intensive than that of complex **2** (Fig. 3) without nitrates. There is a difference between the intensity of the exothermic effect of **1** and **3**, also. The highest exothermic effect follows the decomposition of **1** with a polymeric structure. Despite that **1** is stable at somewhat higher temperatures than **3**, when it decomposes, more energy is released than from complex **3**, which leads to a higher exothermic effect in the case of **1**.

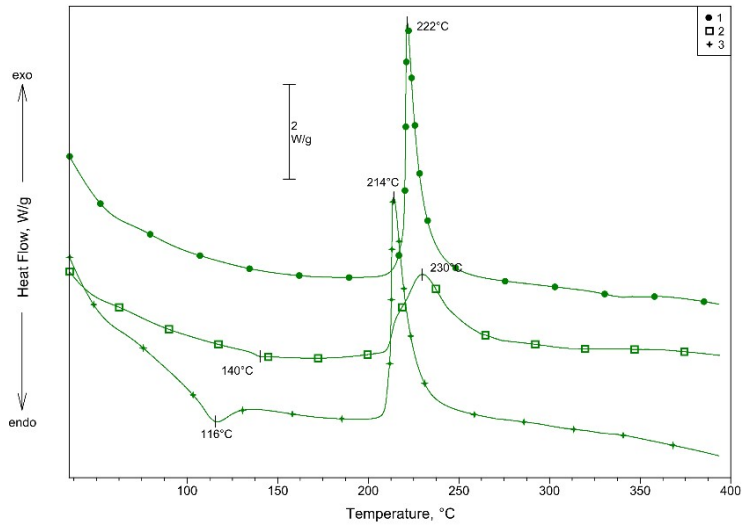

Fig. 3. DSC curves of complexes **1**–**3** in argon.

The TG–MS data prove the conclusions based on TG and DSC curves (Figs. 2 and 3). The first mass loss below 150 °C is in all three compound water evaporation. Even though compound **2** is synthesised in the absence of water and in the presence of NH_3, the following TG–MS signals suggest the presence of water (18 and 17 *m*/*z*) and not ammonia (17 and 16 *m*/*z*, Fig. 4). To follow the main decomposition step of the compounds, besides water (OH^+, H_2O^+), ammonia (NH_2^+, NH_3^+), and chlorine fragments (Cl^+, HCl^+) the signals of the nitrate decompo-

sition products NO^+, N_2O^+ and NO_2^+ were also analysed. From these fragments, the most intensive is NO^+ (30 *m*/*z*), which is usual for nitrate decomposition (Fig. 5).[24] The very small peak of 30 *m*/*z* in complex **2** cannot be correlated to NO^+ release because of the absence of nitrate. However, the mass value of 30 *m*/*z* may be correlated to the fragment N_2H_2 from the nitrogen-rich ligand. As is shown in Fig. S-7 of the Supplementary material, all the detected signals of complex **2** are the most intensive at the beginning of the thermal decomposition process.

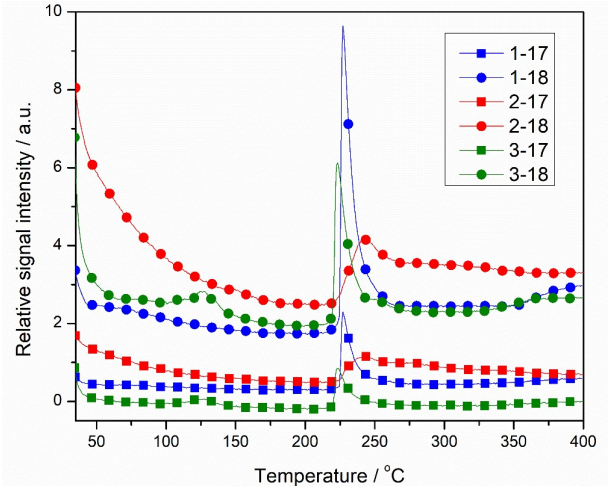

Fig. 4. MS curves of H_2O (17 and 18 *m*/*z*).

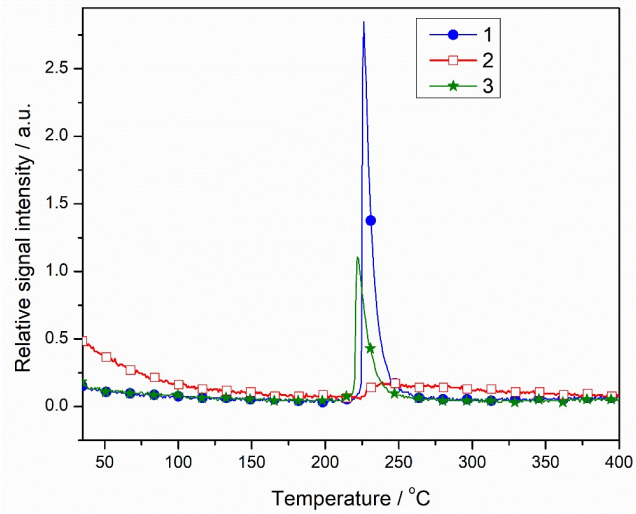

Fig. 5. MS curves of NO (30 *m*/*z*).

CONCLUSION

In the reaction of warm solutions of the ligand, $[H_2L]Cl_2$ and copper(II) nitrate, in the presence of different deprotonating agents, single-crystals of three new coordination compounds were formed – polymeric complex $\{[Cu(L)(\mu\text{-}Cl)]NO_3 \cdot H_2O\}_n$ (**1**) and neutral complexes [Cu(L–H)Cl] (**2**) and $[Cu(L)ClNO_3] \cdot H_2O$ (**3**), where L is 2-acetylpyridine-aminoguanidine. The ligand was coordinated in its neutral form in complexes **1** and **3**, where pyridine and lithium-acetate were used for deprotonation. As a stronger base, ammonia as deprotonating agent, in complex **2**, causes the coordination of the monoanion of the ligand. The Schiff base is coordinated through pyridine, azomethine, and the imine nitrogen atom. This coordination mode results in the formation of two five--membered chelate rings. Copper (II) is situated in the square-pyramidal environment of donor atoms of the ligand and its co-ligands in **1** and **3**, while copper (II) in **2** is placed in a square-planar environment of N-donor atoms and one chlorido ligand. The thermal measurements proved that complexes **1** and **2** are hygroscopic and by increasing the temperature lose the bonded water. Complex **3** also loses its lattice water during heating. All compounds are stable in their anhydrous form up to 200 °C and above this temperature they decompose. The beginning of their decomposition process is more intensive in **1** and **3** because of the presence of nitrate.

Different coordination behaviour of the ligand, in the presence of diprotonation agents with different base constants, can lead to different properties of these novel complexes, and further research will include the investigation of photoluminescence and the antioxidant properties will be analysed.

SUPPLEMENTARY MATERIAL

Additional data and information are available electronically at the pages of journal website: https://www.shd-pub.org.rs/index.php/JSCS/article/view/12476, or from the corresponding author on request. CCDC 2269543-2269546.CCDC 2279826–2279828 contain the supplementary crystallographic data for this paper. These data can be obtained free of charge from The Cambridge Crystallographic Data Centre (https://www.ccdc.cam.ac.uk/structures).

Acknowledgements. The authors gratefully acknowledge the financial support of the Ministry of Science, Technological Development and Innovation of the Republic of Serbia (Grant No. 451-03-47/2023-01/200125), as well as Slovenian–Serbian joint co-operation project funded by Ministry of Science, Technological Development and Innovation of the Republic of Serbia and Slovenian Research and Innovation Agency (2023–2025).

ИЗВОД

РЕАКЦИЈЕ 2-АЦЕТИЛПИРИДИН-АМИНОГВАНИДИНА СА Cu(II) ПОД РАЗЛИЧИТИМ РЕАКЦИОНИМ УСЛОВИМА

МАРИЈАНА С. КОСТИЋ, НИКОЛА Д. РАДНОВИЋ, МАРКО В. РОДИЋ, БЕРТА БАРТА ХОЛО, ЉИЉАНА С. ВОЈИНОВИЋ ЈЕШИЋ и МИРЈАНА М. РАДАНОВИЋ

Универзитет у Новом Саду, Природно–математички факултет, Трг Доситеја Обрадовића 3, 21000 Нови Сад

Деривати аминогванидина су већ дуже време у фокусу истраживања захваљујући разноврсној биолошкој активности као што су антивирусна, антибактеријска, аналгетска, антиоксидативна, као и антиканцерогена активност. Њихови комплекси са металима су такође испитивани и поред биолошки активних деривата аминогванидина велики број ових комплекса такође показује значајну биолошку активност. Осим тога, неки показују значајна фотолуминесцентна својства и користе се за фотоелектронске уређаје. У складу са свим наведеним, у овом раду су приказане синтезе, физичко–хемијска, структурна и термоаналитичка карактеризација комплекса 2-ацетилпиридин аминогванидина (L) са бакром(II). При различитим реакционим условима Cu(II) са L даје комплексе различитог састава. Показано је да се наведена Шифова база може координовати у неутралној или моноанјонској форми у зависности од јачине базе коришћене за депротонацију. У присуству пиридина је добијен координациони полимер, док у присуству амонијака/литијум-ацетата добијена су два различита мономерна комплекса. Одређена су њихова физичко–хемијска и термичка својства, као и молекулска и кристална структура.

(Примљено 7. јула, ревидирано 28. јула, прихваћено 8. септембра 2023)

REFERENCES

1. O. Dömötör, N. V. May, G. T. Gál, G. Spengler, A. Dobrova, V. B. Arion, É. A. Enyedy, *Molecules* **27** (2022) 2044 (https://doi.org/10.3390/MOLECULES27072044/S1)
2. J. Vojtaššák, J. Čársky, L. Danišovič, D. Böhmer, M. Blaško, T. Braxatorisová, *Toxicol. in Vitro* **20** (2006) 868 (https://doi.org/10.1016/j.tiv.2005.12.009)
3. C. Watala, M. Dobaczewski, P. Kazmierczak, J. Gebicki, M. Nocun, I. Zitnanova, O. Ulicna, Z. Durackova, I. Waczulíková, J. Carsky, S. Chlopicki, *Vascul. Pharmacol.* **51** (2009) 275 (https://doi.org/10.1016/j.vph.2009.07.002)
4. Yu. M. Chumakov, V. I. Tsapkov, G. Bocelli, B. Ya. Antosyak, S. G. Shova, A. P. Gulea, *Crystallogr. Rep.* **51** (2006) 60 (https://doi.org/10.1134/S1063774506010123)
5. M. S. More, P. G. Joshi, Y. K. Mishra, P. K. Khanna, *Mater. Today Chem.* **14** (2019) 100195 (https://doi.org/10.1016/j.mtchem.2019.100195)
6. C. Boulechfar, H. Ferkous, A. Delimi, A. Djedouani, A. Kahlouche, A. Boublia, A. S. Darwish, T. Lemaoui, R. Verma, Y. Benguerba, *Inorg. Chem. Commun.* **150** (2023) 110451 (https://doi.org/10.1016/j.inoche.2023.110451)
7. S. S. Chourasiya, D. Kathuria, S. S. Nikam, A. Ramakrishnan, S. Khullar, S. K. Mandal, A. K. Chakraborti, P. V. Bharatam, *J. Org. Chem.* **81** (2016) 7574 (https://doi.org/10.1021/acs.joc.6b01258)
8. M. G. Jelić, D. G. Georgiadou, M. M. Radanović, N. Ž. Romčević, K. P. Giannakopoulos, V. M. Leovac, L. F. Nađ, L. S. Vojinović-Ješić, *Opt. Quantum Electron.* **48** (2016) 276 (https://doi.org/10.1007/s11082-016-0547-5)
9. V. M. Leovac, M. D. Joksović, V. Divjaković, L. S. Jovanović, Ž. Šaranović, A. Pevec, *J. Inorg. Biochem.* **101** (2007) 1094 (https://doi.org/10.1016/j.jinorgbio.2007.04.004)

10. L. S. Vojinović-Ješić, M. M. Radanović, M. V. Rodić, V. Živković-Radovanović, L. S. Jovanović, V. M. Leovac, *Polyhedron* **117** (2016) 526 (https://doi.org/10.1016/J.POLY.2016.06.032)
11. M. M. Radanović, M. V. Rodić, L. S. Vojinović-Ješić, S. Armaković, S. J. Armaković, V. M. Leovac, *Inorg. Chim. Acta* **473** (2018) 160 (https://doi.org/10.1016/J.ICA.2017.12.038)
12. M. Radanovic, S. Novakovic, M. Rodic, L. Vojinovic-Jesic, C. Janiak, V. Leovac, *J. Serb. Chem. Soc.* **87** (2022) 1259 (https://doi.org/10.2298/JSC220613072R)
13. M. M. Radanović, L. S. Vojinović-Ješić, M. G. Jelić, E. Sakellis, B. Barta Holló, V. M. Leovac, M. V. Rodić, *Inorganics (Basel)* **10** (2022) 147 (https://doi.org/10.3390/inorganics10100147)
14. M. M. Radanović, M. V. Rodić, L. S. Vojinović-Ješić, S. Armaković, S. J. Armaković, V. M. Leovac, *Inorg. Chim. Acta* **473** (2018) 160 (https://doi.org/10.1016/j.ica.2017.12.038)
15. G. M. Sheldrick, *Acta Crystallogr. A Found. Adv.* **71** (2015) 3 (https://doi.org/10.1107/S2053273314026370)
16. G. M. Sheldrick, *Acta Crystallogr., C* **71** (2015) 3 (https://doi.org/10.1107/S2053229614024218)
17. A. L. Spek, *Acta Crystallogr., D* **65** (2009) 148 (https://doi.org/10.1107/S090744490804362X)
18. C. R. Groom, I. J. Bruno, M. P. Lightfoot, S. C. Ward, *Acta Crystallogr., B* **72** (2016) 171 (https://doi.org/10.1107/S2052520616003954)
19. I. J. Bruno, J. C. Cole, M. Kessler, J. Luo, W. D. S. Momerwell, L. H. Purkis, B. R. Smith, R. Taylor, R. I. Cooper, S. E. Harris, A. G. Orpen, *J. Chem. Inf. Comput. Sci.* **44** (2004) 2133 (https://doi.org/10.1021/CI049780B)
20. C. F. MacRae, I. Sovago, S. J. Cottrell, P. T. A. Galek, P. McCabe, E. Pidcock, M. Platings, G. P. Shields, J. S. Stevens, M. Towler, P. A. Wood, *Urn:Issn:1600-5767* **53** (2020) 226 (https://doi.org/10.1107/S1600576719014092)
21. K. Nakamoto, *Infrared and Raman spectra of inorganic and coordination compounds. Part B, Applications in coordination, organometallic, and bioinorganic chemistry*, Wiley, New York, 2009 (ISBN 978-0-471-74339-2)
22. A. W. Addison, T. N. Rao, J. Reedijk, J. van Rijn, G. C. Verschoor, *J. Chem. Soc., Dalton Trans.* **0** (1984) 1349 (https://doi.org/10.1039/DT9840001349)
23. L. Yang, D. R. Powell, R. P. Houser, *J. Chem. Soc., Dalton Trans.* (2007) 955 (https://doi.org/10.1039/b617136b)
24. NIST Chemistry WebBook, https://webbook.nist.gov/chemistry/ (accessed June 30, 2023).

Journal of the Serbian Chemical Society
JSCS@tmf.bg.ac.rs • www.shd.org.rs/JSCS
J. Serb. Chem. Soc. *88* (12) S363–S368 (2023) *Supplementary material*

SUPPLEMENTARY MATERIAL TO

Reactions of 2-acetylpyridine-aminoguanidine with Cu(II) under different reaction conditions

MARIJANA S. KOSTIĆ*#, NIKOLA D. RADNOVIĆ#, MARKO V. RODIĆ#, BERTA BARTA HOLLÓ#, LJILJANA S. VOJINOVIĆ-JEŠIĆ# and MIRJANA M. RADANOVIĆ#

University of Novi Sad, Faculty of Sciences, Trg Dositeja Obradovića 3, 21000 Novi Sad, Serbia

J. Serb. Chem. Soc. *88* (12) (2023) 1265–1278

TABLE OF CONTENTS:

{[Cu(L)(μ-Cl)]NO_3·0.25H_2O}$_n$ ***(1)***

Anal. Calcd. for $C_8H_{11.5}N_6O_{3.25}ClCu$: C, 28.02; H, 3.36; N, 24.52 %. Found: C, 27.63; H, 3.68; N, 24.01 %. Conductivity, Λ = 110 S cm^2 mol^{-1} (in MeOH), Λ = 76 S cm^2 mol^{-1} (in DMF). Selected IR bands [wavenumber, cm^{-1}]: 3320 (s), 3182 (s), 1680 (s), 1650 (s), 1603 (m), 1545 (m), 1385 (vs), 1331 (m), 1200 (m), 1156 (w), 1112 (w), 1048 (w), 822 (w), 779 (m), 647 (w).

[Cu(L–H)Cl] ***(2)***

Anal. Calcd. for $C_8H_{10}N_6ClCu$: C, 34.93; H, 3.63; N, 25.45. Found: C, 35.02; H, 3.68; N, 25.63 %. Conductivity, Λ = 5 S cm^2 mol^{-1} (in DMF). Selected IR bands [wavenumber, cm^{-1}]: 3376 (m), 3206 (s), 3122 (m), 1643 (m), 1595 (s), 1516 (s), 1489 (s), 1430 (s), 1366 (m), 1263 (m), 1171 (s), 1086 (m), 1025 (w), 887 (w), 796 (m), 640 (s).

[Cu(L)ClNO_3]·H_2O ***(3)***

Anal. Calcd. for $C_8H_{13}N_6O_4ClCu$: C, 26.28; H, 3.65; N, 23.60. Found: C, 26.97; H, 3.68; N, 23.21 %. Conductivity, Λ = 114 S cm^2 mol^{-1} (in DMF). Selected IR bands [wavenumber, cm^{-1}]: 3538 (m), 3368 (s), 3152 (s), 1647 (vs), 1623 (m), 1601 (s), 1545 (s), 1425 (vs), 1299 (vs), 1267 (s), 1015 (s), 905 (w), 724 (w), 703 (w), 645 (m).

* Corresponding author. E-mail: marijana.kostic@dh.uns.ac.rs

1. X-RAY DATA TABLE

Table S-I. Crystal data, data collection, and refinement details for **1**, **2,** and **3**

Chemical formula	$C_8H_{11.5}N_6O_{3.25}ClCu$ (**1**)	$C_8H_{10}N_6ClCu$ (**2**)	$C_8H_{13}N_6O_4ClCu$ (**3**)
CCDC No.	2279826	2279827	2279828
Temperature, K	295(2)	295(2)	295(2)
Formula weight, g mol^{-1}	342.72	275.20	356.23
Crystal system	monoclinic	triclinic	triclinic
Space group	$P2_1/c$	$P\bar{1}$	$P\bar{1}$
a / Å	15.2534(5)	6.9461(3)	8.8689(2)
b / Å	12.6235(5)	8.8077(4)	9.1112(2)
c / Å	6.9614(3)	9.3443(3)	9.1228(2)
α / °	90	65.659(4)	99.739(2)
β / °	91.933(4)	87.263(3)	91.368(2)
γ / °	90	87.946(3)	112.718(2)
V / Å^3	1339.67(9)	520.19(4)	666.95 (3)
Crystal size, mm^3	0.50×0.21×0.12	0.56 × 0.11 × 0.05	0.48 × 0.41 × 0.23
Reflections collected	11936	12706	25579
Unique reflections	3229	2124	4613
Observed reflections [$I \geq 2\sigma(I)$]	2544	1961	4005
R_{int}	0.030	0.029	0.025
R [$I > 2\sigma(I)$]	0.037	0.021	0.027
R (all data)	0.087	0.056	0.073
Goodness-of-fit, S	1.05	1.09	1.08
$\Delta\rho_{max}$, $\Delta\rho_{min}$, e Å^{-3}	0.29 / −0.25	0.23 / −0.19	0.36 / –0.28

2. ADDITIONAL FIGURES

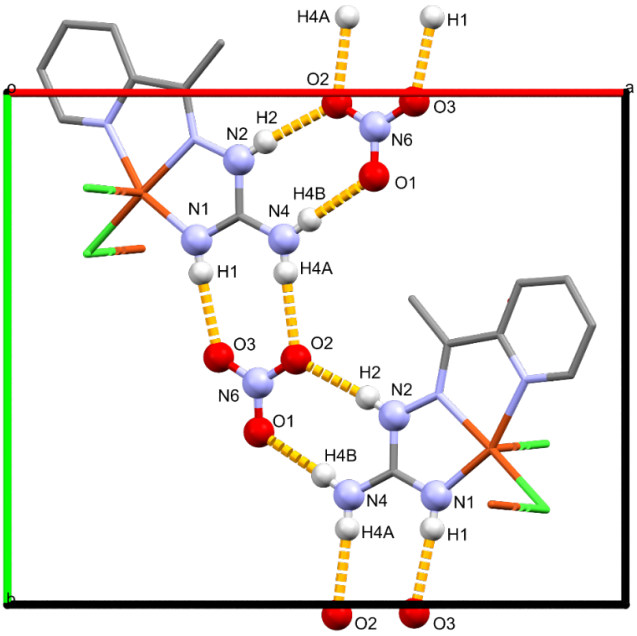

Figure S-1. Hydrogen bonding in **1**

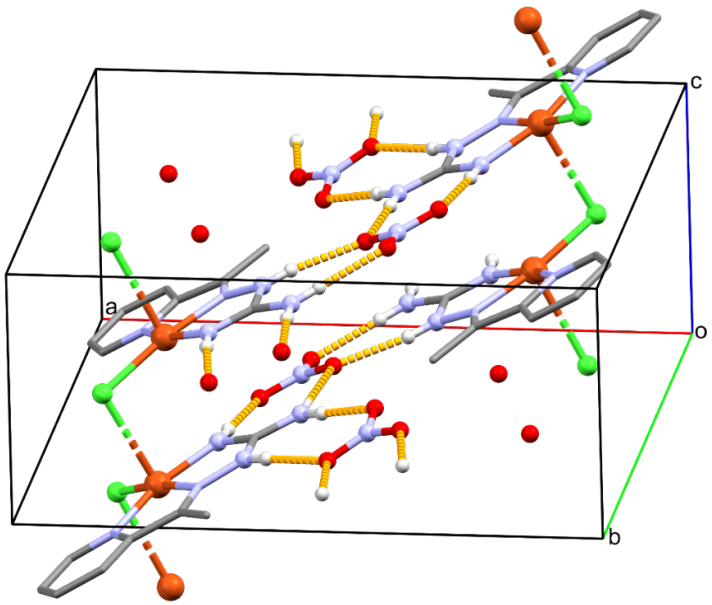

Fig. S-2. Crystal packing of **1** showing the hydrogen bonds that connect two monoperiodic polymer chains

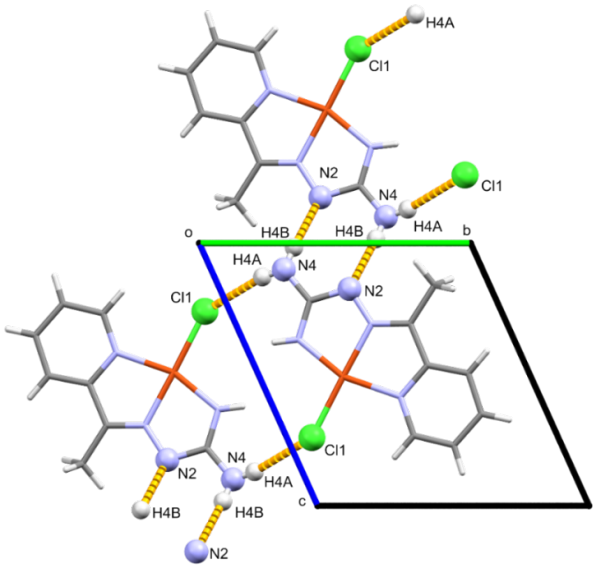

Fig. S-3. Hydrogen bonding in **2**

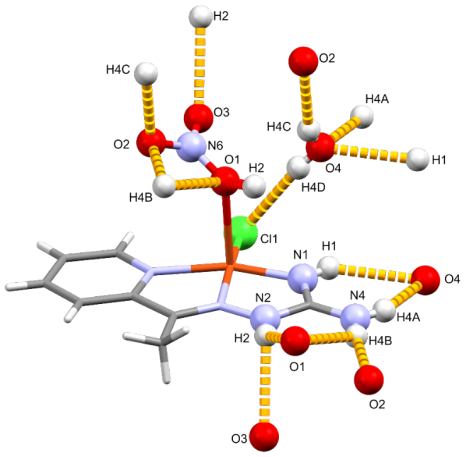

Fig. S-4. Hydrogen bonding in **3**

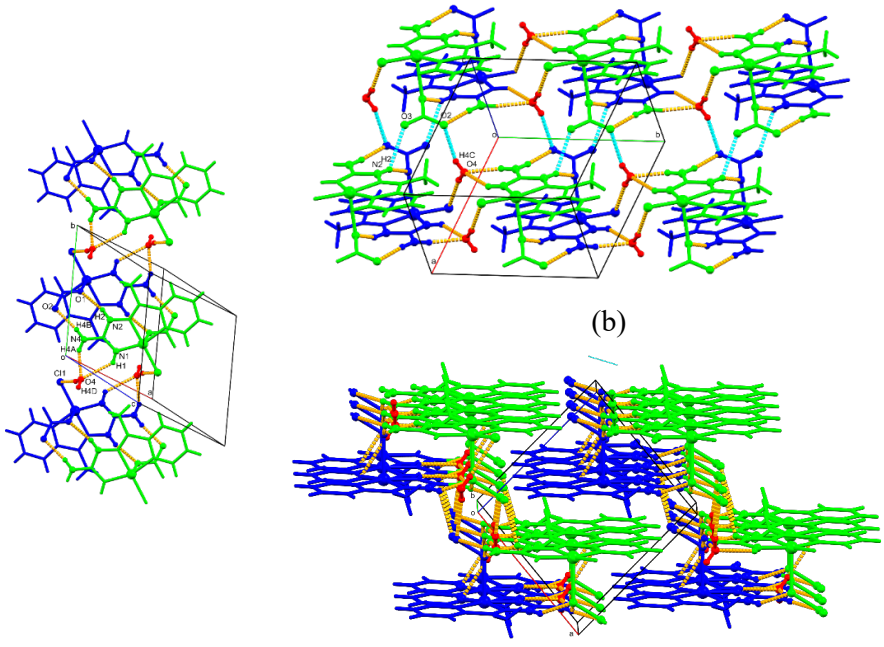

Fig. S-5. Hydrogen bonds responsible for dimer and chain formation (a), interconnecting the chains (b) and crystal packing of **3**

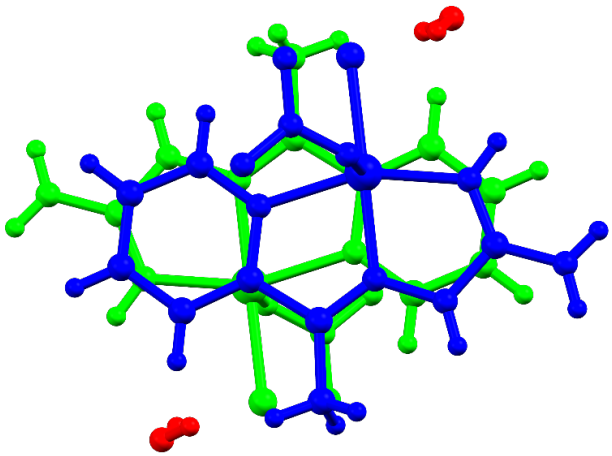

Fig. S-6. Stacking of py ring and aminoguanidine mettalocycle Ж

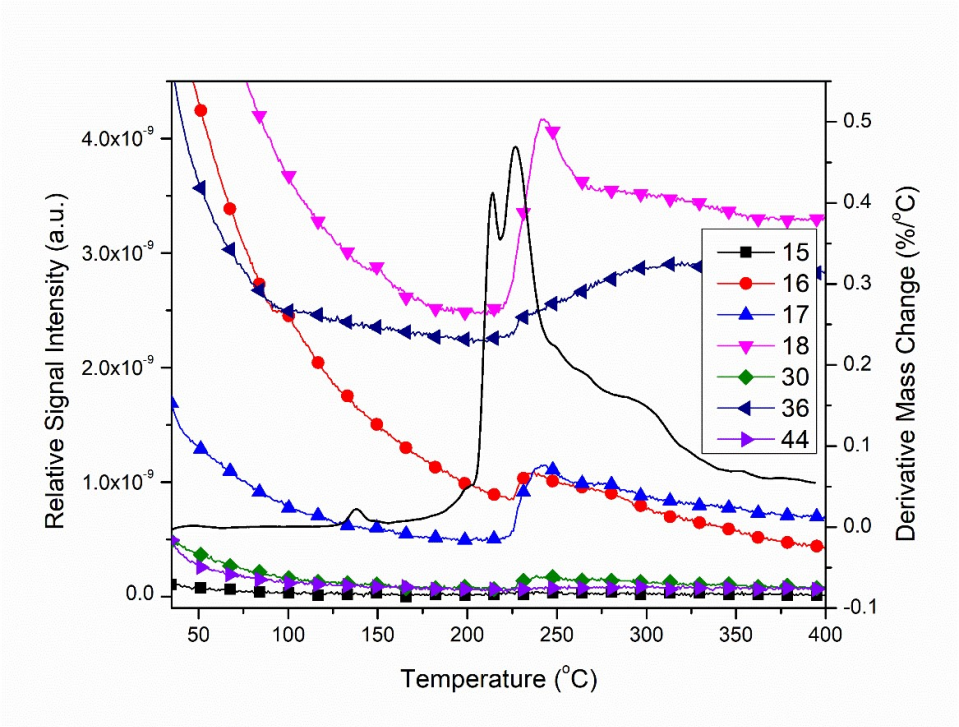

Fig. S-7. Fragments of complex **2** in argon

Journal of the Serbian Chemical Society
JSCS@tmf.bg.ac.rs • www.shd.org.rs/JSCS
J. Serb. Chem. Soc. *88* (12) 1279–1291 (2023)
JSCS–5695
Original scientific paper
Published 19 December 2023

Square-pyramidal mononuclear, dinuclear and polymeric copper(II) complexes with (2-pyridinylmethyl)amino derivatives

STEFAN RICHTER[1], PETER LÖNNECKE[1], DIJANA BOVAN[2], SANJA MIJATOVIĆ[2], DANIJELA MAKSIMOVIĆ-IVANIĆ[2], GORAN N. KALUĐEROVIĆ[3] and EVAMARIE HEY-HAWKINS[1]*

[1]*Universität Leipzig, Faculty of Chemistry and Mineralogy, Institute of Inorganic Chemistry, Johannisallee 29, 04103 Leipzig, Germany,* [2]*Department of Immunology, Institute for Biological Research "Siniša Stanković" National Institute of Republic of Serbia, University of Belgrade, Bulevar despota Stefana 142, 11060 Belgrade, Serbia and* [3]*Department of Engineering and Natural Sciences, University of Applied Sciences Merseburg, Eberhard-Leibnitz-Str. 2, 06217 Merseburg, Germany*

(Received 18 August, revised 26 August, accepted 25 September 2023)

Abstract: The coordination behavior of three ligand precursors 2-[(2-pyridinylmethyl)amino]acetic acid hydrochloride, 4-[(2-pyridinylmethyl)amino]benzoic acid hydrochloride and 4-{[2-(pyridin-2-ylmethylamino)ethylamino]methyl}-benzoic acid hydrochloride, **HL1**·HCl–**HL3**·HCl, respectively, in copper(II) complexes is described. The complexes were characterized by elemental analysis, ESI mass spectrometry and IR spectroscopy, as well as X-ray structural analysis. The reaction of copper(II) with **HL1**·HCl in methanol afforded the polymeric complex $[\{Cu(\mu\text{-}Cl)_2(\mathbf{MeL1}\text{-}\kappa^2N,N')\}_n]$ (**1**) featuring the methyl ester of **L1** (**MeL1**). With **HL2**·HCl or **HL3**·HCl, the dimeric complex $[\{CuCl(\mu\text{-}Cl)(\mathbf{HL2}\text{-}\kappa^2N,N')\}_2]$ (**2**) or the mononuclear complex $[CuCl_2(\mathbf{HL3}\text{-}\kappa^3N,N',N'')]$ (**3**) were obtained. All complexes exhibited square-pyramidal geometries. In **1**, polymeric chains are formed through bridging chlorido ligands without typical hydrogen bonding interaction. Contrarily, the COOH group in **2** is participating in the formation of intermolecular hydrogen bonding forming a supramolecular structure. In **3**, intermolecular hydrogen bonding (Cl···H(O)) leads to a 1-D polymeric structure. The copper(II) complex **2** diminished viability of human 8505C, MCF-7, 518A2 and SW-480 cell lines. The tumoricidal effect of **2** was realized mainly through caspase-mediated apoptosis.

Keywords: copper(II); pyridine; X-ray structure; *in vitro* anticancer activity.

* Corresponding author. E-mail: hey@uni-leipzig.de
https://doi.org/10.2298/JSC230818072R

INTRODUCTION

The Jahn–Teller active copper(II) ion exhibits remarkable flexibility in its coordination sphere, allowing it to adopt a diverse range of coordination geometries, spanning from four-coordinate (tetrahedral or square planar) to six-coordinate elongated octahedral structures.[1] In copper(II) complexes containing halido ligands enhanced flexibility is observed by facilitating halide bridging between copper(II) centers, leading to the formation of extended oligomeric or polymeric complexes.

Pyridine-based multidentate ligands are a highly adaptable group of compounds, primarily because they can be easily functionalized using efficient synthetic methods.[2] The flexibility in their synthesis allows for the creation of custom-made ligands.[3,4] When such molecules are coordinated to metal ions, they enable the manipulation of both the electronic and structural characteristics of the resulting complexes.

Transition metal complexes with *N,N'*-bidentate pyridylmethylamine ligands remain a subject of ongoing interest, primarily due to the high coordination versatility achievable through the introduction of diverse substituents on the amine and/or pyridyl unit.[5–8] Numerous structural variations in pyridylmethylamines and their corresponding complexes have been documented highlighting the significance of their steric and electronic properties in various targeted chemical applications.[9–11] Previous studies have utilized *N*-(2-hydroxybenzyl)-amino acids and *N*-(2-pyridylmethyl)-amino acids as useful polydentate ligands to form multidimensional and oligomeric structures.[12–19]

Here we report the investigation of the influence of the amino *N* substituent in (2-pyridinylmethyl)amino ligands on the solid-state structure of copper(II) complexes. Depending on the substituent polymeric polynuclear $[\{Cu(\mu\text{-}Cl)_2(\mathbf{MeL1}\text{-}\kappa^2N,N')\}_n]$, dinuclear, $[\{CuCl(\mu\text{-}Cl)(\mathbf{HL2}\text{-}\kappa^2N,N')\}_2]$, or mononuclear, $[CuCl_2(\mathbf{HL3}\text{-}\kappa^2N,N',N'')]$, complexes were obtained. The complexes were characterized by elemental analysis, ESI-MS and IR spectroscopy and single crystal structure analysis.

EXPERIMENTAL

Materials and methods

Chemicals and instruments. Methanol, $CuCl_2$, RPMI 1640 medium, fetal bovine serum, propidium iodide (PI), acridine orange (AO), and sulforhodamine B (SRB), were ordered from Sigma-Aldrich (St. Louis, MO). AnnexinV-FITC (AnnV), was obtained from Biotium (Hayward, CA) while Apostat was from R&D (R&D Systems, Minneapolis, MN, USA). For ^{1}H- (300 MHz) and ^{13}C-NMR (75 MHz) spectroscopy (Fourier-300, Bruker) tetra-methylsilane (TMS) was used as an internal standard and deuterated solvent as reference. The melting points were determined in a capillary using a Gallenkamp instrument. Elemental analysis was performed on Thermo Scientific Flash Smart CHNS (Italy). The IR spectra were recorded with an FT-IR spectrometer Spectrum 2000 (Perkin Elmer) using KBr pellets in the range of 4000 to 400 cm^{-1}. The ESI mass spectra in a positive mode were recorded with an FT-ICR

mass spectrometer (Bruker Daltonics). The isotope distribution was determined with the program Molecular Weight Calculator 6.45.[20] The specification of the molecular ion peak refers to the highest signal in the observed isotope pattern. The absorbance for the SRB assay was measured at 540 nm with the reference wavelength at 670 nm. Fluorescence activated cell sorting (FACS) experiments were conducted on CyFlow® Space Partec by using the Partec FloMax® software.

Analytical and spectral data are given in the Supplementary material to this paper.

*Synthesis of the ligand precursors **HL1**·HCl–**HL3**·HCl*

*Synthesis of **HL1**·HCl and **HL2**·HCl*. Ligand precursors **HL1**·HCl (2-[(2-pyridinylmethyl)amino]acetic acid hydrochloride) and **HL2**·HCl (4-[(2-pyridinylmethyl)amino]benzoic acid hydrochloride) were obtained as described in the literature.[13,21]

*Synthesis of 4-{[2-(pyridin-2-ylmethylamino)ethylamino]methyl}benzoic acid hydrochloride **HL3**·HCl*. The compound 4-[(2-aminoethylamino)methyl]benzoic acid (synthetic procedure was described earlier[22]) (1.32 g, 0.007 mol) was reacted with KOH (0.45 g, 0.007 mol) in water (10 mL). The resulting clear light yellow solution was cooled to 0 °C. Pyridine-2-carbaldehyde (0.73 g, 0.007 mol) was then added within 30 min, followed by stirring at 0 °C for 1 h. $NaBH_4$ (0.25 g, 0.007 mol) dissolved in water (5 mL) was slowly added to the reaction solution. The resulting pale yellow suspension was stirred overnight at room temperature. Hydrochloric acid (2 M, 8 mL) was added to the clear yellow solution, foaming vigorously and changing color to orange; the pH of the solution was adjusted to 3. The solvent was then completely removed in vacuum. The crude yellow product was recrystallized from methanol (150 mL). The resulting light yellow solid was filtered off, washed with diethyl ether (50 mL) and dried in vacuum. Properties: yellowish powder; soluble in chloroform, moderately soluble in methanol, DMSO; insoluble in diethyl ether. Yield: 1.05 g (40 %).

*Synthesis of the copper(II) complexes **1**–**3***

*Synthesis of **1***. Solid **HL1**·HCl (300 mg, 1.5 mmol) was added to a solution of $CuCl_2$ (200 mg, 1.5 mmol) in methanol (15 mL). The resulting clear green reaction solution was stirred for three days at room temperature. Afterwards, a light blue precipitate had formed from the bright green reaction solution. This crude product was filtered off and washed with diethyl ether (40 mL) and dried in air.

Properties: green solid; soluble in DMF, DMSO, methanol; moderately soluble in ethanol; insoluble in diethyl ether. Yield: 260 mg (58 %). Decomposition temperature: 212 °C (green to black).

*Synthesis of **2***. A suspension of **HL2**·HCl (396 mg, 1.5 mmol) in methanol (10 mL) was added dropwise within 5 min at room temperature to a bright green solution of $CuCl_2$ (200 mg, 1.5 mmol) in methanol (10 mL). The color of the reaction solution changed from light green to dark green. After stirring overnight, the green precipitate was filtered off and washed with diethyl ether (8 mL). The product was dried in vacuum. Properties: dark green powder; soluble in water, DMSO; moderately soluble in methanol; insoluble in diethyl ether. Yield: 377 mg (70 %). Decomposition temperature: 211 °C (dark green to black).

*Synthesis of **3***. $CuCl_2$ (100 mg, 0.75 mmol) was dissolved in methanol (10 mL) at room temperature. A solution of **HL3**·HCl (280 mg, 0.75 mmol) was added to this bright green solution. After 12 h stirring the light blue precipitate was filtered off and washed with methanol (5 mL) and diethyl ether (5 mL). The product was dried in vacuum. Properties: light blue solid; soluble in water, DMSO; moderately soluble in methanol; insoluble in diethyl ether. Yield: 240 mg (70 %). Decomposition temperature: 190 °C (light blue to black).

Single crystal X-ray structural analysis

The data for the single crystal X-ray structure analyses of **1**–**3** were collected on a Gemini diffractometer (Rigaku Oxford Diffraction) using MoKα radiation and ω-scan rotation. Data reduction was performed with CrysAlis Pro[23] including the program SCALE3 ABSPACK for empirical absorption correction and an analytical numeric absorption correction using a multifaceted crystal model based on expressions derived by Clark and Reid.[24] The structures were solved by direct methods using the program SHELXS-2013 and refined with SHELXL--2018.[25] Crystallographic parameters are collected in Table S-I of the Supplementary material. The structural images were generated and processed with Diamond.[26] Supplementary information of the crystallographic data can be accessed through https://www.ccdc.cam.ac.uk/ /structures/ CCDC 2285917 (**1**), CCDC 2285918 (**2**), CCDC 2287497 (**3**).

In vitro *studies*

Complex **2** was dissolved in DMF at 20 mM (stock solution) and diluted to working concentrations up to 100 μM with completed RPMI 1640 nutrient medium. The tumor cell lines were seeded at 1000 (518A2), 1500 (8505C and SW-480) and 2000 cells/well (MCF-7) and the SRB assay was performed, in triplicate, as described in the literature.[27,28] The assays AnnV/PI, apostat and AO were conducted as described recently.[29,30] For flow cytometry experiments MCF-7 cells were seeded in 6-well plates at 1×10^5 cells/well and concentration applied in treatments was IC_{50} of complex **2**.

RESULTS AND DISCUSSION

Synthesis of copper(II) complexes 1–3

In the present work, two bidentate (**HL1**·HCl and **HL2**·HCl) and one tridentate (**HL3**·HCl) 2-pyridinylmethyl)amino derivatives were reacted with copper(II) chloride in methanol (Scheme 1). The corresponding copper(II) complexes **1**–**3** were obtained in moderate yields. Copper(II) reacts with **HL1**·HCl in methanol with esterification of the carboxylic acid group (complex **1**), as was

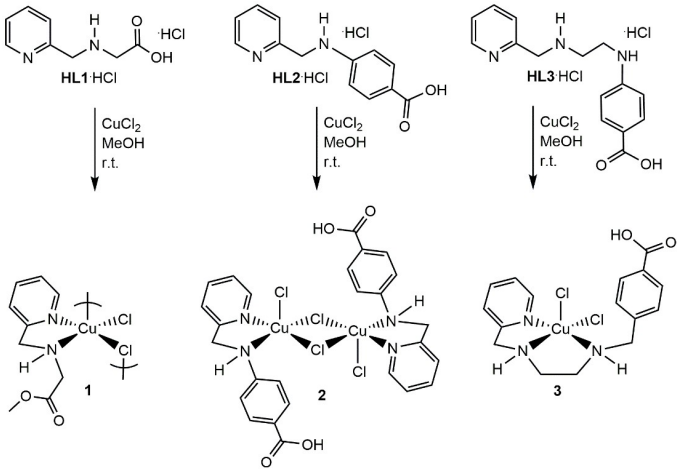

Scheme 1. Synthesis of copper(II) complexes **1**–**3**.

previously also observed for the corresponding cationic monomeric ruthenium(II) *p*-cymene cloride complex with **HL1**.[21] The characterization of the complexes was carried out by mass spectrometry, IR spectroscopy as well as by X-ray single crystal structure analysis.

Characterization

The purity of copper(II) complexes **1**–**3** was confirmed by elemental analysis, verifying their composition. Furthermore, ESI mass spectrometry is particularly informative for copper(II) complexes with chlorido ligands. Considering the natural abundance of only two copper (^{63}Cu 69.17 % and ^{65}Cu 30.83 %)[31] and chlorine isotopes (^{35}Cl 75.77 %, ^{37}Cl 24.23 %),[32] the isotopic patterns of the copper(II) complexes are significantly more line-poor than those of the comparable palladium or platinum complexes.[33,34] Thus, relatively effortless conclusive molecular composition of the respective copper(II) complexes from the isotopic pattern can be obtained. The shape of the isotopic pattern of **1** at 278.2 *m*/*z* suggests only one coordinated chlorido ligand, which makes the corresponding molecular fragment $[\mathbf{1}–Cl]^+$ positively charged. The shape and isotopic ratio of the simulated molecular ion peak agree well, for all three copper(II) complexes, with those of the measured molecular ion peaks. Similarly, for **2** and **3** under the same conditions $[M–Cl]^+$ was observed at *m*/*z* 688.9 and 383.0, respectively. IR spectra of copper(II) complexes **1**–**3** show a characteristic strong absorption band at 1751 and 1608 or 1611 cm^{-1}, which indicates C=O stretching vibration of the ester in **1** or protonated carboxylic groups in **2** and **3**, respectively.[12,21,35,36] Appropriate asymmetric COO vibrations were found at 1357 (**1**), 1261 (**2**) and 1262 cm^{-1} (**3**). For copper(II) complex **1**, N–H vibrations were observed at 3209 cm^{-1}, while **2** and **3** exhibited O–H and N–H vibrations at ca 3420 or 3417 and 3210 or 3208 cm^{-1}, respectively.

*Molecular structure of **1***

Light blue needles of **1** appropriate for X-ray structural analysis were obtained by slow evaporation of a methanol solution. Complex **1** crystallizes in the monoclinic space group $P2_1/c$. The molecular structure is shown in Fig. 1a. Selected bond lengths and angles are summarized in Table I.

A similar copper(II) complex, with a carboxylic acid in the ligand backbone, instead of its methyl ester reported herein (**1**), has already been described.[12] Thus, in that report, coordination in a κ*N*,*N*',κ*O* fashion to copper(II) occurs along with formation a second five-membered ring. The five-membered ring in complex **1** (Cu–N1–C5–C6–N2) has an envelope conformation. Through the index of trigonality τ_5 (0.12), calculated with equation $\tau_5 = (\beta–\alpha)/60$ (α and β are the largest bond angles around the copper(II) ion),[37] the coordination polyhedron around copper(II) is described as a square-pyramid with minor distortion. In the crystal lattice, zig–zag chains typical for copper(II) halido complexes along the

c-axis are formed, where the copper(II) atoms are bridged *via* one chlorido ligand forming a 1D polymer (Fig. 1b).

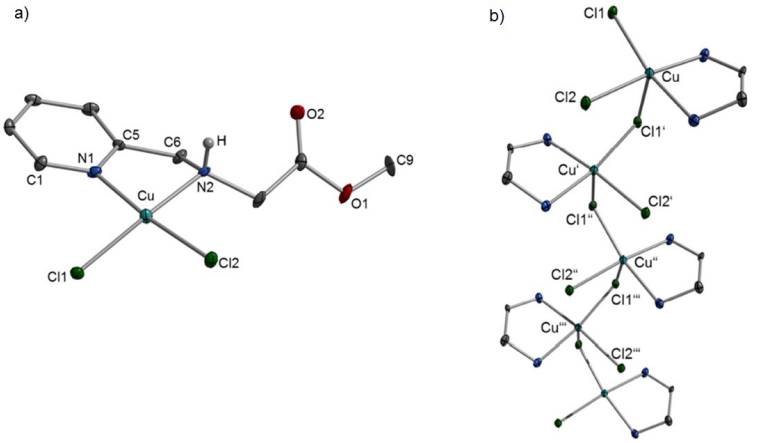

Fig. 1. a) Molecular structure of **1** and b) zig–zag chain along [001]. Only N1, N2, C5 and C6 of the bidentate ligand are shown. The ellipsoids shown correspond to a residence probability of 30 %. For reasons of clarity, only the N–H atom is shown.

TABLE I. Selected bond lengths (Å) and angles (°) in **1**–**3**

Bond length, Å		Bond angle, °	
		1	
Cu−N1	2.017(8)	Cl1−Cu–Cl2	92.49(9)
Cu−N2	2.062(8)	Cl1−Cu–N1	92.9(2)
Cu−Cl1	2.265(2)	Cl1−Cu–N2	167.5(2)
Cu−Cl2	2.297(3)	Cl2−Cu–N2	93.9(2)
Cu'−Cl1	2.699(3)	Cl2−Cu–N1	174.5(2)
		N1−Cu–N2	81.1(3)
		Cu−N1−C1	124.9(7)
Symmetry code ': *x*, 0.5–*y*, 0.5+*z*		Cu−N1−C5	115.2(6)
		2	
Cu−N1	2.005(5)	Cl1−Cu−Cl2	99.10(6)
Cu−N2	2.078(5)	Cl1−Cu−N1	94.1(2)
Cu−Cl1	2.266(2)	Cl1'−Cu−Cl2	93.80(7)
Cu−Cl2	2.248(2)	Cl1'−Cu−N1	94.1(2)
Cu−Cl1'	2.783(2)	Cl1'−Cu−N2	174.7(2)
Cu'−Cl1	2.783(2)	N1−Cu−Cl2	166.6(2)
O1···Cl2	3.024(5)	N1−Cu−N2	81.0(2)
O2···N2	2.832(7)	Cu−N1−C1	114.2(4)
Symmetry code ': *–x* , 1–*y*, 2–*z*		Cu−N1−C5	126.7(4)
		3	
Cu−Cl1	2.2486(7)	Cl1−Cu−Cl2	98.29(2)
Cu−Cl2	2.7100(7)	Cl1−Cu−N1	96.34(6)

TABLE I. Continued

Bond length, Å		Bond angle, °	
3			
Cu−N1	2.015(2)	N1−Cu−N2	81.66(8)
Cu−N2	2.006(2)	N1−Cu−N3	160.07(9)
Cu−N3	2.035(2)	N1−Cu−Cl2	97.26(6)
Cl2···O2‘	3.032(2)	N2−Cu−Cl1	175.99(7)
		N2−Cu−N3	84.23(8)
		N3−Cu−Cl1	96.84(6)
symmetry code’: –*x* , 1–*y*, 2–*z*		N3−Cu−Cl2	95.57(6)

*Molecular structure of **2***

Slow continuous evaporation of a methanol solution of **2** yielded blue needles suitable for single-crystal X-ray structure analysis. The complex crystallizes in the orthorhombic space group *Pccn*. The molecular structure is shown in Fig. 2. Selected bond lengths and angles are summarized in Table II. Complex **2** forms typical chlorido-bridged dimers, with a crystallographic inversion center located in the center of the four-membered Cu–Cl1–Cu'–Cl1' ring. The Cu–Cl1 (2.266(2) Å) and Cu–Cl2 (2.248(2) Å) bond lengths are significantly shorter than the one for Cu'-Cl1 (2.783(2) Å). Coordination of the chelating ligand **HL2** to the copper atom results in a five-membered ring (Cu–N1–C5–C6–N2) in an envelope conformation with λ- or δ-configuration. The bond angles Cu–N1–C1 (114.2(4)°) and Cu–N1–C5 (126.7(4)°) deviate considerably from the ideal angle (120°), but are similar to comparable copper(II) complexes, *i.e.*, [$CuCl_2$(py-2-CH_2NH_2)] and others.[12,38,39] Contrary to general expectation, no carboxylic acid dimers are found in the solid state of **2**. Instead, moderately strong hydrogen bonding occurs between

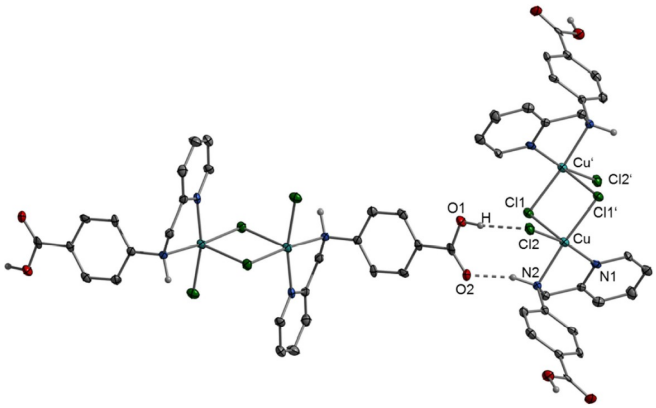

Fig. 2. Intermolecular hydrogen donor-acceptor bonds between two dimers in the solid state of **2**. The ellipsoids shown correspond to a residence probability of 30 %. For clarity, only the N–H and O–H hydrogen atoms are shown.

(O1)H···Cl2 (3.024(5) Å) and O2···H(N2) (2.832(7) Å) (Fig. 2) building (100) oriented layers.[40] The angular structural parameter τ_5 (0.13), a general descriptor of five-coordinate molecules, indicates a square-pyramidal copper(II) complex.

*Molecular structure of **3***

Deep blue plates of complex **3** suitable for X-ray single crystal structure analysis were obtained by slowly cooling a boiling aqueous solution of **3** to room temperature and subsequent storage at 4 °C for 24 h. Complex **3** crystallizes in the monoclinic space group $P2_1/c$. The molecular structure is shown in Fig. 3a. Selected bond lengths and angles are summarized in Table II. **HL3** is coordinated at the copper(II) ion in a $\kappa^3 N,N',N''$ bonding mode generating two five-membered rings which differ in their conformation. Accordingly, ring 1 (Cu–N1–C5––C7–N2) has an envelope conformation and ring 2 (Cu–N2–C7–C8–N3) δ- or λ--conformation. Hydrogen bonds occur between the atoms (O2')H and Cl2 (Fig. 3b), resulting in a 1D chain along [201]. The shortest distance Cl2···O2' is 3.031(2) Å and is in a comparable range to the O1···Cl2 distance of complex **2** (3.024(5) Å). In **3**, the copper(II) ion has a distorted square-pyramidal geometry with an angular structural parameter $\tau_5 = 0.26$.

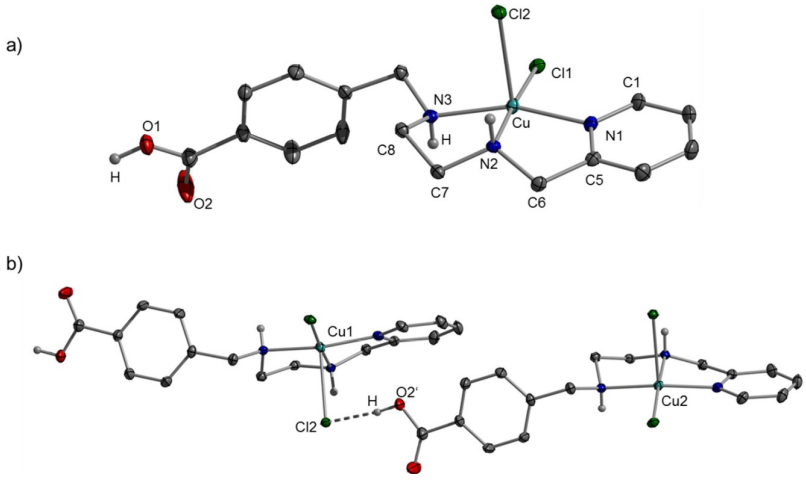

Fig. 3. a) Molecular structure of complex **3** and b) hydrogen bonding in the solid state of **3**. The ellipsoids shown correspond to a residence probability of 30%. For clarity, only the N–H and O–H hydrogen atoms are shown.

In vitro *study of **2***

To assess the *in vitro* potential of copper(II) complexes, as a representative compound complex **2** was selected and tested against four cell lines, namely 8505C, MCF-7, 518A2 and SW-480. The viability was determined using an SRB

assay (Fig. 4). Complex **2** was found to be active on all investigated cell lines with IC_{50} values ranging from 12.5 to 22.5 μM. Its activity was found to be lower on the same cell lines (SRB assay, 96 h of treatment) in comparison to the clinically used drug cisplatin.[41–43]

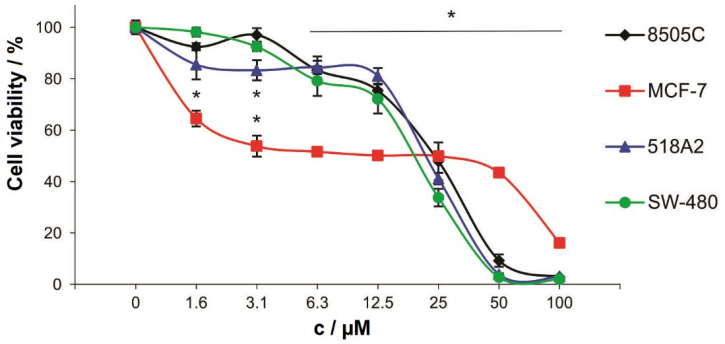

Fig. 4. Dose-dependent response of selected tumor cell lines treated with copper(II) complex **2** (SRB assay, 96 h). IC_{50} concentrations: 8505C, 22.35±2.33; MCF-7, 12.5±0.92; 518A2, 19.95±3.19; SW-480, 22.35±3.75 μM. *: $p < 0.05$ in comparison to control.

MCF-7 cells were chosen for further experiments as the most sensitive cell line displaying a specific plateau effect in response to treatment (Fig. 4). Upon exposure to an IC_{50} dose of copper(II) complex **2**, the MCF-7 cells underwent massive apoptosis (Fig. 5a). This effect was synchronized with intensive total caspase activation despite the fact that these cells are caspase 3 deficient (Fig. 5b).[44,45] Also, complex **2** did not elevate the number of autophagic vesicles in comparison to untreated cells. Even lower in activity than cisplatin, copper(II) complex **2** deserves attention since copper, as essential element, is involved in main cellular functions.[46] Since it was found that tumor cells have a higher demand for copper compared to normal cells, it can be speculated that compounds based on copper(II) will be more efficiently internalized by neoplastic cells thus representing a form of targeted therapy.[47]

CONCLUSION

Preparation and characterization of three copper(II) complexes containing 2-[(2-pyridinylmethyl)amino](methyl acetate) (**1**), 4-[(2-pyridinylmethyl)amino]-benzoic acid (**2**) and 4-{[2-(pyridin-2-ylmethylamino)ethylamino]methyl}benzoic acid (**3**) is described. Elemental analyses verify the purity of the complexes. Furthermore, ESI mass spectrometry and infrared spectroscopy confirm complex formation. In the solid state, complexes form polymeric (**1**), dimeric (**2**) or mononuclear (**3**) structures with copper(II) in a square-pyramidal environment. Complex **1** forms 1D chains *via* bridging chlorido ligands, while dimers of **2** are constructing a supramolecular structure through intermolecular hydrogen bond-

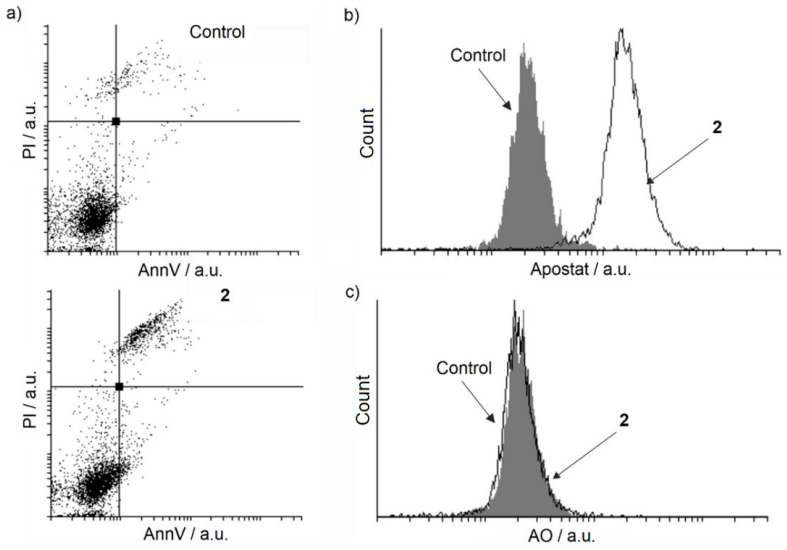

Fig. 5. Triggering of effects of complex **2** on a) apoptosis, b) caspases and c) autophagy in MCF-7 cells with complex **2**.

ing interactions, and complex **3** forms polymeric chains by intermolecular hydrogen bonding. Complex **2** efficiently suppresses the growth of 8505C, MCF-7, 518A2 and SW-480 tumor cell lines. Induction of caspase-dependent apoptosis was found to be a leading cause of the tumoricidal activity of complex **2**.

Acknowledgements. Support from the the Graduate School BuildMoNa (S.R.) and the Ministry of Science, Technological Development and Innovation of the Republic of Serbia (No. 451-03-47/2023-01/200007) is gratefully acknowledged.

ИЗВОД

КВАДРАТНО-ПИРАМИДАЛНИ МОНОНУКЛЕАРНИ, ДИНУКЛЕАРНИ И ПОЛИНУКЛЕАРНИ КОМПЛЕКСИ БАКРА(II) СА (2-ПИРИДИНИЛМЕТИЛ)АМИНО ДЕРИВАТИМА

STEFAN RICHTER[1], PETER LÖNNECKE[1], ДИЈАНА БОВАН[2], САЊА МИЈАТОВИЋ[2], ДАНИЈЕЛА МАКСИМОВИЋ-ИВАНИЋ[2], ГОРАН Н. КАЛУЂЕРОВИЋ[3] и EVAMARIE HEY-HAWKINS[1]

[1]Universität Leipzig, Faculty of Chemistry and Mineralogy, Institute of Inorganic Chemistry, Johannisallee 29, 04103 Leipzig, Germany; [2]Odeljenje za imunologiju, Институт за биолошка истраживања „Синиша Станковић", Институт од националног значаја за Републику Србију, Универзитет у Београду, 11000 Београд и [3]Department of Engineering and Natural Sciences, University of Applied Sciences Merseburg, Eberhard-Leibnitz-Str. 2, 06217 Merseburg, Germany

Описана је координација три лиганд прекурсора 2-[(2-пиридинилметил)амино]сирћетне киселине хидрохлорида, 4-[(2-пиридинилметил)амино]бензоеве киселине хидрохлорида и 4-{[2-(пиридин-2-илметиламино)етиламино]метил}бензоеве киселине хидрохлорида, **HL1**·HCl–**HL3**·HCl, са бакром(II). Награђени комплекси су окарактерисани елементалном анализом, ЕСИ масеном спектрометријом и ИР спектроскопијом, као и

рендгенском структурном анализом. У реакцији бакра(II) са **HL1**·HCl у метанолу формиран је комплекс формуле [{Cu(μ-Cl)$_2$(**MeL1**-κ^2*N*,*N*')}$_n$] уз естерификацију **L1** (**MeL1**). Са **HL2**·HCl, односно **HL3**·HCl бакар(II) је наградио динуклеарни комплекс [{CuCl(μ-Cl)(**HL2**-κ^2*N*,*N*')}$_2$] (**2**), односно мононуклеарни комплекс [CuCl$_2$(**HL3**-κ^3*N*,*N*',*N*'')] (**3**). У сва три комплекса централни јон је у квадратно-пирамидалном окружењу. Код комплекса **1** формирана је полимерна структура преко мостовних хлоридо лиганада, а без типичних водоничних веза. Супротно томе, COOH група у комплексу **2** учествује у грађењу интермолекулске водоничне везе дајући супрамолекуларну структуру. Код комплекса **3** интермолекулсе водоничне везе (Cl···O) образују 1Д полимерну структуру. Комплекс **2** је показао значајну активност на тестираним ћелијама 8505C, MCF-7, 518A2 и SW-480 хуманог порекла. Основни механизам путем кога је реализована туморицидна активност је апоптоза зависна од активације каспаза.

(Примљено 18. августа, ревидирано 26. августа, прихваћено 25. септембра 2023)

REFERENCES

1. M. R. Bond, in *Exploring Chemistry with Pyridine Derivatives*, IntechOpen, Rijeka, 2022 (https://doi.org/10.5772/intechopen.107124)
2. R. Diószegi, D. Bonczidai-Kelemen, A. Cs. Bényei, N. V. May, I. Fábián, N. Lihi, *Inorg. Chem.* **61** (2022) 2319 (https://doi.org/10.1021/acs.inorgchem.1c03728)
3. T. Klemens, K. Czerwińska, A. Szlapa-Kula, S. Kula, A. Świtlicka, S. Kotowicz, M. Siwy, K. Bednarczyk, S. Krompiec, K. Smolarek, S. Maćkowski, W. Danikiewicz, E. Schab-Balcerzak, B. Machura, *Dalton Trans.* **46** (2017) 9605 (https://doi.org/10.1039/C7DT01948C)
4. M. Stojičkov, S. Sturm, B. Čobeljić, A. Pevec, M. Jevtović, A. Scheitler, D. Radanović, L. Senft, I. Turel, K. Andjelković, M. Miehlich, K. Meyer, I. Ivanović-Burmazović, *Europ. J. Inorg. Chem.* **2020** (2020) 3347 (https://doi.org/10.1002/ejic.202000415)
5. S. H. Ahn, J. Shin, S. Nayab, H. Lee, *Bull. Korean Chem. Soc.* **37** (2016) 763 (https://doi.org/10.1002/bkcs.10747)
6. T. Zhu, Z. Guang-Yi, L. Xue-Qiang, X. Sai-Feng, Z. Qian-Jiang, W. Gregory Jackson, W. Zhan-Bing, L. La-Sheng, *Inorg. Chim. Acta* **357** (2004) 953 (https://doi.org/10.1016/j.ica.2003.09.027)
7. A. T. Çolak, O. Z. Yeşilel, O. Büyükgüngör, *Polyhedron* **29** (2010) 2127 (https://doi.org/10.1016/j.poly.2010.03.024)
8. M. Shukla, N. Srivastava, S. Saha, T. R. Rao, S. Sunkari, *Polyhedron* **30** (2011) 754 (https://doi.org/10.1016/j.poly.2010.12.036)
9. S. J. A. Guieu, A. M. M. Lanfredi, C. Massera, L. D. Pachón, P. Gamez, J. Reedijk, *Catal. Today* **96** (2004) 259 (https://doi.org/10.1016/j.cattod.2004.06.149)
10. 10. S.-K. Kang, H.-W. Lee, N. Sengottuvelan, Y.-I. Kim, *Bull. Korean Chem. Soc.* **33** (2012) 95 (https://doi.org/10.5012/bkcs.2012.33.1.95)
11. A. Mondal, S. Sarkar, D. Chopra, T. N. Guru Row, K. Krishna Rajak, *Dalton Trans.* (2004) 3244 (https://doi.org/10.1039/B408316D)
12. X. Wang, J. D. Ranford, J. J. Vittal, *J. Mol. Struct.* **796** (2006) 28 (https://doi.org/10.1016/j.molstruc.2006.03.090)
13. X. Wang, J. J. Vittal, *Inorg. Chem.* **42** (2003) 5135 (https://doi.org/10.1021/ic0344970)
14. A. M. Alam, M. Nethaji, M. Ray, *Angew. Chem. Int. Ed.* **42** (2003) 1940 (https://doi.org/10.1002/anie.200250591)
15. Md. A. Alam, M. Nethaji, M. Ray, *Inorg. Chem.* **44** (2005) 1302 (https://doi.org/10.1021/ic049145n)

16. B.-Y. Lou, D.-Q. Yuan, S.-Y. Gao, R.-H. Wang, Y. Xu, L. Han, M.-C. Hong, *J. Mol. Struct.* **707** (2004) 231 (https://doi.org/10.1016/j.molstruc.2004.07.025)
17. B.-Y. Lou, Y. Xu, D.-Q. Yuan, L. Han, M.-C. Hong, *Acta Cryst. E* **60** (2004) m522 (https://doi.org/ 0.1107/S1600536804007342)
18. B. Sreenivasulu, M. Vetrichelvan, F. Zhao, S. Gao, J. J. Vittal, *Eur. J. Inorg. Chem.* **2005** (2005) 4635 (https://doi.org/10.1002/ejic.200500638)
19. Z. Lü, D. Zhang, S. Gao, D. Zhu, *Inorg. Chem. Commun.* **8** (2005) 746 (https://doi.org/10.1016/j.inoche.2005.05.012)
20. M. Monroe, *Molecular Weight Calculator for Windows*, 2011, https://alchemistmatt.com/mwtwin.html.
21. S. Richter, S. Singh, D. Draca, A. Kate, A. Kumbhar, A. S. Kumbhar, D. Maksimovic--Ivanic, S. Mijatovic, P. Lönnecke, E. Hey-Hawkins, *Dalton Trans.* **45** (2016) 13114 (https://doi.org/10.1039/C6DT01782G)
22. L. I. Shevchenko, P. S. Pel'kis, M. O. Lozinskii, V. N. Kalinin, *Ukr. Khim. Zh.* **50** (1984) 301
23. Rigaku Oxford Diffraction, *CrysAlisPro Software system*, Rigaku Corporation, Wroclaw, 1995–2023
24. R. C. Clark, J. S. Reid, *Acta Cryst., A* **51** (1995) 887 (https://doi.org/10.1107/S0108767395007367)
25. G. M. Sheldrick, *Acta Cryst., C* **71** (2015) 3 (https://doi.org/10.1107/S2053229614024218)
26. K. Putz, K. Brandenburg, *Diamond Crystal and Molecular Structure Visualization*, 2014, https://www.crystalimpact.de/diamond
27. P. Skehan, R. Storeng, D. Scudiero, A. Monks, J. McMahon, D. Vistica, J. T. Warren, H. Bokesch, S. Kenney, M. R. Boyd, *J. Natl. Cancer Inst.* **82** (1990) 1107 (https://doi.org/10.1093/jnci/82.13.1107)
28. V. Vichai, K. Kirtikara, *Nat. Protoc.* **1** (2006) 1112 (https://doi.org/10.1038/nprot.2006.179)
29. L. Useini, T. Komazec, M. Laube, P. Lönnecke, J. Schädlich, S. Mijatović, D. Maksimović-Ivanić, J. Pietzsch, E. Hey-Hawkins, *Adv. Ther.* **6** (2023) 2300117 (https://doi.org/10.1002/adtp.202300117)
30. I. Predarska, M. Saoud, I. Morgan, P. Lönnecke, G. N. Kaluđerović, E. Hey-Hawkins, *Biomolecules* **13** (2023) 595 (https://doi.org/10.3390/biom13040595)
31. Y. Zhang, Z. Bao, N. Lv, K. Chen, C. Zong, H. Yuan, *Frontiers Chem.* **8** (2020) 609 (https://doi.org/10.3389/fchem.2020.00609)
32. J. M. Rosenbaum, R. A. Cliff, M. L. Coleman, *Anal. Chem.* **72** (2000) 2261 (https://doi.org/10.1021/ac991297q)
33. A. J. Dempster, *Nature* **136** (1935) 65 (https://doi.org/10.1038/136065b0)
34. J. B. Creech, J. A. Baker, M. R. Handler, M. Bizzarro, *Chem. Geol.* **363** (2014) 293 (https://doi.org/10.1016/j.chemgeo.2013.11.009)
35. N. Pantelić, B. B. Zmejkovski, B. Kolundžija, M. Đ. Crnogorac, J. M. Vujić, B. Dojčinović, S. R. Trifunović, T. P. Stanojković, T. J. Sabo, G. N. Kaluđerović, *J. Inorg. Biochem.* **172** (2017) 55 (https://doi.org/10.1016/j.jinorgbio.2017.04.001)
36. G. N. Kaluđerović, H. Schmidt, C. Wagner, K. Merzweiler, D. Steinborn, *Collect. Czech. Chem. Commun.* **72** (2007) 560 (https://doi.org/10.1135/cccc20070560)
37. A. W. Addison, T. N. Rao, J. Reedijk, J. van Rijn, G. C. Verschoor, *Dalton Trans.* (1984) 1349 (https://doi.org/10.1039/DT9840001349)

38. Y.-F. Liu, D.-F. Rong, H.-T. Xia, D.-Q. Wang, *Acta Cryst., E* **65** (2009) m1492 (https://doi.org/10.1107/S1600536809044997)
39. B. Zheng, H. Liu, J. Feng, J. Zhang, *Appl. Organometal. Chem.* **28** (2014) 372 (https://doi.org/10.1002/aoc.3138)
40. G. A. Jeffrey, *An Introduction to Hydrogen Bonding*, UK edition, Oxford University Press, New York, 1997
41. C. Vetter, C. Wagner, G. N. Kaluderović, R. Paschke, D. Steinborn, *Inorg. Chim. Acta* **362** (2009) 189 (https://doi.org/10.1016/j.ica.2008.03.085)
42. R. Lindner, G. N. Kaluđerović, R. Paschkec, C. Wagner, D. Steinborn, *Polyhedron* **27** (2008) 914 (https://doi.org/10.1016/j.poly.2007.11.020)
43. G. N. Kaluđerović, T. Krajnović, M. Momčilović, S. Stosic-Grujicic, S. Mijatović, D. Maksimović-Ivanić, E. Hey-Hawkins, *J. Inorg. Biochem.* **153** (2015) 315 (https://doi.org/10.1016/j.jinorgbio.2015.09.006)
44. X.-H. Yang, T. L. Sladek, X. Liu, B. R. Butler, C. J. Froelich, A. D. Thor, *Cancer Res.* **61** (2001) 348 (https://aacrjournals.org/cancerres/article/61/1/348/507421/Reconstitution-of-Caspase-3-Sensitizes-MCF-7?searchresult=1)
45. R. U. Jänicke, M. L. Sprengart, M. R. Wati, A. G. Porter, *J. Biol. Chem.* **273** (1998) 9357 (https://doi.org/10.1074/jbc.273.16.9357)
46. R. Uauy, M. Olivares, M. Gonzalez, *Am. J. Clin. Nutr.* **67** (1998) 952S (https://doi.org/10.1093/ajcn/67.5.952S)
47. V. C. Shanbhag, N. Gudekar, K. Jasmer, C. Papageorgiou, K. Singh, M. J. Petris, *Biochim. Biophys. Acta Mol. Cell Res.* **1868** (2021) 118893 (https://doi.org/10.1016/j.bbamcr.2020.118893).

Journal of the Serbian Chemical Society
JSCS@tmf.bg.ac.rs • www.shd.org.rs/JSCS
J. Serb. Chem. Soc. *88* (12) S369–S370 (2023) *Supplementary material*

SUPPLEMENTARY MATERIAL TO

Square-pyramidal mononuclear, dinuclear and polymeric copper(II) complexes with (2-pyridinylmethyl)amino derivatives

STEFAN RICHTER[1], PETER LÖNNECKE[1], DIJANA BOVAN[2], SANJA MIJATOVIĆ[2], DANIJELA MAKSIMOVIĆ-IVANIĆ[2], GORAN N. KALUĐEROVIĆ[3] and EVAMARIE HEY-HAWKINS[1]*

[1]*Universität Leipzig, Faculty of Chemistry and Mineralogy, Institute of Inorganic Chemistry, Johannisallee 29, 04103 Leipzig, Germany,* [2]*Department of Immunology, Institute for Biological Research "Siniša Stanković" National Institute of Republic of Serbia, University of Belgrade, Bulevar despota Stefana 142, 11060 Belgrade, Serbia and* [3]*Department of Engineering and Natural Sciences, University of Applied Sciences Merseburg, Eberhard-Leibnitz-Str. 2, 06217 Merseburg, Germany*

J. Serb. Chem. Soc. *88* (12) (2023) 1279–1291

ANALYTICAL AND SPECTRAL DATA

4-{[2-(Pyridin-2-ylmethylamino)ethylamino]methyl}benzoic acid hydrochloride ***HL3***·*HCl*

^{1}H NMR (300 MHz, DMSO-d_6, in ppm): δ 3.35−3.41 (m, 4H, CH_2^aCH_2^b), 4.23 (s, 2H, CH_2^c), 4.33 (s, 2H, CH_2^d), 7.41 ('t', 1H, CH^f), 7.56 ('d', 1H, CH^e), 7.70 (d, $^3J_{H,H}$ = 8.0 Hz, 2H, CH^g), 7.87 ('t', 1H, CH^l), 7.95 (d, $^3J_{H,H}$ = 8.0 Hz, 2H, CH^h), 8.59 ('d', 1H, CH^m). ^{13}C{^{1}H} NMR (75 MHz, DMSO-d_6, in ppm): δ 43.2 (s, CH_2^a), 43.4 (s, CH_2^b), 49.9 (s, CH_2^c), 50.9 (s, CH_2^d), 123.3 (s, CH^e), 123.7 (s, CH^f), 129.5 (s, CH^g), 130.1 (s, CH^h), 130.2 (s, C^j), 131.2 (s, C^k), 137.4 (s, CH^l), 149.1 (s, CH^m), 152.4 (s, C^n), 167.1 (s, CO). IR: $\tilde{\nu}$ (cm^{-1}) 3435 (s, br), 2930 (s), 2757 (s), 2696 (s), 2587 (m), 2418 (m), 1683 (s), 1615 (m), 1432 (m), 1320 (m), 1277 (m), 1232 (m), 1106(s), 809 (s), 760 (s).

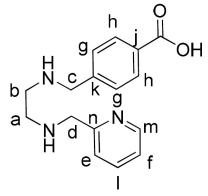

Fig. S-1. Atom numbering scheme of **HL3**.

Compound ***1***

Elemental analysis for $C_9H_{12}Cl_2CuN_2O_2$ (314.65), Calculated: C, 34.35; H, 3.84; N, 8.90 %; Found: C, 34.75, 3.91; N, 9.11 %. ESI-MS (CH_3OH), positive mode: *m*/*z* 278.2 $[M–Cl]^+$.

* Corresponding author. E-mail: hey@uni-leipzig.de

IR: $\tilde{\nu}$ (cm^{-1}) 3419 (br, w), 3209 (s), 3033 (m), 2949 (m), 1751 (s), 1608 (m), 1452 (m), 1440 (m), 1419 (w), 1357 (m), 1240 (s), 1204 (m), 1159 (w), 1131 (w), 1112 (w), 1028 (m), 1008 (m), 931 (w), 772 (s).

*Compound **2***

Elemental analysis for $C_{26}H_{24}Cl_4Cu_2N_4O_4$ (725.37), Calculated: C, 43.05; H, 3.34; N, 7.72 %; Found: C, 42.83, 3.30; N, 7.72 %. ESI-MS (CH_3OH), positive mode: *m*/*z* 688.9 $[M–Cl]^+$. IR: $\tilde{\nu}$ (cm^{-1}) 3421 (br, s), 3210 (m), 2963 (m), 2360 (w), 1717 (m), 1699 (m), 1684 (w), 1608 (s), 1558 (w), 1541 (w), 1507 (w), 1261 (m), 1177 (m), 1104 (m).

*Compound **3***

ESI-MS (CH_3OH), positive mode: *m*/*z* 383.0 $[M–Cl]^+$. IR: $\tilde{\nu}$ (cm^{-1}) 3417 (br, s), 3208 (m), 3157 (m), 2925 (s), 1712 (s), 1670 (m), 1611 (m), 1452 (m), 1319 (w), 1262 (s), 1112 (s), 1023 (s), 801 (m), 769 (m).

TABLE S-I. Crystallographic parameters of copper(II) complexes **1**–**3**; †: twinned crystal needle

Name	**1**†	**2**	**3**
Formula	$C_9H_{12}Cl_2CuN_2O_2$	$C_{26}H_{24}Cl_4Cu_2N_4O_4$	$C_{16}H_{19}Cl_2CuN_3O_2$
Fw (g mol^{-1})	314.65	725.37	419.78
Temperature (K)	130(2)	130(2)	130(2)
crystal color	green	green	blue
crystal size (mm)	0.29 × 0.03 × 0.02	0.15 × 0.03 × 0.01	0.30 × 0.10 × 0.02
crystal system	monoclinic	orthorhombic	monoclinic
space group	$P2_1/c$	*Pccn*	$P2_1/c$
a (Å)	19.195(1)	8.8843(5)	13.2615(4)
b (Å)	8.7089(4)	20.018(1)	10.3590(3)
c (Å)	6.9006(4)	15.899(1)	14.5507(6)
α (°)	90	90	90
β (°)	96.350(5)	90	113.210(4)
γ (°)	90	90	90
V (nm^3)	1.1465(1)	2.8276(3)	1.8371(1)
Z	4	4	4
calcd density (g cm^{-3})	1.823	1.704	1.518
F(000)	636	1464	860
no. of collected reflns	2629	16673	15658
no. of independent reflns	2629	2501	4563
R_{int}	0.0868	0.2079	0.0563
no. of reflns observed	1602	1290	3443
restrains/parameters	0 / 150	2 / 189	0 / 293
R [$I > 2\sigma(I)$]	R_1 = 0.0629, wR_2 = 0.1359	R_1 = 0.0542, wR_2 = 0.0869	R_1 = 0.0406, wR_2 = 0.0758
R (all data)	R_1 = 0,1039, wR_2 = 0,1435	R_1 = 0,1427, wR_2 = 0,1108	R_1 = 0.0635, wR_2 = 0.0844
Goof, *S*	1.006	1.000	1.032
$\Delta\rho_{max}/\Delta\rho_{min}$ (e Å^{-3})	1.234 /−0.625	0.629/−0.497	0.478/−0.377

Journal of the Serbian Chemical Society
JSCS@tmf.bg.ac.rs • www.shd.org.rs/JSCS
J. Serb. Chem. Soc. 88 (12) 1293–1306 (2023)
JSCS–5696
Original scientific paper
Published 19 December 2023

Structure and DNA/BSA binding study of zinc(II) complex with 4-ethynyl-2,2'-bipyridine

TINA P. ANDREJEVIĆ[1#], DARKO P. AŠANIN[2#], AURÉLIEN CROCHET[3], NEVENA LJ. STEVANOVIĆ[1#], IVANA VUČENOVIĆ[4], FABIO ZOBI[3], MILOŠ I. DJURAN[5#] and BILJANA Đ. GLIŠIĆ[1#]*

[1]*University of Kragujevac, Faculty of Science, Department of Chemistry, R. Domanovića 12, 34000 Kragujevac, Serbia,* [2]*University of Kragujevac, Institute for Information Technologies Kragujevac, Department of Science, Jovana Cvijića bb, 34000 Kragujevac, Serbia,* [3]*University of Fribourg, Department of Chemistry, Chemin du Musée 9, CH-1700 Fribourg, Switzerland,* [4]*University of Niš, Faculty of Agriculture Kruševac, Kosančićeva 4, 37000 Kruševac, Serbia and* [5]*Serbian Academy of Sciences and Arts, Knez Mihailova 35, 11000 Belgrade, Serbia*

(Received 5 June, revised 22 June, accepted 8 September 2023)

Abstract: In the present study, a zinc(II) complex with 4-ethynyl-2,2'-bipyridine (ebpy), [Zn(ebpy)Cl_2], was synthesized and characterized by spectroscopic (^{1}H-NMR, IR and UV–Vis) methods and molar conductivity measurement. The crystal structure of the [Zn(ebpy)Cl_2] complex was determined by single-crystal X-ray diffraction analysis, confirming the bidentate coordination of the ebpy ligand through its two nitrogen atoms, while the remaining two coordination sites are occupied by two chloride ions. With the aim to investigate the reactivity of the synthesized zinc(II) complex toward biologically important molecules, its binding affinity to calf thymus DNA (ct-DNA) and bovine serum albumin (BSA) was studied by fluorescence emission spectroscopy. From the obtained results, it can be concluded that [Zn(ebpy)Cl_2] complex binds to bovine serum albumin reversibly, while the combination of ethidium bromide (EthBr) and Hoechst 33258 (2'-(4-hydroxyphenyl)-5-[5-(4-methylpiperazine-1-yl)benzimidazo-2-yl]-benzimidazole) competitive binding study suggests that this complex interacts with ct-DNA through the minor groove binding, which is in agreement with molecular docking study.

Keywords: zinc(II); bipyridine; structural characterization; protein interactions; DNA interactions.

* Corresponding author. E-mail: biljana.glisic@pmf.kg.ac.rs
# Serbian Chemical Society member.
https://doi.org/10.2298/JSC230605066A

INTRODUCTION

Zinc represents an essential trace element for all forms of life.[1] In living systems, the role of zinc can be catalytic or structural, but in some DNA interacting metalloproteins, this metal plays both roles.[2] In the human body, zinc is required for the normal function of immune system, for proper wound healing, the sense of taste and smell, and for the normal growth and development.[3] Besides that, this metal has an important role for the normal function of the brain and can modulate its excitability, and it also influences the learning process.[4] It is also important to mention that zinc supplementation is proposed for application in cancer prevention due to its beneficial effects, such as inhibition of angiogenesis and induction of inflammatory cytokines, leading to the apoptosis of cancer cells.[5]

The great importance of zinc has spawned numerous model complexes and significantly enriched knowledge of its coordination chemistry.[2] In living organisms, zinc exists only in +2 oxidation state, whereby Zn(II) ion has a filled d subshell (d^{10} electronic configuration). In complexes, this metal ion can adopt different coordination number and geometry, including tetrahedrally four-coordinated, trigonal-bipyramidal or square-pyramidal five-coordinated, and octahedrally to trigonal prismatic six-coordinated; all these geometries can also be distorted to different extent.[6] Vahrenkamp proposed that Zn(II) ion acts as both soft and hard Lewis acid, what can be seen from the dominance of the ZnN_2S_2 motif (N represents the donor atom of histidine, while S is from cysteine) in enzymes and zinc fingers.[6] Zinc(II) ion forms tetrahedral complexes with halides and oxygen-donor ligands. Different stable zinc(II) complexes are also known with nitrogen-donor ligands, including amines and azaheterocycles, while some complexes with sulfur-donors have unusual structural properties.[2]

In the last few decades, zinc(II) complexes have attracted great attention for the generation of 1D, 2D and 3D infinite structures and frameworks.[2] Beside its significance in coordination and supramolecular chemistry, numerous zinc(II) complexes have been found to be interesting from the point of view of medicinal chemistry, since these compounds have shown antimicrobial,[7] anticancer,[8] antidiabetic,[9] antioxidant[10] and anti-inflammatory[11] activities. Considering this, we have recently synthesized two mononuclear zinc(II) complexes, $[Zn(py\text{-}2py)X_2]$, X is Cl^- or Br^-, with a 2,2'-bipyridine derivative, namely dimethyl 2,2'-bipyridine-4,5-dicarboxylate (py-2py), and investigated their *in vitro* antimicrobial activity and cytotoxicity on the normal human lung fibroblast cells (MRC-5) and the model organism *Caenorhabditis elegans*.[12] It was found that of the two synthesized zinc(II) complexes, the one with chlorido ligands has shown a higher antifungal activity against the studied *Candida* strains, better ability in preventing *C. albicans* ATCC 10231 biofilm formation, and higher quorum sensing inhibitory potential on the two investigated biosensor strains (*Chromobacterium violaceum*

CV026 and *Serratia marcescens* ATCC 27117).[12] Leading by this study, herein, another 2,2'-bipyridine derivative, namely 4-ethynyl-2,2'-bipyridine (ebpy), reacted with $ZnCl_2$ to yield a mononuclear zinc(II) complex, [Zn(ebpy)Cl_2]. This ligand was previously used for synthesis of platinum(II), ruthenium(II) and rhenium(II) complexes conjugated to vitamin B12 as the formulations of anticancer prodrugs against MCF-7 breast cancer cells.[13] Moreover, a *fac*-$[Mn(CO)_3]^+$ complex bearing ebpy conjugated to vitamin B12, has shown unusual dark and light--induced cytotoxicity.[14] The presently synthesized [Zn(ebpy)Cl_2] complex was characterized by spectroscopy (^{1}H-NMR, IR and UV–Vis) and molar conductivity measurement, while its structure was determined by single-crystal X-ray diffraction analysis. The interactions of this complex with bovine serum albumin (BSA) and calf thymus DNA (ct-DNA) were investigated to check its binding affinity toward these biologically important molecules.

EXPERIMENTAL

Reagents

Zinc(II) chloride, ethanol, acetonitrile, dimethyl sulfoxide (DMSO), deuterated dimethyl sulfoxide (DMSO-d_6), phosphate buffer saline (PBS), bovine serum albumin (BSA), calf thymus DNA (ct-DNA), ethidium bromide (EthBr), Hoechst 33258 (2'-(4-hydroxyphenyl)-5--[5-(4-methylpiperazine-1-yl)benzimidazo-2-yl]-benzimidazole) and *n*-octanol were purchased from the Sigma–Aldrich (St. Louis, MO, USA). All these chemicals were of analytical reagent grade and used without further purification.

Measurements

The elemental analysis of ebpy and [Zn(ebpy)Cl_2] for carbon, hydrogen and nitrogen were performed by the Institute for Information Technologies Kragujevac, University of Kragujevac. The ^{1}H-NMR spectra of ebpy and [Zn(ebpy)Cl_2] were recorded at ambient temperature in DMSO-d_6 on a Varian Gemini 2000 spectrometer at 200 MHz. 5.0 mg of both compounds were dissolved in 0.6 mL of DMSO-d_6 solvent, and the obtained solutions were transferred in 5 mm NMR tube. Chemical shifts, δ, were calibrated relative to those of DMSO-d_6 and are given in ppm, while scalar couplings (J) are reported in Hz. The abbreviations for the peak multiplicities are the follows: *s* (singlet), *d* (doublet), *dd* (doublet of doublets), *t* (triplet) and *m* (multiplet). To follow the solution behaviour of [Zn(ebpy)Cl_2], its ^{1}H-NMR spectrum was recorded right after dissolution of the complex in DMSO-d_6 and after 1 and 2 days standing at ambient temperature. The UV–Vis spectra of ebpy and [Zn(ebpy)Cl_2] were recorded on a Shimadzu UV-1800 spectrophotometer over the wavelength range of 1100–200 nm at ambient temperature. The concentration of solution of these compounds in DMSO used for UV––Vis measurements was 7.41×10^{-5} and 8.40×10^{-5} M, respectively. The measurement of UV––Vis spectrum of [Zn(ebpy)Cl_2] was repeated after 24 and 48 h after its dissolution in DMSO. The IR spectra of ebpy and its zinc(II) complex were recorded on a Perkin Elmer Spectrum 2 spectrometer using KBr pellet technique over the range of 4000–450 cm^{-1} (the used abbreviations: *vs* for very strong, *s* for strong, *m* for medium, *w* for weak). The molar conductivity of [Zn(ebpy)Cl_2] complex was determined on a digital conductivity-meter Crison Multimeter MM 41 after its dissolution in DMSO at ambient temperature at concentration of 1.0×10^{-3} M. Jasco FP-6600 spectrophotometer was used for the measurement of the emission spectra for DNA/BSA interactions of [Zn(ebpy)Cl_2] complex.

Analytical and spectral data, as well as additional details, are given in the Supplementary material to this paper.

Synthesis of ebpy

4-Ethynyl-2,2'-bipyridine (ebpy) was synthesized in accordance with the method previously reported.[15] The purity and constitution of the synthesized compound were confirmed by elemental analysis and ^{1}H-NMR spectroscopy (data given in Supplementary material). The obtained data agree with those for the same compound previously reported.[15]

Synthesis of [Zn(ebpy)Cl$_2$] complex

5.0 mL of ethanolic solution of ebpy (1.0 mmol, 180.1 mg) was added dropwise to a solution of an equimolar amount of $ZnCl_2$ (1.0 mmol, 136.3 mg) in 5.0 mL of ethanol under stirring at ambient temperature. The stirring continued for 3 h at ambient temperature, and after that time, the resulted white precipitate was filtered and recrystallized in acetonitrile. The obtained solution was left to slowly evaporate at ambient temperature. Colorless crystals of [Zn(ebpy)Cl$_2$] complex suitable for single-crystal X-ray analysis were formed after 5 days. Yield: 68 % (215.2 mg).

Crystallographic data collection and refinement of the structure

Crystal data and details of the structure determination for [Zn(ebpy)Cl$_2$] are given in Table S-I of the Supplementary material. A suitable crystal was selected and mounted on a loop in oil on a STOE IPDS 2 diffractometer. The crystal of the complex was kept at 250(2) K during data collection. Using Olex2,[16] the structure was solved with the ShelXT[17] structure solution program using intrinsic phasing and refined with the ShelXL[18] refinement package using least squares minimization.

BSA binding experiment

The protein binding study was performed through fluorescence quenching experiment using BSA (20 μM) in phosphate buffer (PBS, pH 7.4). The quenching of the fluorescence emission intensity of BSA at 366 nm was monitored using [Zn(ebpy)Cl$_2$] as a quencher with the increasing amount (up to 50 μM). The fluorescence emission spectra were recorded in the range of 285–500 nm with an excitation wavelength of 280 nm. It is important to note that the fluorescence spectrum of the [Zn(ebpy)Cl$_2$] in PBS was recorded under the same experimental conditions, and no fluorescence emission was observed.

The Stern–Volmer constant (K_{sv}) for BSA interaction of the [Zn(ebpy)Cl$_2$] was calculated using the following equation:

$$F_0/F = 1 + K_q\tau_0 c(\text{complex}) = 1 + K_{sv}c(\text{complex}) \quad (1)$$

In this equation, F_0 and F represent the emission intensities in the absence and presence of the examined quencher, respectively, K_q is the quenching constant, while τ_0, which amounts 10^{-8} s, is the fluorophore lifetime without the quencher.[19]

The data obtained from the fluorescence measurements were also used to determine the number of the binding sites for the complex to BSA (n) and the equilibrium binding constant, K_A, based on the Scatchard equation:[20]

$$\log (F_0 - F)/F = \log K_A + n\log c(\text{complex}) \quad (2)$$

Lipophilicity assay

The flask-shaking method[21] was used for determination of the partition coefficient (log P) as a measure of lipophilicity for [Zn(ebpy)Cl$_2$]. This complex was dissolved in DMSO and added to water/*n*-octanol system. The obtained solution was vortexed for 1 h at ambient tem-

perature and, after that, left to stand for additional 24 h until the separation of the two phases was achieved. The absorbance value was determined from the calibration curve and used for calculation of the concentration of the complex in *n*-octanol phase (c_o) and water phase (c_w). The following equation was applied for calculation of the log *P* value:

$$\log P = \log (c_O/c_W) \quad (3)$$

DNA binding experiment

PBS buffer was used for the preparation of a stock solution of ct-DNA (1.43×10^{-2} M), which concentration was determined from the UV absorbance value at 260 nm and the molar extinction coefficient, $\varepsilon = 6.6\times10^3$ M^{-1} cm^{-1}.[22] Stock solutions of EthBr (10.1 mM), Hoechst 33258 (10 mM) and zinc(II) complex (10 mM) were prepared in DMSO.

The competitive binding studies were performed at pH 7.4 in PBS, whereas the ratio [ct-DNA]:[EthBr/Hoechst 33258] was 10:1, while the concentration of the complex gradually increased (up to 100 μM). The spectra for the competitive interaction between EthBr and the complex toward ct-DNA were measured in the range of 525–750 nm, with the excitation wavelength of 520 nm, while the range for Hoechst 33258 competitive binding study was 351–750 nm, with the excitation wavelength of 346 nm. The K_{sv}, K_q and K_A constants, and the *n* number were calculated as described above for BSA binding experiment.[19,20]

Docking study

Docking calculations were performed as previously described.[23] The DNA target for the investigated zinc(II) complex was selected from Protein Data Bank (pdb code: 1BNA), as the double stranded (d(CpGpCpGpApApTpTpCpGpCpG) dodecamer with two G≡C rich regions flanking one A=T rich region.[24] Molecular docking calculations were carried out with the AutoDock Vina (version 1.2.0)[25] and the AutoDock4 (version 4.2.6)[26] software packages. The Biovia Discovery Studio Visualizer software (version 21.1.0.20298) was employed to analyze possible interactions between the complex and the DNA target.

RESULTS AND DISCUSSION

The ligand 4-ethynyl-2,2'-bipyridine (ebpy) was prepared in accordance with the method previously described[15] and its purity was confirmed by elemental analysis and ^{1}H-NMR spectroscopy. Zinc(II) complex, [Zn(ebpy)Cl_2], was synthesized by mixing equimolar amounts of $ZnCl_2$ and ebpy in ethanol at ambient temperature (Scheme 1).

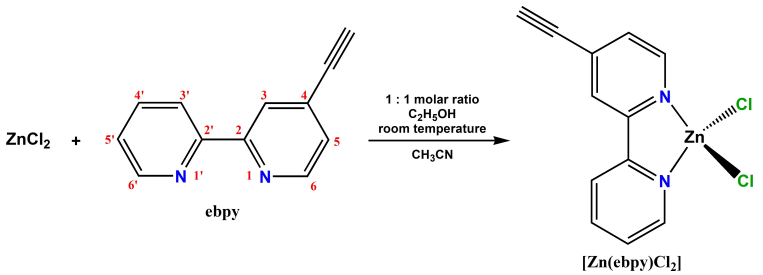

Scheme 1. Schematic presentation of the synthesis of [Zn(ebpy)Cl_2]. Numeration of atoms in ebpy was done in accordance with IUPAC recommendations and does not match that applied in the X-ray analysis of zinc(II) complex.

The obtained white precipitate was filtered and recrystallized in acetonitrile to yield the colourless crystals of [Zn(ebpy)Cl_2] suitable for single-crystal X-ray diffraction analysis. In addition, ^{1}H-NMR, IR and UV–Vis spectroscopy and molar conductivity measurement were applied for characterization of the synthesized complex.

Solid state studies

The [Zn(ebpy)Cl_2] complex crystallizes in the monoclinic space group $P2_1/m$. The molecular structure of this complex with the anisotropic displacement ellipsoids and the atom numbering scheme is shown in Fig. 1, while its selected bond lengths (Å) and bond angles (°) with the estimated standard deviations are presented in Table S-II of the Supplementary material.

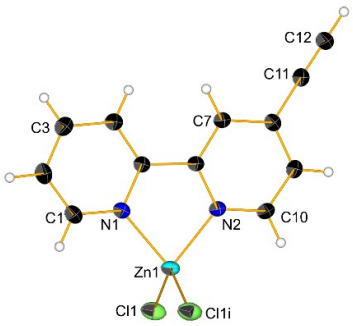

Fig. 1. Molecular structure of [Zn(ebpy)Cl_2] complex. Displacement ellipsoids are drawn at 50 % probability level and H atoms are represented by spheres of arbitrary size. Symmetry code: (*i*) *x*, 1/2–*y*, *z*.

As can be seen in Fig. 1, [Zn(ebpy)Cl_2] complex is a mononuclear species, in which the Zn(II) ion is coordinated by the ebpy acting as a bidentate ligand through its two nitrogen atoms and two chlorido ligands resulting in N_2Cl_2 coordination environment around the metal ion. The complex adopts a slightly distorted tetrahedral geometry, with the value of tetrahedral index τ_4[27] of 0.92. This tetrahedral index can be calculated as:

$$\tau_4 = (360° - (\beta + \alpha))/141° \quad (4)$$

where β and α are the largest angles around the Zn(II) ion (β = Cl1^i–Zn1–Cl1= = 116.77(4)° and α = N1–Zn1–Cl1^i = 113.93(3)°), while τ_4 value for the ideal tetrahedral geometry amounts 1.[27] This distortion from the ideal tetrahedral geometry can be attributed to the relatively low bite angle of ebpy of 80.46(10)°. The bond lengths and angles presented in Table S-II for [Zn(ebpy)Cl_2] are in accordance with those reported in the Cambridge Crystallographic Database (version 5.44, April 2023)[28] for the structurally similar zinc(II) complexes with bidentately coordinated 2,2'-bipyridine and its substituted derivatives. In the crystal structure of the [Zn(ebpy)Cl_2] complex, stacking interactions (π–π and weak C–H···X) are present and can contribute to the stabilization of the structure.

IR spectroscopy is a useful tool for identification of functional groups in a molecule, since each chemical bond has a specific energy absorption band. The IR spectrum of [Zn(ebpy)Cl_2] complex in the range of 4000–450 cm^{-1} agrees with its structure determined by single-crystal X-ray diffraction analysis. In this spectrum, the bands attributed to the characteristic vibrations of ebpy coordinated to the Zn(II) ion can be detected. Thus, the bands at 3215, 2109 and 623 cm^{-1} in the IR spectrum of the synthesized zinc(II) complex can be ascribed to $\nu(C_{alkyne}–H)$, $\nu(C\equiv C)$ and $\gamma(C_{alkyne}–H)$ vibrations, respectively, suggesting the presence of terminal alkyne (*i.e.*, monosubstituted) in its structure. The other most important bands are those which originate from the vibrations of heteroaromatic rings (analytical data are given in the Supplementary material).

Solution studies

^{1}H-NMR spectra of ebpy and [Zn(ebpy)Cl_2] were recorded in DMSO-d_6 to verify the coordination mode of this ligand to the Zn(II) ion in solution (Fig. S--1). As can be seen from Fig. S-1, the number of signals due to the ebpy in the zinc(II) complex was the same as that of the free ligand. Four resonances at δ 7.67, 8.12, 8.57 and 8.72 ppm are observed in the aromatic region of the ^{1}H--NMR spectrum of [Zn(ebpy)Cl_2] complex, due to C5H/C5'H, C4'H, C3H/C3'H and C6H/C6'H protons, respectively. In most cases, the chemical shifts of these protons are downfield shifted from those of the corresponding protons of uncoordinated ebpy. It is interesting to mention that the $\Delta(^1H)_{coord}$ coordination shift (determined in respect to uncoordinated ebpy) for C3H/C3'H protons (+0.18 ppm) is larger than those for C6H/C6'H protons (+0.00 ppm), which are adjacent to the pyridine nitrogen binding atoms (Fig. S-1). These protons appear at δ 8.39 and 8.72 ppm in the ^{1}H-NMR spectrum of the uncoordinated ebpy ligand, respectively. In the aliphatic region of the ^{1}H-NMR spectrum of [Zn(ebpy)Cl_2], a signal due to the acetylene proton is present at 4.84 ppm and it is shifted downfield after ebpy ligand coordination to the Zn(II) ion ($\Delta(^1H)_{coord}$ = +0.15 ppm). It is important to note that there are no visible changes in ^{1}H-NMR spectrum of [Zn(ebpy)Cl_2] recorded 2 days after its dissolution in DMSO-d_6 in respect to that recorded immediately (Fig. S-2), confirming the bidentate coordination of ebpy to the Zn(II) ion over this time period.

Non-electrolytic nature of [Zn(ebpy)Cl_2] in DMSO solution was confirmed by molar conductivity measurement.[29] Furthermore, the value of the molar conductance of this complex determined immediately after its dissolution (4.82 Ω^{-1} cm^2 mol^{-1}) remains almost the same for 2 days.

The UV–Vis spectrum of [Zn(ebpy)Cl_2] was recorded in DMSO at ambient temperature and compared with the corresponding spectrum of ebpy ligand. By comparison of these two spectra, it can be concluded that the absorbance peak at 283 nm and a shoulder at 308 nm in the UV–Vis spectrum of [Zn(ebpy)Cl_2] are

due to the intra-ligand charge transfer transitions.[30] With the aim to additionally confirm the stability of [Zn(ebpy)Cl_2] complex in DMSO, the measurement of its UV–Vis spectrum was repeated 24 and 48 h after its dissolution (Fig. S-3). As can be seen, the shape of spectra, position, and intensity of the absorption maxima of [Zn(ebpy)Cl_2] did not change for the investigated period, additionally confirming its solution stability.

BSA binding study

Serum albumin, the most abundant protein in the bloodstream, has a significant role in the transport of various compounds to the target organs and tissues. In the present study, fluorescence emission spectroscopy was used for studying the interaction of the [Zn(ebpy)Cl_2] with bovine serum albumin, BSA. After addition of this complex to BSA solution (20 μM), a decrease of the BSA fluorescence intensity was observed (33 % of its initial intensity), suggesting that [Zn(ebpy)Cl_2] complex interacts with the studied protein (Fig. 2). As a result of this interaction, a blue shift of 3 nm in the emission maximum was observed, being in accordance with the binding of zinc(II) complex with the hydrophobic active site of BSA.[31]

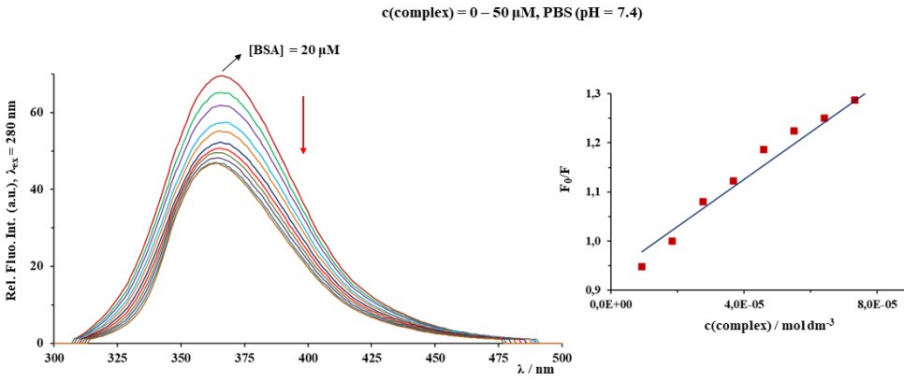

Fig. 2. Fluorescence emission spectra of BSA in the presence of an increasing amount of [Zn(ebpy)Cl_2]. The red arrow shows the changes of fluorescence intensity after the addition of this complex. Stern–Volmer plot of F_0/F *vs.* *c*(complex) is inserted.

The fluorescence quenching data for [Zn(ebpy)Cl_2] was analyzed using the Stern–Volmer and Scatchard equations given in the Experimental section. The determined values of K_{sv}, K_q and K_A constants, and *n* number of binding sites of the zinc(II) complex per BSA are given in Table I. These values indicate that [Zn(ebpy)Cl_2] has a moderate affinity toward BSA, whereas one site per protein is available for its binding. The BSA binding constants of the recently synthesized [Zn(py-2py)X_2] complexes, X is Cl^- or Br^-, py-2py is dimethyl 2,2'-bipyr-

idine-4,5-dicarboxylate,[12] are 3.5 – 100 fold higher than those calculated for [Zn(ebpy)Cl_2] complex. Considering that the value of K_q constant for [Zn(ebpy)Cl_2] complex is higher than the limiting diffusion rate constant of the biomolecule (2×10^{10} M^{-1} s^{-1}),[32] it can be concluded that the mechanism of BSA fluorescence quenching is static. Although the value of K_A constant for the investigated complex shows its affinity for BSA, it is significantly lower than 10^{15} M^{-1}.[33] This indicates that upon arrival to the target site, [Zn(ebpy)Cl_2] will be released from the serum protein.

TABLE I. Values of binding constants of [Zn(ebpy)Cl_2] with BSA

K_{sv} / M^{-1}	Hypochromism, %	K_q / M^{-1} s^{-1}	K_A / M^{-1}	n
$(5.13\pm0.02)\times10^3$	33.5	5.13×10^{11}	2.35×10^3	0.90

Lipophilicity assay

The lipophilicity of a compound, expressed as a partition coefficient (log P) between the hydrophobic octanol phase and the hydrophilic water phase, indicates its ability to be transported through the lipid structures.[21] The log P value for [Zn(ebpy)Cl_2] is 1.35, being in the range of −0.4 to 5.6, reported previously for different therapeutic agents.[34] Besides that, the molecular weight of this complex is lower than 500, and follows the Lipinski's rule of five for orally used therapeutic agents.[35]

DNA competitive binding study

To further investigate the reactivity of [Zn(ebpy)Cl_2] towards DNA as a potential biological target, its interaction with ct-DNA was followed using the fluorescence quenching method in a competitive study with an intercalator ethidium bromide (EthBr) and with a minor groove binder Hoechst 33258 (2'-(4-hydroxyphenyl)-5-[5-(4-methylpiperazine-1-yl)benzimidazo-2-yl]-benzimidazole; Hoe). The emission spectra of ct-DNA–EthBr and ct-DNA–Hoe solutions, in which the ratio [ct-DNA]:[EthBr/Hoe] is 10:1, were recorded after the adding the increasing concentration of the [Zn(ebpy)Cl_2] (0–100 μM). The fluorescence titration spectra are presented in Fig. 3, while the corresponding numerical data calculated by the Stern–Volmer and Scatchard equations are given in Table II.

As it was mentioned above, EthBr intercalates between adjacent base pairs in the ct-DNA double helix, leading to the fluorescence enhancement.[19] After addition of an investigated compound, a decrease in the fluorescence emission intensity of the ct-DNA–EthBr system will be observed if it substitutes EthBr and intercalates into ct-DNA or if it binds to this system and forms a non-fluorescent species.[19] As can be seen from Table II, the value of K_A constant for binding of [Zn(ebpy)Cl_2] to the ct-DNA–EthBr system is significantly lower than that for EthBr ($K_A = 2\times10^6$ M^{-1}),[32] being in accordance with its non-intercalative nature.

This is also in accordance with the very low percentage of hypochromism of only 6% (Table II). On the other hand, the value of K_A constant for binding of [Zn(ebpy)Cl$_2$] to the ct-DNA–Hoe system, with the order being 10^4, shows the possibility of its interaction with ct-DNA *via* minor groove binding. In both cases, the values of K_q constants indicate that the mechanism of fluorescence quenching is static.[32]

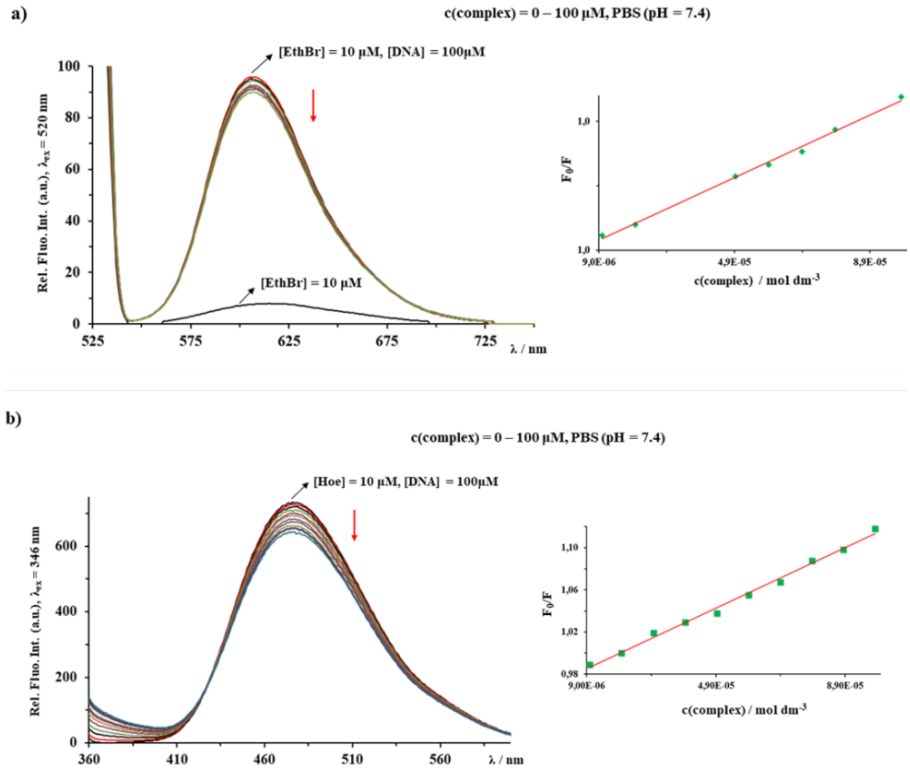

Fig. 3. Fluorescence emission spectra of: a) ct-DNA–EthBr and b) ct-DNA–Hoe systems in the presence of an increasing concentration of [Zn(ebpy)Cl$_2$]. The red arrows show the changes of fluorescence intensity after the adding the zinc(II) complex. Stern–Volmer plots of F_0/F *vs.* *c*(complex) are also inserted.

The non-intercalative nature and minor groove binding of [Zn(ebpy)Cl$_2$] were confirmed by docking calculations using a double stranded d(CpGpCpGpApApTpTpCpGpCpG) dodecamer (Fig. 4). Molecular docking results indicate that minor groove binding is the most stable binding mode for [Zn(ebpy)Cl$_2$]. The binding energy (or docking affinity) of the complex for the

model dodecamer is –6.7 kcal* mol^{-1}. The [Zn(ebpy)Cl$_2$] does not intercalate into base pairs. Its docking mode is not stabilized by π–π stacking interactions, but only by long distance, rather weak coulombic interactions between the Zn(II) ion and the negatively charged phosphates in the DNA backbone.

TABLE II. Values of binding constants of [Zn(ebpy)Cl$_2$] with ct-DNA in the presence of EthBr and Hoe

Binding structure	K_{sv} / 10^2 M^{-1}	Hypochromism, %	K_q / 10^{11} M^{-1} s^{-1}	K_A / M^{-1}	n
ct-DNA–EthBr	5.87±0.01	6.1	0.587	67.6	0.77
ct-DNA–Hoe	14.8±0.1	12.2	1.48	1.09×10^4	1.22

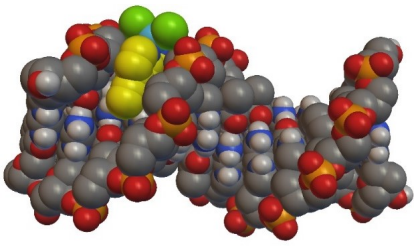

Fig. 4. Space-filling model of computer-generated lowest energy binding pose of [Zn(ebpy)Cl$_2$] with DNA (d(CpGpCpGpApApTpTpCpGpCpG) dodecamer sequence).

CONCLUSION

We have shown that the reaction between equimolar amounts of 4-ethynyl-2,2'-bipyridine (ebpy) and ZnCl$_2$ in ethanol leads to the formation of mononuclear zinc(II) complex, [Zn(ebpy)Cl$_2$]. The crystallographic results revealed that this complex has a slightly distorted tetrahedral geometry with ebpy being bidentately coordinated to the Zn(II) ion, while the remaining two sites are occupied by chlorido ligands. The synthesized [Zn(ebpy)Cl$_2$] complex has an affinity to bind to BSA reversibly, while toward ct-DNA, it behaves as a minor groove binder. Considering the biological importance of zinc(II) complexes and their potential application as metal-based therapeutics, further studies will be aimed on the investigation of antimicrobial and antiproliferative activities of the presently synthesized zinc(II) complex and its structural analogues.

SUPPLEMENTARY MATERIAL

Additional data and information are available electronically at the pages of journal website: https://www.shd-pub.org.rs/index.php/JSCS/article/view/12428, or from the corresponding author on request. CCDC 2266337 contains the supplementary crystallographic data for this article. These data can be obtained free of charge from The Cambridge Crystallographic Data Centre via https://www.ccdc.cam.ac.uk/structures/.

Acknowledgements. This research has received funding from the Ministry of Science, Technological Development and Innovation of the Republic of Serbia (Agreements No. 451-

* 1 kcal = 4184 J

-03-47/2023-01/200122 and 451-03-47/2023-01/200378) and the Serbian Academy of Sciences and Arts under project No. F128.

ИЗВОД

СТРУКТУРА И ИСПИТИВАЊЕ DNA/BSA ИНТЕРАКЦИЈА КОМПЛЕКСА ЦИНКА(II) СА 4-ЕТИНИЛ-2,2'-БИПИРИДИНОМ

ТИНА П. АНДРЕЈЕВИЋ[1], ДАРКО П. АШАНИН[2], AURÉLIEN CROCHET[3], НЕВЕНА Љ. СТЕВАНОВИЋ[1], ИВАНА ВУЧЕНОВИЋ[4], FABIO ZOBI[3], МИЛОШ И. ЂУРАН[5] и БИЉАНА Ђ. ГЛИШИЋ[1]

[1]Универзитет у Крагујевцу, Природно–математички факултет, Институт за хемију, Р. Домановића 12, 34000 Крагујевац, [2]Универзитет у Крагујевцу, Институт за информационе технологије Крагујевац, Департман за природно-математичке науке, Јована Цвијића бб, 34000 Крагујевац, [3]University of Fribourg, Department of Chemistry, Chemin du Musée 9, CH-1700 Fribourg, Switzerland, [4]Универзитет у Нишу, Пољопривредни факултет Крушевац, Косанчићева 4, 37000 Крушевац и [5]Српска академија наука и уметности, Кнез Михаилова 35, 11000 Београд

У овом раду, синтетисан је и применом спектроскопских (^{1}H-NMR, IR и UV–Vis) метода и мерењем моларне проводљивости окарактерисан комплекс цинка(II) са 4-етинил-2,2'-бипиридином (ebpy), [Zn(ebpy)Cl_2]. Кристална структура [Zn(ebpy)Cl_2] комплекса је одређена применом дифракције X-зрака са монокристала, при чему су добијени кристалографски подаци потврдили да се ebpy лиганд бидентатно координује за јон метала преко два атома азота, док преостала два координациона места заузимају два хлоридо лиганда. У циљу одређивања реактивности синтетисаног комплекса цинка(II) са биолошки значајним молекулима, испитиване су његове интеракције са ДНК молекулом тимуса телета (ct-DNA) и албумином говеђег серума (BSA) применом флуоресцентне емисионе спектроскопије. На основу добијених спектроскопских резултата, може се закључити да се [Zn(ebpy)Cl_2] комплекс реверзибилно везује за BSA, док компетитивно испитивање везивања етидијум-бромида (EthBr) и Hoechst 33258 (2'-(4-хидроксифенил)-5-[5-(4-метилпиперазин-1-ил)бензимидазо-2-ил]-бензимидазол) указује да се цинк(II) комплекс везује за ct-DNA преко малог жлеба, што је у складу са резултатима молекулског доковања.

(Примљено 5. јуна, ревидирано 22. јуна, прихваћено 8. септембра 2023)

REFERENCES

1. S. Frassinetti, G. L. Bronzetti, L. Caltavuturo, M. Cini, C. Della Croce, *J. Environ. Pathol. Toxicol. Oncol*. **25** (2006) 597 (https://dx.doi.org/10.1615/JEnvironPatholToxicolOncol.v25.i3.40)
2. J. Burgess, R. H. Prince, in *Encyclopedia of Inorganic Chemistry*, John Wiley & Sons, Ltd., New York, 2006 (https://dx.doi.org/10.1002/0470862106.ia260)
3. J. Osredkar, N. Sustar, *J. Clin. Toxicol*. **S3** (2011) 495 (https://doi.org/0.4172/2161-0495.S3-001)
4. B. K. Y. Bitanihirwe, M. G. Cunningham, *Synapse* **63** (2009) 1029 (https://doi.org/10.1002/syn.20683)
5. A. S. Prasad, F. W. J. Beck, D. C. Snell, M. Kucuk, *Nutr. Cancer* **61** (2009) 879 (https://doi.org/10.1080/01635580903285122)
6. H. Vahrenkamp, *Dalton Trans*. (2007) 4751 (https://doi.org/10.1039/B712138E)
7. S. N. Sovari, F. Zobi, *Chemistry* **2** (2020) 418 (https://doi.org/10.3390/chemistry2020026)
8. M. Pellei, F. Del Bello, M. Porchia, C. Santini, *Coord. Chem. Rev.* **445** (2021) 214088 (https://doi.org/10.1016/j.ccr.2021.214088)

9. Y. Yoshikawa, H. Yasui, *Curr. Top. Med. Chem.* **12** (2012) 210 (https://doi.org/10.2174/156802612799078874)
10. G. Psomas, *Coord. Chem. Rev.* **412** (2020) 213259 (https://doi.org/10.1016/j.ccr.2020.213259)
11. Q. Zhou, T. W. Hambley, B. J. Kennedy, P. A. Lay, P. Turner, B. Warwick, J. R. Biffin, H. L. Regtop, *Inorg. Chem*. **39** (2000) 3742 (https://doi.org/10.1016/10.1021/ic991477i)
12. T. P. Andrejević, I. Aleksic, J. Kljun, B. V. Pantović, D. Milivojevic, S. Vojnovic, I. Turel, M. I. Djuran, B. Đ. Glišić, *Inorganics* **10** (2022) 71 (https://doi.org/10.3390/inorganics10060071)
13. J. Rossier, D. Hauser, E. Kottelat, B. Rothen-Rutishauser, F. Zobi, *Dalton Trans*. **46** (2017) 2159 (https://doi.org/10.1039/C6DT04443C)
14. J. Rossier, J. Delasoie, L. Haeni, D. Hauser, B. Rothen-Rutishauser, F. Zobi, *J. Inorg. Biochem*. 209 (2020) 111122 (https://doi.org/10.1016/j.jinorgbio.2020.111122)
15. N. Zabarska, D. Sorsche, F. W. Heinemann, S. Glump, S. Rau, *Eur. J. Inorg. Chem.* **2015** (2015) 4869 (https://doi.org/10.1002/ejic.201500630)
16. O. V. Dolomanov, L. J. Bourhis, R. J. Gildea, J. A. K. Howard, H. Puschmann, *J. Appl. Crystallogr.* **42** (2009) 339 (https://doi.org/10.1107/S0021889808042726)
17. G. M. Sheldrick, *Acta Crystallogr., A* **71** (2015) 3 (https://doi.org/10.1107/S2053273314026370)
18. G. M. Sheldrick, *Acta Crystallogr., C* **71** (2015) 3 (https://doi.org/10.1107/S2053229614024218)
19. P. Smoleński, C. Pettinari, F. Marchetti, M. F. C. Guedes da Silva, G. Lupidi, G. V. B. Patzmay, D. Petrelli, L. A. Vitali, A. J. L. Pomberio, *Inorg. Chem.* **54** (2015) 434 (https://doi.org/10.1021/ic501855k)
20. D. S. Raja, N. S. P. Bhuvanesh, K. Natarajan, *Inorg. Chem.* **50** (2011) 12852 (https://doi.org/10.1021/ic2020308)
21. C. A. Puckett, J. K. Barton, *J. Am. Chem. Soc.* **129** (2007) 46 (https://doi.org/10.1021/ja0677564)
22. R. Bera, B. K. Sahoo, K. S. Ghosh, S. Dasgupta, *Int. J. Biol. Macromol.* **42** (2008) 14 (https://doi.org/10.1016/j.ijbiomac.2007.08.010)
23. K. Schindler, Y. Cortat, M. Nedyalkova, A. Crochet, M. Lattuada, A. Pavic, F. Zobi, *Pharmaceuticals* **15** (2022) 1107 (https://doi.org/10.3390/ph15091107)
24. H. R. Drew, R. M. Wing, T. Takano, C. Broka, S. Tanaka, K. Itakura, R. E. Dickerson, *Proc. Natl. Acad. Sci. U.S.A.* **78** (1981) 2179 (https://doi.org/10.1073/pnas.78.4.2179)
25. O. Trott, A. J. Olson, *J. Comput. Chem*. **31** (2010) 455 (https://doi.org/10.1002/jcc.21334)
26. G. M. Morris, R. Huey, W. Lindstrom, M. F. Sanner, R. K. Belew, D. S. Goodsell, A. J. Olson, *J. Comput. Chem.* **30** (2009) 2785 (https://doi.org/10.1002/jcc.21256)
27. L. Yang, D.R. Powell, R. P. Houser, *Dalton Trans*. (2007) 955 (https://doi.org/10.1039/B617136B)
28. F. H. Allen, *Acta Crystallogr.,B* **58** (2002) 380 (https://doi.org/10.1107/S0108768102003890)
29. I. Ali, W. A. Wani, K. Saleem, *Synth. React. Inorg. Met.-Org. Chem.* **43** (2013) 1162 (https://doi.org/10.1080/15533174.2012.756898)
30. T. P. Andrejević, B. Warżajtis, B. Đ. Glišić, S. Vojnovic, M. Mojicevic, N. Lj. Stevanović, J. Nikodinovic-Runic, U. Rychlewska, M. I. Djuran, *J. Inorg. Biochem.* **208** (2020) 111089 (https://doi.org/10.1016/j.jinorgbio.2020.111089)
31. V. T. Yilmaz, C. Icsel, J. Batur, S. Aydinlik, M. Cengiz, O. Buyukgungor, *Dalton Trans*. **46** (2017) 8110 (https://doi.org/10.1039/c7dt01286a)

32. Y. Shi, C. Guo, Y. Sun, Z. Liu, F. Xu, Y. Zhang, Z. Wen, Z. Li, *Biomacromolecules* **12** (2011) 797 (https://doi.org/10.1021/bm101414w)
33. O. H. Laitinen, V. P. Hytönen, H. R. Nordlund, M. S. Kulomaa, *Cell. Mol. Life Sci.* **63** (2006) 2992 (https://doi.org/10.1007/s00018-006-6288-z)
34. A. K. Ghose, V. N. Viswanadhan, J. J. Wendoloski, *J. Comb. Chem.* **1** (1999) 55 (https://doi.org/10.1021/cc9800071)
35. C. A. Lipinski, F. Lombardo, B. W. Dominy, P. J. Feeney, *Adv. Drug Deliv. Rev.* **23** (1997) 3 (https://doi.org/10.1016/S0169-409X(96)00423-1).

Journal of the Serbian Chemical Society
JSCS@tmf.bg.ac.rs • www.shd.org.rs/JSCS
J. Serb. Chem. Soc. *88* (12) S371–S374 (2023) *Supplementary material*

SUPPLEMENTARY MATERIAL TO

Structure and DNA/BSA binding study of zinc(II) complex with 4-ethynyl-2,2'-bipyridine

TINA P. ANDREJEVIĆ[1], DARKO P. AŠANIN[2], AURÉLIEN CROCHET[3], NEVENA LJ. STEVANOVIĆ[1], IVANA VUČENOVIĆ[4], FABIO ZOBI[3], MILOŠ I. DJURAN[5] and BILJANA Đ. GLIŠIĆ[1]*

[1]University of Kragujevac, Faculty of Science, Department of Chemistry, R. Domanovića 12, 34000 Kragujevac, Serbia, [2]University of Kragujevac, Institute for Information Technologies Kragujevac, Department of Science, Jovana Cvijića bb, 34000 Kragujevac, Serbia, [3]University of Fribourg, Department of Chemistry, Chemin du Musée 9, CH-1700 Fribourg, Switzerland, [4]University of Niš, Faculty of Agriculture Kruševac, Kosančićeva 4, 37000 Kruševac, Serbia and [5]Serbian Academy of Sciences and Arts, Knez Mihailova 35, 11000 Belgrade, Serbia

J. Serb. Chem. Soc. *88* (12) (2023) 1293–1306

TABLE OF CONTENTS

* Corresponding author. E-mail: biljana.glisic@pmf.kg.ac.rs

ANALYTICAL DATA FOR EBPY LIGAND AND THE COMPLEX

Anal. Calcd. for $C_{12}H_8N_2$ (MW 180.21): C, 79.98; H, 4.47; N, 15.55 %. Found: C, 79.82; H, 4.52; N, 15.68 %. ^{1}H NMR (200 MHz, DMSO-d_6): δ = 4.69 (*s*, 1H, CCH), 7.52 (*m*, 2H, C5H and C5'H), 7.98 (*dd*, J = 8.6, 6.9 Hz, 1H, C4'H), 8.39 (*d*, J = 6.9 Hz, 2H, C3H and C3'H), 8.72 (*d*, J = 5.0 Hz, C6H and C6'H) ppm. IR (KBr, ν, cm^{-1}): 3224m (ν(C_{alkyne}–H)), 3059w, 3029w, 3011w (ν(C_{ar}–H)), 2108m (ν(C≡C)), 1584vs, 1564m, 1540s, 1457vs (ν(C_{ar}=C_{ar}) and ν(C_{ar}=N)), 794s (γ(C_{ar}–H)), 626m (γ(C_{alkyne}–H)). UV-Vis (DMSO, λ_{max}, nm): 283 (ε = 1.0 × 10^4 M^{-1} cm^{-1}), 308 (*sh*, ε = 5.3 × 10^3 M^{-1} cm^{-1}). Λ_M (DMSO): 1.50 Ω^{-1}cm^{2}mol^{-1}.

Anal. Calcd. for $C_{12}H_8Cl_2N_2Zn$ (MW 316.47): C, 45.54; H, 2.55; N, 8.85 %. Found: C, 45.41; H, 2.52; N, 8.92 %. ^{1}H NMR (200 MHz, DMSO-d_6): δ = 4.84 (*s*, 1H, CCH), 7.67 (*m*, 2H, C5H and C5'H), 8.12 (*t*, J = 7.4 Hz, 1H, C4'H), 8.57 (*s*, 2H, C3H and C3'H), 8.72 (*d*, J = 4.8 Hz, C6H and C6'H) ppm. IR (KBr, ν, cm^{-1}): 3215s (ν(C_{alkyne}–H)), 3114w, 3080w, 3057w (ν(C_{ar}–H)), 2109m (ν(C≡C)), 1604vs, 1571w, 1542m, 1480m, 1440s, 1406s (ν(C_{ar}=C_{ar}) and ν(C_{ar}=N)), 792s (γ(C_{ar}–H)), 623m (γ(C_{alkyne}–H)). UV-Vis (DMSO, λ_{max}, nm): 283 (ε = 9.3 × 10^3 M^{-1} cm^{-1}), 308 (*sh*, ε = 4.8 × 10^3 M^{-1} cm^{-1}). Λ_M (DMSO): 4.82 Ω^{-1}cm^{2}mol^{-1}.

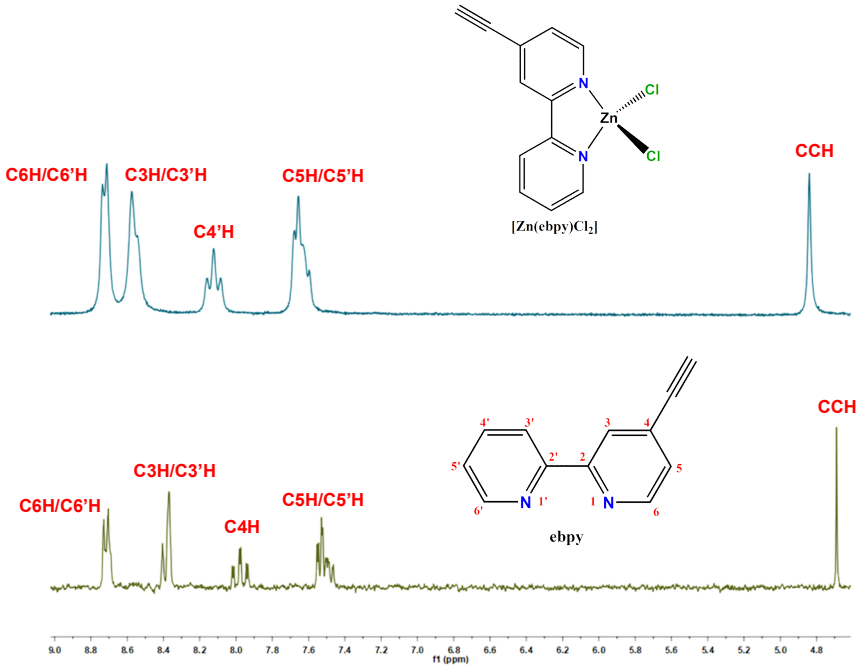

Fig. S-1. The parts of ^{1}H NMR spectrum of [Zn(ebpy)Cl_2] measured in DMSO-d_6 in comparison to that of ebpy.

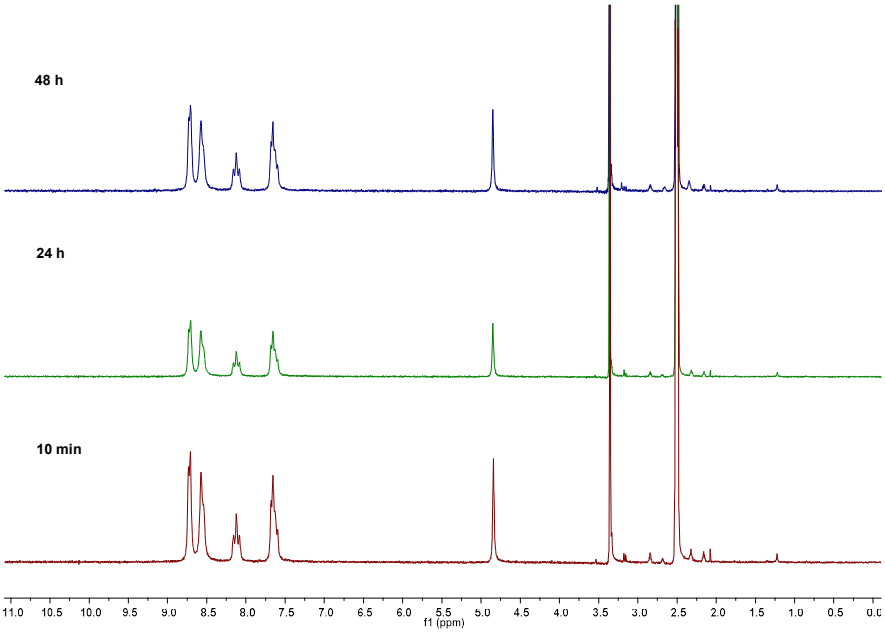

Fig. S-2. Time-dependent ^{1}H NMR spectra of [Zn(ebpy)Cl$_2$] measured in DMSO-d_6 at ambient temperature over 48 h.

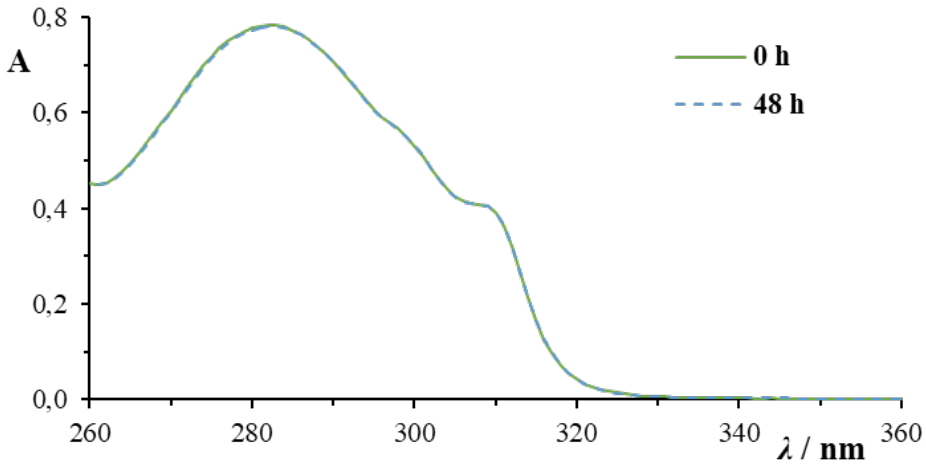

Fig. S-3. UV-Vis spectra of [Zn(ebpy)Cl$_2$] measured in DMSO right after its dissolution and after 48 h standing at ambient temperature.

TABLE S-I. Details of the crystal structure determination of $[Zn(ebpy)Cl_2]$

	$[Zn(ebpy)Cl_2]$
Empirical formula	$C_{12}H_8Cl_2N_2Zn$
Molecular weight	316.47
Crystal system, space group	monoclinic, $P2_1/m$
a (Å)	7.9738(7)
b (Å)	7.2991(8)
c (Å)	11.0462(10)
β (°)	98.749(7)
V (Å^3)	635.43(11)
F_{000}	316
Z	2
X-radiation, λ /Å	Mo-K_α 0.71073
data collect. temperat. / K	250(2)
Calculated density (g cm^{-3})	1.654
Absorption coefficient (mm^{-1})	2.329
Crystal size (mm^3)	0.19 × 0.143 × 0.08
2θ range (°)	3.73 to 52.644
index ranges h, k, l	-9 ... 9, -9 ... 9, -13 ... 13
No. of collected and independent reflections	5319, 1363
R_{int}	0.0361
Data / restraints / parameters	1363 / 0 / 100
Goodness-on-fit on F^2	1.079
Final R indices [$I \geq 2\sigma(I)$]	0.0280, 0.0660
Final R indices (all data)	0.0332, 0.0702
Difference density: max, min (e Å^{-3})	0.27, -0.33
CCDC number	2266337

TABLE S-II. Selected bond distances (Å) and valence angles (°) in $[Zn(ebpy)Cl_2]$

$[Zn(ebpy)Cl_2]$	
Zn1—N1	2.045(3)
Zn1—N2	2.048(3)
Zn1—Cl1	2.1981(7)
Cl1^i—Zn1—Cl1	116.77(4)
N1—Zn1—Cl1^i	113.93(3)
N1—Zn1—Cl1	113.93(3)
N1—Zn1—N2	80.46(10)
N2—Zn1—Cl1^i	113.25(3)
N2—Zn1—Cl1	113.25(3)
C1—N1—Zn1	126.5(2)
C5—N1— Zn1	114.5(2)
C6—N2— Zn1	114.2(2)
C10—N2— Zn1	126.8(2)

Symmetry code: (i) x, 1/2-y, z

Journal of the Serbian Chemical Society
JSCS@tmf.bg.ac.rs • www.shd.org.rs/JSCS
J. Serb. Chem. Soc. 88 (12) 1307–1317 (2023)
JSCS–5697
Original scientific paper
Published 19 December 2023

DNA/BSA interactions and cytotoxic studies of tetradentate *N*,*N*,*O*,*O*-Schiff base copper(II) complexes

ALEKSANDAR MIJATOVIĆ[1#], ANGELINA Z. CAKOVIĆ[2#], ALEKSANDAR LOLIĆ[3], SNEŽANA SRETENOVIĆ[4], MARKO N. ŽIVANOVIĆ[5], DRAGANA S. ŠEKLIĆ[5], JOVANA BOGOJESKI[2#] and BILJANA V. PETROVIĆ[2*#]

[1]*University of Belgrade – Faculty of Mining and Geology, Đušina 7, 11000 Belgrade, Serbia,* [2]*University of Kragujevac, Faculty of Science, R. Domanovića 12, 34000 Kragujevac, Serbia,* [3]*University of Belgrade – Faculty of Chemistry, Studentski trg 12–16, 11000 Belgrade, Serbia,* [4]*University of Kragujevac, Faculty of Medicinal Science, Department of Internal medicine, S. Markovic 69, 34000 Kragujevac, Serbia and* [5]*University of Kragujevac, Institute for Information Technologies Kragujevac, Jovana Cvijića bb, 34000 Kragujevac, Serbia*

(Received 14 June, revised 18 June, accepted 8 September 2023)

Abstract: Three Schiff base Cu(II) complexes, (*N*,*N'-bis*(acetylacetone)propylenediimine)copper(II) complex, [Cu(acac$_2$pn)] (**1**), (*N*,*N'-bis*-(benzoylacetone)propylenediimine)copper(II) complex, [Cu(phacac$_2$pn)] (**2**) and (*N*,*N'-bis*--(trifluoroacetylacetone)propylenediimine)copper(II) complex, [Cu(tfacac$_2$pn)] (**3**), were used to investigate the interactions with calf thymus DNA (ct-DNA) and bovine serum albumin (BSA) using the electronic absorption and spectroscopic fluorescence methods. UV–Vis absorption studies showed that studied complexes interact with DNA molecule and exhibit moderate binding affinity. Fluorescence studies of complexes **1**–**3** also showed a possibility for DNA intercalation as well as a relatively high binding ability toward BSA. Among the tested complexes, the highest affinity for DNA and BSA molecules was shown by complex **1**. Cytotoxic analyses, performed on human colorectal carcinoma HCT-116 and healthy lung fibroblast MRC-5 cell lines, showed that complex **2** exhibited activity on both cell lines, while complexes **1** and **3** did not show any activity.

Keywords: antitumor; mechanism; cell line; biomolecule; affinity; drug design.

INTRODUCTION

Inorganic medicinal chemistry is an extensive interdisciplinary field in which main research areas is focused on the design and synthesis of transition metal ion complexes as new anticancer agents. Within the transition metals,

* Corresponding author. E-mail: biljana.petrovic@pmf.kg.ac.rs
# Serbian Chemical Society member.
https://doi.org/10.2298/JSC230614063M

redox-active copper is of particular interest because it is endogenous to humans and has a strong affinity for nucleobases. Copper(II) complexes have shown remarkable potential due to their antimicrobial, anti-inflammatory and cytotoxic activities.[1–4]

Schiff bases are good chelating agents that are popular among the researchers because of their simple and inexpensive synthesis. Some fine-tuning of molecular electronic properties makes Schiff bases extremely attractive for the development of pharmacological agents.[5,6] Besides the fact that many transition metal ion complexes containing Schiff bases have shown excellent anticancer activity, the anticancer activity of some Schiff bases increases when they are used as ligands.[5–10] Certain Schiff base Cu(II) complexes showed potent cytotoxic activity against human colorectal and breast cancer cells.[11–14]

The primal intracellular target for most anticancer drugs is the DNA molecule.[15,16] Therefore, when developing new anticancer drugs, it is crucial to determine the compounds interactions with DNA under physiological conditions. Transition metal ion complexes interact with DNA *via* covalent or non-covalent interactions (intercalation, groove binding, and electrostatic interactions). In addition to DNA, transition metal complexes can also interact with some proteins. Serum albumin proteins are essential for the transport and delivery of pharmaceutical agents to tissues and cells.[17,18] Considering this, the study of the interactions of anticancer agents with albumin provides valuable information about the structural features of the agents and their pharmacological response. Originally, it was believed that only DNA-binding properties were relevant for determination of the anticancer activity of agents. However, protein binding properties are essential for the pharmacokinetics and pharmacodynamics of drugs.[18] Generally, noncovalent binding is the most important binding mode for anticancer drug-protein interactions.

This work aimed to study the DNA/BSA interactions of three structurally similar Cu(II) complexes (Fig. 1) in which copper(II) ion is coordinated to two nitrogen and two oxygen donor atoms.[19–21] The influence of different substi-

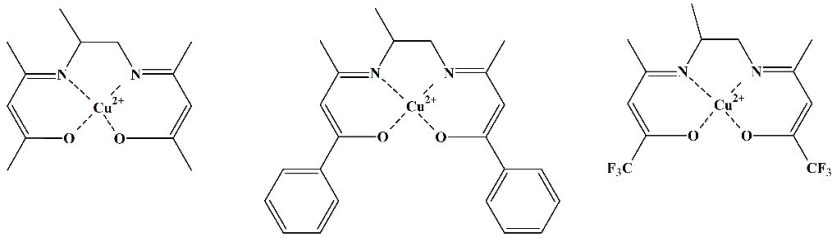

1 [Cu(acac2pn)] **2** [Cu(phacac2pn)] **3** [Cu(tfacac2pn)]

Fig. 1. Structures of the studied Cu(II) complexes.

tuents on the activity of complexes was determined. These studies were carried out using calf thymus DNA (ct-DNA) and bovine serum albumin (BSA). The work also shows the results of the *in vitro* cytotoxic assay against human colorectal carcinoma cells HCT-116, which are compared with the effects on healthy human MRC-5 fibroblast cells of the human pleura.

EXPERIMENTAL

Materials and methods

The complexes, (*N*,*N'*-bis(acetylacetone)propylenediimine)copper(II) complex, [Cu(acac2pn)] (**1**), (*N*,*N'*-bis-(benzoylacetone)propylenediimine)copper(II) complex, [Cu(phacac$_2$pn)] (**2**) and (*N*,*N'*-bis-(trifluoroacetylacetone)propylenediimine)copper(II) complex, [Cu(tfacac$_2$pn)] (**3**), were synthesized according to the previously published procedures.[19-21] The obtained complexes were characterized by UV–Vis, IR and mass spectrometry (LTQ Orbitrap XL), Figs. S-1–S-5 of the Supplementary material to this paper. Acetylacetone was obtained from Merck. Phosphate buffer (PBS) were obtained from Fluka. Ethanol absolute anhydrous, chloroform and dichloromethane were obtained from Carlo Erba. Copper(II) acetate hydrate was obtained from Kemika, Zagreb. Bovine serum albumin (BSA), calf thymus DNA (ct-DNA), ethidium bromide (EB) and 1,2-diaminoethane (en) were purchased from Sigma–Aldrich and were used as received without further purification. For *in vitro* experiments all reagents were of the molecular biology grade. Dulbecco's modified eagle medium (DMEM) and phosphate-buffered saline (PBS) were obtained from GIBCO, Invitrogen, USA. Fetal bovine serum (FBS) and trypsin-EDTA were from PAA (The Cell Culture Company, Pasching, Austria). Water was of Millipore quality and it was autoclaved before use in any experiments. All other chemicals were of the highest purity, commercially available, and were used without further purification.

Instrumentation

Perkin-Elmer Lambda 25 double-beam spectrophotometer with a 3.0 mL quartz cuvette and 1.0 cm path length was used for the recording of UV–Vis spectra. ct-DNA solutions were prepared by dissolving the commercially obtained ct-DNA in PBS, with a ratio of the absorbances at 260 and 280 nm between 1.8–1.9, indicating that ct-DNA was adequately free of protein.

Concentration of the ct-DNA solution was determined using A_{260} with $\varepsilon = 6600$ M^{-1} cm^{-1}.[22,23] RF-1501 PC spectrofluorometer was used to record fluorescence spectra in the range 550–750 nm. Fluorescence intensity was measured at an excitation wavelength of 527 nm and emission wavelength of 612 nm. For all experiments the slit widths for excitation and emission (10 nm each) and scan rate were kept constant. Spectrophotometric analyses of cell cytotoxicity were conducted on Multiskan SkyHigh UV/Vis spectrophotometer (ThermoFisher Scientific).

DNA-binding studies

UV–Vis spectroscopy studies. The interactions of studied complexes with ct-DNA were examined using UV–Vis spectroscopy in order to determine the possible binding modes. The intrinsic equilibrium binding constants, K_b, were determined using Eq. (S-1), Supplementary material. DNA binding experiments were performed at room temperature and all absorbance measurements were made in a buffered solution (0.01 M PBS, pH 7.4). The series of solutions containing studied complexes and DNA were prepared by mixing a constant concentration of complex solutions (8 μM) with an increase of DNA concentration from 0 to 40 μM.

Fluorescence quenching studies. Fluorescence spectroscopy was also used to study the interactions of studied complexes with ct-DNA. For fluorescence determination the complex––DNA solutions were prepared by mixing constant DNA–EtBr solutions (DNA EtBr ratio was 1:1) with different concentrations of Cu(II) complex. Concentration of DNA was 25 μM, ethidium bromide (EtBr) was 25 μM while complex concentrations varied from 0 to 50 μM. The system was shaken and incubated at room temperature for 5 minutes before measurement. Stern–Volmer equation (Eq. (S-2)) was used to calculate the fluorescence quenching constant K_{sv}.

BSA-binding studies. Solutions of complexes **1**–**3** and BSA (2 μM) were prepared in 0.01 M phosphate buffer solution. During the fluorescence quenching experiments, the concentration of BSA was kept constant. The quenching of the emission intensity of the tryptophan residues in the BSA at 352 nm was followed using complexes **1**–**3** as quenchers with increasing concentration in the range of 0–30 μM. The fluorescence spectra were recorded in the range of 300–500 nm at an excitation wavelength of 295 nm. The data of the binding of Cu(II) complexes were analyzed using the Stern–Volmer equation. Observed diagrams were used to confirm the interactions of the complexes with albumin and to calculate the corresponding constants.

In vitro *cell cytotoxicity analyses*

The HCT-116, colorectal carcinoma cell line, and MRC-5, healthy lung fibroblast cell line, were cultured in Dulbecco's modified eagle medium (DMEM) supplemented with 10 % fetal bovine serum (FBS), 100 IU/mL penicillin and 100 μg/mL streptomycin. For *in vitro* cytotoxicity analyses, 10^4 cells per well in 96-well microtiter plates were seeded overnight and treated with complexes for 24 and 72 h. After treatment incubation, the cell viability was estimated by standard MTT assay, briefly described in our previous studies.[24,25]

RESULTS AND DISCUSSION

DNA-binding studies

The DNA molecule has long been recognized as a main binding target in the human body for the transition metal ion complexes exhibiting anticancer activity. Consequently, the first step when examining the mechanism of action of different transition metal ion complexes is usually the investigation of their affinity for DNA binding.[26–28] Electronic absorption spectroscopy is a commonly used method for verifying the extent and nature of the binding between the metal complexes and the DNA molecule. The absorption intensity of the complexes can decrease (hypochromism) or increase (hyperchromism) upon addition of the DNA, with a slight shift in absorption wavelength, indicating an interaction between complexes and DNA.[28] Within this work, the interactions of complexes **1**–**3** with ct-DNA were examined using UV–Vis titrations. During the titration, the concentrations of complex solutions were kept constant (8 μM; PBS) while the concentrations of ct-DNA solution were increasing (0–40 μM). The equilibrium binding constants, K_b, were calculated using Eq. (S-1). Fig. 2 shows the changes in the UV–Vis spectra of complex **1** in the presence of the increasing ct-DNA concentrations. The observed results for complexes **2** and **3** are shown in Fig. S-6 of the Supplementary material.

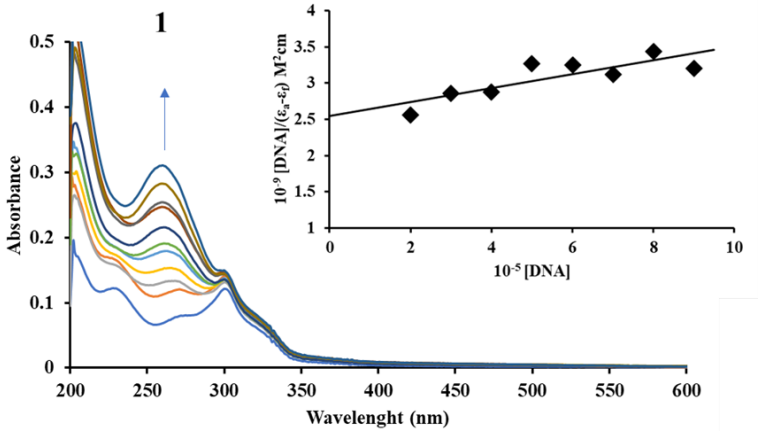

Fig. 2. UV–Vis titration spectra of 8 μM solution of complex 1 in 0.01 M PBS with the addition of the increasing ct-DNA concentration (0–40 μM). Arrow shows hyperchromism in the spectral band. Inset: plots of [DNA]/($\varepsilon_a - \varepsilon_f$) *vs*. [DNA] for the titration of the complex **1** with ct-DNA; with ■ are shown the experimental data points and the full line represents the exponential fitting of the data.

Addition of the ct-DNA solution to the solution of the studied complexes resulted in an intensity increase of the spectra shown in Figs. 2 and S-6 with a slight shift of the maximum peak (2-3 nm red shift). These observations indicate a moderate ability of the studied complexes to interact with ct-DNA, probably by external contact.[29] The intrinsic binding constants for DNA interactions of the complexes were calculated using Eq. (S1) and listed in Table I. The order of the reactivity for the complexes is **1** > **3** > **2**. Complex **1** has the highest value of K_b constant in the order of 10^4, while the other two complexes have similar values in the order of 10^3, indicating a moderate possibility for DNA interactions.

TABLE I. The obtained K_b and K_{sv} constant values for DNA and BSA interactions of complexes **1**–**3**

Complex	ct-DNA		BSA
	K_b / 10^3 M^{-1}	K_{sv} / 10^3 M^{-1}	K_{sv} / 10^4 M^{-1}
1	32±1	2.1±0.1	3.6±0.1
2	2.7±0.1	2.9±0.1	1.8±0.1
3	4.4±0.1	2.7±0.1	1.2±0.1

The fluorescence spectroscopic method is the most accurate and reliable method for studying the relative binding of small molecules to DNA. It is usually used to accurately determine if intercalation is the binding mode of complexes **1**–**3** toward ct-DNA. EtBr is a classical intercalator with significant fluorescence emission intensity at 612 nm[30] when bound to DNA. The changes observed in

the spectra of EtBr–ct-DNA are often used to study the DNA binding affinity of transition metal ion complexes. Namely, the quenching of the EtBr–ct-DNA fluorescence emission occurs upon addition of a compound capable to intercalate between the DNA strands displacing the EtBr from EtBr–ct-DNA. The fluorescence quenching curves of EtBr–ct-DNA in the absence and presence of the complex **2** is shown in Fig. 3, and for complexes **1** and **3** in Fig. S-7 of the Supplementary material. Addition of the increasing amounts (up to r = 1.0) of complexes (0–50 μM) resulted in an intensity decrease of the emission band at 612 nm, indicating competition of the complexes with EtBr in binding toward DNA. The obtained results indicate that complexes **1**–**3** displace EtBr from the aduct DNA–EtBr, exhibiting the possibility for intercalation.[31,32]

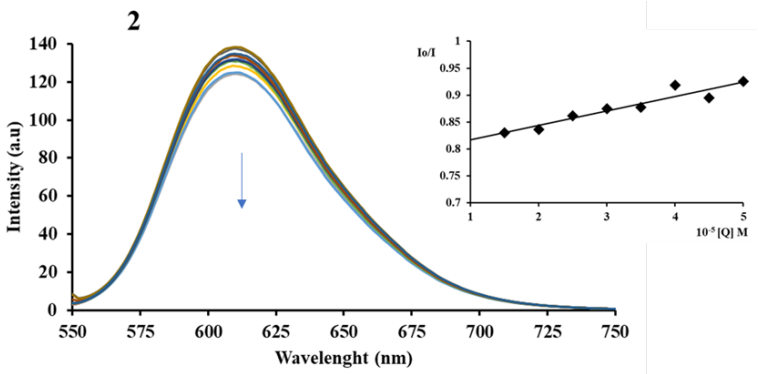

Fig. 3. Fluorescence titration spectra of EtBr–DNA (25 μM) in the presence of varying amounts of complex **2** (phosphate buffer solution = 0,01 M, pH 7.4). The arrow shows changes in fluorescence intensity upon increasing the concentration of complex (0–50 μM). Inset: plots of I_o/I *vs.* [Q]; with ■ are shown the experimental data points and the full line represents the exponential fitting of the data.

The dynamic quenching constant, K_{sv}, was determined from the slope of the linear plots by Eq. (S-2). The calculated K_{sv} values are listed in Table I. Complexes exhibited similar values of the quenching constant, indicating their moderate efficiency in the replacement of the EtBr from EtBr–DNA adduct.

BSA-binding studies

As it was mentioned before, serum albumin plays an important role in the transport and delivery of many pharmaceutical drugs to tissues and cells. Since albumin is the most abundant protein in the bloodstream, the studies of the binding of different biologically active compounds to albumin provide very useful information about their potential activity.[33,34] The interactions of metal drugs with proteins, related to the binding of complexes to albumin, are crucial for their biological distribution, toxicity and even mechanism of action. Moreover, the

binding of drugs to proteins can affect (either enhance or reduce) their biological properties. BSA is intensively studied serum albumin due to its structural homology with human serum albumin (HSA). A BSA solution shows intense fluorescence emission at 352 nm when excited at 295 nm.[35] Addition of complexes **1**–**3** to a BSA solution affects the BSA fluorescence spectra, Figs. 4 and S-8.

The observed quenching can be attributed to the changes in the tertiary structure of the protein after binding of complex. The values of the dynamic quenching constant, K_{SV}, and quenching constant, kq (M^{-1} s^{-1}) for the interaction with BSA were derived according to the Stern–Volmer quenching equation (Eq. (S2)) and listed in Table I.

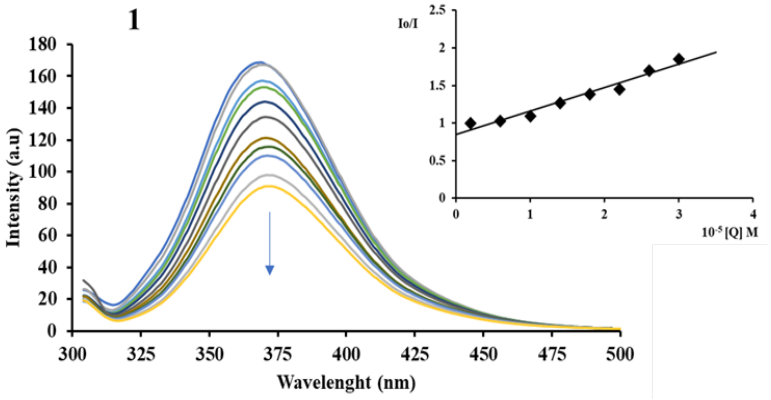

Fig. 4. Fluorescence titration spectra of BSA (2 μM) with different concentrations of complex 1 (phosphate buffer solution = 0,01 M, pH 7.4). Arrow shows the changes in the fluorescence intensity upon increasing the concentration of complex (0–30 μM). Inset: Stern–Volmer plots of the interaction of complex **1** with BSA.

The values presented in Table I are relatively high, suggesting that complexes **1**–**3** interact better with BSA than with DNA. The highest constant was determined for complex **1**, while complexes **2** and **3** showed similar values. The higher affinity of complexes **1**–**3** for the BSA molecule can also be seen from Fig. 5, which compares the K_{SV} values for the interactions with ct-DNA and BSA.

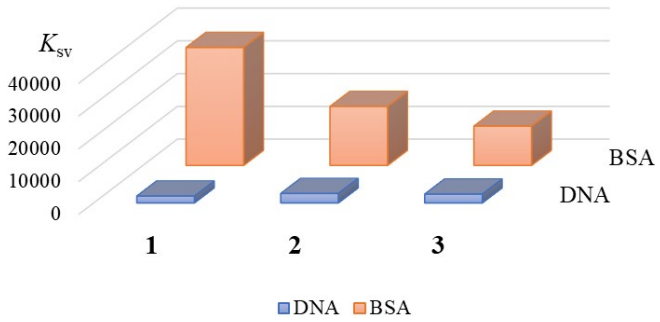

Fig. 5. Comparison of the obtained K_{sv} values for the interactions of complexes **1**–**3** with BSA and with ct-DNA.

The highest constant was determined for complex **1**, while the lowest was for complex **3**. Considering this, the greatest reactivity is shown by a complex that has two methyl groups in its structure while the lowest was shown by complex that has two CF_3 groups in the structures. Based on the obtained results it can be concluded that the binding of complexes strongly depends on steric effects of voluminous phenyl group as well as on electronic effects of CF_3 groups. Previously published results with similar Cu(II) complexes that differ in structure only by the ethylenediamine-bridge part, showed slightly higher reactivity to HSA, than the examined complexes to BSA with a similar order of reactivity.[36]

*Cytotoxicity of the complexes **1**–**3***

The observed results of the interactions of complexes **1**–**3** with DNA suggest that cells surviving treatment with these chemicals may be affected. Considering this, cancer cells and healthy cells were treated, and the results of cell viability are shown in Figs. S-9–S-14 and in Table II.

TABLE II. Cytotoxicity results (IC_{50} / μM) of the investigated Cu(II) complexes on HCT-116 and MRC-5 cells

Complex	HCT-116		MRC-5	
	Time, h		Time, h	
	24	72	24	72
1	>500	>500	>500	187.88
2	346.41	168.25	90.94	78.01
3	>500	>500	>500	>500

The complexes decreased cell viability in a concentration- and time-dependent manner. Complex **2** exerted the strongest effect on HCT-116 cells with an IC_{50} value of 168.25 μM at 72 h. Complexes **1** and **3** exerted no cytotoxic effects. On the other hand, in MRC-5 cells, we observed that complexes **2** red-

uced cell viability the most, complex 1 induced moderate effect, while complexes 3 had no effect.

CONCLUSION

Based on the results obtained by examining the interactions of complexes **1**–**3** with DNA and BSA molecules, it was found that they interact with ct-DNA molecule in a moderate manner. Moreover, the studied complexes showed good quenching of BSA fluorescence and good binding ability to this protein with relatively high binding constants. Among the tested complexes, the highest affinity for DNA and BSA molecules was shown by complex **1**, which has two methyl groups in the structure of the ligand. Cytotoxicity tests showed that complex **2** exerted the strongest effect on HCT-116 cells. These results could contribute to a better understanding of the interactions of novel transition metal ion complexes with biologically important molecules, such as DNA and proteins. In addition, this study could provide useful information as a basis for the design of new molecules with desired biological activities.

SUPPLEMENTARY MATERIAL

Additional data and information are available electronically at the pages of journal website: https://www.shd-pub.org.rs/index.php/JSCS/article/view/12435, or from the corresponding author on request.

Acknowledgement. The authors gratefully acknowledge the financial support of the Ministry of Science, Technological Development and Innovation of the Republic of Serbia, Contract numbers: 451-03-47/2023-01/200122, 451-03-47/2023-01/200126, 451-03-47/2023-01/200126, 451-03-47/2023-01/200125.

ИЗВОД

ДНК/BSA ИНТЕРАКЦИЈЕ И ЦИТОТОКСИЧНОСТ КОМПЛЕКСА БАКРА(II) СА ШИФОВИМ БАЗАМА КАО ЛИГАНДИМА

АЛЕКСАНДАР МИЈАТОВИЋ[1], АНГЕЛИНА З. ЦАКОВИЋ[2], АЛЕКСАНДАР ЛОЛИЋ[3], СНЕЖАНА СРЕТЕНОВИЋ[4], МАРКО Н. ЖИВАНОВИЋ[5], ДРАГАНА С. ШЕКЛИЋ[5], ЈОВАНА БОГОЈЕСКИ[2] и БИЉАНА В. ПЕТРОВИЋ[2]

[1]Универзитет у Београду – Рударско–геолошки факултет, Ђушина 7, 11000 Београд, [2]Универзитет у Крагујевцу, Природно–математички факултет, Р. Домановића 12, 34000 Крагујевац, [3]Универзитет у Београду, Хемијски факултет, Студентски трг 12–16, Београд, [4]Универзитет у Крагујевцу, Медицински факултет, Одсек за интерну медицину, С. Марковић 69, 34000 Крагујевац и [5]Универзитет у Крагујевцу, Институт за информационе технологије Крагујевац, Јована Цвијића бб, 34000 Крагујевац

Три комплекса Cu(II) јона са Шифовим базама као лигандима, (*N*,*N'-bis*-(ацетилацетон)пропилендиимин)бакар(II) комплекс, [Cu(acac$_2$pn)] (**1**), (*N*,*N'-bis*-(бензоилилацетон)пропилендиимин)бакар(II) комплекс, [Cu(phacac$_2$pn)] (**2**), и (*N*,*N'-bis*-(бензоилилацетон)пропилендиимин)бакар(II) комплекс, [Cu(tfacac$_2$pn)] (**3**) коришћени су за испитивање интеракција са ДНК (ct-ДНА) и говеђим серум албумином (BSA), користећи апсорпциону спектрофотометрију и флуоросценцију. Испитивања помоћу UV–Vis спектрофотометрије су показала да проучавани комплекси показују умерени афинитет за интеракцију са молекулом ДНК. Резултати испитивања флуоресценције комплекса **1**–**3** су показали да комплекси имају могућност интеркалације са молекулом ДНК, као и

релативно високу способност везивања за BSA. Од свих проучаваних комплекса, највећи афинитет за интеракцију са ДНК и BSA показао је комплекс **1**. Цитотоксичност комплекса испитивана је на ћелијским линијама људског колоректалног карцинома HCT--116 и на здравим фибробластима плућа MRC-5. Резултати су показали да комплекс **2** показује активност на обе ћелијске линије, док су комплекси **1** и **3** неактивни.

(Примљено 14. јуна, ревидирано 18. јуна, прихваћено 8. септембра 2023)

REFERENCES

1. J. C. Dabrowiak, *Metals in Medicine*, 2nd ed., Wiley, New York, 2017 (ISBN:9781119191377, (https://doi.org/10.1002/9781119191377))
2. S. Medicia, M. Peanaa, V. M. Nurchib, J. I. Lachowiczb, G. Crisponib, M. A. Zoroddua, *Coord. Chem. Rev*. **284** (2015) 329 (https://doi.org/10.1016/j.ccr.2014.08.002)
3. F. Tistao, C. Marzano, M. Porchia, M. Pellei, C. Santini, *Med. Res. Rev*. **30** (2010) 708 (https://doi.org/10.1002/med.20174)
4. C. Marzano, M. Pellei, F. Tristao, C. Santini, *Anticancer Agents Med. Chem.* **9** (2009) 185 (https://doi.org/10.2174/187152009787313837)
5. M. Karmakar, S. Chattopadhyay, *J. Mol. Struct*. **1186** (2019) 155 (https://doi.org/10.1016/J.MOLSTRUC.2019.02.091)
6. C. Boulechfar, H. Ferkous, A. Delimi, A. Djedouani, A. Kahlouche, A. Boublia, A.S. Darwish, T. Lemaoui, R. Verma, Y. Benguerba, *Inorg. Chem. Commun.* **150** (2023) 110451 (https://doi.org/10.1016/j.inoche.2023.110451)
7. S. Yamada, *Coord. Chem. Rev.* **1** (1966) 415 (https://doi.org/10.1016/S0010-8545(00)80184-8)
8. L. H. A. Rahman, R. M. E. Khatib, L. A. E. Nassr, A. M. A. Dief, F. E. Lashin, *Spectrochim. Acta, A* **111** (2013) 266 (https://doi.org/10.1016/j.saa.2013.03.061)
9. L. H. A. Rahman, R. M. E. Khatib, L. A. E. Nassr, A. M. A. Dief, A. A. Seleem, *Spectrochim. Acta, A* **117** (2014) 366 (https://doi.org/10.1016/j.saa.2013.07.056)
10. X. G. Ran, L. Y. Wang, Y. C. Lin, J. Hao, D. R. Cao, *Appl. Organometal. Chem.* **24** (2010) 741 (https://doi.org/10.1002/aoc.1678)
11. F. Zhao, W. Wang, W. Lu, L. Xu, S. Yang, X. Cai, M. Zhou, M. Lei, M. Ma, H. Xu, F. Cao, *Eur. J. Med. Chem*. **146** (2018) 451 (https://doi.org/10.1016/j.ejmech.2018.01.041)
12. R. Fekri, M. Salehi, A. Asadi, M. Kubicki, *Inorg. Chim. Acta* **484** (2018) 245 (https://doi.org/10.1016/J.ICA.2018.09.022)
13. L. N. Ji, X. H. Zou, J. G. Liu, *Coord. Chem. Rev*. **216** (2001) 513 (https://doi.org/10.1016/S0010-8545(01)00338-1)
14. A. Nori, J. Kopecek, *Adv. Drug Delivery Rev.* **57** (2005) 609 (https://doi.org/10.1016/j.addr.2004.10.006)
15. R. K. Gupta, R. Pandey, G. Sharma, R. Prasad, B. Koch, S. Srikrishna, P. Z. Li, Q. Xu, D. S. Pandey, *Inorg. Chem.* **52** (2013) 3687 (https://doi.org/10.1021/ic302196v)
16. M. Ganeshpandian, R. Loganathan, E. Suresh, A. Riyasdeen, M. A. Akbarshad, M. Palaniandavar, *Dalton Trans*. **43** (2014) 1203 (https://doi.org/10.1039/C3DT51641E)
17. R. Baosic, D. Milojkovic-Opsenica, Z. Tesic, *J. Planar Chromatogr. – Mod. TLC* **16** (2003) 412 (https://doi.org/10.1556/JPC.15.2002.4.4)
18. P. J. Mc Carthy, R. J. Hovey, K. Ueno, A. E. Martel, *J. Am. Chem. Soc*. **77** (1955) 5820 (https://doi.org/10.1021/ja01627a011)
19. N. Stevanovic, D. Apostolovic, M. Milcic, A. Lolic, M. van Hage, T. Cirkovic Velickovic, R. Baosic, *New J. Chem.* **45** (2021) 6231 (https://doi.org/10.1039/d1nj00040c)

20. F. Dimiza, S. Fountoulaki, A. N. Papadopoulos, C. A. Kontogiorgis, V. Tangoulis, C. P. Raptopoulou, V. Psycharis, A. Terzis, D. P. Kessissoglou, G. Psomas, *Dalton Trans.* **40** (2011) 8555 (https://doi.org/10.1039/c1dt10714c)
21. F. Dimiza, F. Perdih, V. Tangoulis, I. Turel, D. P. Kessissoglou, G. Psomas, *J. Inorg. Biochem*. **105** (2011) 476 (https://doi.org/10.1016/j.jinorgbio.2010.08.013)
22. P. Čanović, J. Bogojeski, J.V. Košarić, S.D. Marković, M.N. Živanović. *Turk. J. Biol*. **41** (2017) 141 (https://doi.org/10.3906/BIY-1605-77)
23. J. V. Košarić, D. M. Cvetković, M. N. Živanović, M. G. Ćurčić, D. S. Šeklić, Z. M. Bugarčić, S. D. Marković. *J. Buon.* **19** (2014) 283 (https://jbuon.com/archive/19-1-283.pdf)
24. A. Petrović, M. M. Milutinović, E. T. Petri, M. Živanović, N. Milivojević, R. Puchta, A. Scheurer, J. Korzekwa, O. R. Klisurić, J. Bogojeski, *Inorg. Chem*. **58** (2019) 307 (https://doi.org/10.1021/acs.inorgchem.8b02390)
25. O. Novakova, H. Chen, O. Vrana, A. Rodger, P. J. Sadler, V. Brabec, *Biochemistry* **42** (2003) 11544 (https://doi.org/10.1021/bi034933u)
26. E. S. Koumousi, M. Zampakou, C. P. Raptopoulou, V. Psycharis, C. M. Beavers, S. J. Teat, G. Psomas and T. C. Stamatatos, *Inorg. Chem.* **5** (2012) 7699 (https://doi.org/10.1021/ic300739x)
27. M. M. Milutinović, J. V. Bogojeski, O. Klisurić, A. Scheurer, S. K. C. Elmroth, Ž. D. Bugarčić, *Dalton Trans.* **45** (2016) 15481 (https://doi.org/10.1039/c6dt02772e)
28. J. M. Kelly, A. B. Tossi, D. J. McConnell, C. Oh Uigin, *Nucleic Acids Res*. **13** (1985) 6017 (https://doi.org/10.1093/nar/13.17.6017)
29. B. C. Boger, B. E. Fink, S. R. Brunette, W. C. Tse, M. P. Hedrick, *J. Am. Chem. Soc*. **123** (2001) 5878 (https://doi.org/10.1021/ja010041a)
30. D. Senthil Raja, N. S. P. Bhuvanesh, K. Natarajan, *Inorg. Chem.* **50** (2011) 12852 (https://doi.org/10.1021/ic2020308)
31. J. Steinhardt, J. Krijn and J. G. Leidy, *Biochemistry* **10** (1971) 4005 (https://doi.org/10.1021/bi00798a001)
32. Y. Song, Y. Liu, W. Liu, F. A. Villamena and J. L. Zweier, *RSC Adv.* **4** (2014) 47649 (https://doi.org/10.1039/C4RA04616A)
33. F. Wang, W. Huang, Z. Dai, *J. Mol. Struct*. **875** (2008) 509 (https://doi.org/10.1016/j.molstruc.2007.05.034)
34. A. Mijatović, N. Gligorijevic, D. Cocic, S. Spasic, A. Lolić, S. Aranđelović, M. Nikolić, R. Baošić, *J. Inorg. Biochem*. **244** (2023) 112224 (https://doi.org/10.1016/j.jinorgbio.2023.112224).

Journal of the Serbian Chemical Society
JSCS@tmf.bg.ac.rs • www.shd.org.rs/JSCS
J. Serb. Chem. Soc. *88* (12) S375–S382 (2023) *Supplementary material*

SUPPLEMENTARY MATERIAL TO

DNA/BSA interactions and cytotoxic studies of tetradentate *N*,*N*,*O*,*O*-Schiff base copper(II) complexes

ALEKSANDAR MIJATOVIĆ[1#], ANGELINA Z. CAKOVIĆ[2#], ALEKSANDAR LOLIĆ[3], SNEŽANA SRETENOVIĆ[4], MARKO N. ŽIVANOVIĆ[5], DRAGANA S. ŠEKLIĆ[5], JOVANA BOGOJESKI[2#] and BILJANA V. PETROVIĆ[2*#]

[1]University of Belgrade – Faculty of Mining and Geology, Đušina 7, 11000 Belgrade, Serbia, [2]University of Kragujevac, Faculty of Science, R. Domanovića 12, 34000 Kragujevac, Serbia, [3]University of Belgrade – Faculty of Chemistry, Studentski trg 12–16, 11000 Belgrade, Serbia, [4]University of Kragujevac, Faculty of Medicinal Science, Department of Internal medicine, S. Markovic 69, 34000 Kragujevac, Serbia and [5]University of Kragujevac, Institute for Information Technologies Kragujevac, Jovana Cvijića bb, 34000 Kragujevac, Serbia

J. Serb. Chem. Soc. *88* (12) (2023) 1307–1317

THE INTRINSIC EQUILIBRIUM BINDING CONSTANT FOR DNA STUDIES

$$\frac{[DNA]}{\varepsilon_A - \varepsilon_f} = \frac{[DNA]}{\varepsilon_b - \varepsilon_f} \pm \frac{1}{K_b / (\varepsilon_b - \varepsilon_f)} \qquad \text{(Equation S-1)}$$

To determine the intrinsic binding constant K_b, the ratio of the intercept of the curve [DNA]/(ε_A - ε_f) versus [DNA], where [DNA] is the DNA concentration in base pairs and the slope was used. The apparent extinction coefficient ε_A is consistent with A_{obsd}/[complex]. The extinction coefficients ε_f and ε_b refer to the unbound and fully bound complex, respectively.

STERN-VOLMER EQUATION FOR DNA AND BSA STUDIES

Stern-Volmer quenching constant, K_{sv}, for DNA and BSA as well as the quenching rate constant, k_q, for BSA were calculated using the Stern-Volmer equation:

$$\frac{I_0}{I} = 1 + K_{sv}[Q] \qquad \text{(Equation S-2)}$$

In Equation S-2, the total concentration of the quencher is given by [Q], while I_0 describes the emission intensity in the absence of the quencher and the emission intensity in the presence of the quencher is described by I.

* Corresponding author. E-mail: biljana.petrovic@pmf.kg.ac.rs

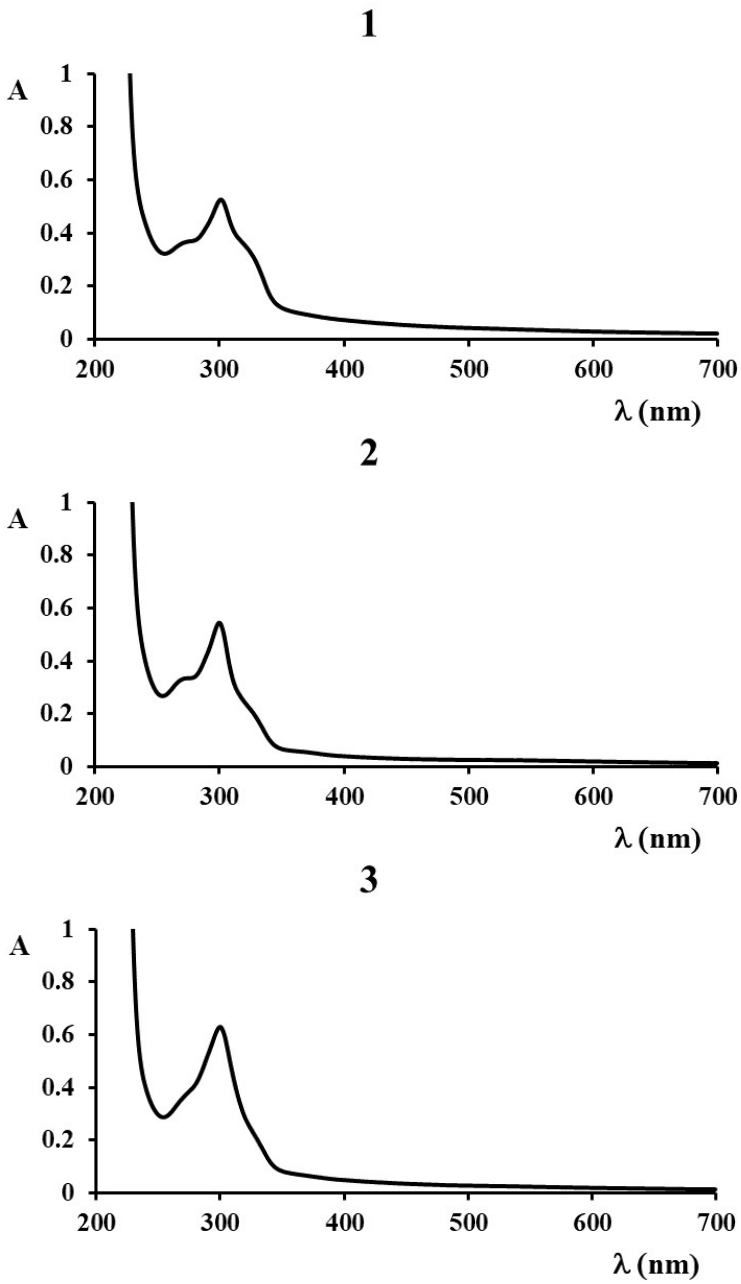

Fig. S-1. UV-Vis spectra of studied complexes [Cu(acac2pn)] (1), [Cu(phacac2pn)] (2), [Cu(tfacac2pn)] (3)

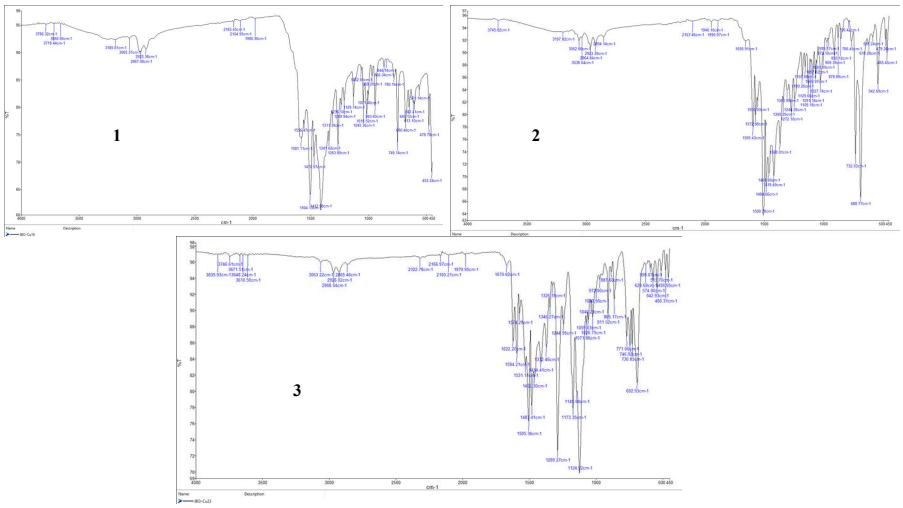

Fig. S-2. IR spectra of studied complexes [Cu(acac2pn)] (1), [Cu(phacac2pn)] (2), [Cu(tfacac2pn)] (3)

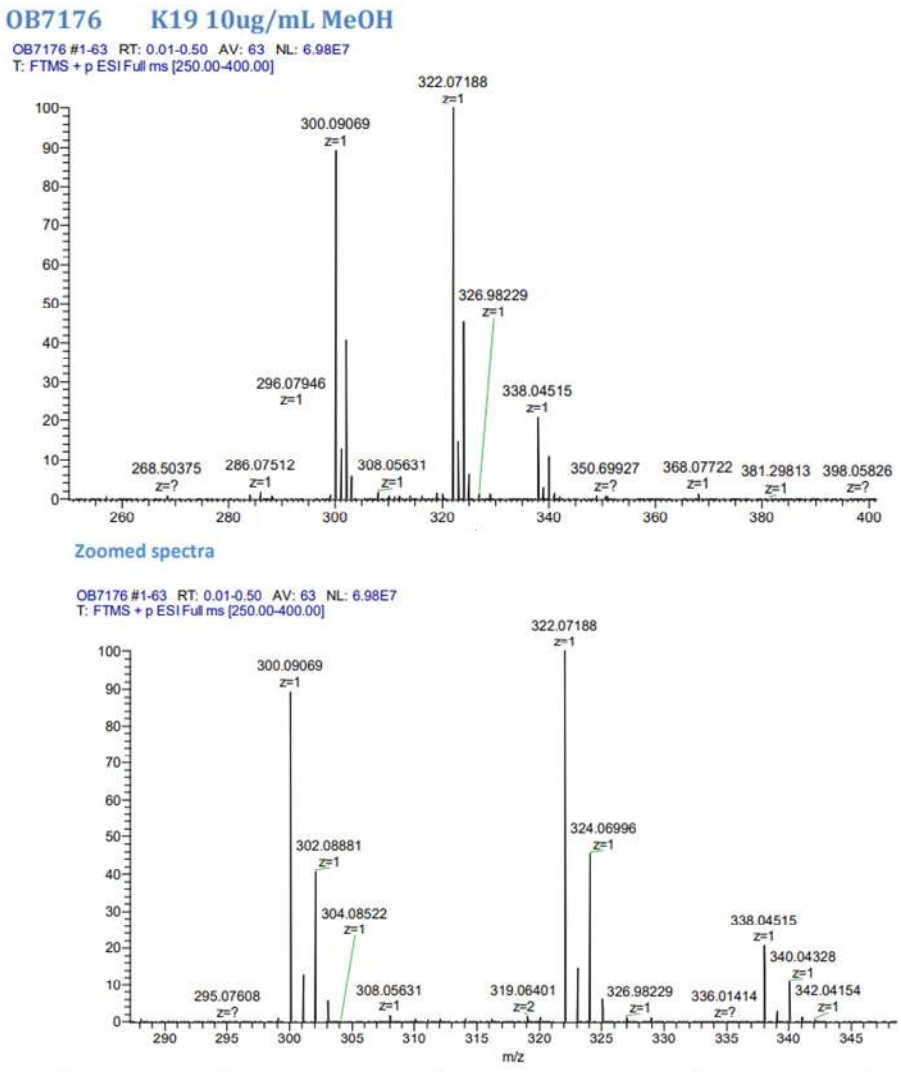

Exact mass	Observed mass	Observed ion type	Error (ppm)
300.08935	300.09069	$[M+H]^+$	4.47
322.0713	322.07188	$[M+Na]^+$	1.80

Fig. S-3. Mass spectra for complex [Cu(acac2pn)] (1) (10 ng/mL MeOH).

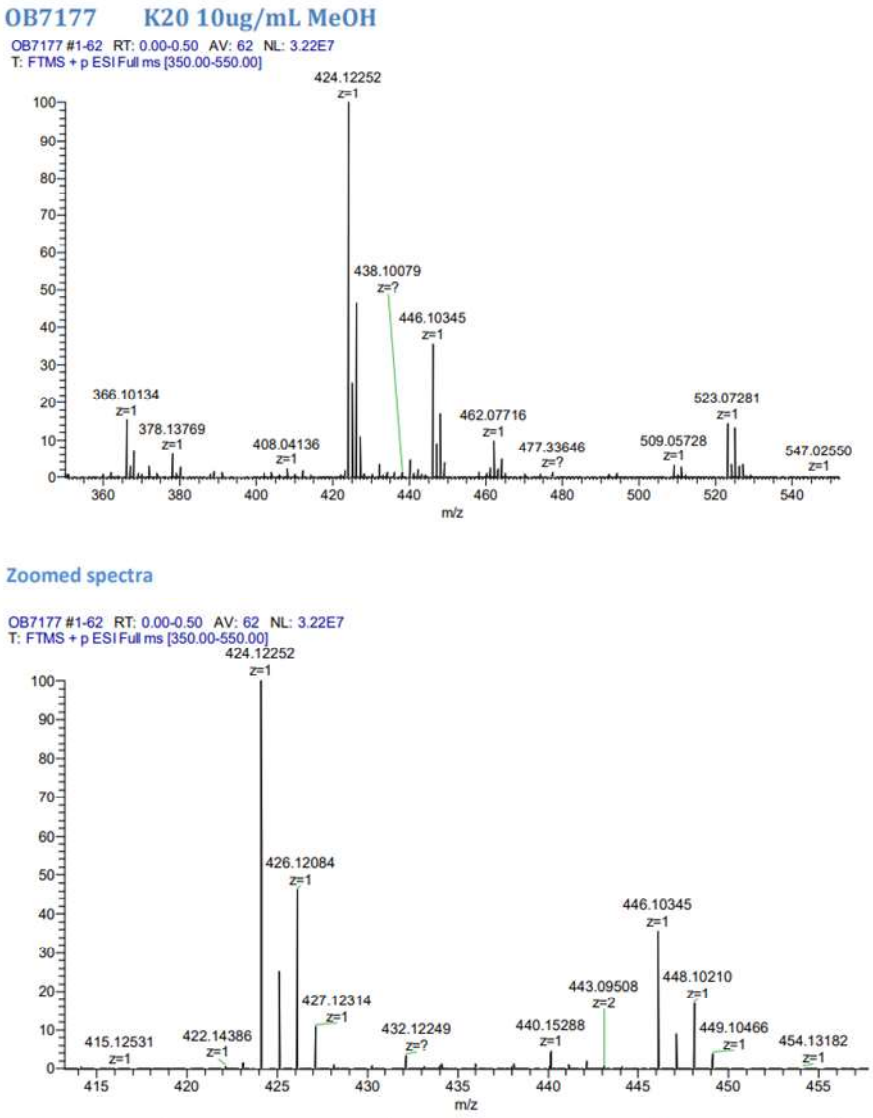

Exact mass	Observed mass	Observed ion type	Error (ppm)
424.12065	424.12252	$[M+H]^+$	4.41
446.1026	446.10345	$[M+Na]^+$	1.91

Fig. S-4. Mass spectra for complex [Cu(phacac2pn)] (2) (10 ng/mL MeOH).

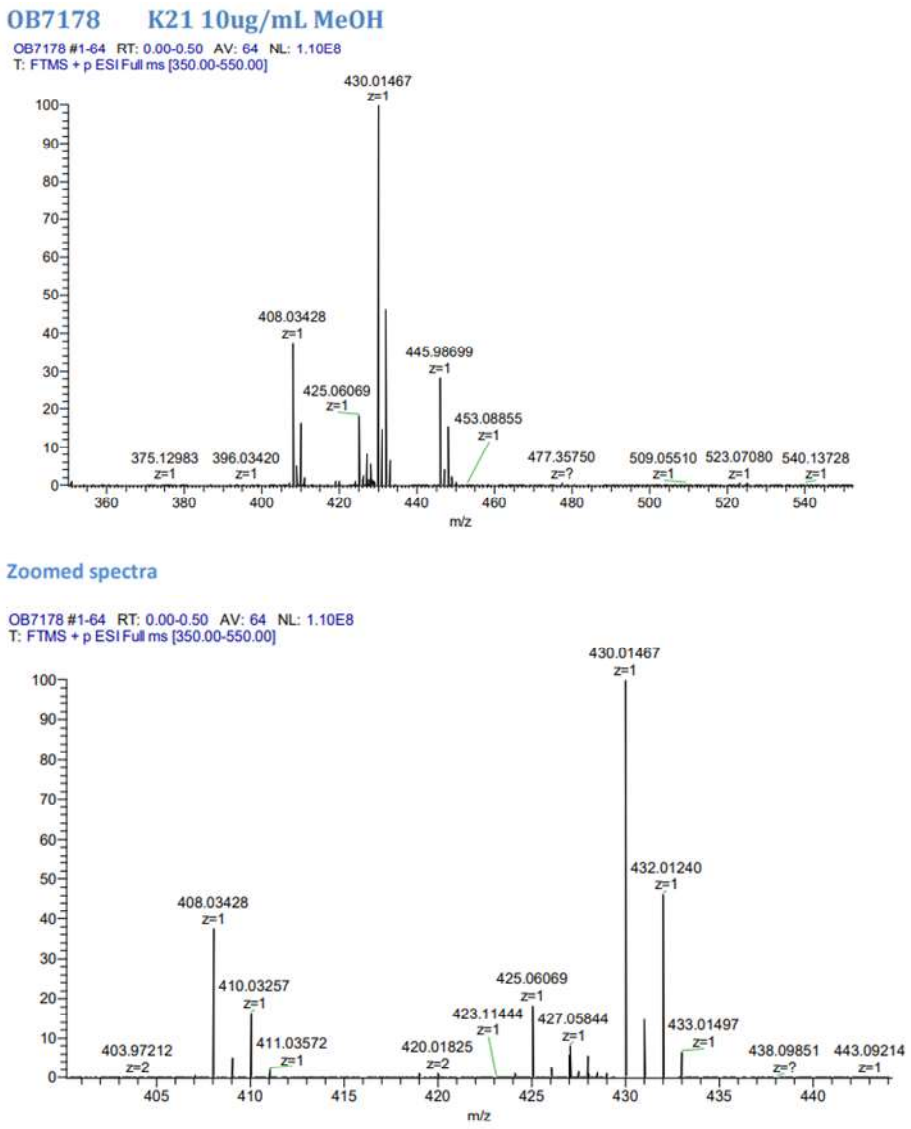

Exact mass	Observed mass	Observed ion type	Error (ppm)
408.03282	408.03428	$[M+H]^+$	3.52
430.01477	430.01467	$[M+Na]^+$	0.23

Fig. S-5. Mass spectra for complex [Cu(tfacac2pn)] (3) (10 ng/mL MeOH).

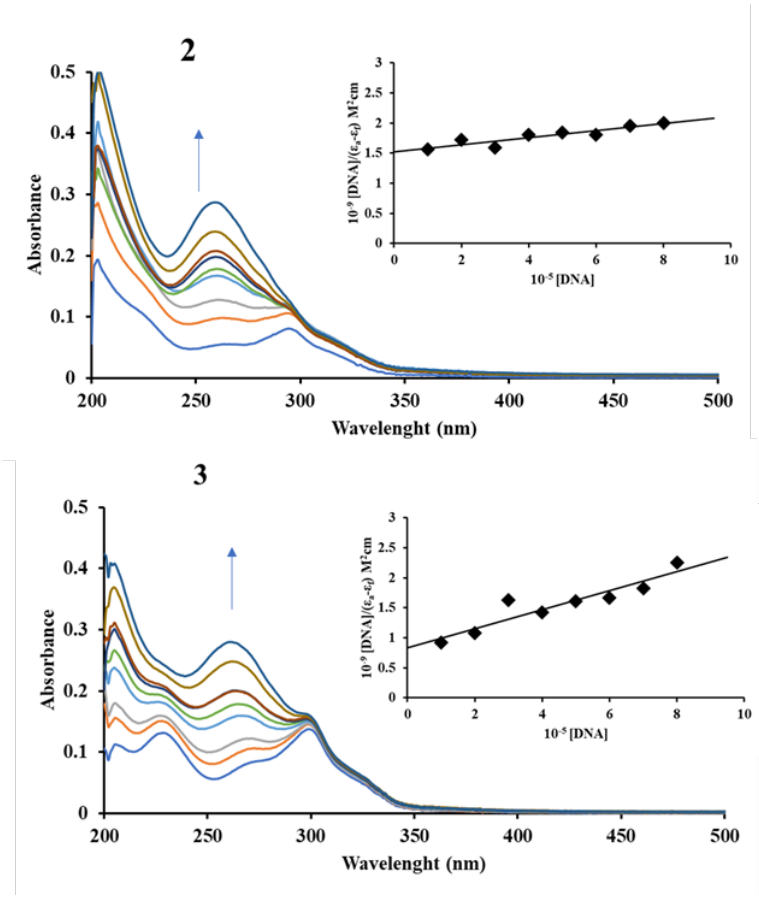

Fig. S-6. UV-Vis titration spectra for 8 μM solution of complexes **2** and **3** in 0,01 M PBS with increasing ct-DNA concentration (0 - 40 μM). Arrow shows hyperchromism in the spectral band. Insepts: Plots of [DNA]/($\varepsilon_a - \varepsilon_f$) versus [DNA] for the titration of the complexes with ct-DNA; with (■) are shown the experimentl data points and the full line represents the exponential fitting of the data.

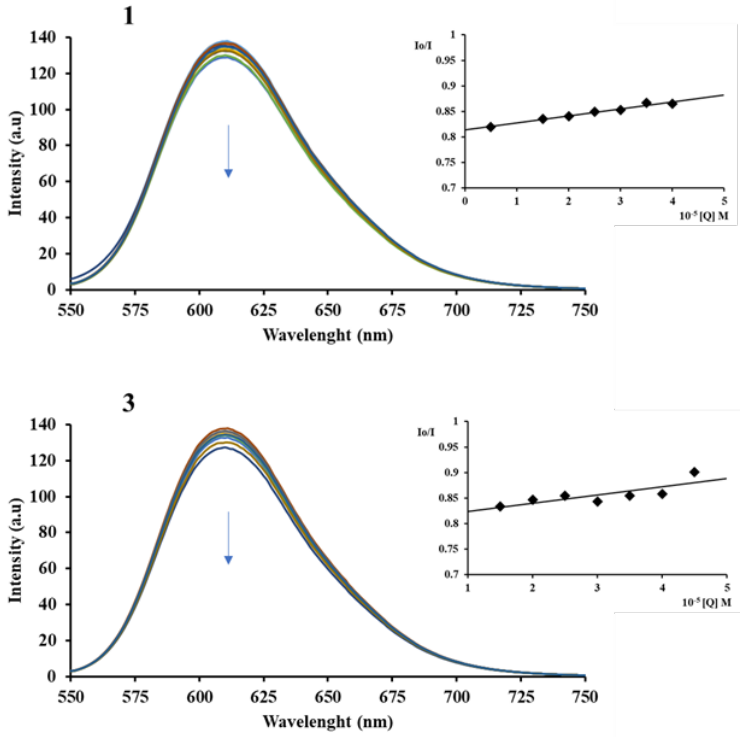

Fig. S-7. Fluorescence titration spectra of EtBr-DNA and of EtBr (25 μM) bound to DNA (25 μM) in the presence of varying amounts of complexes **1** and **3** (phosphate buffer solution = 0,01 M, pH = 7.4). Arrow shows changes in fluorescence intensity upon increasing concentration of complexes (0-50 μM). Insert: plots of I_o/I versus [Q]; with (■) are shown the experimental data points and the full line represents the exponential fitting of the data.

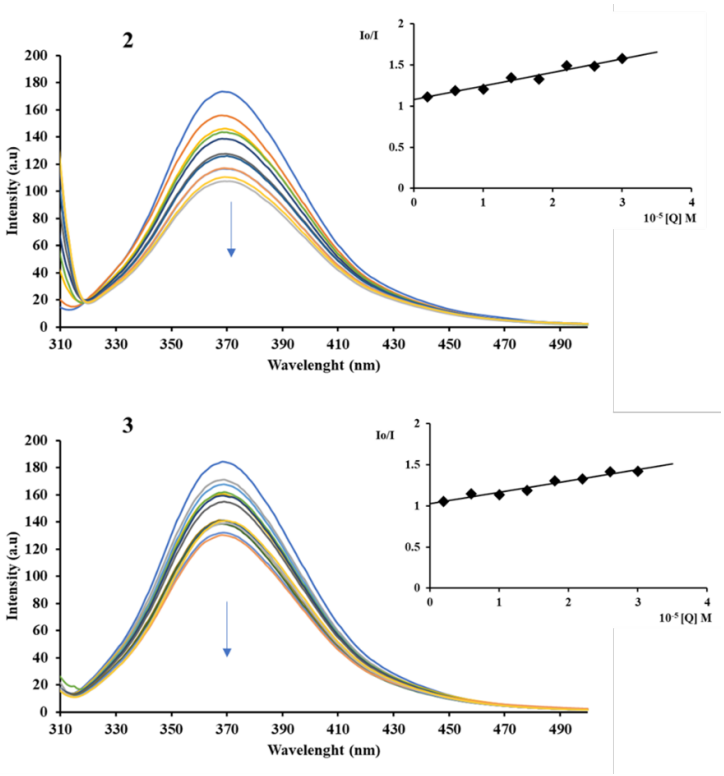

Fig. S-8. Fluorescence titration spectra of BSA (2 μM) at different concentrations of complexes **2** and **3** (phosphate buffer solution = 0,01 M, pH = 7.4). Arrow shows changes in fluorescence intensity upon increasing concentration of complexes (0-30 μM). Insets: Stern-Volmer plots of the interaction with BSA.

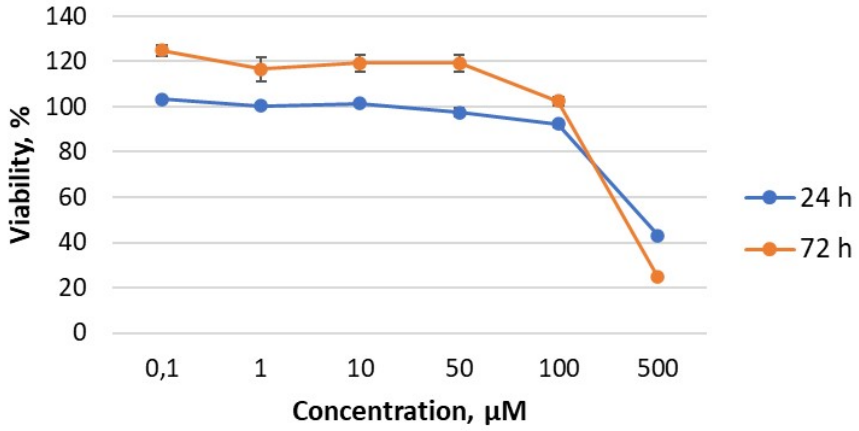

Fig. S-9. Effects of **1** on HCT-116 cells, expressed as the complex concentations related to the number of viable cells after 24 and 72 h of exposure.

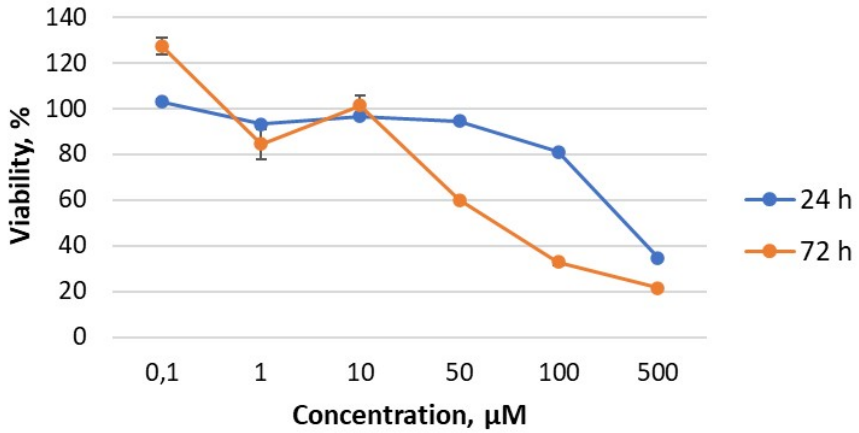

Fig. S-10. Effects of **2** on HCT-116 cells, expressed as the complex concentrations related to the number of viable cells after 24 and 72 h of exposure.

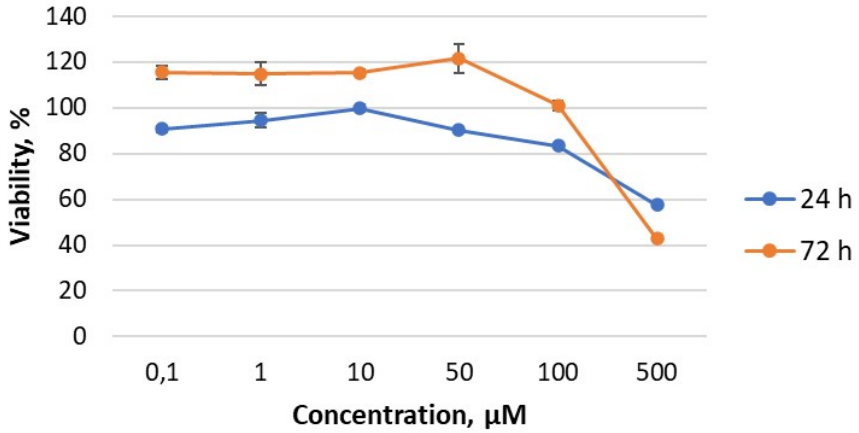

Fig. S-11. Effects of **3** on HCT-116 cells, expressed as the complex concentrations related to the number of viable cells after 24 and 72 h of exposure.

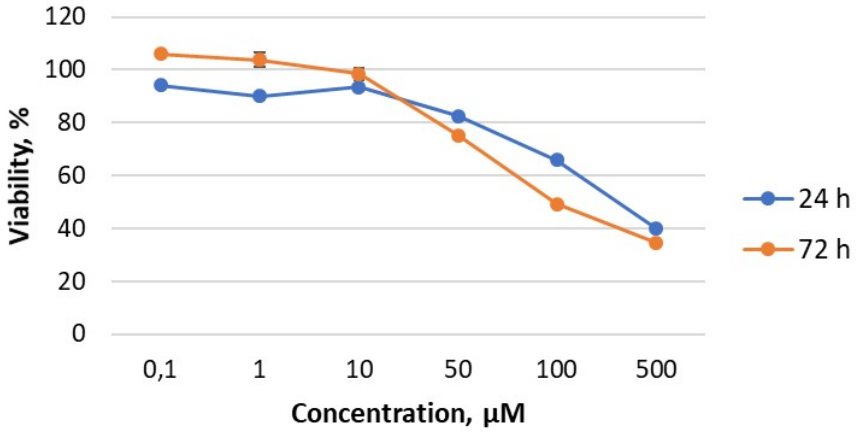

Fig. S-12. Effects of complex **1** on to MRC-5 cells, expressed as the complex concentrations related to the number of viable cells after 24 and 72 h of exposure.

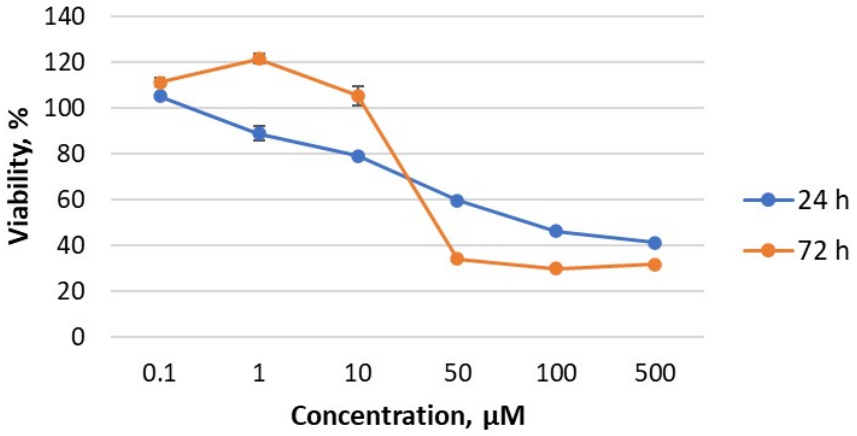

Fig. S-13. Effects of complex **2** on to MRC-5 cells, expressed as the complex concentrations related to the number of viable cells after 24 and 72 h of exposure.

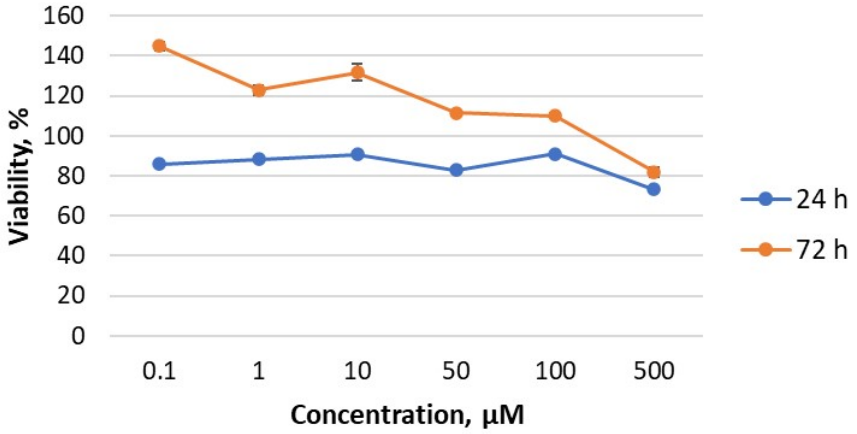

Fig. S-14. Effects of complex **3** on to MRC-5 cells, expressed as the complex concentrations related to the number of viable cells after 24 and 72 h of exposure.

Journal of the Serbian Chemical Society
JSCS@tmf.bg.ac.rs • www.shd.org.rs/JSCS
J. Serb. Chem. Soc. *88* (12) 1319–1334 (2023)
JSCS–5698
Original scientific paper
Published 19 December 2023

Diorganotin(IV) complexes with hydroxamic acids derivatives of some histone deacetylases inhibitors

DANIJELA N. NIKOLIĆ[1,2#], MARIJA S. GENČIĆ[1]*, JELENA M. AKSIĆ[1], NIKO S. RADULOVIĆ[1#], DUŠAN S. DIMIĆ[3#] and GORAN N. KALUĐEROVIĆ[2]**

[1]University of Niš, Faculty of Sciences and Mathematics, Department of Chemistry, Višegradska 33, 18000 Niš, Serbia, [2]University of Applied Sciences Merseburg, Department of Engineering and Natural Sciences, Eberhard-Leibnitz-Straße 2, DE-06217 Merseburg, Germany and [3]University of Belgrade, Faculty of Physical Chemistry, Studentski trg 12–16, 11000 Belgrade, Serbia

(Received 30 June, revised 18 July, accepted 8 September 2023)

Abstract: Organotin(IV) compounds show great potential as antitumor metallodrugs with lower toxicity and higher antiproliferative activity. Histone deacetylases (HDAC) inhibitors are characterised by high bioavailability and low toxicity. In this research, the two novel octahedral organotin(IV) complexes of physiologically active hydroxamate-based ligands, *N*-hydroxy-4-phenylbutanamide (**HL$_1$**) and *N*-hydroxy-2-propylpentanamide (**HL$_2$**), have been prepared and characterized using FTIR, ^{1}H-, ^{13}C- and ^{119}Sn-NMR spectroscopy. Particular emphasis was put on the binding characteristics of ligands. The structures were additionally analysed by the density functional theory at B3LYP-D3BJ/6--311++G(d,p)(H,C,N,O)/LanL2DZ(Sn) level. The theoretical IR and NMR spectra were compared to the spectroscopic data, and it was concluded that the predicted structures described well the experimental ones. The stability of different isomers of **HL$_1$** and **HL$_2$** was assessed by the natural bond orbital analysis, and the importance of intramolecular hydrogen bond was outlined. The interactions between donor atoms and Sn were investigated and correlated with the changes in chemical shift and the wavenumbers of characteristic vibrations.

Keywords: diphenyltin(IV); *N*-hydroxy-4-phenylbutanamide; *N*-hydroxy-2-propylpentanamide; spectral characterization; DFT; NBO.

*,** Corresponding authors. E-mail: (*)marija.gencic@pmf.edu.rs; (**)goran.kaluderovic@hs-merseburg.de
Serbian Chemical Society member.
https://doi.org/10.2298/JSC230630064N

INTRODUCTION

Histone deacetylases (HDACs) are key enzymes involved in the regulation of various physiological cellular processes, such as transcription, by catalysing the hydrolysis of the ε-acetylated lysine chain in histones, but they are also being increasingly implicated in tumorigenesis. It is proven that HDAC inhibitors could elicit anticancer effects in tumour cells by their ability to impose cell cycle arrest, differentiation, DNA damage, autophagy, and/or apoptosis.[1,2] The traditional HDAC inhibitors are divided into four main groups: *i*) hydroxamic acids or hydroxamates, such as suberanilohydroxamic acid; *ii*) cyclic peptides, including depsipeptide; *iii*) benzamides, *e.g.*, chidamide; *iv*) short-chain fatty acids, including butyric, 4-phenylbutanoic and valproic acid (Fig. 1).[2] Previous studies have shown that combining the bioavailability and low toxicity of short-chain fatty acids with the bidentate binding ability of hydroxamates to the active site Zn^{2+} could be beneficial, resulting in analogues with enhanced potency (*e.g.*, *N*-hydroxy-4-phenylbutanamide) and/or altered HDAC isoform selectivity (*e.g.*, *N*-hydroxy-2-propylpentanamide).[3,4]

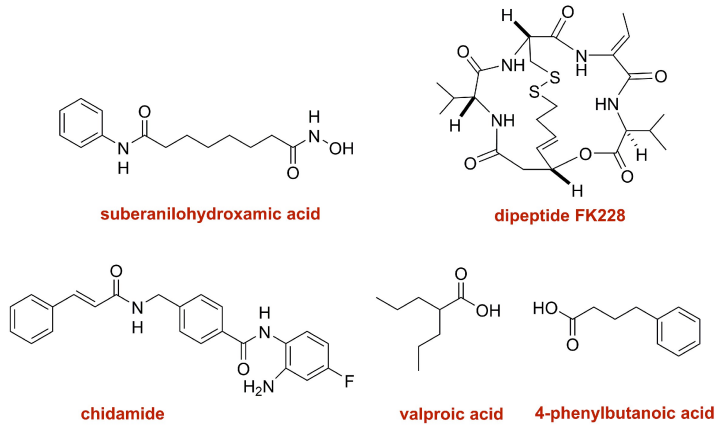

Fig. 1. Structures of HDAC inhibitors classes representatives.

Due to drug resistance, a broad spectrum of activity and toxicity-related issues of platinum-based antitumor chemotherapeutics, numerous efforts have been devoted to developing more effective non-platinum alternatives. Among them, organotin(IV) complexes have emerged as potential antitumor metallodrugs due to lower toxicity, specifically targeted drug uptake by the cancerous cells, higher antiproliferative activity, and/or better excretion properties than platinum-based counterparts.[5,6] It has been shown that the number (mono-, di- or tri-) and type of alkyl/aryl groups linked to the central tin atom, the nature of the organic ligand, and the number of free coordination positions offered could play an

important role in the antiproliferative action of the organotin(IV) compounds.[7] A dozen of di- and tri-organotin(IV) complexes bearing different hydroxamic acids as ligands were prepared and structurally characterised recently, and it was discovered that some of them display potent cytotoxic and/or antimicrobial activities.[2,8–10] Tin compounds can also be used as photo-stabilizers for poly(vinyl chloride).[11–13]

Thus, this work deals with the preparation and characterization (FTIR, ^{1}H-, ^{13}C- and ^{119}Sn-NMR spectroscopy) of two new complexes **1** and **2** in which the known biologically active hydroxamate-based ligands, *N*-hydroxy-4-phenylbutanamide (**HL$_1$**) and *N*-hydroxy-2-propylpentanamide (**HL$_2$**), respectively, were combined with an diphenyltin(IV) moiety (Scheme 1). The structure and spectroscopic properties of compounds **1** and **2** were additionally confirmed by the quantum-chemical optimizations at B3LYP-D3BJ/6-311++G(d,p)(H,C,N,O)//LanL2DZ(Sn) level of theory. The intramolecular interactions governing the stability were analysed by the natural bond orbital theory.

EXPERIMENTAL AND THEORETICAL METHODS

General methods

All commercially available chemicals and solvents were used as purchased without further purification. Valproic acid was prepared *via* the standard malonate ester synthesis.[14] The identity and purity of the synthetic standard were confirmed by NMR and GC–MS analysis (trimethylsilyl derivative).

^{1}H-NMR (400 MHz; including ^{1}H-NMR selective homonuclear decoupling experiments), ^{13}C-NMR, DEPT-90, DEPT-135, NOESY and gradient ^{1}H–^{1}H COSY, HSQC and HMBC spectra were recorded on a Bruker Avance III 400 spectrometer (Bruker, Switzerland), while ^{119}Sn-NMR spectra were recorded on a Bruker Avance DRX 400 spectrometer. NMR spectra were measured at 25 °C in deuterated chloroform ($CDCl_3$) and/or deuterated dimethyl sulfoxide (DMSO-d_6). Chemical shifts (δ) given in ppm were referenced to tetramethylsilane (TMS) and/or residual non-deuterated/deuterated solvent peak as an internal standard. IR measurements (neat, attenuated total reflectance) were carried out on a Thermo Nicolet 6700 FTIR instrument (Waltham, USA) and the vibration frequencies are reported in wavenumbers (cm^{-1}). The elemental analyses were carried out in a Vario EL III elemental analyser (Elementar Analysensysteme GmbH, Hanau, Germany) to determine C, H and N.

Analytical and spectral data of the synthesized compounds are given in Supplementary material to this paper.

General procedure for preparation of hydroxamate ligand precursors

A slightly modified previously published procedure was applied.[15] 4-Phenylbutanoic acid and valproic acid were converted to the corresponding acid chlorides by $SOCl_2$ and used without further purification. Et_3N (19.5 mL, 0.14 mol) was added dropwise to precooled (0 °C) solution of $NH_2OH{\times}HCl$ (9.7 g, 0.14 mol) in H_2O (35.9 mL). Then the reaction mixture was stirred at 0 °C for 30 min, following the addition of the solution of acid chloride (7 mmol) in dry THF (14.4 mL). The reaction mixture was stirred for an additional 60 min and warmed to room temperature. Layers were separated and the aqueous solution was extracted with CH_2Cl_2 (2×30 mL). The combined organic phases were dried with anhydrous $MgSO_4$ and

concentrated in *vacuo* to give the corresponding hydroxamic acid. *N*-hydroxy-4-phenylbutanamide (**HL_1**) and *N*-hydroxy-2-propylpentanamide (**HL_2**) were obtained as colourless crystals (in 34.5 and 45.7 % yield, respectively) and according to NMR analyses were sufficiently pure to be used further without purification (see Supplementary material). NMR data for ligands **HL_1** and **HL_2** were in general agreement with those previously reported.[3,4]

General procedure for preparation of diphenyltin(IV) complexes

A modified procedure by Li and co-workers (2004) was applied.[2] Typically, Ph_2SnCl_2 (0.15 mmol) was added to the methanolic solution (3 mL) of the hydroxamic acid **HL_1** or **HL_2** (0.3 mmol) and KOH (0.3 mmol). The reaction mixture was stirred under N_2 at room temperature overnight. The white solid formed (KCl) was filtered off and the obtained filtrate was concentrated under a vacuum to yield the corresponding diorganotin(IV) complex.

Theoretical methods

The structures of ligands and organotin(IV) complexes were optimized in the Gaussian program package[16] by employing B3LYP-D3BJ[17,18] functional in conjunction with 6-311++G(d,p)[19] basis set for H, C, N and O, and LanL2DZ basis set for Sn.[20,21] The optimizations were performed without any geometrical constraints, and the absence of imaginary frequencies proved that the minima on the energy surface was found. The vibrational spectra were analysed and viewed in the Gauss View program.[22] The solvent environment was modelled by the conductor-like polarizable continuum (CPCM) model[23] for the measurements performed in chloroform and DMSO. The NMR spectra were predicted by the gauge independent atomic orbital approach (GAIO)[24] in the Gaussian Program package. The intramolecular interactions governing the stability of the ligand isomers and complexes were examined by the natural bond orbital (NBO) analysis.[25]

RESULTS AND DISCUSSION

Synthesis and characterization

The organotin(IV) hydroxamates **1** and **2** were prepared at room temperature by the reaction of one equivalent of Ph_2SnCl_2 with two equivalents of ligand (**HL_1** or **HL_2**, respectively) in MeOH in the presence of an equimolar amount of KOH as a base (Scheme 1). Complexes **1** and **2** were obtained as colourless solids in very good yields and their purity was confirmed by C, H, and N elemental analysis. Compounds were further characterized by IR and multinuclear (^{1}H-, ^{13}C- and ^{119}Sn-) NMR spectroscopy. The numbering of atoms in Scheme 1 was only used for NMR data assignation.

To investigate the vibrational modes of hydroxamic acids and how they change with complexation, the FTIR spectra of solid **HL_1** and **HL_2** and their organotin(IV) complexes **1** and **2**, respectively, were scanned in the range from 4500 to 400 cm^{-1} (Figs. S-1–S-4). The ligand precursors showed the band at 3174 and 3176 cm^{-1}, respectively, assigned to the N-H stretching vibrations, which was broader and less intense when they were complexed to a metal cation. The shift towards lower frequencies of the ν(C=O) from 1650 and 1627 cm^{-1} in the ligand precursors **HL_1** and **HL_2** to 1596 and 1589 cm^{-1} in complexes **1** and **2**, respectively, indicated that the ligand coordinates through oxygen atom. This

moderate to significant change in ν(C=O) vibration wavenumber could be indicative of the lengthening and weakening of the carbonyl bond.[10] The C–N stretching and N–H bending vibrations were found at 1536 cm^{-1} in the **HL_2** spectrum. Herein, the same vibrations were also influenced by the complexation, as it appeared as a broader band centred at 1525 cm^{-1} in the corresponding organotin compound. The observed shifts are suggestive of bonding through carbonyl and hydroxamic oxygens (O,O coordination) and non-participation of nitrogen in bonding. Moreover, in the IR spectrum of complex **2** two additional bands at 728 and 697 cm^{-1} that were not present in the spectrum of ligand precursor **HL_2**, assigned as C–H wag and ring bend of the phenyl group, respectively, clearly indicated the introduction of Ph_2Sn moiety in this molecule. New bands at about 540 cm^{-1} (also not present in the ligand precursor) corresponding to ν(Sn–O) further confirm the formation of organotin(IV) complexes **1** and **2**, respectively.[2]

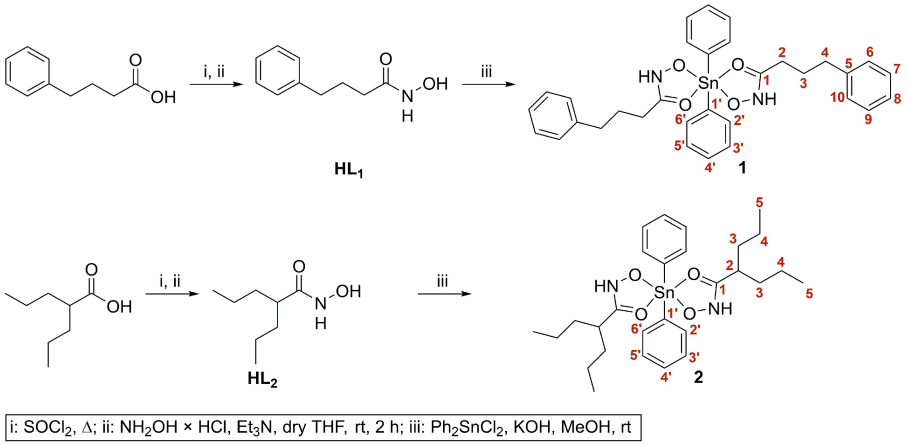

Scheme 1. Synthetic route to complexes **1** and **2**.

A comparison of ^{1}H- and ^{13}C-NMR spectra of diorganotin(IV) hydroxamates **1** and **2** with that of the ligand precursors (**HL_1** and **HL_2**, respectively) and of the starting material Ph_2SnCl_2, has further supported their formation. Hydroxamic acid **HL_1** in $CDCl_3$ exhibited characteristic proton and carbon resonances for monosubstituted phenyl ring and three CH_2 groups belonging to propane-1,3--diyl fragment (Fig. 2, Figs. S-5 and S-6 of the Supplementary material). Alongside the mentioned resonances the two additional broad singlets corresponding to N–H and O–H protons, at 10.39 and 8.77 ppm, respectively, were observed in the ^{1}H-NMR spectrum (in DMSO-d_6). The NMR spectra of the ligand precursor **HL_2** were also recorded in both $CDCl_3$ and DMSO-d_6. Among the aliphatic protons, the terminal methyl groups appeared as a triplet at 0.88 ppm (J^3 = 7.2 Hz), while CH and CH_2 groups were observed as four complex multiplets (Fig. S-7 of

the Supplementary material) in $CDCl_3$. According to the interactions noted in the HSQC and ^1H-^1H COSY spectra the methylene groups in position 3 are anisochronous (Fig. 3A). These diastereotopic methylene groups exhibit a double magnetic nonequivalence: the two CH_2 groups have different chemical shifts and the protons within them are nonequivalent as well and feature complex splitting patterns (*e.g.*, overlapping pairs of *dtd* or *ddt*). Therefore, it appears that a specific conformation around the C(2)H–C(3)H_2 bond was preferred in ligand **HL_2** leading to the magnetic nonequivalence of methylene groups. As expected, there were two methylene carbon signals in the ^{13}C-NMR spectrum (at 34.83 and 20.80 ppm), along with one resonance for each of the carbonyl (at 174.47 ppm), methine (at 44.15 ppm), and methyl carbon (14.15 ppm) atoms (Fig. S-8 of the Supplementary material). In addition to four chemical shifts in the aliphatic region, the signals of the labile N–H and OH-protons were observed at 10.36 and 8.68 ppm, respectively, in ^1H-NMR of ligand precursor in DMSO-d_6 (Fig. S-9 of the Supplementary material).

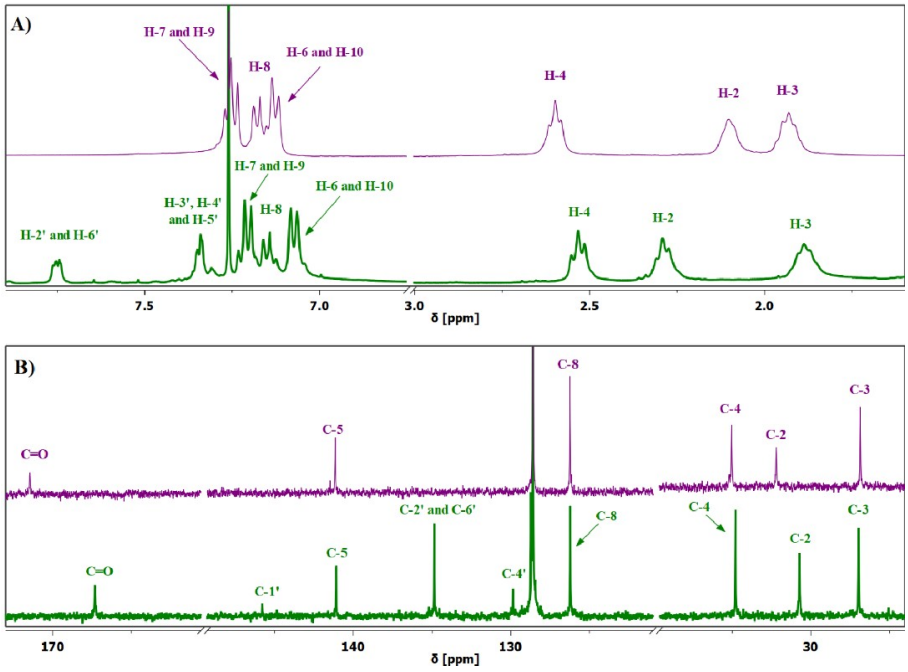

Fig. 2. Comparison of the ^1H- (A) and ^{13}C-NMR (B) spectra of ligand **HL_1** (violet line) and complex **1** (green line) in $CDCl_3$.

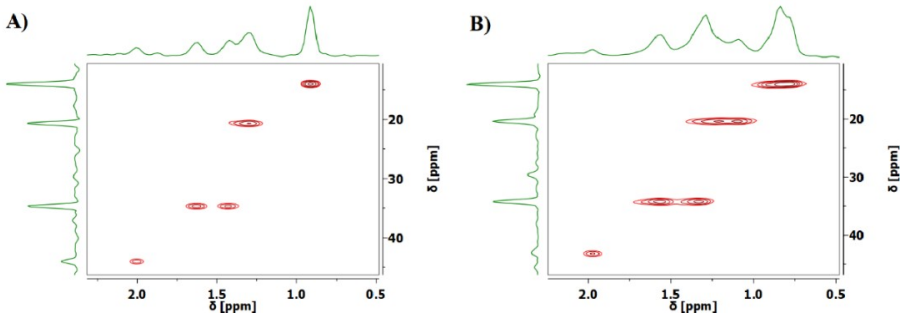

Fig. 3. Expansions of the aliphatic regions of HSQC spectra of ligand $\mathbf{HL_2}$ (A) and complex **2** (B).

Despite their comprehensive chemistry and biology, the structures of hydroxamic acids in solution are still a matter of wide debate. If there is restricted rotation around the C–N bond then *Z* and *E* isomers should exist, while tautomerism could lead to the two additional enolic forms of hydroximic acid (Fig. 4A).[26] The previous theoretical and NMR studies showed that primary hydroxamic acids tend to adopt the more stable keto-*E* and/or keto-*Z* conformations. Moreover, it was found that the prevalence of certain conformations strongly depends on concentration, temperature and the nature of the solvent.[27] Each of analysed ligands, $\mathbf{HL_1}$ and $\mathbf{HL_2}$, showed a single set of characteristic resonances in both the ^{1}H- and ^{13}C-NMR spectra in DMSO-d_6 at room temperature (Figs. S-9 and S-10 of the Supplementary material), and this is consistent either with the presence of only one conformer (*E* or *Z*, due to the high rotational barrier) or a rapid interconversion between the two conformations, so that only one average set of signals is observed in the spectrum. Whatever the preferred conformation is, it is out of the question that hydroxamic acid must be in the prearranged keto-*Z* conformation in order to chelate the metal ion effectively. Thus clearly, the solvent in which metal complexation takes place (in our case methanol) has to play a crucial role in facilitating the required conformation changes necessary for (O,O) coordination.[28] Indeed, it is supposed that protic solvents, such as methanol, stabilize the keto-*Z* conformation by forming intermolecular hydrogen bonds (Fig. 4B).[27]

The appearance of characteristic chemical shifts of phenyl groups attached to the tin centre in the ^{1}H and ^{13}C spectra of complex **1** and **2** (in $CDCl_3$), which were absent in the spectra of free ligands, clearly reveals the assimilation of the diphenyltin(IV) moiety (Figs. S-11–S-14 of the Supplementary material). Moreover, the carbonyl carbon (C=O) resonances that appeared at 170.73 and 174.47 ppm in the ^{13}C spectra of the hydroxamic acids, $\mathbf{HL_1}$ and $\mathbf{HL_2}$, respectively, were shifted upfield in the corresponding complex (to 167.32 and 169.52 ppm, respectively), indicating an increase in electron density at the carbon atom when

the oxygen is chelated to the tin atom (Fig. 2B, Figs. S-12 and S-14). In complex **1**, this effect was also noted for α-methylene carbon atom (C2, see Scheme 1; $\Delta\delta$ = –0.76), while in complex **2**, even the δ-carbon atom (C5, see Scheme 1) experienced some marginal magnetic shielding ($\Delta\delta$ in the range from –0.80 to –0.05 and gradually decreased with the distance from C=O group). In contrast, the resonances of all other carbon atoms in complex **1** were shifted downfield compared to the free ligand ($\Delta\delta$ in the range from 0.46 to 0.82).

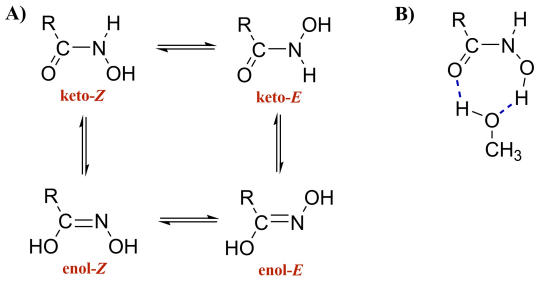

Fig. 4. Plausible conformations of a hydroxamic acid (A) and intramolecular H-bonding of hydroxamic acid in keto-*Z* conformation with methanol (B).

In the ^{1}H-NMR spectra of **1** and **2** in $CDCl_3$ also all the expected chemical shifts could be identified, with some evident coordination induced shifts in comparison to the appropriate ligand precursor (Fig. 2B, Figs. S-11 and S-13). In complex **1**, the methylene protons next to the hydroxamate C=O group (H-2), which are the closest to the coordination centre, were most notably shifted to higher frequencies ($\Delta\delta$ = 0.18). This deshielding of the H-2 protons may be attributed to the magnetic anisotropy of the phenyl and/or carbonyl groups (Fig. 2B). The complete assignments of the ^{1}H- and ^{13}C-NMR spectra of complex **1** in $CDCl_3$ were achieved by a combination of data from DEPT, ^{1}H–^{1}H COSY, NOESY, HMQC and HMBC spectra. The precise values of proton chemical shifts and coupling constants were determined using manual iterative full spin analysis (MestReNova 11.0.3–18688, Mestrelab Research, Santiago de Compostela, Spain). Unfortunately, the complete assignment of ^{1}H-NMR data of complex **2** in $CDCl_3$ was hampered by the fact that upon complexation of hydroxamic acid **HL_2** the methylene groups in position 4 and methyl groups from *N*--hydroxy-2-propylpentanamide moiety became magnetically nonequivalent as well (Fig. 3B) and that some of the resonances originating from phenyl groups overlapped with the residual solvent signal. Therefore, the chemical shifts were estimated based on the observed HSQC interactions.

Finally, the tin chemical shift (^{119}Sn) values often indicate the coordination number around the tin centre and, thus, provide valuable information about the geometry of organotin(IV) complexes.[29] In the ^{119}Sn-NMR spectra of **1** and **2** (in

$CDCl_3$; Figs. S-15 and S-16) one sharp signal (at –402.41 and –349.95 ppm, respectively) was present, which strongly supports the octahedral geometry of this tin(IV) complex.[2,8]

Theoretical analysis of ligands and complexes

The quantum-chemical methods were first employed to investigate the stability of different ligands **HL_1** and **HL_2** conformers to verify the experimental observation of the keto-*Z* isomer dominance. The optimized structures of ligands in vacuum are shown in Figs. 5 and S-17. Table I lists the electronic energies of the conformers calculated in vacuum relative to the most stable conformer.

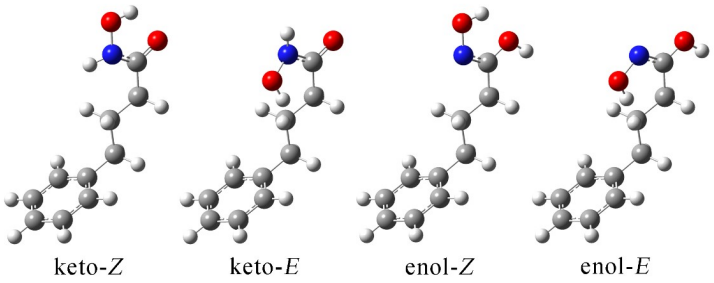

Fig. 5. Optimized isomers in vacuum (B3LYP-D3BJ/6-311++G(d,p) level of theory) of **HL_1**.

TABLE I. Relative electronic and free energies (in kJ mol^{-1}) to the most stable conformer (calculated at B3LYP-D3BJ/6-311++G(d,p) level of theory) for ligands **HL_1** and **HL_2**

Isomer	Electronic energies		Free energies	
	HL_1	**HL_2**	**HL_1**	**HL_2**
Keto-*Z*	0	0	0	0
Keto-*E*	4.5	9.1	4.1	9.8
Enol-*Z*	39.1	41.1	40.6	41.10
Enol-*E*	52.6	58.5	54.7	58.0

The results from Table I prove that the keto-*Z* isomers of both **HL_1** and **HL_2** were the most stable when both electronic and free energies were concerned. This result was expected due to the forming of the intramolecular hydrogen bond between the hydroxyl and carbonyl groups. The Second-order perturbation theory results, within NBO analysis, allowed the quantification of the stabilisation energy of this interaction.[30] The intramolecular hydrogen bonds, denoted as LP(O)→σ(O−H), had energies of 17.8 (**HL_1**) and 19.7 kJ mol^{-1} (**HL_2**). Higher stabilization energy in the case of the second hydroxamic acid ligand was probably due to the positive inductive effect of heptane-4-yl moiety, while in the case of **HL_1**, the electron density is distributed through the phenyl group and hydroxylamide parts. Another important stabilisation interaction is LP(N)→π(C=O),

with 76.4 and 61 kJ mol^{-1} stabilization energies for **HL$_1$** and **HL$_2$**, respectively. This interaction represents charge delocalisation within the amide group. The other reason for the preferability of this isomer is the formation of the intermolecular hydrogen bonds with solvent molecules and the lowest steric hindrance, as previously discussed in the experimental part. Once the rotation around the N atom occurred, the keto-*E* isomers were formed. These conformers do not contain intramolecular hydrogen bond, and the stabilisation energies originating from LP(N)→π(C=O) are lower for several kJ mol^{-1}. The rotational barriers of 4.5 and 9.1 kJ mol^{-1} are still sufficiently low to allow the presence of a keto-*E* isomer in the solution. The formation of a double bond between carbon and nitrogen atom made the system much more rigid. In the case of enol-*Z* isomers, the intramolecular hydrogen bond is formed. Due to the system's rigidity, the distance between the hydrogen atom donor and acceptor in hydrogen bond is much longer than in keto-*Z* isomers leading to lower stabilisation energies of 7.3 (**HL$_1$**) and 7.9 kJ mol^{-1} (**HL$_2$**). The stabilization of enol-*E* isomers is the lowest compared to the other three in both ligands.

The applicability of the chosen level of theory for the optimisation of ligand structures was further examined by comparing the experimental and the theoretical IR and NMR spectra. The most prominent bands of N–H and O–H stretching vibrations of structures optimised in vacuum were around 3624 (3174 in experimental spectrum, N–H) and 3561 cm^{-1} (O–H). Lower wavenumber for the N–H stretching vibration results from the intramolecular hydrogen bond formation. These values were significantly higher than those experimentally observed because the experimental spectra were recorded in the solid sample, while the optimizations were performed on an isolated molecule in vacuum.[31] Due to the intermolecular interactions, the wavenumbers shift to lower values. On the other hand, the C=O stretching vibrations were observed at 1663 (**HL$_1$**) and 1661 cm^{-1} (**HL$_2$**) for the structures optimized in vacuum. These values reproduce well the experimental ones considering all of the optimization limitations (1647 and 1627 cm^{-1} in experimental spectra, respectively). The C–N stretching and N–H bending vibrations were found at 1557 cm^{-1} in the spectra of both **HL$_1$** and **HL$_2$**, which is several cm^{-1} higher than in the experimental spectrum (1541 and 1536 cm^{-1}).

When NMR spectra are concerned, Table II lists the experimental and theoretical values of the chemical shifts of **HL$_1$**, while the analogous table for **HL$_2$** is presented in the Supplementary material. The experimental and theoretical chemical shifts were compared by calculating the correlation coefficient (*R*) and the mean absolute error (*MAE*). The theoretical shifts were obtained for the structures optimised in chloroform. The calculated chemical shifts were overestimated, and the correction factors were determined from the dependency between experimental and theoretical values. These factors were 0.95 and 0.94 for ^{1}H-

and ^{13}C-NMR spectra of **HL_1**. The calculated values show a high *R* value and low *MAE* (0.14 (^{1}H-NMR) and 2.4 ppm (^{13}C-NMR)), proving the reproducibility of the experimental data. The lowest values of the chemical shifts in ^{1}H-NMR spectra were obtained for the hydrogen atoms of the aliphatic chain between 1.93 and 2.60 ppm in the experimental and between 1.51 and 2.53 ppm in the theoretical spectrum. As expected, the chemical shifts of hydrogen atoms attached to aromatic carbon atoms were in a narrow range. The largest discrepancies between the experimental and the theoretical data were calculated for the hydrogen atoms attached to oxygen and nitrogen atoms (>1.5 ppm) due to the formation of stabilisation interactions with the solvent molecules. When ^{13}C-NMR chemical shifts are concerned, the values for carbon atoms of the aromatic ring were almost equal, because the similarity of the chemical environment of carbon atoms was not significantly influenced by the present aliphatic chain. The similar results was obtained for ligand **HL_2**.

TABLE II. Experimental and theoretical (at B3LYP-D3BJ/6-311++G(d,p) level of theory) of **HL_1**

^{1}H Chemical shifts, ppm			^{13}C Chemical shifts, ppm		
H atom	Experimental	Theoretical	C atom	Experimental	Theoretical
C3-H	1.93	1.51	C3	26.1	30.8
C2-H	2.10	2.44	C2	31.5	37.5
C4-H	2.60	2.53	C4	34.3	39.8
C6-H	7.13	7.50	C8	125.5	125.0
C10-H	7.13	7.50	C6	127.9	127.5
C8-H	7.18	7.50	C10	127.9	127.4
C7-H	7.25	7.69	C7	127.9	127.7
C9-H	7.25	7.50	C9	127.9	127.7
O-H	8.77	7.18	C5	140.4	143.3
N-H	10.39	7.85	C1	170.7	166.8
R		0.993	*R*		0.995
MAE / ppm		0.14	*MAE* / ppm		2.4

Once the reproducibility of experimental spectral data was shown, it could be concluded that the optimized structures represented well the structures in solution. The same methodology was applied for the structural analysis of complexes **1** and **2**. The optimized structures are given in Fig. 6, although other conformers could also possibly exist. The complexation occurs through two oxygen atoms and Sn as the central metal ion. The ligands are positioned symmetrically around the Sn ion. The bond distances between deprotonated hydroxyl group oxygen and Sn were, on average, 2.20 Å, while between the carbonyl oxygen and Sn were 2.29 Å. The optimised structure also supported the experimental finding that a bond was not formed between Sn and the nitrogen atom. The NBO analysis gave the stabilisation energies formed between oxygen atoms and Sn. In

the case of complex **1**, the stabilisation interactions between hydroxyl group oxygen and Sn had an energy of 222 kJ mol^{-1}, and between the carbonyl oxygen and Sn, 180 kJ mol^{-1}. These energies explained the difference in the bond lengths between Sn and O atoms. The stronger interactions were formed between **HL$_2$** and Sn (LP($O_{hydroxyl}$)→LP(Sn) (266 kJ mol^{-1}) and LP($O_{carbonyl}$)→LP(Sn) (133 kJ mol^{-1})). The electron density is mostly localised on the hydroxylamide group, as previously explained for the isolated ligand.

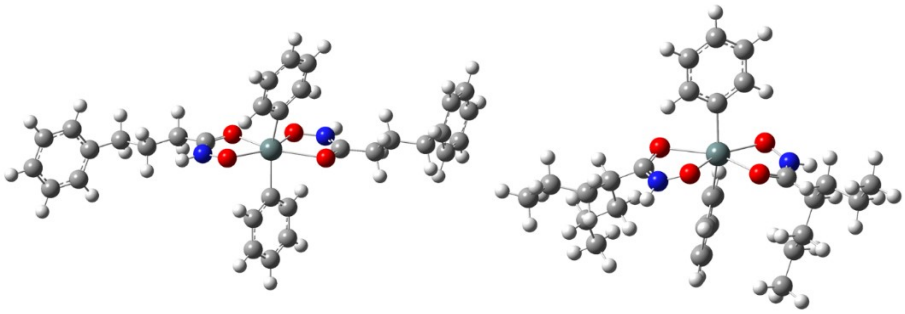

Fig. 6. Optimized structures (at B3LYP-D3BJ/6-311++G(d,p)(H,C,N,O)/LanL2DZ(Sn) of complexes **1** (left) and **2** (right).

Upon the complexation, the characteristic frequencies of the groups included in the compound formation were changed as experimentally observed. The C=O stretching vibration wavenumber lowered to 1610 (**HL$_1$**) and 1598 cm^{-1} (**HL$_2$**) in the theoretical spectra of compounds optimised in vacuum (1596 and 1589 cm^{-1} in experimental spectra). The difference of around 50 cm^{-1}, due to the formation of the complex, was equal in the experimental and predicted spectra. The same was observed for the C–N stretching and N–H bending vibrations. In the lower part of the theoretical spectrum, a band at 546 cm^{-1} assigned to ν(Sn–O) was obtained, similar to the experimental spectrum (540 cm^{-1}), as an important finding to support the formation of organotin(IV) complexes **1** and **2**.

The experimental and the theoretical NMR spectra of complexes **1** and **2** were also compared. Tables III and S-II list the experimental and theoretical chemical shifts in chloroform. The correlation coefficients between experimental and theoretical values are 0.995 for both ^{1}H- and ^{13}C-NMR spectra of complex **1**, with *MAE* values being 0.11 and 2.1 ppm, respectively. A shift in values was observed for the carbonyl oxygen (166.8 ppm in the spectrum of **HL$_1$** and 163.9 ppm in a spectrum of complex **1**), thus proving that this group is included in the complex formation, as it is experimentally confirmed. Similar was observed for **HL$_2$** and complex **2**. Change in chemical shift of C2 of 1.8 ppm was also induced upon complexation. The rest of the values remained almost the same (for example, δ(C5) was found to be 143.3 (**HL$_1$**) and 143.8 ppm (**1**)).

Based on the comparison between the experimental and the theoretical IR and NMR spectra of complexes **1** and **2**, it can be concluded that the predicted structure from Scheme 1 was confirmed.

TABLE III. Experimental and theoretical (at B3LYP-D3BJ/6-311++G(d,p) level of theory) of complex **1**

^{1}H chemical shifts, ppm			^{13}C chemical shifts, ppm		
H atom	Experimental	Theoretical	C atom	Experimental	Theoretical
C3-H	1.89	1.46	C3	27.0	31.3
C2-H	2.28	2.23	C2	30.7	35.7
C4-H	2.53	2.43	C4	34.8	39.8
C6-H	7.07	7.17	C8	126.2	125.5
C10-H	7.07	7.17	C7	128.6	128.4
C8-H	7.15	7.12	C9	128.6	128.3
C7-H	7.22	7.22	C6	128.6	127.9
C9-H	7.22	7.22	C10	128.6	127.9
C4'-H	7.34	7.22	C3'	128.7	127.8
C3'-H	7.35	7.22	C5'	128.7	127.0
C5'-H	7.35	7.22	C4'	129.9	128.4
C2'-H	7.75	7.85	C2'	134.9	134.0
C6'-H	7.75	7.98	C6'	134.9	135.1
R		0.995	C5	141.1	143.8
MAE / ppm		0.11	C1'	145.8	150.9
			C1	167.3	163.9
			R		0.995
			MAE / ppm		2.1

CONCLUSION

The two new diphenyltin(IV) complexes of biologically active hydroxamate--based ligands, *N*-hydroxy-4-phenylbutanamide (**HL$_1$**) and *N*-hydroxy-2-propyl-pentanamide (**HL$_2$**), have been synthesised and characterized by IR, ^{1}H-, ^{13}C- and ^{119}Sn-NMR spectroscopies. The bonding through hydroxamic and carbonyl oxygens (O,O coordination mode) has been indicated by the presence of characteristic bands in the IR spectra. The six-coordinate octahedral geometry around tin has been proposed based on ^{119}Sn-NMR data. All the expected chemical shifts were present in the ^{1}H- and ^{13}C-NMR spectra of complexes **1** and **2**. Some evident coordination-induced shifts could be noted compared to the ligand precursors. The complete assignments of the ^{1}H- and ^{13}C-NMR spectra of complex **1** in $CDCl_3$ were achieved by combining the data from 2D NMR spectra and ^{1}H--NMR simulation. The relative stability of different conformers of **HL$_1$** and **HL$_2$** was explained through the intramolecular hydrogen bond formation and LP(N)$\rightarrow$ $\rightarrow\pi$(C=O) stabilisation interaction. The theoretical IR and NMR spectra of the ligands reproduced well the experimental results. The structure optimisation of complexes **1** and **2** proved the binding mode through the oxygen atoms, with

stronger bonds formed with hydroxyl oxygen (shorter bond and higher stabilization interaction energy) than with carbonyl oxygen. The changes in IR spectra upon complexation were successfully modelled by quantum-chemical calculations. High values of correlation coefficient (>0.991) and low mean absolute error values for comparing the experimental and the calculated NMR chemical shifts proved the predicted structure. Further studies on biological activity of herein described complexes are to be performed, having in mind the well-known biological potential of both ligands and Sn.

SUPPLEMENTARY MATERIAL

Additional data and information are available electronically at the pages of journal website: https://www.shd-pub.org.rs/index.php/JSCS/article/view/12461, or from the corresponding author on request.

Acknowledgments. The work was supported by the Ministry of Science, Technological Development and Innovation of Serbia (contract number: 451-03-47/2023-01/200124 and 451-03-47/2023-01/200146). This research is a part of Danijela N. Nikolić's PhD Thesis supervised by Marija S. Genčić. D.D. wishes to express his gratitude to Filip Vlahović, PhD, for his generous help with the optimization of organotin(IV) compounds.

И З В О Д

ДИОРГАНОКАЛАЈ(IV) КОМПЛЕКСИ СА ХИДРОКСАМАТНИМ ДЕРИВАТИМА КИСЕЛИНА КРАТКОГ НИЗА КОЈЕ ПРЕДАСТАВЉАЈУ HDAC ИНХИБИТОРЕ

ДАНИЈЕЛА Н. НИКОЛИЋ[1,2], МАРИЈА С. ГЕНЧИЋ[1], ЈЕЛЕНА М. АКСИЋ[1], НИКО С. РАДУЛОВИЋ[1], ДУШАН С. ДИМИЋ[3] и ГОРАН Н. КАЛУЂЕРОВИЋ[2]

[1]Универзитет у Нишу, Природно–математички факултет, Департман за хемију, Вишеградска 33, 18000 Ниш, [2]University of Applied Sciences Merseburg, Department of Engineering and Natural Sciences, Eberhard-Leibnitz-Straße 2, DE-06217 Merseburg, Germany и [3]Универзитет у Београду, Факултет за физичку хемију, Студентски трг 12–16, 11000 Београд

Органокалајна(IV) једињења показују велики значај као антитуморски металолекови са ниском токсичношћу и изразитом антипролиферативном активношћу. Инхибиторе хистон деацетилазе карактеришу велика биодоступност и ниска токсичност. У овом раду је описана синтеза и карактеризација (FTIC, ^{1}H-, ^{13}C- и ^{119}Sn-NMR спектроскопија) два нова комплекса дифенилкалаја(IV) са биолошки активним хидроксаматним лигандима, *N*-хидрокси-4-фенилбутанамидом (**HL$_1$**) и *N*-хидрокси-2-пропилпентанамидом (**HL$_2$**). Посебна пажња је посвећена предвиђању начина везивања лиганада у добијеним комплексима. Структуре су додатно испитане применом теорије функционала густине на B3LYP-D3BJ/6-311++G(d,p)(H,C,N,O)/LanL2DZ(Sn) нивоу. Теоријски IC и NMR спектри су упоређени са спектроскопским подацима и закључено је да предвиђене структуре добро описују експерименталне. Стабилност различитих изомера **HL$_1$** и **HL$_2$** је испитана теоријом природних орбитала и приказан је значај интрамолекулске водоничне везе. Интеракције између донорских атома и Sn су испитане и корелисане са променом у хемијским померањима и таласним бројевима карактеристичних вибрација.

(Примљено 30. јуна, ревидирано 18. јула, прихваћено 8. септембра 2023)

REFERENCES

1. J. Chen, D. Faller, R. Spanjaard, *Curr. Cancer Drug Targets* **3** (2003) 219 (https://doi.org/10.2174/1568009033481994)
2. G. Li, Y. Tian, W.-G. Zhu, Front. *Cell Dev. Biol.* **8** (2020) (https://doi.org/10.3389/fcell.2020.576946)
3. J. L. Tischler, B. Abuaita, S. C. Cuthpert, C. Fage, K. Murphy, A. Saxe, E. B. Furr, J. Hedrick, J. Meyers, D. Snare, A. R. Zand, *J. Enzyme Inhib. Med. Chem.* **23** (2008) 549 (https://doi.org/10.1080/14756360701715703)
4. D. M. Fass, R. Shah, B. Ghosh, K. Hennig, S. Norton, W.-N. Zhao, S. A. Reis, P. S. Klein, R. Mazitschek, R. L. Maglathlin, T. A. Lewis, S. J. Haggarty, *ACS Med. Chem. Lett.* **2** (2011) 39 (https://doi.org/10.1021/ml1001954)
5. J. Devi, M. Yadav, D. K. Jindal, D. Kumar, Y. Poornachandra, *Appl. Organomet. Chem.* **33** (2019) 1 (https://doi.org/10.1002/aoc.5154)
6. S. N. Syed Annuar, N. F. Kamaludin, N. Awang, K. M. Chan, *Front. Chem.* **9** (2021) (https://doi.org/10.3389/fchem.2021.657599)
7. S. Hadjikakou, N. Hadjiliadis, *Coord. Chem. Rev.* **253** (2009) 235 (https://doi.org/10.1016/j.ccr.2007.12.026)
8. X. Shang, E. C. B. A. Alegria, M. F. C. Guedes da Silva, M. L. Kuznetsov, Q. Li, A. J. L. Pombeiro, *J. Inorg. Biochem.* **117** (2012) 147 (https://doi.org/10.1016/j.jinorgbio.2012.08.019)
9. S. Kumari, N. Sharma, *J. Coord. Chem.* **72** (2019) 584 (https://doi.org/10.1080/00958972.2019.1573993)
10. V. K. Choudhary, A. K. Bhatt, N. Sharma, *J. Coord. Chem.* **72** (2019) 372 (https://doi.org/10.1080/00958972.2019.1573993)
11. N. Naoom, E. Yousif, D. S. Ahmed, B. M. Kariuki, G. A. El-Hiti, *Polymers* **14** (2022) 4590 (https://doi.org/10.3390/polym14214590)
12. R. R. Arraq, A. G. Hadi, D. A. Ahmed, G. A. El-Hiti, B. M. Kariuki, A. A. Husain, M. Bufaroosha, E. Yousif, *Polymers* **15** (2023) 550 (https://doi.org/10.3390/polym15030550)
13. R. Haddad, S. Khadum, M. Ali, A. Majeed, A. Husain, M. Bufaroosha, D. Ahmed, E. Yousif, *Bull. Chem. Soc. Ethiop*. **37** (2023) 771 (https://dx.doi.org/10.4314/bcse.v37i3.18)
14. M. S. Genčić, N. M. Stojanović, M. Z. Mladenović, N. S. Radulović, *Neurochem. Int.* **161** (2022) 105433 (https://doi.org/10.1016/j.neuint.2022.105433)
15. U. Gravemann, J. Volland, H. Nau, *Neurotoxicol. Teratol.* **30** (2008) 390 (https://doi.org/10.1016/j.ntt.2008.03.060)
16. http://www.gaussian.com
17. A. D. Becke, *Phys. Rev., A* **38** (1988) 3098 (https://doi.org/10.1103/PhysRevA.38.3098)
18. A.D. Becke, E.R. Johnson, *J. Chem. Phys.* **123** (2005) 154101 (https://doi.org/10.1063/1.2065267)
19. T. H. Dunning, *J. Chem. Phys.* **90** (1989) 1007 (https://doi.org/10.1103/10.1063/1.456153)
20. P. J. Hay, W. R. Wadt, *J. Chem. Phys.* **82** (1985) 299 (https://doi.org/10.1063/1.448975)
21. P. J. Hay, W. R. Wadt, *J. Chem. Phys.* **82** (1985) 270 (https://doi.org/10.1063/1.448799)
22. *Gauss View, Version 5*, Semichem Inc., Shawnee, KS, 2009
23. A. V. Marenich, C. J. Cramer, D. G. Truhlar, *J. Phys. Chem., B* **113** (2009) 6378 (https://doi.org/10.1021/jp810292n)
24. J. A. Bohmann, F. Weinhold, T. C. Farrar, *J. Chem. Phys.* **107** (1997) 1173 (https://doi.org/10.1063/1.474464)

25. J. P. Foster, F. Weinhold, *J. Am. Chem. Soc.* **102** (1980) 7211 (https://doi.org/10.1021/ja00544a007)
26. D. A. Brown, W. K. Glass, R. Mageswaran, S. A. Mohammed, *Magn. Reson. Chem.* **29** (1991) 40 (https://doi.org/10.1002/mrc.1260290109)
27. B. García, S. Ibeas, J. M. Leal, F. Secco, M. Venturini, M. L. Senent, A. Niño, C. Muñoz, *Inorg. Chem.* **44** (2005) 2908 (https://doi.org/10.1021/ic049438g)
28. D. A. Brown, R. A. Coogan, N. J. Fitzpatrick, W. K. Glass, D. E. Abukshima, L. Shiels, M. Ahlgrén, K. Smolander, T. T. Pakkanen, T. A. Pakkanen, M. Peräkylä, *J. Chem. Soc., Perkin Trans.* **2** (1996) 2673 (https://doi.org/10.1039/P29960002673)
29. J. Adeyemi, D. Onwudiwe, *Molecules* **23** (2018) 2571 (https://doi.org/10.3390/molecules23102571)
30. D. S. Dimić, Z. S. Marković, L. Saso, E. H. Avdović, J. R. Đorović, I. P. Petrović, M. J. Stanisavljević, D. D. Stevanović, I. Potočňák, E. Samoľová, S. R. Trifunović, J. M. Dimitrić Marković, *Oxid. Med. Cell. Longev.* **2019** (2019) 2069250 (https://doi.org/10.1155/2019/2069250)
31. T. Eichhorn, F. Kolbe, S. Mišić, D. Dimić, I. Morgan, M. Saoud, D. Milenković, Z. Marković, T. Rüffer, J. Dimitrić Marković, G. N. Kaluđerović, *Int. J. Mol. Sci.* **24** (2023) (https://doi.org/10.3390/ijms24010689).

Journal of the Serbian Chemical Society
JSCS@tmf.bg.ac.rs • www.shd.org.rs/JSCS
J. Serb. Chem. Soc. *88* (12) S387–S398 (2023) *Supplementary material*

SUPPLEMENTARY MATERIAL TO

Diorganotin(IV) complexes with hydroxamic acids derivatives of some histone deacetylases inhibitors

DANIJELA N. NIKOLIĆ[1,2], MARIJA S. GENČIĆ[1]*, JELENA M. AKSIĆ[1], NIKO S. RADULOVIĆ[1], DUŠAN S. DIMIĆ[3] and GORAN N. KALUĐEROVIĆ[2]**

[1]University of Niš, Faculty of Sciences and Mathematics, Department of Chemistry, Višegradska 33, 18000 Niš, Serbia, [2]University of Applied Sciences Merseburg, Department of Engineering and Natural Sciences, Eberhard-Leibnitz-Straße 2, DE-06217 Merseburg, Germany and [3]University of Belgrade, Faculty of Physical Chemistry, Studentski trg 12–16, 11000 Belgrade, Serbia

J. Serb. Chem. Soc. *88* (12) (2023) 1319–1334

SPECTRAL AND ANALYTICAL DATA OF LIGAND PRECURSORS AND COMPLEXES

*N-hydroxy-4-phenylbutanamide (**HL**$_1$):* Yield 434 mg (34.3%). Colorless crystals. IR (ATR): 3174w (ν(N-H)), 2979m, 2946m (ν$(CH_2)_{as}$), 2602m, 2496m, 1647m (ν(C=O)), 1474s (δ$(CH_2)_{sc}$), 1383m, 1364w, 1172m, 1035s, 851w, 807m, 757m (γ(C-H), 700m (Φ(C=C)), cm^{-1}. ^{1}H NMR (400 MHz, $CDCl_3$, δ): 7.25 (*dd,* 2H, J_3 = 7.5, 7.0, H-7 and H-9), 7.18 (*d,* 1H, J_3 = 7.0, H-8), 7.13 (*d,* 2H, J_3 = 7.5, H-6 and H-10), 2.60 (*t,* 2H, J_3 = 7.3, H-4), 2.10 (*bt,* 2H, J_3 = 7.0, H-2), 1.93 (*tt,* 2H, J_3 = 7.3, 7.0, H-3). ^{13}C NMR (100.6 MHz, $CDCl_3$, δ): 170.73 (C=O), 140.44 (C-5), 127.87 (C-6 and C-10 or C-7 and C-9), 127.85 (C-6 and C-10 or C-7 and C-9), 125.50 (C-8), 34.33 (C-4), 31.49 (C-2), 26.13 (C-3). ^{1}H NMR (400 MHz, DMSO-d_6, δ): 10.39 (*bs,* 1H, N-H), 8.77 (*bs,* 1H, O-H), 7.28 (*m*, 2H, H-6 and H-10), 7.18 (*m*, 3H, H-7, H-8 and H-9), 2.55 (*t,* 2H, J_3 = 7.1, H-4), 1.98 (*t*, 2H, J_3 = 7.4, H-2), 1.80 (*tt*, J_3 = 7.4, 7.1, 2H, H-3).^{13}C NMR (100.6 MHz, DMSO-d_6, δ): 169.12 (C=O), 141.90 (C-5), 128.54 (C-6 and C-10), 126.03 (C-7, C-8 and C-9), 34.85 (C-4), 32.02 (C-2), 27.25 (C-3).

*N-hydroxy-2-propylpentanamide (**HL**$_2$):* Yield 508 mg (45.7%). Colorless crystals. IR (ATR): 3176w (ν(N-H)), 3026w, 2957m (ν$(CH_3)_{as}$), 2930m (ν$(CH_2)_{as}$), 2873m (ν$(CH_2)_s$), 1627s (ν(C=O)), 1536m (ν(C-N) + ν$(CNH)_{bend}$), 1464s (δ$(CH_2)_{sc}$), 1381m, 1273w, 1113w, 1041m, 990w, 949m, 891w, 756m, cm^{-1}. ^{1}H NMR (400 MHz, $CDCl_3$, δ): 1.98 (*m*, 1H, H-2), 1.60 (*m*, 2H, H-3A), 1.40 (*m*, 2H, H-3B), 1.28 (*m*, 4H, H-4), 0.88 (*t,* J_3 = 7.2, 6H, H-5).^{13}C NMR (100.6 MHz, $CDCl_3$, δ): 174.47 (C=O), 44.15 (C-2), 34.83 (C-3), 20.80 (C-4), 14.15 (C-5). ^{1}H NMR (400 MHz, DMSO-d_6, δ): 10.36 (*s,* 1H, N-H), 8.68 (*s,* 1H, O-H), 1.96 (*m,* 1H, H-2), 1.43 (*m,* 2H, H-3A), 1.20 (*m,* 6H, H-3B and H-4), 0.83 (*t,* 6H, J_3 = 7.2, H-5). ^{13}C NMR (100.6 MHz, DMSO-d_6, δ): 171.39 (C=O), 41.89 (C-2), 34.45 (C-3), 19.97 (C-4), 13.78 (C-5).

*,** Corresponding authors. E-mail: (*)marija.gencic@pmf.edu.rs; (**)goran.kaluderovic@hs-merseburg.de

*[$Ph_2Sn(L_1)_2$] (**1**)*: Yield 164 mg (94.8%). Colorless solid. IR (ATR): 3141w (ν(N-H)), 2929w (ν$(CH_2)_{as}$), 1596m (ν(C=O)), 1519m (ν(C-N) + ν$(CNH)_{bend}$), 1496m, 1454m (δ$(CH_2)_{sc}$), 1430m, 1363w, 1299w, 1152w, 1087w, 1071m, 992m, 952m, 731m (γ(C-H), 700s (Φ(C=C)), 540m (ν(Sn-O)), cm^{-1}. ^{1}H NMR (400 MHz, $CDCl_3$, δ): 7.75 (*dd,* 4H , J_3 = 6.60, J_4 = 2.90, H-2' and H-6'), 7.345 (*dd,* 4H, J_3 = 7.00, 6.60, H-3' and H-5'), 7.335 (*dd,* 2H, J_3 = 7.00, J_4 = 2.90, H-4'), 7.22 (*dd,* 4H, J_3 = 7.60, 7.20, H-7 and H-9), 7.15 (*dd*, 2H, J_3 = 7.60, J_4 = 1.70, H-8), 7.07 (*ddd*, 4H, J_3 = 7.20, J_4 = 1.70, –1.00, H-6 and H-10), 2.53 (*td,* 4H, J_3 = 7.70, J_4 = –1.00, H-4), 2.28 (*t,* 4H, J_3 = 7.00, H-2), 1.89 (*tt,* 4H, J_3 = 7.70, 7.00. H-3). ^{13}C NMR (100.6 MHz, $CDCl_3$, δ): 167.32 (C=O), 145.79 (C-1'), 141.10 (C-5), 134.86 (C-2' and C-6'), 129.86 (C-4'), 128.70 (C-3' and C-5'), 128.61 (C-6 and C-10), 128.59 (C-7 and C-9), 126.21 (C-8), 34.79 (C-4), 30.73 (C-2), 26.95 (C-3). ^{119}Sn NMR (149.2 MHz, $CDCl_3$, δ): –402.41 (*s,* Sn). Combustion analysis for $C_{15}H_{18}N_2O_4Sn$: Calculated. C 61.05 H 5.45, N 4.42; found C 60.93 H 5.57, N 4.45.

*[$Ph_2Sn(L_2)_2$] (**2**)*: Yield 98 mg (89 %). Colorless solid. IR (ATR): 3176w (ν(N-H)), 3048w, 2956s (ν$(CH_3)_{as}$), 2930m (ν$(CH_2)_{as}$), 2871m (ν$(CH_2)_s$), 1589s (ν(C=O)), 1525m (ν(C-N) + ν$(CNH)_{bend}$), 1464m (δ$(CH_2)_{sc}$), 1429m, 1380m, 1277w, 1120m, 1073m, 1045m, 995m, 953m, 899w, 728m (γ(C-H), 697s (Φ(C=C)), 540m (ν(Sn-O)), cm^{-1}. ^{1}H NMR (400 MHz, $CHCl_3$, δ): 7.59 (*m,* 4H, H-2' or H-3'), 7.30 (*m,* 2H, H-4'), 7.27 (*m,* 4H, H-2' or H-3'), 1.96 (*m,* 2H, H-2), 1.54 (*m,* 4H, H-3A), 1.28 (*m,* 8H, H-3B and H-4A), 1.07 (*m,* 4H, H-4B), 0.76 (*m*, 12H, CH_{3A} and CH_{3B}). ^{13}C NMR (100.6 MHz, $CDCl_3$, δ): 169.52 (C=O), 148.29 (C-1'), 135.56 (C-2' or C-3'), 128.38 (C-4'), 127.94 (C-2' or C-3'), 43.35 (C-2), 34.35 (C-3), 20.49 (C-4), 14.10 (C-5). ^{119}Sn NMR (149.2 MHz, $CDCl_3$, δ): –349.95 (*s,* Sn). Combustion analysis for $C_{28}H_{42}N_2O_4Sn$: Calculated. C 57.06, H 7.18, N 4.75; found C 57.45, H 7.32, N 4.70.

IR SPECTRA OF LIGAND PRECURSORS AND COMPLEXES

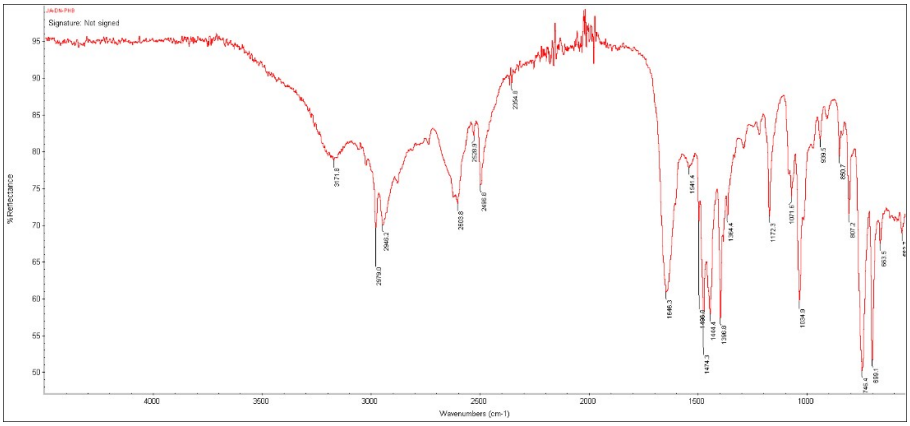

Fig. S-1. FTIR spectrum of *N*-hydroxy-4-phenylbutanamide (**HL$_1$**)

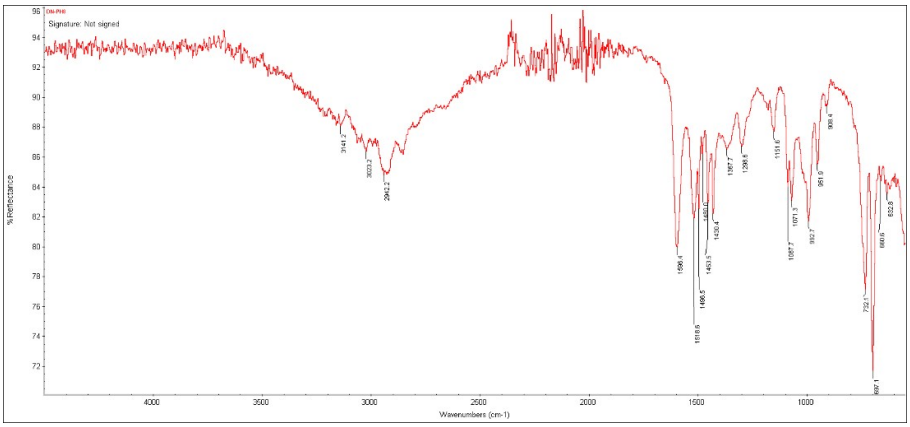

Fig. S-2. FTIR spectrum of [$Ph_2Sn(L_1)_2$] (**1**)

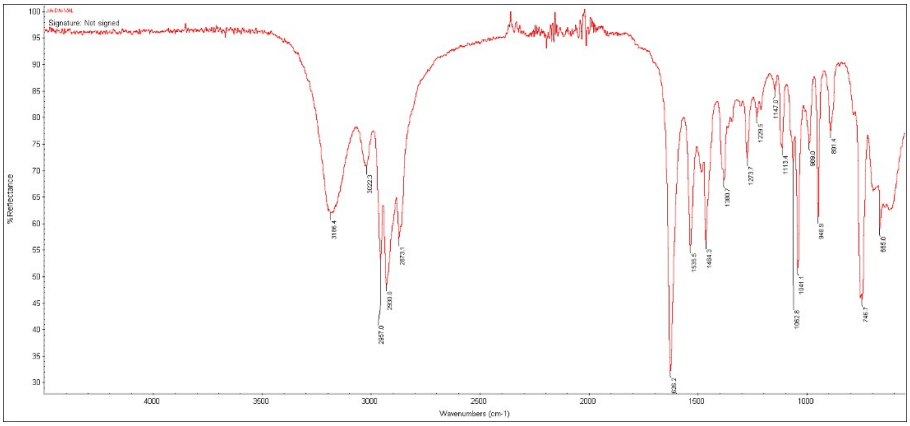

Fig. S-3. FTIR spectrum of *N*-hydroxy-2-propylpentanamide (**HL_2**)

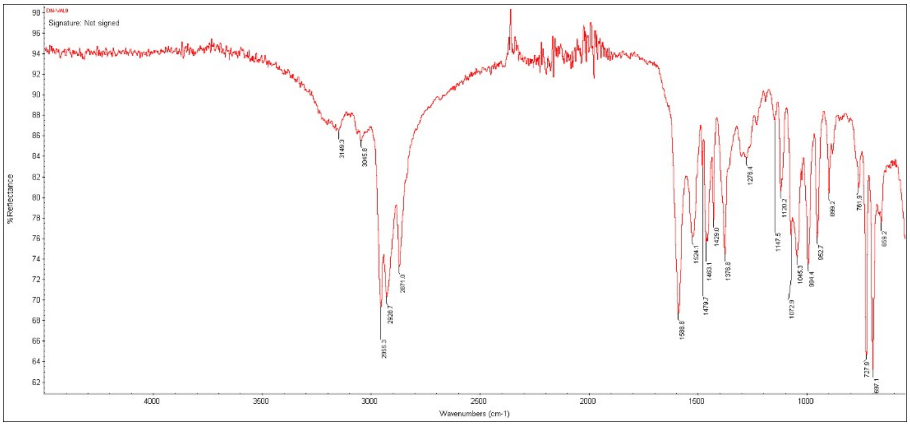

Fig. S-4. FTIR spectrum of $[Ph_2Sn(L_2)_2]$ (**2**)

NMR SPECTRA OF LIGAND PRECURSORS AND COMPLEXES

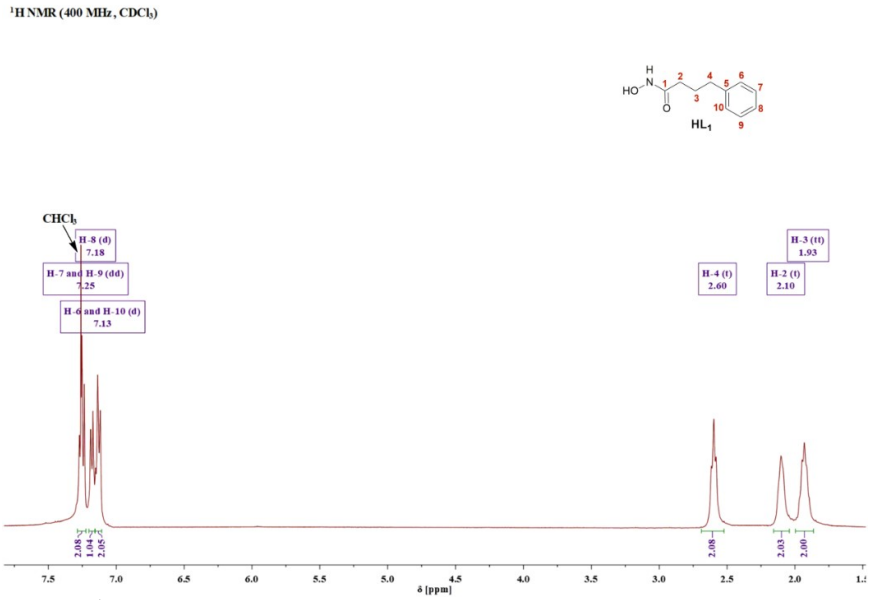

Fig. S-5. ^{1}H NMR spectrum (400 MHz, $CDCl_3$) of *N*-hydroxy-4-phenylbutanamide (**HL$_1$**)

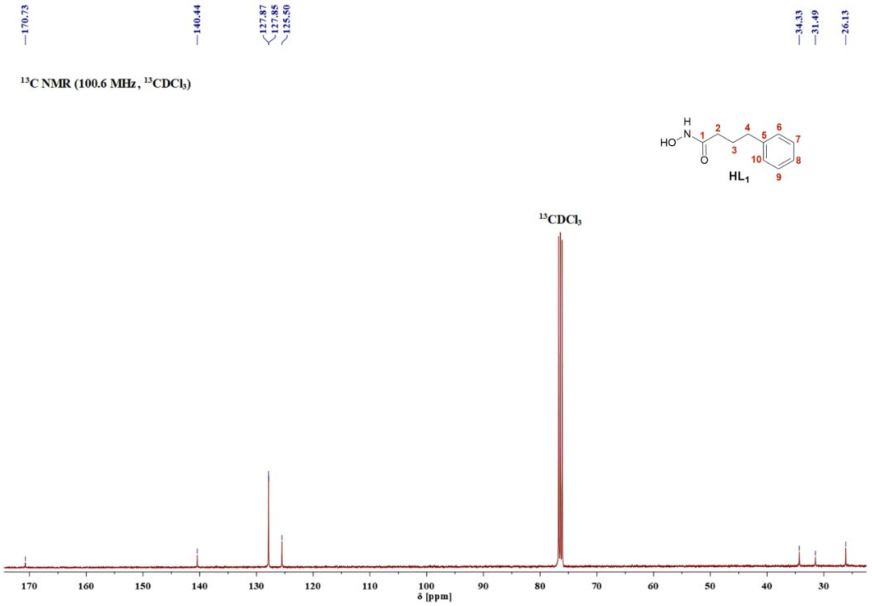

Fig. S-6. ^{13}C NMR spectrum (100.6 MHz, $CDCl_3$) of *N*-hydroxy-4-phenylbutanamide (**HL$_1$**)

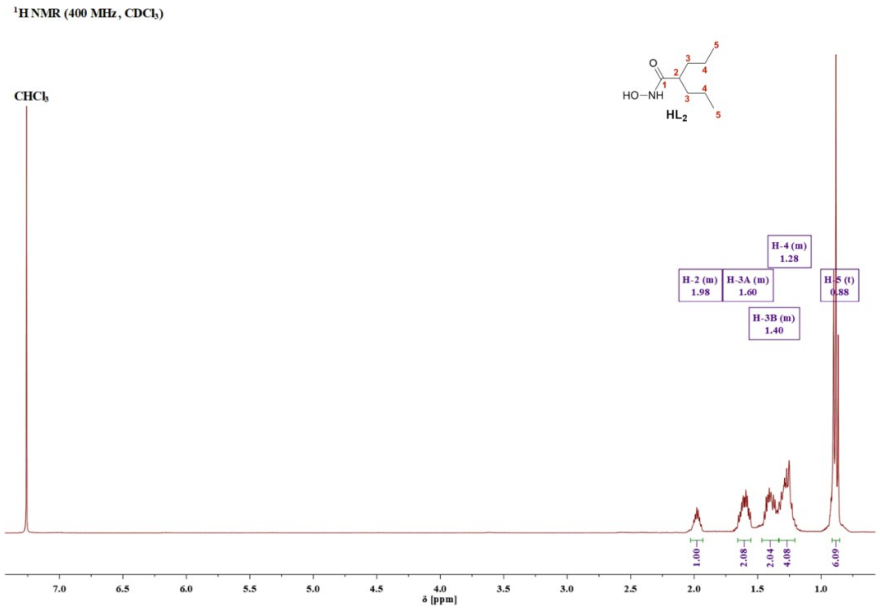

Fig. S-7. ^{1}H NMR spectrum (400 MHz, $CDCl_3$) of *N*-hydroxy-2-propylpentanamide (**HL_2**)

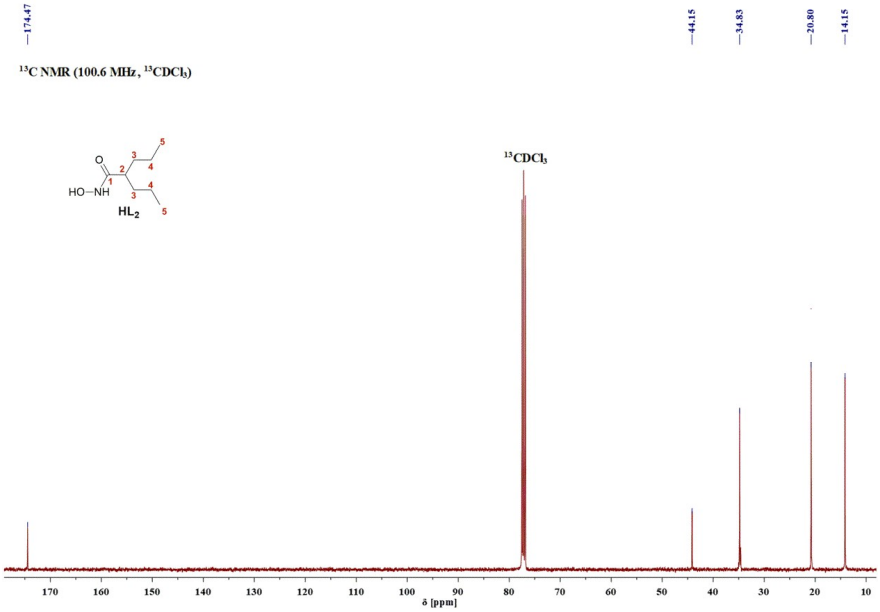

Fig. S-8. ^{13}C NMR spectrum (100.6 MHz, $CDCl_3$) of *N*-hydroxy-2-propylpentanamide (**HL_2**)

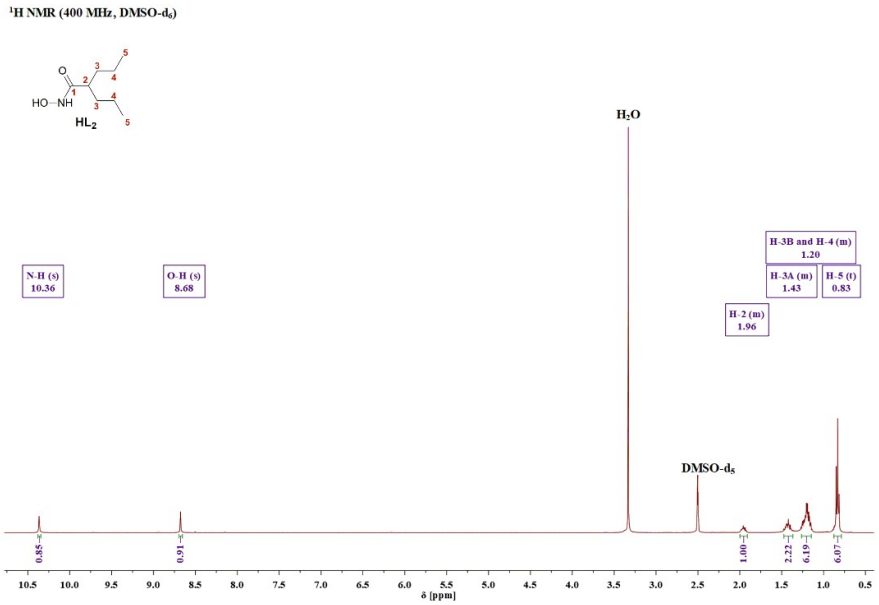

Fig. S-9. ^{1}H NMR spectrum (400 MHz, DMSO-d_6) of *N*-hydroxy-2-propylpentanamide (**HL$_2$**)

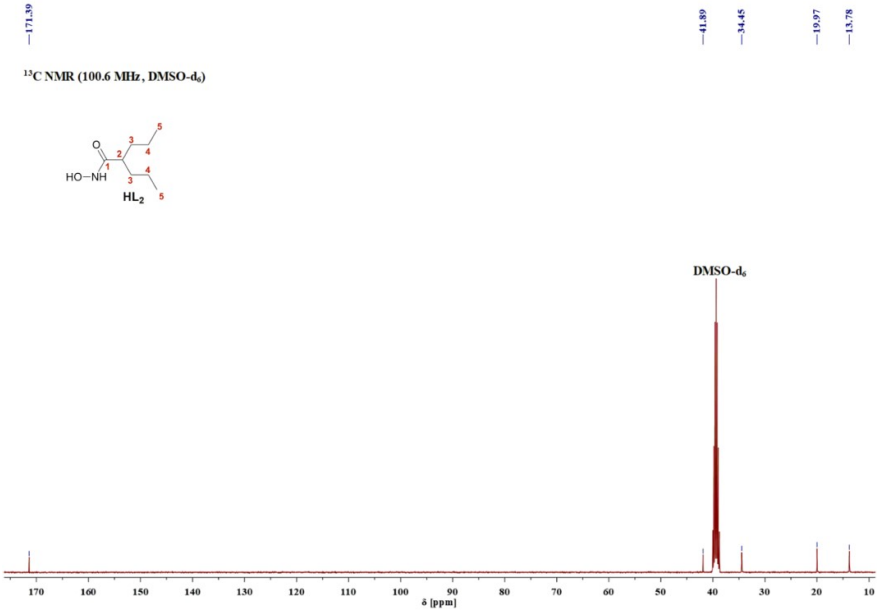

Fig. S-10. ^{13}C NMR spectrum (100.6 MHz, DMSO-d_6) of *N*-hydroxy-2-propylpentanamide (**HL$_2$**)

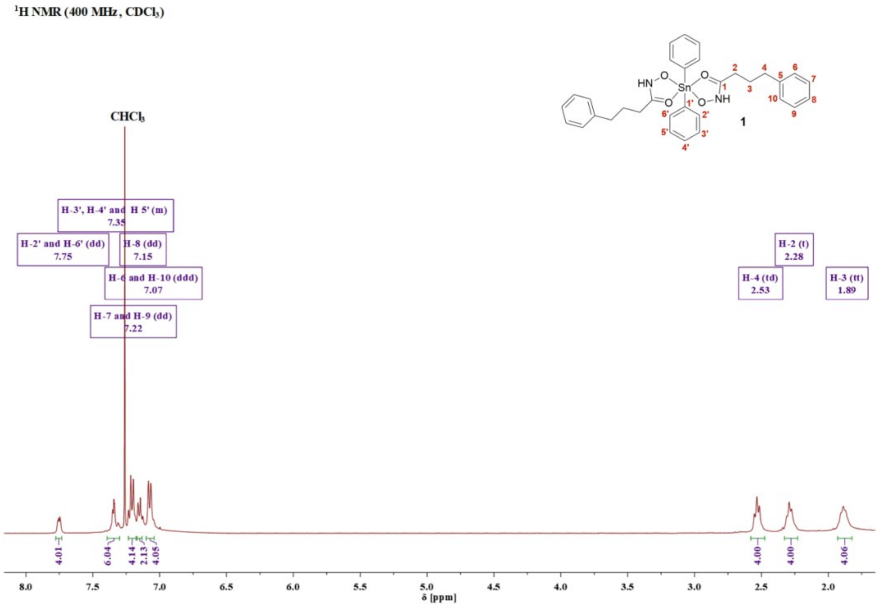

Fig. S-11. ^{1}H NMR spectrum (400 MHz, $CDCl_3$) of $[Ph_2Sn(L_1)_2]$ (**1**)

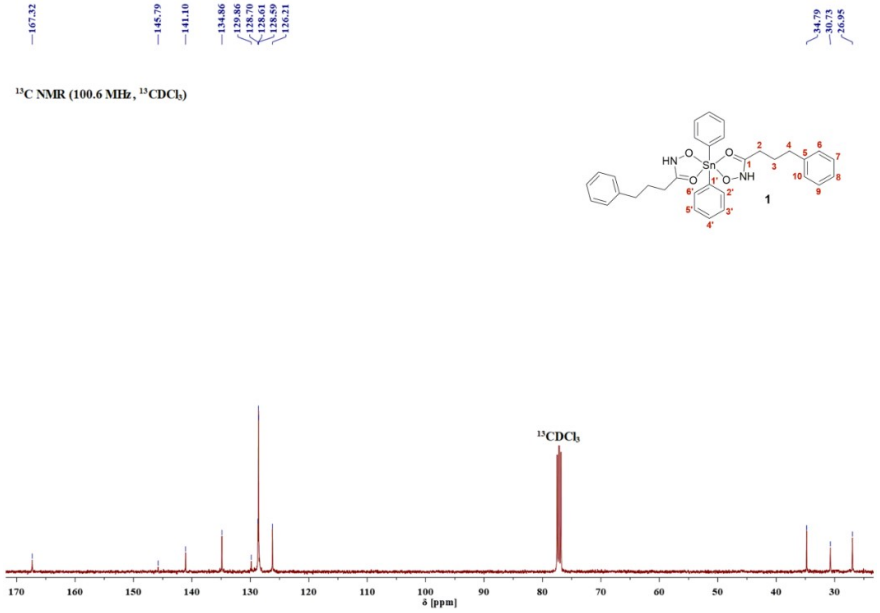

Fig. S-12. ^{13}C NMR spectrum (100.6 MHz, $CDCl_3$) of $[Ph_2Sn(L_1)_2]$ (**1**)

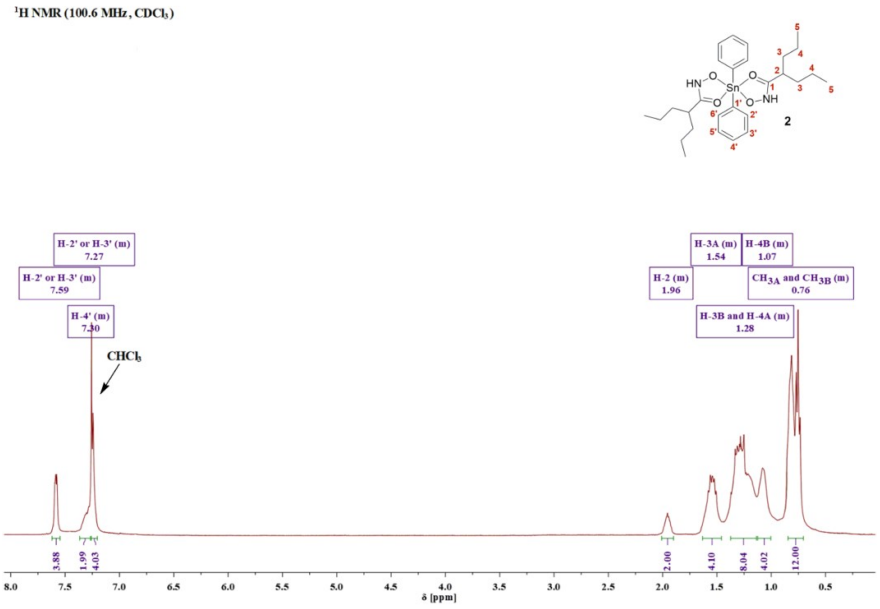

Fig. S-13. ^{1}H NMR spectrum (400 MHz, $CDCl_3$) of $[Ph_2Sn(L_2)_2]$ (**2**)

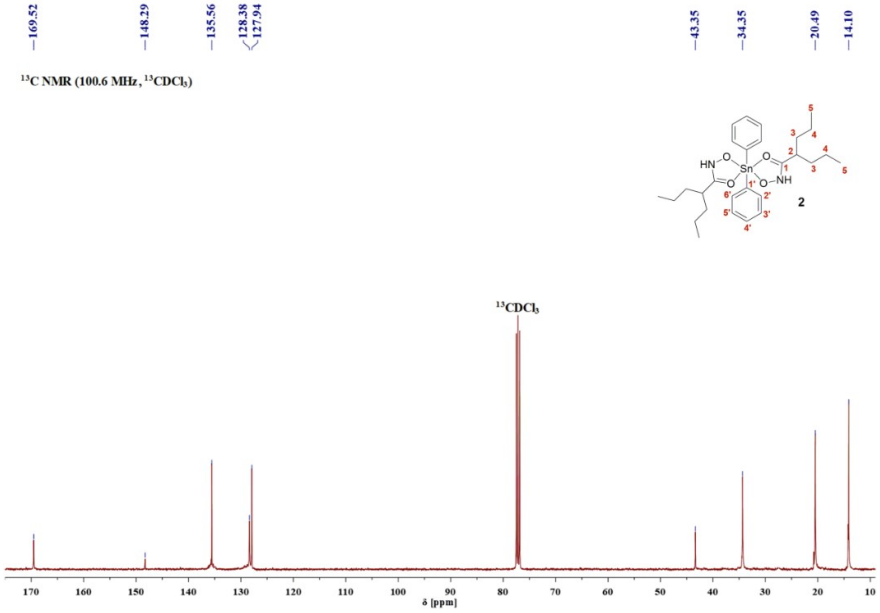

Fig. S-14. ^{13}C NMR spectrum (100.6 MHz, $^{13}CDCl_3$) of $[Ph_2Sn(L_2)_2]$ (**2**)

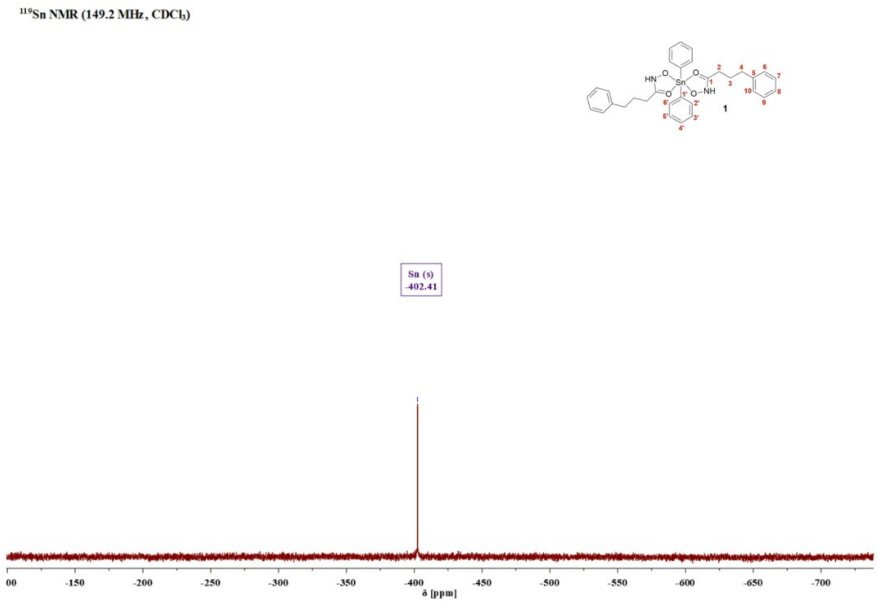

Fig. S-15. ^{119}Sn NMR spectrum (149.2 MHz, $CDCl_3$) of $[Ph_2Sn(L_1)_2]$ (**1**)

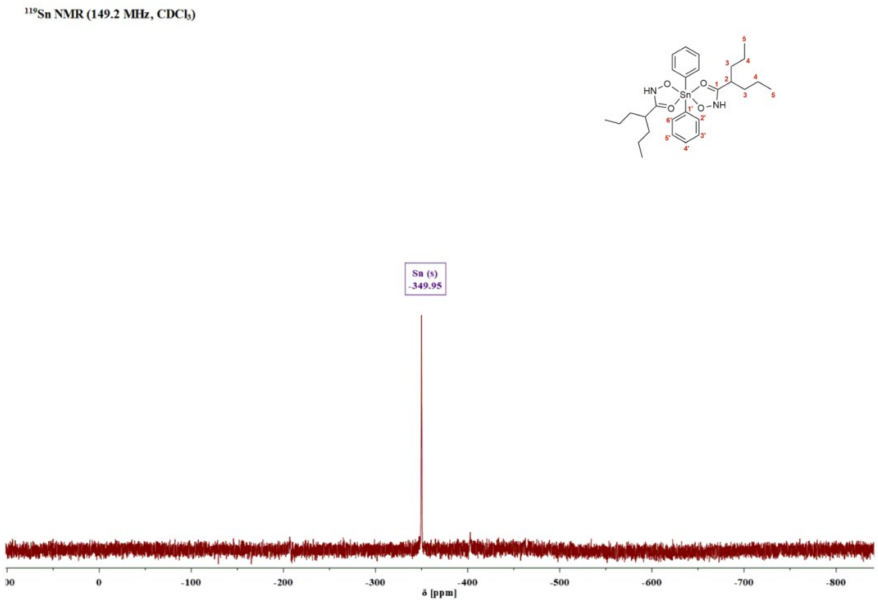

Fig. S-16. ^{119}Sn NMR spectrum (149.2 MHz, $CDCl_3$) of $[Ph_2Sn(L_2)_2]$ (**2**)

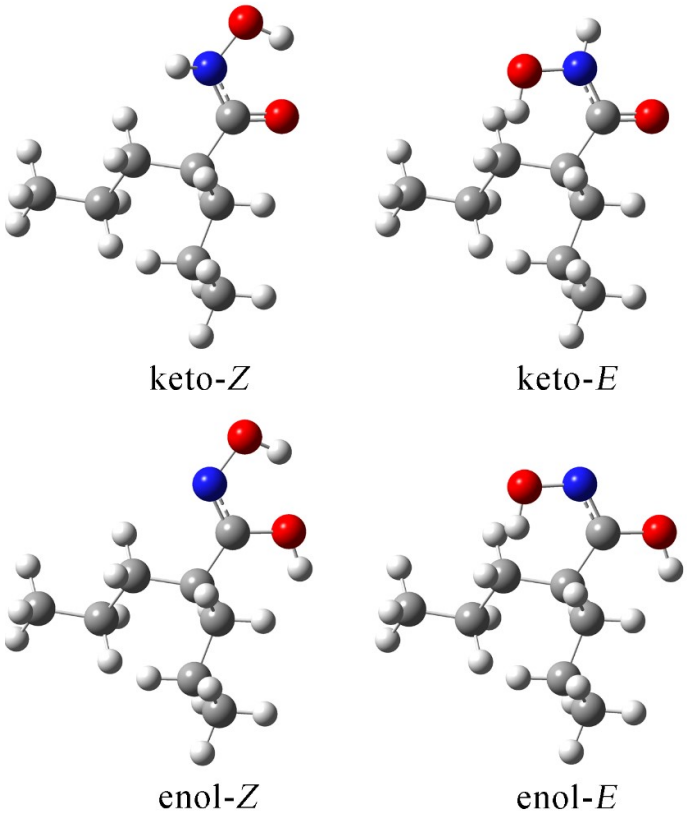

Fig. S-17. Optimized isomers (B3LYP-D3BJ/6-311++G(d,p) level of theory) of **HL_2**

Table S-I. Experimental and theoretical (at B3LYP-D3BJ/6-311++G(d,p) level of theory) of **HL_2**

^{1}H chemical shifts [ppm]			^{13}C chemical shifts [ppm]		
H atom	Experimental	Theoretical	C atom	Experimental	Theoretical
C5-H	0.88	0.88	C5	14.2	15.8
C4-H	1.28	1.28	C4	20.8	27.2
C3-H	1.40	1.30	C3	34.8	38.5
C2-H	1.98	2.06	C2	44.1	49.6
O-H	8.68	6.98	C1	174.5	171.5
N-H	10.36	7.66			
R		0.978	R		0.994
MAE [ppm]		0.04	MAE [ppm]		4.0

Table S-II. Experimental and theoretical (at B3LYP-D3BJ/6-311++G(d,p) level of theory) of complex **2**.

^{1}H chemical shifts [ppm]			^{13}C chemical shifts [ppm]		
H atom	Experimental	Theoretical	C atom	Experimental	Theoretical
C5-H	0.76	0.58	C5	14.1	16.5
C4-HA	1.07	0.78	C4	20.5	22.0
C4-HB	1.28	0.89	C3	34.4	38.1
C3-HA	1.28	0.95	C2	43.4	48.0
C3-HB	1.54	1.29	C2’	127.9	133.7
C2-H	1.96	1.53	C6’	127.9	125.0
C2’-H	7.27	7.22	C4’	128.3	128.7
C6’-H	7.27	7.22	C3’	135.6	130.0
C4’-H	7.30	7.28	C5’	135.6	130.0
C3’-H	7.59	7.54	C1’	148.3	147.7
C5’-H	7.59	8.08	C1	169.5	169.6
R		0.992	R		0.991
MAE [ppm]		0.22	MAE [ppm]		3.0

Journal of the Serbian Chemical Society
JSCS@tmf.bg.ac.rs • www.shd.org.rs/JSCS
J. Serb. Chem. Soc. *88* (12) 1335–1354 (2023)
JSCS–5699
Original scientific paper
Published 19 December 2023

Synthesis, spectroscopic characterization and DFT analysis of dichlorido(η^6-*p*-cymene)ruthenium(II) complexes with isonicotinate-polyethylene glycol ester ligands

THOMAS EICHHORN[1•], DUŠAN DIMIĆ[2•#], ZORAN MARKOVIĆ[3] and GORAN N. KALUĐEROVIĆ[1*]

[1]*Department of Engineering and Natural Sciences, University of Applied Sciences Merseburg, Eberhard-Leibnitz-Straße 2, 06217 Merseburg, Germany,* [2]*University of Belgrade, Faculty of Physical Chemistry, Studentski trg 12–16, 11000 Belgrade, Serbia and* [3]*Institute of Information Technologies, University of Kragujevac, Jovana Cvijića bb, 34000 Kragujevac, Serbia*

(Received 12 April, revised 26 June, accepted 18 September 2023)

Abstract: Ruthenium complexes have gained significant attention due to the ruthenium similarity to iron, lower toxicity, and higher anticancer effectiveness than other compounds. In this contribution, five new isonicotinate-polyethylene glycol ester ligands were synthesised and characterised by NMR and IR spectroscopies. The corresponding Ru(II) complexes were also obtained, and their structure was investigated by traditional methods. The optimisation of structures was performed at B3LYP/6-31+G(d,p) level of theory for H, C, N and O atoms and B3LYP/LanL2DZ for Ru. The intramolecular stabilisation interactions were assessed through the natural bond orbital approach. The NMR chemical shifts were predicted by the gauge independent atomic orbital method and compared to the experimental values. High correlation coefficients and low mean absolute errors between these data sets proved that the predicted structures described well the experimental ones. The theoretical and experimental IR spectra were also compared, and differences in the most notable bands were described. One of the ligands (**L5**) and complexes (**5**) showed fluorescent properties due to methylisatoic moiety. The electronic spectra of this compound were modelled by the time dependent-density functional theory method. The difference of 11 nm between the experimental and the theoretical wavelength was explained by the interactions between the solvent and the solute. Further biological and theoretical studies are advised for this series of compounds.

Keywords: ruthenium(II) complexes; DFT; NBO; isonicotinate; IR; NMR.

* Corresponding author. E-mail: goran.kaluderovic@hs-merseburg.de
• Equaly contributed.
Serbian Chemical Society member.
https://doi.org/10.2298/JSC230412070E

INTRODUCTION

Cancer is a leading cause of death worldwide, representing a multifactorial and complex disease. The discovery of cisplatin in the 60s of the twentieth century marked the beginning of using complex compounds in treating different cancers.[1] Although proven effective, this compound has some severe side effects, including myelosuppression, emesis, nephrotoxicity and alopecia, besides possible inherent resistance observed in some cancer types.[1,2] Therefore, the attention has been focused on similar compounds with higher effectiveness and lower toxicity. Complexes based on platinum-type metals, such as palladium, ruthenium, iridium, rhodium and osmium, represent possible substitutes for cisplatin.[3–5] Due to its similarity in chemical behaviour to iron, ruthenium is characterised by higher human organism tolerance and higher selectivity. *In vitro* studies[6] focus mostly on Ru(II)-arene and Ru(II)-polypyridine complexes.

The development of so-called "half sandwich" Ru(II)-arene compounds (or "piano-stool" complexes) is underway as these compounds offer diversity in the possible substituents that influence the biological activity.[4,7] The general formula of these compounds is [(η^6-arene)Ru(*YZ*)(*X*)], in which *YZ* can be either a bidentate ligand or two monodentate ligands.[7] Compounds having neutral monodentate ligands commonly contain, beside η^6-arene, two chlorido ligands. The solubility of Ru(II) complexes in water represented a severe drawback for their application in medicine. The ionic complexes have much greater potential, and the research nowadays focuses on the compounds with the increased halide ligands groups.[8,9] Some of the examples of Ru(III) compounds that entered clinical trials are imidazolium *trans*-[tetrachlorido(dimethyl sulfoxide)(1-*H*-imidazole)ruthenate(III)] (NAMI-A), indazolium *trans*-[tetrachloridobis(1-*H*-indazole)ruthenate(III)] (KP1019) and their sodium analogues.[1] Depending on the choice of ligands, Ru(II) compounds also possess some antiradical activity towards the reactive species, such as hydroxyl radical.[10]

The coordination properties of nicotinic and isonicotinic acid to lanthanide ions were described 1970s.[11] The study by Schobert and Biersack investigated *cis*-dichloridoplatinum(II) complexes with aminomethylnicotinate and isonicotinate ligands, in which these compounds acted as bidentate ligands.[12] Rhenium(I)--polypyridine complexes coordinated to ethyl-isonicotinate exhibited luminescence that depended on polypyridine moiety and that could be used as photosensitizers for the singlet oxygen production in cells.[13] Mixed metal complexes of copper(II) and vanadium(V) incorporating isonicotinate ligands were obtained by Wang and coworkers.[14] Four new uranium(VI) isonicotinate framework solids had a range of dimensionalities from zero-dimensional to two-dimensional compounds and were described by Kim and coworkers.[15]

This research aims to describe the synthesis and structural characterization of five new isonicotinate-polyethylene glycol ester ligands and their correspond-

ing Ru(II) complexes. NMR, IR, MS, UV–Vis, fluorescence spectroscopies and elemental analysis are used in this contribution to determine the structures of compounds. The structures of the obtained compounds were also validated by predicting IR, NMR and UV–Vis spectra calculated using the density functional theory (DFT) results and comparing them with the experimental ones. Interactions governing the stability of ligands and complexes are also examined in detail by the natural bond orbital (NBO) theory.

EXPERIMENTAL AND THEORETICAL METHODS

Materials and methods

Preparative technique. Ligand precursors were prepared in dry toluene and acetonitrile. All reactions of ruthenium(II) complexes were carried out under argon by using the standard Schlenk line technique. Diethyl ether and toluene were distilled from sodium benzophenone. Dichloromethane was distilled from calcium hydride. 2-Propanol was dried with molecular sieve 3 Å and degassed with argon before use. Ethylene glycol was freshly distilled and stored with a molecular sieve 4 Å. All other poly(ethylene oxide) compounds and poly(ethylene oxide) monomethyl ethers were dried with sodium sulphate. Ligand precursor (**L1**·HCl) and appropriate ruthenium(II) complex (**1**) were previously reported[16] and used here for comparison and theoretical calculations.

Purchased materials. Isonicotinic acid, thionyl chloride, diethylene glycol and α-terpinene were purchased from Acros Organics. Triethylene glycol, tetraethylene glycol and diethylene glycol monomethyl ether were ordered from Merck. Glycol monomethyl ether and triethylene glycol monomethyl ether were purchased from Fluka. Ruthenium(III) chloride hydrate was also commercially available from Alfa Aesar.

Instrumental methods

All samples were measured in 5 mm NMR tubes at 300 K; other conditions are noted. ^{1}H- and ^{13}C-NMR spectra were recorded on Varian Unity 500 or Varian Gemini 400 spectrometers. The chemical shift of ^{1}H-NMR spectra is relative to signals of undeuterated solvents, C*H*Cl$_3$ (δ = 7.26 ppm) and *H*DO (δ = 4.79 ppm). ^{13}C-NMR spectra are calibrated to solvent *C*DCl$_3$ (δ = 77.16 ppm) and all signals noted in the experimental part are singlets. IR spectra were measured from 4000–250 cm^{-1} with a Bruker Tensor 27 FT-IR-spectrometer with diamond ATR. High-resolution ESI mass spectra were obtained from a Bruker Apex III Fourier transform ion cyclotron resonance (FTR-ICR) mass spectrometer (Bruker Daltonics) equipped with an infinity cell, a 7.0 T superconducting magnet (Bruker), an rf-only hexapole ion guide and an external Apollo electrospray ion source (Agilent, off-axis spray). The sample solutions were introduced continuously via a syringe pump with a flow rate of 120 μL h^{-1}. The ligand precursors are noted without hydrochloride as [M+H]$^+$. UV–Vis spectra were recorded on an HP 8453 (Hewlett–Packard GmbH, Waldbronn Analytical Division, Germany), and the fluorescence spectra were recorded on the Fluoromax 2 (Horiba Jobin Yvon GmbH, Unterhaching, Germany). All measurements were performed at room temperature and in cuvettes from Hellma GmbH & Co. KG (Müllheim, Germany, d = 1 cm).

Theoretical methods

All structures were optimized using the Gaussian 09 Program Package[17] without any geometrical constraints. The global hybrid generalised gradient approximation (GAA) functional B3LYP[18] and 6-311++G(d,p)[19] basis set was employed to optimize the ligand structure.

Ligands were optimized in protonated form to follow the experimentally obtained hydrochloride salts. For Ru(II) complexes, B3LYP functional in conjunction with the basis sets 6-31++G(d,p) for H, C, N and Cl, and LanL2DZ[20,21] were employed. The absence of imaginary frequencies showed that the minima of the potential energy surface were obtained. The vibrational frequencies were analysed and visualized in the GausView program.[22] The correction factors for the selected level of theory were obtained on the National Institute of Standards and Technology website (https://cccbdb.nist.gov/vsfx.asp). The influence of solvents on the simulated NMR (D_2O, $CDCl_3$) and UV–Vis (H_2O) spectra was simulated using the Conductor-like polarizable continuum model (CPCM).[23] The intramolecular interactions governing structure stability were analysed by the natural bond orbital[24] (NBO) approach, as implemented in the Gaussian Program package. The ^{1}H- and ^{13}C-NMR chemical shifts were calculated by the gauge independent atomic orbital (GIAO)[25,26] Approach. The TMS as an internal standard for NMR measurements was also optimised at the mentioned level of theory, and NMR spectra were predicted. The electronic transitions were calculated by the time dependent-density functional theory (TD-DFT).[27]

*General procedure for the synthesis of isonicotinate esters (**L2**·HCl–**L5**·HCl)*

The isonicotinic acid (Table I), and dimethylformamide (0.03 g, 0.4 mmol) were cooled to 15 °C, and the excess thionyl chloride (5 mL, 70 mmol) was added dropwise. The reaction mixture was stirred at 40 °C for one hour. The formed light yellow acyl chloride hydrochloride was obtained by evaporating the solvent and the rest of the thionyl chloride and dried *in vacuo*. The obtained acyl chloride hydrochloride was used *in situ* to prepare poly(ethylene glycol) esters (Fig. 1). The acyl chloride hydrochloride was suspended in toluene (40 mL). The appropriate poly(ethylene oxide) monomethyl ether was added at 15 °C and stirred overnight at room temperature. The product precipitated during the reaction was filtered off and washed with toluene (recrystallization from ethanol, method A). If viscous oils were obtained, toluene was removed *in vacuo* and impurities were removed by the extraction with acetone/diethyl ether (method B).

Properties, analytical and spectral data of the synthesized compounds are given in Supplementary material to this paper.

TABLE I. Reaction details for the preparation of ruthenium(II) complexes **2**–**5**

Complex	n({$RuCl_2(\eta^6$-*p*-cymene)$\}_2$) mmol	n(**L2**·HCl–**L5**) mmol	Reaction time, h	Yield, %
2	0.10	0.22	1	96
3	0.10	0.24	1	97
4	0.15	0.37	2	72
5	0.055	0.113	2	65

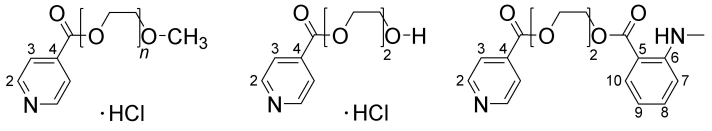

Fig. 1. Poly(ethylene oxide) monomethyl ether (n 1–3) esters of isonicotinic acid (**L1**·HCl–**L3**·HCl), di(ethylene oxide) monoester of isonicotinic acid (**L4**·HCl) and fluorescent ligand (**L5**) with assignment for NMR characterization.

*2-(2-Hydroxyethoxy)ethyl isonicotinate hydrochloride (**L4**·HCl)*. Isonicotinic acid (1.23 g, 10 mmol) and dimethylformamide (0.03 g, 0.4 mmol) were cooled to 15 °C, and the excess thionyl chloride (5 mL, 70 mmol) was added slowly. The suspension was stirred, heated to 40 °C for 1 h and turned light yellow. The formed isonicotinic acyl chloride hydrochloride was obtained by evaporation of the reaction mixture, dried *in vacuo*, and used *in situ* to prepare **L4**·HCl.

The isonicotinic acyl chloride hydrochloride was suspended in toluene (20 mL). Diethylene glycol (5.7 mL, 60 mmol) was added and the mixture was stirred overnight at rt. The crude product precipitated during the reaction, and toluene was removed *in vacuo*. The product was extracted with acetone/diethyl ether and multiple times redissolved in acetone and precipitated with excess diethyl ether. Yield: 0.34 g (14 %).

*2-[2-(2-Methylamino-benzoyloxy)ethoxy]ethyl isonicotinate (**L5**)*. **L4**·HCl (62 mg, 0.25 mmol), methylisatoic acid anhydride (54.3 mg, 0.31 mmol) and potassium carbonate (60 mg, 0.5 mmol) were suspended in acetonitrile (20 mL) and stirred at 60 °C for 3 h. The precipitate was filtered off and washed with dichloromethane (2×5 mL). The crude product was obtained by evaporation of the volatiles and purified by centrifugally accelerated thin-layer chromatography with an eluent system of dichloromethane and ethanol ($V_{CH_2Cl_2}/V_{EtOH}$ = 40:1). The fractions containing the product (R_f = 0.24) were combined, and the volatiles evaporated. Yield: 63 mg (73 %).

*General procedure for the synthesis of mononuclear ruthenium(II) complexes **2**–**4***

The appropriate ligand/ligand precursor was suspended in isopropanol (20 mL) and stirred at rt. Dichlorido(η^6-*p*-cymene)ruthenium(II) dimer was added, and the orange reaction mixture was heated to 40 °C (for details see Table I). The suspension turned light orange or yellow and was cooled to –47 °C. The product was precipitated and filtered off (Fig. 2), washed with diethyl ether (4×2 mL) and dried in air.

Properties, analytical and spectral data of the synthesized compounds are given in Supplementary material.

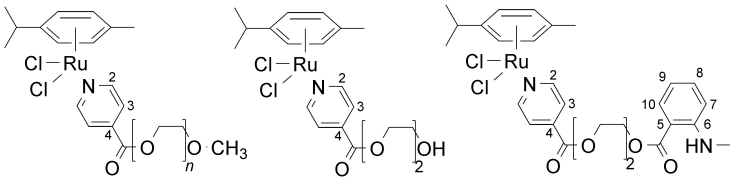

Fig. 2. Chemical structures of mononuclear Ru(II) complexes with ligands **L2**–**L5** (*n* 2–3).

RESULTS AND DISCUSSION

*Poly(ethylene oxide) esters of isonicotinic acid (**L2**–**L4**·HCl and **L5**) and corresponding Ru(II) complexes (**2**–**5**)*

Synthesis. All prepared ligand precursors were synthesised by a similar procedure described in the literature.[28,29] The appropriate acyl chloride was first synthesised by reacting isonicotinic acid with thionyl chloride (Scheme 1). This reaction was catalysed by dimethylformamide (DMF) within 1 h.[30] The proposed

mechanism includes several steps. In the first step, the sulphur atom of thionyl chloride is attacked by the carboxylic acid to give an unstable intermediate, a mixed anhydride. The released hydrogen chloride protonates the carboxylic oxygen atom and makes the carboxylic carbon atom strongly electrophilic. Afterward, the chloride anion attacks the carbon atom, and the intermediate reacts, yielding the desired acyl chloride, sulphur dioxide, and hydrogen chloride.[31,32]

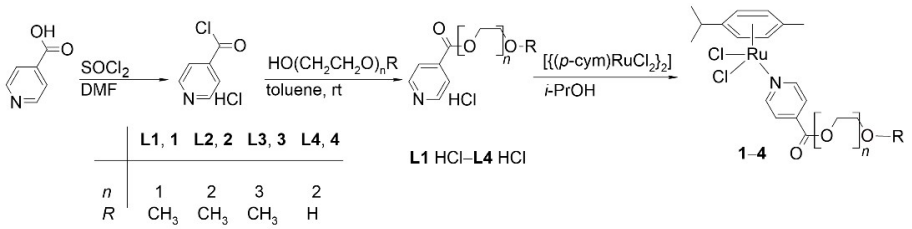

Scheme 1. Synthesis route of poly(ethylene oxide) esters of *iso*nicotinic acid (**L1**–**L4**·HCl).

The acyl chloride was obtained as a light yellow, crystalline powder that reacted exothermically with dried alcohols leading to the release of hydrogen chloride.[33] The reaction mixture, one equivalent acyl chloride with one equivalent alcohol, was stirred at room temperature overnight using dry toluene as solvent (no side products were formed, Scheme 1), yielding the desired product quantitatively.

The structures of ligands were confirmed by the NMR, IR, and ESI-HRMS techniques. The first two are discussed in detail below. The following values were obtained for the mass peaks of the protonated ligands $[L+H]^+$ with the deviation from the calculated values shown in parenthesis: *m*/*z* 226.10738 (**L2**, 0.0 ppm), 270.13351 (**L3**, 0.3 ppm) , 212.09176 (**L4**, 0.3 ppm) and 345.14451 (**L5,** 0.1 ppm).

*Structure and stability of **L1**–**L3** and **1**–**3***. The structures of all ligands optimised at the B3LYP/6-311++G(d,p) level of theory are shown in Fig. 3. This theory level was previously applied to optimize the similar compounds and the spectra assignation.[34,35] As it can be seen, the structure of ligands **L1**–**L3** consists of an aromatic ring adjacent to the ester group and a flexible aliphatic chain (Fig. 3). The planarity of the first part of the compounds is due to the elongated delocalization between the aromatic ring and ester group. In this case, a strong electron donation from the ester group to the aromatic ring is shown in the NBO analysis below. To evaluate the validity of the chosen level of theory for the structural determination of the obtained esters, the optimised bond lengths and angles of previously published **L1**[16] were compared to those of pure isonicotinic acid.[36] This comparison was performed by calculating the mean absolute error (*MAE*) between experimental and theoretical bond lengths and angles. This para-

meter estimates the average absolute difference between two sets of data. The *MAE* values obtained after the comparison are 0.02 Å and 3.1° for bond lengths and angles. The complete list of values is shown in the Supplementary material. After a closer inspection of the data, it is clear that the differences are because isonicotinic acid is in the zwitterionic form in the crystal structure, with the amino group protonated and carboxyl group deprotonated, which leads to the elongation of N−C bonds and equilibration of two C=O bonds. Nevertheless, these results show that the optimized structure resembles the expected crystallographic structure. In case of other two ligands, any significant changes in this part of molecule are not expected. All of the C−O in the aliphatic chain have uniform length of 1.43 Å.

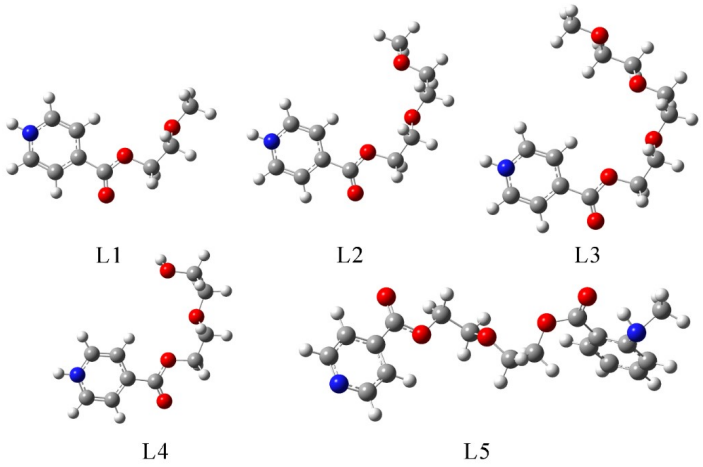

Fig. 3. Optimized ligand structures at B3LYP/6-311++G(d,p) level of theory.

The stability of ligands is governed by intramolecular interactions, as examined in the NBO framework. The most numerous interactions include π(C−C)→ →π*(C−C). These interactions have energies between 95 and 76 kJ mol^{-1} (Table S-I of the Supplementary material). The nitrogen atom is part of the aromatic ring, and its lone pairs are included in the stabilisation of the ring structure. Interactions of the type π(C−N)→π*(C−C) and π(C−C)→π*(C−N) have energies of 60 and 109 kJ mol^{-1}, respectively. The lone pair of nitrogen atoms also stabilise neighbouring C−C atoms, LP(N)→π*(C−C), with the energy of 41 kJ mol^{-1}. The carboxyl group interacts strongly with the aromatic ring. The interconnection between the aromatic ring and carboxylic group is stabilised by the interaction with an energy of 10 kJ mol^{-1}. The planarity of this part of the molecule is possible through strong LP(O)→π*(C−C) interaction with an energy of 75 kJ mol^{-1}. The strongest interactions are within the carboxyl group, LP(O)→

$\rightarrow\pi^*$(C−O), with an energy of 135 kJ mol^{-1}. The rest of the aliphatic chain is stabilised by much weaker interactions that allow free rotation of the groups. The interactions in other ligands are not influenced by the elongation, as these groups are interconnected by the oxygen atoms that act as electron donors to both sides of a chain, but the leakage of electron density is not possible from one side to the other.

The bond is formed between Ru(II) and pyridine nitrogen atom upon complexation. The predicted structures of complexes were optimized at B3LYP/6--31G(d,p)(H, C, O, N, Cl)/LanL2DZ (Ru) level of theory.[37–39] In a previous contribution, this level of theory was applied to [{RuCl(η^6-*p*-cymene)}$_2$(μ-Cl)(μ-1--*N,N'*-naphthyl)]Cl compound and it was shown that the optimised structure represented the crystallographic one well, with the detailed spectra assignment.[10] The optimised structure of **1**, as a representative of the whole class **1**–**3** complexes, is presented in Fig. 4. The optimised structure contains *p*-cymene and **L1** ligand and two chlorine atoms bonded to Ru(II). The resemblance between **L1** and isonicotinoic acid was shown previously, and the same line of reasoning can be applied to the expected similarity between the experimental and the theoretical structures of *p*-cymene moiety.[10] The optimised Ru−Cl bonds have 2.43 and 2.45 Å, almost identical to previously determined lengths in crystal structures of similar compounds.[40] The Ru−N bond length is 2.18 Å, similar to the previously discussed compounds. These bond lengths are not affected by the length of an aliphatic chain of ligands. The optimised bond angles Cl−Ru−Cl and N−Ru−Cl are 90 and 64°, respectively. These angles, again, follow the experimentally determined values. The interactions between Ru(II) and surrounding groups were analysed in the next paragraph through the NBO approach, with the compound **1** given as an example.

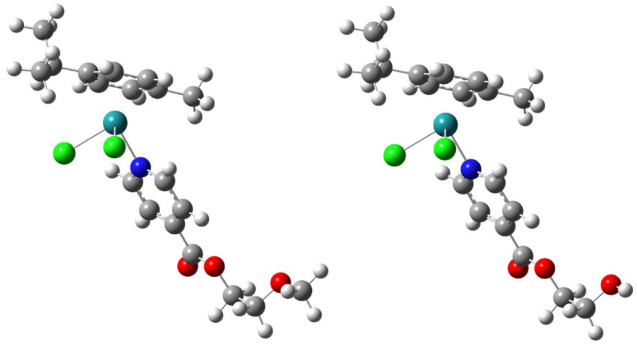

1 4

Fig. 4. Optimized structures of **1** and **4** at B3LYP/6-31+G(d,p)(H,C,N,O,Cl)/LanL2DZ(Ru) level of theory (the following colours represent atoms: white – hydrogen, grey – carbon, blue – nitrogen, green – chlorine, teal – ruthenium).

The stabilisation interactions within the **L1** moiety within **1** are almost identical to those previously discussed. The *p*-cymene moiety contains an aromatic ring with methyl and isopropyl groups. The strongest stabilisation interactions within *p*-cymene denoted as π(C−C)→π*(C−C), have energies between 46 and 55 kJ mol^{-1} (Table S-I). The π electron cloud also interacts with Ru(II) through π(C−C)→LP*(Ru), which includes different carbon-carbon pairs of the aromatic ring. These interactions have energies between 60 and 80 kJ mol^{-1}, proving the Ru(II)-*p*-cymene group's stability. The interactions denoted as LP(Ru)→π*(C−C) were also observed with similar energies. The nitrogen atom of the pyridine ring interacts with Ru(II) through the interactions with an energy of 146 kJ mol^{-1}. The weak interactions denoted as LP(N)→σ*(Ru−Cl) have energies of around 27 kJ mol^{-1}. The carbon–nitrogen bonds stabilize the Ru(II) through π(C−N)→ →LP*(Ru) interactions with energies of 50 kJ mol^{-1}. The stabilisation interaction between nitrogen atom and Ru(II) was observed in other compounds in literature.[41,42] Chlorido ligands also interact with the central metal ion by donating electron pairs. These interactions between lone pairs, LP(Cl)→LP*(Ru), have energies between 34 and 75 kJ mol^{-1}. The weak interactions LP(Cl)→σ(Ru−Cl) of several kJ mol^{-1} stabilise the overall structure. Based on the given values, it can be concluded that the donor atoms, namely chlorine, nitrogen, and aromatic moiety, interact with Ru ions through interactions of similar strength. The aliphatic chain length does not influence these interactions as these groups are further from the interacting nitrogen atom.

Experimental and theoretical NMR spectra. The synthesised **L2**–**L3**·HCl ligands were characterised by NMR spectroscopy. Ligand precursor, previously reported, **L1**·HCl and appropriate ruthenium(II) complex **1**[16] were used for comparison, and the results are given in the mentioned reference. The NMR spectra were modelled for the structures optimized in D_2O and $CDCl_3$ to mimic the experimental conditions. The theoretical chemical shifts were calculated relative to TMS. The experimental and theoretical values for the chemical shifts of **L1**·HCl and **1**, as representative examples, are given in Tables S-II and S-III of the Supplementary material. These values were compared by calculating the *MAE* and correlation coefficient for ^{1}H- and ^{13}C-NMR spectra. The atomic enumeration is shown in Figs. 1 and 2, and it should be remembered that the aromatic carbon atoms are symmetric; therefore, a lower number of resonances is observed.

The results from Tables S-II and S-III show that the theoretical chemical shifts are in agreement with the experimental ones. The calculated values were overestimated, and the correction factor was obtained from the dependency between experimental and theoretical values (0.94 for ^{1}H- and 0.97 for ^{13}C--NMR). When ^{1}H-NMR spectra are concerned, the correlation factors between the two sets of values were 0.97/0.99 for **L1·HCl** and **1**. The *MAE* value was

0.27 ppm in the case of **L1**·HCl and 0.44 ppm in the case of **1**. These high correlation factors and low *MAE* values result from the relative rigidity of the overall structure represented by aromatic rings and structures with elongated delocalisation. These results prove the applicability of the selected level of theory for the representation of the newly obtained Ru(II) complexes. The lowest value of chemical shifts was obtained for the methoxy group in the aliphatic chain (3.48 ppm in the experimental and 3.28 ppm in the theoretical spectrum). The proximity of oxygen atoms increased chemical shifts to 3.92 ($OC\underline{H}_2$) and 4.67 ($COOC\underline{H}_2$) ppm in the experimental spectrum. These values are, on average, 0.3 ppm different in the theoretical spectrum. In the pyridine ring, the appropriate chemical shifts are much higher and depend on the proximity of the nitrogen atom. Two sets of resonances at 8.62 and 9.05 ppm represent the hydrogen atoms in the experimental spectrum. Once the complex is formed, the largest difference was observed for the hydrogen atoms adjacent to nitrogen (9.23 *vs*. 9.05 ppm, and 7.86 *vs*. 8.62 ppm), proving that a new interaction between nitrogen and Ru(II) is formed, inducing the changes in the electron density of the ring. The ^{1}H-NMR chemical shifts of protons form the *p*-cymene moiety have the expected values common for other similar compounds.[40]

The ^{13}C-NMR chemical shifts are more commonly used for the comparison due to the lower possibility for rotation. In the ligand structure, the lowest chemical shifts were obtained for the carbon atoms of the aliphatic chain (58.2 ($O\underline{C}H_3$), 65.9 ($\underline{C}H_2OOC$) and 69.6 ($\underline{C}H_2O$) ppm). These carbon atoms are located at 62.8, 73.9, and 73.7 ppm in the theoretical spectrum. The presence of two oxygen atoms in the carboxyl group significantly increases the chemical shift value to 163.4 in the experimental and 161.4 ppm in the theoretical spectrum. Carbon atoms of the pyridine ring also have the expected values. The carbon atoms adjacent to nitrogen in the pyridine ring increase the chemical shift value upon complexation (142.7 to 155.9 ppm). The rest of the carbon atoms retain the position of the resonances present in **L1**·HCl. The same applies to chemical shifts of carbon atoms in the *p*-cymene moiety.

Experimental and theoretical IR spectra. The experimental and theoretical IR spectra were also compared in order to investigate the applicability of the selected level of theory. The theoretical vibrational motion was visualised in GausView,[22] as previously mentioned. The theoretical wavenumber values were overestimated, and the correction factors suggested by the National Institute for Standards and Technology (NIST) for the given level of theory were used. The IR spectra of **L1**·HCl and **1** will be discussed as the representative examples of ligands **L1**–**L3**·HCl and complexes **1**–**3**. The detailed spectral characterisation for other ligands and complexes is presented under the synthetic procedure and characterisation in the previous Methodology section.

The IR spectrum of **L1**·HCl contains four characteristic bands found at approximately 1730, 1280, 1110 and 750 cm^{-1}. The first band at 1730 cm^{-1} in the experimental spectrum is assigned to the C=O ester group vibration. In the theoretical spectrum, this band is positioned at 1756 cm^{-1}, which is well reproduced, bearing in mind that the IR spectrum was recorded for a solid sample, and the theoretical calculations were performed for an isolated compound. The band at 1280 cm^{-1} is a typical absorption band for carbon–oxygen single bonds in ether and ester groups[43] This C–O stretching vibration in the theoretical spectrum is at 1270 cm^{-1}. The strong, broad band at 1110/1123 cm^{-1} in the experimental/theoretical spectra of **L1**·HCl corresponds to the ester/ether vibration. The band at approximately 750 cm^{-1} results from vibrations of the pyridine ring in both spectra but can be overlapped by carbon-hydrogen vibrations in the fingerprint region.[44]

Further specific bands, which are weaker in the spectra, are observed near 3020 cm^{-1} for heteroaromatic vibrations and near 2980 cm^{-1} for alkyl groups of the poly(ethylene oxide) spacer.[44] The positions of these bands are also similar in the theoretical spectrum. In the IR spectrum of **1**, the most prominent bands are located at 1730, 1275 and 1119 cm^{-1}, almost identical to the previously discussed values. A new strong band is positioned at 276 cm^{-1}, corresponding to the Ru–Cl stretching vibration. The similar values were obtained for the trichloridotriaquoruthenium(III) complex[45].

*2-(2-Hydroxyethoxy)ethyl ester of isonicotinic acid (**L4**·HCl) and corresponding Ru(II) complex (**4**)*

Synthesis. The appropriate acyl chloride hydrochloride was obtained using the modified method for **L1**·2HCl–**L3**·HCl. The synthesis is changed using excess alcohol to the acyl chloride hydrochloride (6 eq.) in toluene. The crude product is obtained as viscous oil with a high percentage of diethylene glycol and small amounts of **L1**·2HCl or **L4**·2HCl. The product is extracted with acetone/ /diethyl ether ($V_{Acetone}/V_{Et2O}$ = 5:1) and precipitated with diethyl ether several times. ESI–HRMS analysis was performed under the same conditions as **L1**·HCl. Results showed the expected mass peaks of the $[M+H]^+$.

*Structure and stability of **L4**·HCl and **4***. The structures of **L4**·HCl and **4** are presented in Figs. 3 and 4. The structure of **L4**·HCl greatly resembles the structure of **L2**·HCl, but the methoxy group is exchanged with the hydroxyl group. This change is not expected to influence the stability and structural features of the ligand significantly. The weaker stabilisation interaction was obtained in the aliphatic chain (LP(O)→σ(C–C)), with an energy of 4.8 in **L4**·HCl *vs.* 5.1 kJ mol^{-1} in **L1**·HCl (Table S-I). This change in the group does not influence the complexation route and the geometry of the complex **4** compared to **2**.

Experimental and theoretical NMR spectra. The experimental and theoretical NMR spectra of **L4**·HCl and **4** also resemble those previously mentioned in

L2·HCl and **2**. The NMR chemical shifts of **L4**·HCl and **4** are presented in Tables S-IV and S-V of the Supplementary material. As in the previous case, the obtained values were overestimated, and the correction coefficients were determined as the slope in the dependency of experimental on theoretical values. In the ^{1}H-NMR spectrum of **L4**·HCl, four hydrogen atoms of the aliphatic chain (HOC$\underline{H_2}$C$\underline{H_2}$) have the same chemical shifts at 3.77 ppm in the experimental spectrum. In the theoretical spectrum, the chemical environments of these protons are different due to the calculations performed for the compounds in vacuum and without free rotation. Other hydrogen atoms have their expected positions. The hydrogen atom of the OH group was not observed in the experimental range. The carbon atom adjacent to OH has a higher chemical shift value than the corresponding one with OCH_3 group (in **L2**·HCl; 71.8 *vs*. 69.6 ppm). The MAE values for ^{1}H- and ^{13}C-NMR spectra of **L4**·HCl are 0.24 and 4.1 ppm, with high correlation coefficients ($R > 0.98$). Upon the formation of **4**, the most notable differences are observed in the chemical shifts of carbon atoms in the pyridine ring. The *MAE* value for ^{13}C-NMR chemical shifts is 4.5 ppm, with *R* equal to 0.98. A higher *R*-value was calculated for ^{1}H-NMR chemical shifts of **4**. These results prove the applicability of the chosen level of theory for the representation of both ligand and complex.

Experimental and theoretical IR spectra. The experimental and theoretical IR spectra were compared as additional proof of the structural representation of **L4**·HCl and **4**. The same method was applied for the correction of theoretical wavenumber values. The IR spectrum **L4**·HCl is characterised by a broad peak at 3350 cm^{-1} attributed to the O−H stretching vibration. In the theoretical spectrum, this band is shown at 3737 cm^{-1}. This difference is expected as the optimization was performed on the isolated molecule in a vacuum. When the intermolecular interactions are formed, the O−H bond length increases, and the wavenumber lowers. The most intense peak is at 1730 in the experimental and 1755 cm^{-1} in the theoretical spectra of **L4**·HCl, assigned to the C=O vibration. The vibrations of carbon–oxygen bonds at 1280 and 1110 cm^{-1} are similar to those previously discussed for **L1**·HCl. The heteroaromatic vibrations at 750 cm^{-1} are observed in the same region as the bands of other ligand precursors (**L1**·2HCl–**L3**·HCl). These results correlate well with all other synthesised esters. In the experimental and theoretical spectra of **4**, the bands of aliphatic and aromatic C−H stretching vibrations increase in intensity due to *p*-cymene moiety. The remaining bands are not significantly affected except for forming new bands assigned to Ru−Cl vibrations.

*2-[2-(2-Methylamino-benzoyloxy)ethoxy]ethyl isonicotinate (**L5**) and corresponding Ru(II) complex (**5**)*

Synthesis. Ligand **L5** was prepared in the reaction between **L4**·HCl and methylisatoic acid anhydride in the presence of potassium carbonate, as pre-

sented below. The reaction mixture was stirred for three hours at 60 °C in acetonitrile, and the reaction progress was followed with thin-layer chromatography (Scheme 2). Another reaction setup with toluene as solvent and at a higher temperature yielded only small amounts of the desired product. The crude product was purified by the centrifugally accelerated thin-layer chromatography with an eluent system of dichloromethane and ethanol. The analysis with ESI-HRMS resulted in the expected mass peak of the protonated molecule (m/z = 345.14451) $[M+H]^+$. The product was obtained in good yield (73 %).

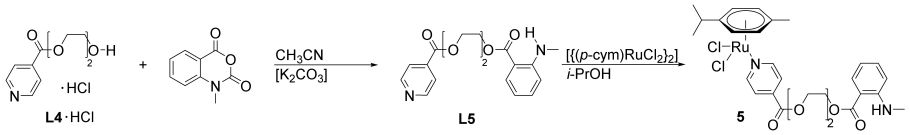

Scheme 2. Preparation of the fluorescent ligand **L5** and corresponding ruthenium(II) complex (**5**).

*Structure and stability of **L5** and **5***. The optimised structures of **L5** and **5** are shown in Figs. 3 and 5. Ligand **L5** has the most complex structure of the described compounds, as there is an additional condensed structure of methylisatoic acid moiety attached to the PEG chain. As previously discussed, the complexation does not influence the stabilisation interactions within the ligand structure; therefore, the NBO analysis of **L5** and **5** is shown together. Besides stabilisation interactions in the pyridine ring, aliphatic chain, and *p*-cymene moiety, strong interactions were observed at the intersection of the aliphatic chain and methylisatonic acid moiety. The lone pair on the carboxylic oxygen atom stabilises the neighbouring C–O and C–C bonds by 132 and 71 kJ mol^{-1}, respectively (Table S-I). The adjacent oxygen atom stabilises the carboxylic group through the

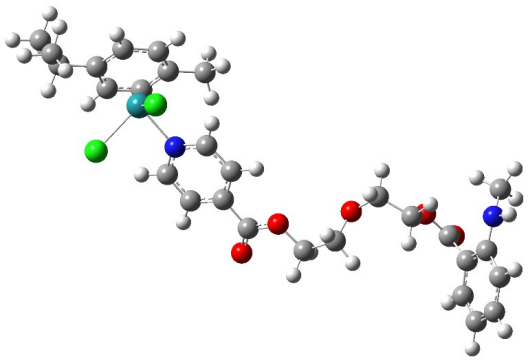

Fig. 5. Optimized structure of **5** at B3LYP/6-31+G(d,p)(H,C,N,O,Cl)/LanL2DZ(Ru) level of theory (the following colours represent atoms: white –hydrogen, grey – carbon, blue – nitrogen, green – chlorine, teal – ruthenium).

LP(O)→π*(C−O) interaction with energy equal to 105 kJ mol^{-1}. The stabilisation interactions within the aromatic ring have similar energies to those of pyridine and *p*-cymene moieties, between 45 and 55 kJ mol^{-1}. The nitrogen atom increases the stability of this ring through the positive resonance effect and the electron delocalisation. Including these groups does not influence the part of the ligand directly attached to Ru(II), as there is a long chain with the electronegative atom intersections that prevents electron delocalisation through the entire molecule. The structure of the ligand and the corresponding complex is further analysed by NMR and IR spectroscopies.

Experimental and theoretical NMR spectra. The NMR spectra of **L5** and **5** are given in the Supplementary material (Tables S-VI and S-VII). The ^{1}H-NMR spectrum of **5** shows several changes and additional resonances compared to the characterised ligand precursor (**L4**·HCl). First, the resonances of the isonicotinate moiety are shifted to a higher field ($\Delta\delta(H^2)$ = –0.3 ppm, $\Delta\delta(H^3)$ = –0.8 ppm). The corresponding carbon atoms give resonances, which are observed in almost the same position as the earlier discussed free ligands (**L5**: $\delta(C^2)$ = 149.8 ppm, $\delta(C^3)$ = 123.4 ppm, **L4**·HCl: $\delta(C^2)$ = 149.4 ppm, $\delta(C^3)$ = 123.0 ppm). Additionally to the previously described ligand precursors herein, in ^{13}C-NMR spectra there is the presence of two chemical shifts above 160 ppm (164.9 and 168.5 ppm) corresponding to COO and CON groups from isonicotinic and methylisatoic moieties, respectively. Two resonances near 4.5 ppm are assigned to protons, which directly bond to the ester groups and show no coupling with each other. More resonances are observed for the new aromatic system, the fluorescent group. The chemical shifts belonging to the aromatic regions of the fluorescent moiety range from 6.5–7.9 ppm. One doublet of the fluorescent moiety is shifted to approximately 7.9 ppm (compared to methylisatoic acid anhydride) and overlaps with the doublet of the isonicotinate group at 7.8 ppm. Another resonance for the methyl group bound to the nitrogen atom of the amine pendant group is found at 2.9 ppm. The theoretical spectrum of **L5** at B3LYP/6-311++G(d,p) level of theory reproduces well the experimental one. The *MAE* values for ^{1}H- and ^{13}C-NMR spectra are 0.40 and 4.3 ppm, which aligns with the previous predictions of other ligands. The most notable differences in the calculated spectrum were observed for the carboxyl carbon atoms, averaging 6 ppm. When **5** is formed, the differences in chemical shifts were obtained for the carbon atoms adjacent to the nitrogen atom of the pyridine ring. These shifts were 6 ppm (149.8 in **L5** and 155.9 ppm in **5**). The rest of the carbon and hydrogen atoms do not show significant changes. The correlation coefficients between the experimental and the theoretical chemical shifts are 0.94 and 0.95 for ^{1}H- and ^{13}C--spectra, with *MAE* values of 0.79 and 6.0 ppm. These results again prove the theoretical representation of ligand and complex, even when the elongated structure of **L5** is concerned.

Experimental and theoretical IR spectra. In addition to the specific bands observed at 1718 cm^{-1} for the carbonyl group of the isonicotinate part, at 1260 and 1120 cm^{-1} for carbon–oxygen bonds and 750 cm^{-1} for aromatic bending vibrations, two strong bands are significant for this ligand precursor. The first new sharp band at 3370 cm^{-1} can be assigned to a stretching vibration of the secondary amine.[43] This band is located at 3382 cm^{-1} (scaled) in the theoretical spectrum. The difference of 18 cm^{-1} is due to the physical state of the recorded sample, but it is still within the expected difference. The second strong band at 1684 cm^{-1} is generated by the carbonyl stretching vibration of the newly formed ester bond of the fluorescent benzene ring and is observed in other esters of *N*--methylisatoic anhydride, too.[46,47] The band assigned to this vibration in the theoretical spectrum is 1648 cm^{-1}. The vibration of this carboxyl group is lower than the one previously observed in ligands **L1**–**L4**·HCl due to the proximity of the aromatic ring, which extends the electron delocalisation and elongates the respective C=O band. These bands characteristic of ligand are positioned at 3372 and 1676 cm^{-1} in the experimental spectrum of **5**, which proves the assumption that this part of the ligand is not under the influence of metal ions, as shown previously in the NMR spectrum. In the theoretical spectrum, these wavenumbers are higher for several cm^{-1} but within the expected range.

*Experimental and theoretical UV–Vis/fluorescence spectra of **L5***. The UV––Vis and fluorescence spectra of **L5** and **5** in $CHCl_3$ are presented in Fig. 6. The UV–Vis spectrum of **L5** has a broad peak at 355 nm. The emission spectrum is measured with an excitation wavelength of 372 nm and in a range from 387–550 nm. The excitation pattern was analysed with an emission wavelength of 418 nm from 200–400 nm. Ligand **L5** shows a broad excitation spectrum, and the maximum excitation intensity is at 371 nm, additionally, two shoulders are observed at 342 and 266 nm. The first shoulder at a lower wavelength shows a high intensity and reaches 89 % of the intensity of the peak at 371 nm. The second shoulder is weaker and reaches only 24 % of the highest intensity. Due to these two shoulders, the excitation spectrum ranges approximately 160 nm (240–400 nm). Complex **5** shows peaks at the same position, just their intensity is much lower that of those in **L5** spectrum. Similarity in position can be explained by the weak influence of the metal ion on the overall electron density of the groups included in the transitions. The decrease in intensity is due to the competing deactivation processes and the energy dissipation through vibration and partial rotation.

The structure of **L5** optimized at B3LYP/6-311++G(d,p) level of theory in $CHCl_3$ was used to predict the electronic spectrum. In the range of experimental values, the theoretical spectrum is dominated by an intensive peak at 344 nm, assigned to HOMO→LUMO (99 %) transition, with an oscillator strength of 0.1283. The calculated wavelength differs by around 10 nm from the experimental one, and it can be assumed that the interactions with the solvent would inf-

luence an additional shift in the spectrum, although strong interactions with $CHCl_3$ are not expected due to the low solvent's low dipole moment. In the theoretical spectrum of **5** a much higher number of weak transitions can be observed. These transitions are attributed to the metal-ligand electron transitions. The most intense transition is positioned at 360 nm, with the oscillator strength of 0.1165, denoted as HOMO→LUMO+3 (97 %). This result shows that the experimental value of 355 nm is well-reproduced in the theoretical spectrum of **5**. Also, a shift between theoretical values of transitions assigned to ligand can be a consequence of the level of theory used and change in electron density upon complexation.

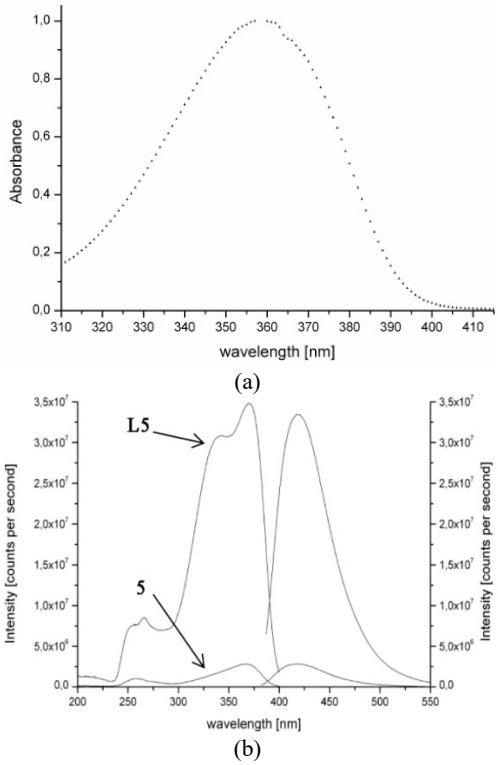

Fig. 6. UV–Vis/fluorescence spectra of ligand **L5** (a) and **5** (b).

CONCLUSION

Ligands **L2**–**L4**·HCl were prepared in the reaction between appropriate acyl chloride and dried alcohols. The theoretical structures, including already reported **L1**·HCl, were obtained at the B3LYP/6-31+G(d,p)(H,C,N,O,Cl)/LanL2DZ(Ru) level of theory. Due to the elongated delocalisation between the aromatic ring and ester group, the strongest stabilisation interactions included π(C−C)→ →π*(C−C) and LP(O)→π*(C−C), as determined by the NBO approach. The pyr-

idine ring was also stabilised by the LP(N)→π*(C−C), with an energy of 41 kJ mol^{-1}. The bond is formed between Ru(II) and pyridine nitrogen upon complexation. Two Ru−Cl bonds have 2.43 and 2.45 Å, while the Ru−N bond length was 2.18 Å. The optimised bond angles were in the expected range. High correlation coefficients (>0.98) were calculated for the experimental and theoretical ^{1}H- and ^{13}C-NMR chemical shifts. As a representative example, the *MAE* values were 0.23 and 4.3 ppm for ^{1}H- and ^{13}C-NMR spectra of **L1**. The IR spectra were well reproduced, with differences explained by the physical state of the substance. The NMR and IR spectra of **L4**·HCl and the corresponding complex **4** also proved the applicability of the chosen theory of level. The additional moiety in ligand **L5** led to high-intensity fluorescent emission. This group was stabilised by the interactions between carboxyl group and π-electron cloud of aromatic ring. The fluorescence emission peak of **L5** was obtained at 372 nm for the excitation wavelength of 418 nm. The experimental and theoretical wavelengths of the most intense transition in the UV–Vis spectrum of **L5** were 355 and 344 nm, respectively. Much more successful overlap between the experimental and the theoretical values was obtained for the UV–Vis spectrum of **5**, with 5 nm difference. This difference was explained by the stabilisation due to the solvent-solute interactions. As the stability and the structure of these compounds were obtained, further biological activity studies are advised.

SUPPLEMENTARY MATERIAL

Additional data and information are available electronically at the pages of journal website: https://www.shd-pub.org.rs/index.php/JSCS/article/view/12353, or from the corresponding author on request.

ИЗВОД

СИНТЕЗА, СПЕКТРОСКОПСКА И DFT АНАЛИЗА ДИХЛОРИДО(η^6-*p*-ЦИМЕН)РУТЕНИЈУМ(II) КОМПЛЕКСА СА ИЗОНИКОТИНАТ-ПОЛИЕТИЛЕН ГЛИКОЛ ЕСТАРСКИМ ЛИГАНДИМА

THOMAS EICHHORN[1], ДУШАН ДИМИЋ[2], ЗОРАН МАРКОВИЋ[3] и ГОРАН Н. КАЛУЂЕРОВИЋ[1]

[1]Department of Engineering and Natural Sciences, University of Applied Sciences Merseburg, Eberhard-Leibnitz-Straße 2, 06217 Merseburg, Germany, [2]Универзитет у Београду, Факултет за физичку хемију, Студентски трг 12–16, 11000 Београд [3]Институт за информационе технологије, Универзитет у Крагујевцу, Јована Цвијића бб, 34000 Крагујевац

Комплекси рутенијума су значајни због рутенијумове сличности гвожђу, мање токсичности, и веће антиканцер ефикасности. У овом раду, пет нових изоникотинат-полиетилен-гликол естарских лиганада је синтетисано и окарактерисано NMR и IC спекроскопијама. Одговарајући Ru(II) комплекси су такође добијени и њихова структура одређена стандардним методама. Оптимизација структуре је урађена на B3LYP/6-31+G(d,p) нивоу теорије за H, C, N и O атоме и B3LYP/LanL2DZ за Ru. Интрамолекулске стабилизационе интеракције су испитане анализом природних орбитала. Хемијски помераји у NMR спектрима су предвиђени GIAO (*gauge independent atomic orbital*) методом и упоређени са експерименталним вредностима. Високи коефицијент корелације и ниска средња вредност апсолутне разлике између ових скупова вредности доказују да пред-

виђене структуре добро описују експерименталне. Теоријски и експериментални IC спектри су такође упоређени, а разлике у положајима трака објашњене. Један од лиганада (**L5**) и комплекса (**5**) је показао флуоресцентне особине због присуства метилисатоичне групе. Електронски спектри овог једињења су моделовани временски зависном DFT методом. Разлика од 11 nm између експерименталне и теоријске таласне дужине је објашњена интеракцијама између растворка и растварача. За ову серију једињења су препоручене даље биолошке и теоријске анализе.

(Примљено 12. априла, ревидирано 26. јуна, прихваћено 18. септембра 2023)

REFERENCES

1. R. G. Kenny, C. J. Marmion, *Chem. Rev.* **119** (2019) 1058 (https://doi.org/10.1021/acs.chemrev.8b00271)
2. T. C. Johnstone, K. Suntharalingam, S. J. Lippard, *Chem. Rev.* **116** (2016) 3436 (https://doi.org/10.1021/acs.chemrev.5b00597)
3. S. Thota, D. A. Rodrigues, D. C. Crans, E. J. Barreiro, *J. Med. Chem.* **61** (2018) 5805 (https://doi.org/10.1021/acs.jmedchem.7b01689)
4. A. Rilak Simović, R. Masnikosa, I. Bratsos, E. Alessio, *Coord. Chem. Rev.* **398** (2019) 113011 (https://doi.org/10.1016/j.ccr.2019.07.008)
5. L. Conti, E. Macedi, C. Giorgi, B. Valtancoli, V. Fusi, *Coord. Chem. Rev.* **469** (2022) 214656 (https://doi.org/10.1016/j.ccr.2022.214656)
6. S. Y. Lee, C. Y. Kim, T.-G. Nam, *Drug Des. Devel. Ther.* **14** (2020) 5375 (https://doi.org/10.2147/DDDT.S275007)
7. B. Therrien, *Coord. Chem. Rev.* **253** (2009) 493 (https://doi.org/10.1016/j.ccr.2008.04.014)
8. M. J. Clarke, *Coord. Chem. Rev.* **232** (2002) 69 (https://doi.org/10.1016/S0010-8545(02)00025-5)
9. G. S. Smith, B. Therrien, *Dalt. Trans.* **40** (2011) 10793 (https://doi.org/10.1039/C1DT11007A)
10. D. S. Dimić, G. N. Kaluđerović, E. H. Avdović, D. A. Milenković, M. N. Živanović, I. Potočňák, E. Samoľová, M. S. Dimitrijević, L. Saso, Z. S. Marković, J. M. Dimitrić Marković, *Int. J. Mol. Sci.* **23** (2022) 1001 (https://doi.org/10.3390/ijms23021001)
11. G. Jia, G.-L. Law, K.-L. Wong, P. A. Tanner, W.-T. Wong, *Inorg. Chem.* **47** (2008) 9431 (https://doi.org/10.1021/ic8010103)
12. R. Schobert, B. Biersack, *Inorg. Chim. Acta* **358** (2005) 3369 (https://doi.org/10.1016/j.ica.2005.05.015)
13. L. D. Ramos, G. Cerchiaro, K. P. Morelli Frin, *Inorg. Chim. Acta* **501** (2020) 119329 (https://doi.org/10.1016/j.ica.2019.119329)
14. C.-M. Wang, Y.-L. Chuang, S.-T. Chuang, K.-H. Lii, *J. Solid State Chem.* **177** (2004) 2305 (https://doi.org/10.1016/j.jssc.2004.02.030)
15. J.-Y. Kim, A. J. Norquist, D. O'Hare, *Chem. Mater.* **15** (2003) 1970 (https://doi.org/10.1021/cm021722n)
16. T. Eichhorn, E. Hey-Hawkins, D. Maksimović-Ivanić, M. Mojić, J. Schmidt, S. Mijatović, H. Schmidt, G. N. Kaluderović, *Appl. Organomet. Chem.* **29** (2015) 20 (https://doi.org/10.1002/aoc.3238)
17. *Gaussian 09, Revision A.02*, Gaussian Inc., Wallingford, CT, 2009
18. A. D. Becke, *J. Chem. Phys.* **98** (1993) 5648 (https://doi.org/10.1063/1.464913)
19. T. H. Dunning, *J. Chem. Phys.* **90** (1989) 1007 (https://doi.org/10.1063/1.456153)
20. P. J. Hay, W. R. Wadt, *J. Chem. Phys.* **82** (1985) 299 (https://doi.org/10.1063/1.448975)

21. P. J. Hay, W. R. Wadt, *J. Chem. Phys.* **82** (1985) 270 (https://doi.org/10.1063/1.448799)
22. R. Dennington, K. Todd, J. Millam, *Gauss View, Version 5*, Semichem Inc., Shawnee, KS, 2009
23. A. V. Marenich, C. J. Cramer, D. G. Truhlar, *J. Phys. Chem., B* **113** (2009) 6378 (https://doi.org/10.1021/jp810292n)
24. A. E. Reed, R. B. Weinstock, F. Weinhold, *J. Chem. Phys.* **83** (1985) 735 (https://doi.org/10.1063/1.449486)
25. R. Zieliński, H. Szymusiak, *Pol. J. Food Nutr. Sci.* **12** (2003) 157 (http://journal.pan.olsztyn.pl/pdf-98612-30420?filename=APPLICATION%20OF%20DFT.pdf)
26. J. A. Bohmann, F. Weinhold, T. C. Farrar, *J. Chem. Phys.* **107** (1997) 1173 (https://doi.org/10.1063/1.474464)
27. D. Jacquemin, J. Preat, V. Wathelet, E. A. Perpète, *Chem. Phys.* **328** (2006) 324 (https://doi.org/10.1016/j.chemphys.2006.07.037)
28. G. R. Newkome, K. J. Theriot, V. K. Gupta, R. N. Balz, F. R. Fronczek, *Inorg. Chim. Acta* **114** (1986) 21 (https://doi.org/10.1016/S0020-1693(00)84582-X)
29. C. O. Badgett, C. F. Woodward, *J. Am. Chem. Soc.* **69** (1947) 2907 (https://doi.org/10.1021/ja01203a501)
30. H. H. Bosshard, R. Mory, M. Schmid, H. Zollinger, *Helv. Chim. Acta* **42** (1959) 1653 (https://doi.org/10.1002/hlca.19590420526)
31. J. Clayden, N. Greeves, S. Warren, *Organic Chemistry*, 2nd ed., Oxford University Press, Oxford, 2012 (ISBN: 978-0-19-927029-3)
32. A. Wollrab, *Organische Chemie*, 2nd ed., Springer Verlag, Berlin, 2012 (ISBN:978-3-642-45143-0)
33. *Organikum*, 22nd ed., Wiley VCH, Weinheim, 2004 (ISBN: 978-3-527-33968-6)
34. G. Świderski, M. Kalinowska, R. Świsłocka, S. Wojtulewski, W. Lewandowski, *Spectrochim. Acta, A* **100** (2013) 41 (https://doi.org/10.1016/j.saa.2012.02.047)
35. S. Ramalingam, S. Periandy, S. Mohan, *Spectrochim. Acta, A* **77** (2010) 73 (https://doi.org/10.1016/j.saa.2010.04.027))
36. A. G. Medvedev, A. A. Mikhailov, P. V. Prikhodchenko, T. A. Tripol'skaya, O. Lev, A. V. Churakov, *Russ. Chem. Bull.* **62** (2013) 1871 (https://link.springer.com/article/10.1007/s11172-013-0269-9)
37. M. Al-Noaimi, M. A. AlDamen, *Inorg. Chim. Acta* **387** (2012) 45 (https://doi.org/10.1016/j.ica.2011.12.050)
38. V. Uahengo, P. Cai, J. Naimhwaka, A. Rahman, L. S. Daniel, H. Bhakhoa, L. Rhyman, P. Ramasami, *Polyhedron* **173** (2019) 114106 (https://doi.org/10.1016/j.poly.2019.114106)
39. A. A. Sikalov, V. V. Pavlovskiy, A. A. Kirilchuk, *Inorg. Chem. Commun.* **99** (2019) 156 (https://doi.org/10.1016/j.inoche.2018.11.020)
40. T. Eichhorn, F. Kolbe, S. Mišić, D. Dimić, I. Morgan, M. Saoud, D. Milenković, Z. Marković, T. Rüffer, J. Dimitrić Marković, G. N. Kaluđerović, *Int. J. Mol. Sci.* **24** (2023) 689 (https://doi.org/10.3390/ijms24010689)
41. A. Mondal, U. Sen, N. Roy, V. Muthukumar, S. K. Sahoo, B. Bose, P. Paira, *Dalt. Trans.* **50** (2021) 979 (https://doi.org/10.1039/D0DT03107K)
42. M. T. Rupp, N. Shevchenko, G. S. Hanan, D. G. Kurth, *Coord. Chem. Rev.* **446** (2021) 214127 (https://doi.org/10.1016/j.ccr.2021.214127)
43. E. Pretsch, P. Bühlmann, C. Affolter, *Structure Determination of organic compounds*, 3rd ed., Springer Verlag, Berlin, 2000 (ISBN: 978-3-662-62439-5)

44. M. Hesse, H. Meier, B. Zeeh, *Spektroskopische Methoden in der organischen Chemie*, 7th ed., Georg Thieme Verlag, Stuttgart, 2002 (http://dx.doi.org/10.1055/b-002-46985)
45. J. R. Durig, W. A. McAllister, E. E. Mercer, *J. Inorg. Nucl. Chem.* **29** (1967) 1441 (https://doi.org/10.1016/0022-1902(67)80244-6)
46. I. Chevrier, J. L. Sagué, P. S. Brunetto, N. Khanna, Z. Rajacic, K. M. Fromm, *Dalton Trans.* **42** (2013) 217 (https://doi.org/10.1039/C2DT31259J)
47. D. Roell, T. W. Rösler, S. Degen, R. Matusch, A. Baniahmad, *Chem. Biol. Drug Des.* **77** (2011) 450. (https://doi.org/10.1111/j.1747-0285.2011.01116.x).

Journal of the Serbian Chemical Society
JSCS@tmf.bg.ac.rs • www.shd.org.rs/JSCS
J. Serb. Chem. Soc. *88* (12) S399–S406 (2023) *Supplementary material*

SUPPLEMENTARY MATERIAL TO

Synthesis, spectroscopic characterization and DFT analysis of dichlorido(η^6-*p*-cymene)ruthenium(II) complexes with isonicotinate-polyethylene glycol ester ligands

THOMAS EICHHORN[1], DUŠAN DIMIĆ[2], ZORAN MARKOVIĆ[3] and GORAN N. KALUĐEROVIĆ[1]*

[1]*Department of Engineering and Natural Sciences, University of Applied Sciences Merseburg, Eberhard-Leibnitz-Straße 2, 06217 Merseburg, Germany,* [2]*University of Belgrade, Faculty of Physical Chemistry, Studentski trg 12–16, 11000 Belgrade, Serbia and* [3]*Institute of Information Technologies, University of Kragujevac, Jovana Cvijića bb, 34000 Kragujevac, Serbia*

J. Serb. Chem. Soc. *88* (12) (2023) 1335–1354

ANALYTICAL AND SPECTRAL DATA OF THE SYNTHESIZED COMPOUNDS

2-(2-Methoxyethoxy)ethyl iso-nicotinate hydrochloride (L2·HCl)

Properties: Viscous, hygroscopic oil; soluble in water, methanol, ethanol, *iso*propanol, insoluble in diethyl ether.

^{1}H-NMR (400 MHz, D_2O): δ 3.33 (s, 3H, OCH_3), 3.63, 3.74 (m, 4H, $CH_3OCH_2CH_2$), 3.95 (m, 2H, $COOCH_2CH_2$), 4.63 (m, 2H, $COOCH_2$), 8.59 (d, $^3J_{H,H}$ = 6.8 Hz, 2H, H^3), 9.03 (d, $^3J_{H,H}$ = 6.8 Hz, 2H, H^2). ^{13}C-NMR (100 MHz, D_2O): δ 58.0 (CH_3O), 66.0 (CH_2OOC), 68.1, 69.5, 70.9 (CH_2O), 126.9 (C^3), 142.6 (C^2), 145.9 (C^4), 163.2 (*C*OO). ESI-HRMS (CH_3OH), positive mode: Calcd for $[C_{11}H_{16}NO_4]^+$ 226.10738, *m*/*z* 226.10738 $[M+H]^+$. IR: ν (cm^{-1}) 3068(w), 2877(w), 2400(b), 2100(w), 2022(w), 1916(w), 1731(s), 1635(w), 1605(m), 1501(w), 1450(w), 1282(s), 1239(m), 1198(w), 1100(s), 998(m), 845(m), 754(s), 684(m), 359(w). Yield: 88%.

2-[2-(2-Methoxyethoxy)ethoxy]ethyl iso-nicotinate hydrochloride (L3·HCl)

Properties: Viscous, hygroscopic oil; soluble in water, methanol, ethanol, *iso*propanol, chloroform, and dichloromethane, insoluble in diethyl ether.

^{1}H-NMR (400 MHz, D_2O): δ 3.35 (s, 3H, OCH_3), 3.60, 3.70, 3.72, 3.79 (m, 8H, OCH_2CH_2O), 3.98 (m, 2H, $COOCH_2CH_2$), 4.66 (m, 2H, $COOCH_2$), 8.62 (d, $^3J_{H,H}$ = 6.8 Hz, 2H, H^3), 9.04 (d, $^3J_{H,H}$ = 6.8 Hz, 2H, H^2). ^{13}C-NMR (100 MHz, D_2O): δ 58.0 (CH_3O), 66.1 (CH_2OOC), 68.2, 69.4, 69.5, 69.7, 70.9 (CH_2O), 127.0 (C^3), 142.6 (C^2), 145.9 (C^4), 163.3 (*C*OO). ESI-HRMS (CH_3OH), positive mode: Calcd for $[C_{13}H_{20}NO_5]^+$ 270.13360, *m*/*z* 270.13351 $[M+H]^+$. IR: ν (cm^{-1}) 3073(w), 2875(w), 2400(b), 2100(w), 2026(w), 1916(w), 1730(s), 1635(w), 1607(m), 1500(w), 1450(w), 1282(s), 1239(m), 1198(w), 1098(s), 998(m), 845(m), 758(s), 685(m), 363(w). Yield: 95%.

* Corresponding author. E-mail: goran.kaluderovic@hs-merseburg.de

2-(2-Hydroxyethoxy)ethyl isonicotinate hydrochloride (L4·HCl)

Properties: Viscous, colourless oil; soluble in water, methanol, ethanol, *iso*propanol, acetone, chloroform, and dichloromethane, insoluble in diethyl ether.

^{1}H-NMR (400 MHz, D_2O): δ 3.77 (m, 4H, HOCH_2CH_2), 4.00 (m, 2H, COOCH_2CH_2), 4.69 (m, 2H, COOCH_2), 8.60 (d, $^{3}J_{H,H}$ = 6.8 Hz, 2H, H^3), 9.04 (d, $^{3}J_{H,H}$ = 6.8 Hz, 2H, H^2). ^{13}C-NMR (100 MHz, D_2O): δ 60.3 (*C*H_2OH), 66.1 (*C*H_2OOC), 68.1 (*C*H_2CH$_2$OOC), 71.8 (*C*H_2CH2OH), 126.9 (C^3), 142.7 (C^2), 145.9 (C^4), 163.4 (*C*OO). ESI-HRMS (CH_3OH), positive mode: Calcd for $[C_{10}H_{14}NO_4]^+$ 212.09173, *m*/*z* 212.09176 $[M+H]^+$. IR: ν (cm^{-1}) 3350(b), 3080(w), 2872(w), 2440(b), 2100(w), 1730(s), 1637(w), 1604(w), 1502(w), 1451(w), 1404(w), 1282(s), 1119(s), 1068(m), 1002(m), 925(w), 889(w), 839(m), 754(s), 678(m), 520(w), 357(w), 255(w).

2-[2-(2-Methylamino-benzoyloxy)ethoxy]ethyl iso-nicotinate (L5)

Properties: Viscous oil, which crystallized upon standing, soluble in methanol, ethanol, *iso*propanol, chloroform, and dichloromethane, and insoluble in diethyl ether and water.

^{1}H-NMR (400 MHz, $CDCl_3$): δ 2.89 (s, 3H, NCH_3), 3.87 (m, 4H, OCH_2), 4.43, 4.53 (t, $^{3}J_{H,H}$ = 6.8 Hz, 4H, COOCH_2), 6.53 (t, $^{3}J_{H,H}$ = 7.6 Hz, 1H, H^9), 6.65 (d, $^{3}J_{H,H}$ = 8.5 Hz, 1H, H^7), 7.37 (ddd, $^{3}J_{H8,H7}$ = 7.8 Hz, $^{3}J_{H8,H9}$ = 7.1 Hz, $^{4}J_{H8,H10}$ = 1.7 Hz, 1H, H^8), 7.84 (d, $^{3}J_{H,H}$ = 6.0 Hz, 2H, H^3), 7.88 (dd, $^{3}J_{H10,H9}$ = 8.0 Hz, $^{4}J_{H10,H8}$ = 1.6 Hz 1H, H^{10}), 8.71 (d, $^{3}J_{H,H}$ = 6.1 Hz, 2H, H^2). ^{13}C-NMR (100 MHz, $CDCl_3$): δ 29.7 (N*C*H$_3$), 63.2, 65.0 (*C*H$_2$OOC), 69.0, 69.4 (*C*H$_2$CH$_2$OOC), 109.7 (C^5), 110.9 (C^7), 114.5 (C^9), 123.4 (C^3), 131.7 (C^{10}), 135.0 (C^8), 138.1 (C^4), 149.8 (C^2), 152.2 (C^6), 164.9, 168.5 (*C*OO). ESI-HRMS (CH_3OH), positive mode: Calcd for $[C_{18}H_{21}N_2O_5]^+$ 345.14450, *m*/*z* 345.14451 $[M+H]^+$. IR: ν (cm^{-1}) 3372(m), 2950(w), 2885(w), 2825(w), 1718(s), 1684(s), 1603(w), 1580(m), 1518(m), 1454(w), 1431(m), 1408(m), 1375(m), 1322(m), 1278(m), 1261(s), 1243(s), 1180(s), 1134(s), 1117(s), 1093(s), 1063(m), 1040(m), 1021(m), 952(m), 894(w), 877(w), 867(w), 850(w), 753(s), 700(s), 675(m), 605(m), 575(m), 533(m), 512(m), 275(m), 217 (w). UV-vis (1.74×10^{-4} M, $CHCl_3$, 298 K): λ_{max} 358 nm (ε = 5747 M^{-1} cm^{-1}).

*Dichlorido(*η^6-p-*cymene)(diethylene glycol monomethyl ether isonicotinate-*κ*N)ruthenium(II) (**2**)*

Properties: Orange powder; soluble in chloroform, dichloromethane, dimethylformamide, acetone, and acetonitrile, moderately soluble in methanol, ethanol, *iso*propanol, and tetrahydrofuran, insoluble in diethyl ether and toluene.

EA: Anal. Found: C, 47.00; H, 5.18; N, 2.65. Calcd for $C_{21}H_{29}Cl_2NO_4Ru$ (531.43): C, 47.46; H, 5.50; N, 2.64. ^{1}H-NMR (400 MHz, $CDCl_3$): δ 1.31 (d, $^{3}J_{H,H}$ = 7.0 Hz, 6H, CH(CH_3)$_2$), 2.09 (s, 3H, CCH_3), 2.98 (sept, $^{3}J_{H,H}$ = 7.0 Hz, 1H, C*H*(CH$_3$)$_2$), 3.38 (s, 3H, OCH_3), 3.56, 3.68 (m, 4H, OCH_2), 3.83 (t, $^{3}J_{H,H}$ = 4.7 Hz, 2H, COOCH$_2$CH_2), 4.53 (t, $^{3}J_{H,H}$ = 4.6 Hz, 2H, COOCH_2), 5.23 (d, $^{3}J_{H,H}$ = 5.9 Hz, 2H, C*H*CCH$_3$), 5.45 (d, $^{3}J_{H,H}$ = 5.8 Hz, 2H, C*H*CHCCH$_3$), 7.85 (d, $^{3}J_{H,H}$ = 6.5 Hz, 2H, H^3), 9.23 (d, $^{3}J_{H,H}$ = 6.5 Hz, 2H, H^2). ^{13}C-NMR (100 MHz, $CDCl_3$): δ 18.4 (C*C*H$_3$), 22.4 (C(*C*H$_3$)$_2$), 30.8 (*C*(CH$_3$)$_2$), 59.2 (*C*H$_3$O), 65.1 (*C*H$_2$OOC), 70.3 (*C*H$_2$O), 82.5, 83.3 (*C*H), 97.5, 103.9 (*C*CH), 123.7 (C^3), 138.7 (C^4), 155.9 (C^2), 163.9 (*C*OO). ESI-HRMS (CH_3OH), positive mode: Calcd for $[C_{21}H_{29}ClNO_4{}^{96}Ru]^+$ 490.08556, *m*/*z* 490.08544 $[M-Cl]^+$. IR: ν (cm^{-1}) 3062(w), 2964(w), 2878(w), 1728(s), 1556(w), 1468(w), 1451(w), 1414(m), 1377(w), 1323(w), 1275(s), 1228(w), 1202(w), 1107(s), 1056(m), 1027(m), 863(m), 769(m), 695(m), 659(w), 451(w), 371(w), 284(s), 232(s).

*Dichlorido(*η^6-p-*cymene)(triethylene glycol monomethyl ether iso-nicotinate-κN)ruthenium(II)* ***(3)***

Properties: Orange powder; soluble in chloroform, dichloromethane, dimethylformamide, acetone, and acetonitrile, moderately soluble in methanol, ethanol, *iso*propanol, and tetrahydrofuran, insoluble in diethyl ether and toluene.

EA: Anal. Found: C, 47.58; H, 5.31; N, 2.47. Calcd for $C_{23}H_{33}Cl_2NO_5Ru$ (575.49): C, 48.00; H, 5.78; N, 2.43. ^{1}H-NMR (400 MHz, $CDCl_3$): δ 1.31 (d, $^3J_{H,H}$ = 6.9 Hz, 6H, CH(CH_3)$_2$), 2.09 (s, 3H, CCH_3), 2.98 (sept, $^3J_{H,H}$ = 6.9 Hz, 1H, CH(CH$_3$)$_2$), 3.37 (s, 3H, OCH_3), 3.54, 3.64, 3.67, 3.68 (m, 8H, OCH_2), 3.83 (t, $^3J_{H,H}$ = 4.6 Hz, 2H, COOCH$_2$CH_2), 4.52 (t, $^3J_{H,H}$ = 4.6 Hz, 2H, COOCH_2), 5.23 (d, $^3J_{H,H}$ = 5.9 Hz, 2H, CHCCH$_3$), 5.45 (d, $^3J_{H,H}$ = 5.9 Hz, 2H, CHCHCCH$_3$), 7.85 (d, $^3J_{H,H}$ = 6.5 Hz, 2H, H^3), 9.22 (d, $^3J_{H,H}$ = 6.5 Hz, 2H, H^2). ^{13}C-NMR (100 MHz, $CDCl_3$): δ 18.4 (CCH$_3$), 22.4 (C(CH_3)$_2$), 30.8 (C(CH$_3$)$_2$), 59.2 (CH$_3$O), 65.5 (CH$_2$OOC), 69.0, 70.7, 70.8, 70.8, 72.1 (CH$_2$O), 82.5, 83.2 (CH), 97.5, 103.9 (CCH), 123.7 (C^3), 138.8 (C^4), 155.9 (C^2), 163.9 (COO). ESI-HRMS (CH$_3$OH), positive mode: Calcd for $[C_{23}H_{33}ClNO_5{}^{96}Ru]^+$ 534.11178, *m*/*z* 534.11174 [M-Cl]$^+$. IR: ν (cm^{-1}) 3063(w), 2964(w), 2876(w), 1732(s), 1556(w), 1475(w), 1451(w), 1414(m), 1367(w), 1319(w), 1279(s), 1202(w), 1144(m), 1104(s), 1090(s), 1053(m), 1028(m), 947(w), 867(m), 849(m), 802(w), 769(m), 695(m), 659(w), 518(w), 455(w), 371(w), 283(s), 232(s).

*Dichlorido(*η^6-p-*cymene)((3-oxa-5-hydroxy)-pentyl isonicotinate-κN)ruthenium(II)* ***(4)***

Properties: Orange powder; soluble in chloroform, dichloromethane, dimethylformamide, acetone, and acetonitrile, moderately soluble in methanol, ethanol, *iso*propanol, and tetrahydrofuran, insoluble in diethyl ether and toluene.

EA: Anal. Found: C, 45.98; H, 5.16; N, 2.70. Calcd for $C_{20}H_{27}Cl_2NO_4Ru$ (518.21): C, 46.36; H, 5.25; N, 2.70. ^{1}H-NMR (400 MHz, $CDCl_3$): δ 1.32 (d, $^3J_{H,H}$ = 6.9 Hz, 6H, CH(CH_3)$_2$), 2.10 (s, 3H, CCH_3), 2.99 (sept, $^3J_{H,H}$ = 6.9 Hz, 1H, CH(CH$_3$)$_2$), 3.64, 3.76, 3.85 (m, 6H, OCH_2), 4.54 (m, 2H, COOCH_2), 5.24 (d, $^3J_{H,H}$ = 5.9 Hz, 2H, CHCCH$_3$), 5.46 (d, $^3J_{H,H}$ = 5.8 Hz, 2H, CHCHCCH$_3$), 7.85 (d, $^3J_{H,H}$ = 6.4 Hz, 2H, H^3), 9.24 (d, $^3J_{H,H}$ = 6.4 Hz, 2H, H^2). ^{13}C-NMR (100 MHz, $CDCl_3$): δ 18.4 (CCH$_3$), 22.4 (C(CH_3)$_2$), 30.8 (C(CH$_3$)$_2$), 61.9, 65.4, 68.9, 72.6 (CH$_2$O), 82.5, 83.2 (CH), 97.6, 104.0 (CCH), 123.7 (C^3), 138.7 (C^4), 156.0 (C^2), 164.0 (COO). ESI-HRMS (CH$_3$OH), positive mode: Calcd for $[C_{20}H_{27}ClNO_4{}^{96}Ru]^+$ 476.06991, *m*/*z* 476.06973 [M-Cl]$^+$. IR: ν (cm^{-1}) 3450(b), 3063(w), 2962(w), 2878(w), 1728(s), 1471(w), 1414(m), 1382(w), 1323(w), 1278(s), 1228(m), 1120(s), 1061(s), 932(w), 866(m), 800(w), 771(s), 698(m), 659(w), 451(w), 400(w), 371(w), 355(w), 286(s), 233(s).

*Dichlorido(*η^6-p-*cymene)[2-{2-(2-methylamino-benzoyloxy)-ethoxy}-ethyl isonicotinate*-κN*]ruthenium(II)* ***(5)***

Properties: Yellow powder; soluble in chloroform, dichloromethane, moderately soluble in methanol, ethanol, *iso*propanol, insoluble in diethyl ether.

EA: Anal. Found: C, 51.83; H, 4.99; N, 4.09. Calcd for $C_{28}H_{34}Cl_2N_2O_5Ru$ (650.56): C, 51.70; H, 5.27; N, 4.31. ^{1}H-NMR (400 MHz, $CDCl_3$): δ 1.30 (d, $^3J_{H,H}$ = 6.9 Hz, 6H, CH(CH_3)$_2$), 2.07 (s, 3H, CCH_3), 2.90 (s, 3H, NCH_3), 2.97 (sept, $^3J_{H,H}$ = 6.9 Hz, 1H, CH(CH$_3$)$_2$), 3.86 (m, 4H, OCH_2), 4.43, 4.52 (m, 4H, COOCH_2CH_2), 5.21 (d, $^3J_{H,H}$ = 5.5 Hz, 2H, CHCCH$_3$), 5.44 (d, $^3J_{H,H}$ = 5.5 Hz, 2H, CHCHCCH$_3$), 6.59 (t, $^3J_{H,H}$ = 7.5 Hz, 1H, H^9), 6.69 (d, $^3J_{H,H}$ = 8.3 Hz, 1H, H^7), 7.40 (t, $^3J_{H,H}$ = 7.8 Hz, 1H, H^8), 7.79 (d, $^3J_{H,H}$ = 5.8 Hz, 2H, H^3), 7.90 (d, $^3J_{H,H}$ = 8.0 Hz, 1H, H^{10}), 9.17 (d, $^3J_{H,H}$ = 5.8 Hz, 2H, H^2). ^{13}C-NMR (100 MHz, $CDCl_3$): δ 18.3 (CCH$_3$), 22.4 (C(CH_3)$_2$), 29.8 ((b), NCH_3), 30.8 (C(CH$_3$)$_2$), 63.2, 65.3 (CH$_2$OOC), 68.9, 69.4 (CH$_2$OCH_2), 82.5, 83.2 (CH$_{cym}$), 97.5, 103.9 (CCH$_{cym}$), 109.8 ((b),

C[5]), 111.2 ((b), *C*[7]), 114.7 ((b), *C*[9]), 123.6 (*C*[3]), 131.6 (*C*[10]), 135.0 (*C*[8]), 138.6 (*C*[4]), 152.2 ((b), *C*[6]), 155.9 (*C*[2]), 163.9, 168.4 (*C*OO). ESI-HRMS (CH_3OH), positive mode: Calcd for $[C_{28}H_{34}ClN_2O_5{}^{96}Ru]^+$ 609.12267, *m*/*z* 609.12286 $[M\text{-}Cl]^+$. IR: ν (cm^{-1}) 3372(w), 3059(w), 2964(w), 2872(w), 2819(w), 1734(s), 1676(s), 1604(w), 1576(m), 1516(m), 1442(w), 1413(m), 1378(w), 1322(w), 1278(s), 1236(s), 1120(s), 1084(s), 1057(m), 948(w), 858(m), 762(s), 702(s), 662(w), 528(m), 283(s), 234(s). UV-vis (7.01×10^{-5} M, $CHCl_3$, 298 K): λ_{max} 351 nm (ε = 11689 M×cm^{-1}). Fluorescence (7.01×10^{-5} M, $CHCl_3$, 298 K): $\lambda_{max,\ excitation}$ 367 nm, $\lambda_{max,\ emission}$ 418 nm.

Table S-I. Second order perturbation theory parameters and occupancies for the selected interactions within investigated ligands and complexes

	L1	
Donor (i)	Acceptor (j)	E2/ kJ mol-1
π(C−C)	π*(C−C)	76
π(C−C)	π*(C−C)	95
π(C−N)	π*(C−C)	60
π(C−C)	π*(C−N)	109
LP(N)	π*(C−C)	41
LP(O)	π*(C−C)	75
LP(O)	π*(C−O)	135
	1	
π(C−C)	π*(C−C)	46
π(C−C)	π*(C−C)	55
π(C−C)	LP*(Ru)	60
π(C−C)	LP*(Ru)	80
LP(N)	σ*(Ru−Cl)	27
π(C−N)	LP*(Ru)	50
LP(Cl)	LP*(Ru)	34
LP(Cl)	LP*(Ru)	75
LP(Cl)	σ(Ru−Cl)	5
	L4	
LP(O)	σ(C−C)	4.8
	L5	
LP(O)	σ(C−C)	71
LP(O)	σ(C−O)	132
LP(O)	π*(C−O)	105

TABLE S-II. Experimental and theoretical ^{13}C-NMR chemical shifts (in ppm) of **L1** and **1**

Carbon atom	Ligand **L1·HCl**		Complex **1**	
	Experimental	Theoretical	Experimental	Theoretical
C^2	142.7	140.8	155.9	148.8
C^3	126.9	127.5	123.7	118.0
C^4	145.7	145.0	138.8	136.2
CH_3O	58.2	62.8	59.2	58.0
CH_2OOC	65.9	73.9	65.5	67.8
CH_2O	69.6	73.7	69.0	69.7
*C*OO	163.4	158.6	163.9	159.2
C*C*H3			18.4	18.9
C(*C*H3)2			22.4	22.7
C(CH3)2			30.8	35.5
C_{arm}			70.8	83.2
C_{arm}			72.1	83.6
C_{arm}			82.5	84.5
C_{arm}			83.3	86.9
*C*H			97.5	99.9
*C*CH			103.9	111.4
	R	0.99	R	0.98
	MAE [ppm]	3.5	MAE [ppm]	4.6

Table S-III. Experimental and theoretical ^{1}H NMR chemical shifts (in ppm) of **L1·HCl** and **1**

Hydrogen atom	Ligand **L1·HCl**		Complex **1**	
	Experimental	Theoretical	Experimental	Theoretical
OCH_3	3.48	3.28	3.42	3.39
OCH_2	3.92	3.60	3.72	3.55
$COOCH_2$	4.67	4.31	4.52	4.17
C^3–*H*	8.62	8.61	7.86	7.62
C^2–*H*	9.05	8.61	9.23	8.64
$CH(CH_3)_2$			1.31	1.31
CCH_3			2.09	1.67
$CH(CH_3)_2$			2.98	3.00
C_{arm}–H			5.23	4.69
C_{arm}–H			5.45	4.95
	R	0.97	R	0.99
	MAE [ppm]	0.27	MAE [ppm]	0.44

Table S-IV. Experimental and theoretical ^{13}C NMR chemical shifts (in ppm) of **L4**·HCl and **4**

Carbon atom	**L4·HCl**		**4**	
	Experimental	Theoretical	Experimental	Theoretical
C^2	142.7	155.2	156.0	150.9
C^3	126.9	127.5	138.7	119.5
C^4	145.9	141.1	123.7	134.3
CH_2CH_2OH	71.8	67.4	72.6	73.4
CH_2CH_2OOC	68.1	63.8	65.4	66.7
CH_2OOC	66.1	62.9	68.9	68.5
CH_2OH	60.3	59.2	61.9	60.4
COO	163.4	161.7	164.0	161.4
CCH3			18.4	18.8
C(CH3)2			22.4	27.2
C(CH3)2			30.8	35.9
C_{arm}			82.5	84.4
C_{arm}			82.5	85.34
C_{arm}			83.2	85.9
C_{arm}			83.2	87.0
CH			97.6	100.6
CCH			104.0	114.1
	R	0.98	R	0.98
	MAE [ppm]	4.1	MAE [ppm]	4.5

Table S-V. Experimental and theoretical ^1H NMR chemical shifts (in ppm) of **L4**·HCl and **4**

Hydrogen atom	**L4·HCl**		**4**	
	Experimental	Theoretical	Experimental	Theoretical
OCH_2	3.77	3.71	3.85	3.96
$HOCH_2CH_2$	3.77	3.55	3.64	3.93
$COOCH_2CH2$	4.00	3.74	3.76	3.87
$COOCH_2$	4.69	44.26	4.54	4.45
C^3-*H*	8.60	8.64	9.24	9.13
C^2-*H*	9.04	9.45	7.85	8.09
$CH(CH_3)_2$			1.32	1.38
CCH_3			2.10	1.81
$CH(CH_3)_2$			2.99	3.21
C_{arm}-H			5.24	5.01
C_{arm}-H			5.46	5.21
	R	0.99	R	0.99
	MAE [ppm]	0.24	MAE [ppm]	0.18

Table S-VI. Experimental and theoretical ^{13}C NMR chemical shifts (in ppm) of **L5** and **5**

Carbon atom	**L5**		**5**	
	Experimental	Theoretical	Experimental	Theoretical
C^2	149.8	148.5	155.9	151.1
C^3	123.4	123.4	123.6	119.7
C^4	138.1	136.2	138.6	134.4
C^5	109.7	127.6	109.8	128.7
C^6	152.2	150.9	152.2	126.0
C^7	110.9	110.3	111.2	125.1
C^8	135.0	135.7	135.0	127.7
C^9	114.5	130.8	114.7	123.9
C^{10}	131.7	129.6	131.6	122.7
N*C*H3	29.7	29.1	29.8	29.7
CH_2CH_2OOC	69.4	67.2	69.4	68.6
CH_2OOC	65.0	64.0	65.3	67.3
CH_2CH_2OOC	69.0	62.8	68.9	72.3
CH_2OOC	63.2	61.1	63.2	69.3
*C*OO	168.5	164.2	168.4	169.4
*C*OO	164.9	156.2	163.9	161.7
C*C*H_3			18.3	19.1
C(*C*H_3)$_2$			22.4	22.8
C(CH_3)$_2$			30.8	36.3
C_{arm}			82.5	85.2
C_{arm}			82.5	85.2
C_{arm}			83.2	85.8
C_{arm}			83.2	88.3
*C*H			97.5	114.3
*C*CH			103.9	102.5
	R	0.96	R	0.95
	MAE [ppm]	4.2	MAE [ppm]	6.0

Table S-VII. Experimental and theoretical ^{1}H NMR chemical shifts (in ppm) of **L5** and **5**

Hydrogen atom	**L5**		**5**	
	Experimental	Theoretical	Experimental	Theoretical
NCH_3	2.89	2.53	2.90	2.69
OCH_2	3.87	3.88	3.86	2.85
$COOCH_2CH_2$	4.43	3.44	4.43	3.27
$COOCH_2CH_2$	4.53	3.51	4.52	3.40
C^3-*H*	7.84	8.23	7.79	7.07
C^2-*H*	8.71	9.05	9.17	8.16
C^7-*H*	6.65	6.81	6.69	6.74
C^8-*H*	7.37	7.68	7.40	6.89
C^9-*H*	6.53	6.81	6.59	6.74
C^{10}-*H*	7.88	7.73	7.90	6.74
$CH(CH_3)_2$			1.30	0.30
CCH_3			2.07	0.79
$CH(CH_3)_2$			2.97	2.09
	R	0.95	R	0.94
	MAE [ppm]	0.40	MAE [ppm]	0.79

Journal of the Serbian Chemical Society
JSCS@tmf.bg.ac.rs • www.shd.org.rs/JSCS
J. Serb. Chem. Soc. 88 (12) 1355–1367 (2023)
JSCS–5700
Original scientific paper
Published 19 December 2023

Zn(II) complex with pyridine based 1,3-selenazolyl-hydrazone: Synthesis, structural characterization and DFT study

JOVANA B. ARAŠKOV[1#], PREDRAG G. RISTIĆ[1*#], ALEKSANDAR VIŠNJEVAC[2**], ANDREJ LJ. MILIVOJAC[3], DRAGANA M. MITIĆ[3], NENAD R. FILIPOVIĆ[4#] and TAMARA R. TODOROVIĆ[1#]

[1]University of Belgrade – Faculty of Chemistry, Studentski trg 12–16, 11000 Belgrade, Serbia, [2]Division of Physical Chemistry, Institute Ruđer Bošković, Bijenička cesta 54, Zagreb 10000, Croatia, [3]Innovation Centre of Faculty of Chemistry, University of Belgrade, Studentski trg 12–16, 11000 Belgrade, Serbia and [4]University of Belgrade – Faculty of Agriculture, Nemanjina 6, 11000 Belgrade, Serbia

(Received 31 August, revised 25 September, accepted 13 October 2023)

Abstract: An octahedral complex of Zn(II) with a ligand from a class of pyridine-based 1,3-selenazolyl-hydrazones was synthesized and characterized by IR and NMR spectroscopy and single crystal X-ray diffraction analysis. The purity of the complex was confirmed by elemental analysis. Two ligands are coordinated in the neutral *NNN*-tridentate form forming a complex cation, while the positive charge is neutralized by $[ZnCl_4]^{2-}$. Complex crystallizes in monoclinic *C*2/*c* space group with the Zn atoms situated in a special position. The packing features of the novel complex were analyzed using Hirshfeld surfaces, construction of 2D pseudosymmetric plot and DFT quantum mechanical calculations and compared with the previously published sulfur-based isostere. The key difference in the structures, imposed by replacement of sulfur with selenium, were identified.

Keywords: Zn(II) complex; selenazolyl-hydrazones; X-ray crystal structure; isosteres; selenium; intermolecular energies.

INTRODUCTION

Zinc is one of the most studied elements in pharmacological research due to the fact that it is found in about 10 % of all enzymes in human body. Also, zinc is a versatile element extensively employed in various area of material chemistry research, including nanomaterial synthesis,[1,2] photocatalytic,[3] photoluminescence[4,5] and electrochemical[6] studies. The possibility of achieving different coordination numbers from 2 to 9 (most often 4-6)[7], affinity to *N*,*O*,*S*-donor

* Corresponding authors. E-mail: (*)predrag@chem.bg.ac.rs, (**)visnevac@irb.hr
# Serbian Chemical Society member.
https://doi.org/10.2298/JSC230831079A

atoms and high bioavailability makes Zn(II) an excellent candidate for the synthesis of complexes for specific application. By choosing the starting Zn(II) salt it is possible to control the nuclearity, geometry and type of complexes.

A crystallographic study of complexes provides insight into the geometrical parameters, the orientation of the hydrophilic/phobic parts of the ligands, as well as the types and distribution of weak intermolecular interactions which are important for examining potential application.[8,9]

N-heteroaromatic (1,3-thiazolyl-2-yl)-hydrazones are a widely studied class of compounds as a potential anticancer,[10,11] antioxidant,[12–18] antibacterial,[19–22] antifungal[23–28] and antiparazitic agents.[29,30] By suitable selection of *N*-heteroaromatic moiety and substituents on 1,3-thiazole ring, it is possible to design and direct the coordination mode. An isosteric replacement of sulfur with selenium can lead not only to increase of structural diversity, but also to improvement of pharmacological properties and achievement of a better intake of selenium.[31]

Selenium is a micronutrient that supports the processes of the immune response, fertility, proper function of thyroid hormones, regulation of redox balance in cells and cancer chemoprevention.[32] Also, there are several studies that explain the fact that selenium as a part of organic molecule is more acceptable to the human body than selenium in an inorganic form (such as SeO_3^{2-}).[32,33] In support of the growing field of research on 1,3-selenazole derivatives is the fact that there are 69 crystal structures deposited in CSD[7] containing substituted 1,3-selenazole ring. Two of 69 crystal structures containing the hydrazone pharmacophore as a substituent in 2-position of 1,3-selenazole ring. Eight of the 69 crystal structures are complexes of Zn(II), Co(III) and Cd(II) with *N*-heteroaromatic (1,3-selenazolyl-2-yl)-hydrazones. Since the properties of a complex is dependent not only on the nature of the ligand, but also on weak interactions, this paper presents a crystallographic study and analysis of intermolecular interactions in the crystal structure of novel Zn(II) complex with 2-(2-(pyridine-2-ylmethylene)hydrazonyl)-4--(4-methoxyphenyl)-1,3-selenazole ($HLSe^2$) and comparison with a previously published sulfur isostere.[4]

EXPERIMENTAL

Materials and methods

Potassium selenocyanate (99 %), hydrazine hydrate (99 %), 2-formylpyridine (99 %) and 2-4'-methoxyacetophenone (98 %) were obtained from Acros Organics. Anhydrous $ZnCl_2$ (99 %) was obtained from Merck. All solvents were obtained from commercial suppliers and used without further purification. Purity of complex was confirmed by elemental analysis (C, H, N) by the standard micromethods using the Elementar Vario EL III CHNS/O analyzer. Infra-red (IR) spectra were recorded on a Thermo Scientific Nicolet Summit FT-IR spectrometer by the attenuated total reflection (ATR) technique in the region 4000–400 cm^{-1}. Molar conductivities were measured at room temperature (298 K) on the Crison multimeter MM41. The NMR spectra were performed on a Varian/Aglient 400 MHz. Chemical shifts are given on δ scale relative to tetramethylsilane (TMS) as internal standard for ^1H and ^{13}C. IR and NMR spectra,

as well as analytical and spectral data, are given in Figs. S-1–S-3 of the Supplementary material to this paper.

Synthesis

The ligand based on (1,3-selenazol-2-yl)hydrazone was synthesized according to a previously published procedure.[34] The ligand (50 mg, 0.14 mmol) was dissolved in 10 ml of hot MeOH. When the ligand was dissolved, the solid $ZnCl_2$ (19 mg, 0.14 mmol) was added. The dark orange solution was refluxed for 1 h. After 2 days, orange single crystals of the complex suitable for single crystal X-ray diffraction analysis crystallized from the mother liquor. The crystals were collected by filtration, washed with cold methanol (4 °C) and diethyl ether and dried in a desiccator. Yield: 0.057 g (83 %).

X-ray structural analysis (XRD)

The **2-Cl-Se** (Zn(II) complex with 2-(2-(pyridin-2-ylmethylene)hydrazonyl)-4-(4-methoxyphenyl)-1,3-selenazole) was obtained as single crystal, so its structure in solid state was solved by single crystal X-ray diffraction analysis. Diffraction data for **2-Cl-Se** were collected at 298 K at Xcalibur Ruby Nova diffractometer using monochromatic CuKα (λ = 1.54184 Å) radiation. Collection, data reduction and unit cell refinement was performed using CrysAlisPro.[35] Structure refinement was performed using SHELXL-2016/4.[36] Collected data were corrected for absorption effects using multiple scan absorption correction method. Most of the hydrogen atoms are placed in ideal geometric positions while some are found in the differential Fourier map. Calculations for verification of molecular structures, parameters of crystal packing as well as preparation of illustrations of molecular structures and crystal packing were performed using Platon,[37] Mercury.[38] WinGX[39] and OLEX2[40] programs. Crystallographic information file is deposited in CSD under the following number – 2291805. Crystal data and structure refinement are given in Table S-I of the Supplementary material. Tables of bond angles and lengths are given in Supplementary material (Tables S-II and S-III).

Hirshfeld surfaces and analysis of intermolecular interactions

Hirschfeld surfaces and pseudosymmetric fingerprint plots of intermolecular interactions were generated using crystallographic information file (CIF). Before calculation, bond lengths involving hydrogen atoms were normalized to standard values estimated by neutron diffraction. Visualization of surfaces and presentation of results as d_{norm}, shape indexes and curvedness, as well as calculations of 2D plots with d_e and d_i distance values were done using CrystalExplorer 21[41]. The distance from the surface to the nearest nucleus of the atom on the outside of the surface is denoted as *de*, while the distance from the surface to the closest nucleus of the atom on the inside of the surface is denoted as *di*. The surfaces are mapped over a standard color scale, and 2D fingerprint plots are calculated using *de* and *di* values in the range 0.4−2.8 Å.

Calculation of intermolecular interaction energies

Intermolecular interaction energies were calculated using molecular electron densities derived from wavefunctions computed by Gaussian09[42] coupled with CrystalExplorer21[41] using B3LYP functional[43–46] and DGDZVP basis set.[47,48] CIF is used as input file while bond lengths involving hydrogen atoms were normalized to standard values estimated by neutron diffraction. For calculation purposes, a cluster is constructed around the central molecule which implies real molecular environments and usage of corresponding atomic coordinates at a distance of 3.8 Å from the central molecule. Calculated wave functions were automatically

generated for all symmetrically connected molecules within the cluster and Energy frameworks[49] were constructed for the supercell (2×2×2).

RESULTS AND DISCUSSION

Synthesis and spectroscopic characterization

The complex was synthesized by direct reaction between anhydrous $ZnCl_2$ and $HLSe^2$ (in equimolar ratio) in methanol under reflux conditions (Scheme 1). Based on the results of elemental analysis and molar conductivity measurements, the following molecular formula of the complex was determined: $[Zn(HLSe^2)_2][ZnCl_4]$. The presence of the valence C=N vibration of thiazole ring and the imine bond in IR spectrum was observed at 1564 and 1526 cm^{-1}, respectively. These bands are shifted in the spectrum of **2-Cl-Se** at 1610 and 1546 cm^{-1}, respectively, which indicates coordination of the ligands *via* thiazole and imine nitrogens. Band at 3099 cm^{-1} originates from valence N–H vibration which implies that the ligands are coordinated in a neutral form. In ^{1}H-NMR spectrum presence of N–H at 12.46 ppm additionally confirms coordination of ligands in neutral form. Aromatic protons are in range 6.93–8.54 ppm. At 3.75 ppm singlet originating from the proton of the methoxy group on the periphery of the ligand was observed.

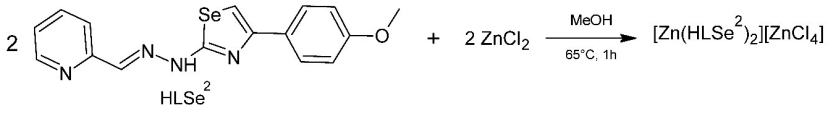

Scheme 1. Synthesis of **2-Cl-Se**.

Molecular structure analysis

Complex **2-Cl-Se** crystallize in the monoclinic *C*2/*c* space group. The complex cation consists of Zn(II) atom and two meridionally positioned ligands coordinated in a neutral form, where the positive charge of the complex cation is neutralized by the tetrachloridozincate(II) anion. (Fig. 1). The geometry of the coordination environment is distorted octahedral where each ligand forms the NNN-chelate tridentate coordination *via* pyridine, imine and azomethine nitrogen atoms. The angular distortion from the ideal octahedron geometry is caused by the position of nitrogen atoms and planarity of the ligand. The Zn atoms are in a special position (Wyckoff letter *e*, site symmetry 2) which causes that the asymmetric unit consists of one half of the complex cation and one half of the tetrachloridozincate(II) anion.

In order to visually describe the geometrical differences in the molecular geometry between the isostructural **2-Cl** (Zn(II) complex with 2-(2-(pyridin-2-ylmethylene)hydrazonyl)-4-(4-methoxyphenyl)-1,3-thiazole) and **2-Cl-Se**, the cations were overlapped over the donor atoms and the deviations from the root

mean planes through the aromatic rings were measured. The substitution of sulfur by selenium atom leads to slight deviations: the mean planes drawn through the rings **A** and **A'** deviate by 3.90°, **B** and **B'** by 2.39°, while the corresponding angle between **C** and **C'** is 2.89° (Fig. 2). The measured deviations are in accordance with the size of sulfur and selenium atoms.

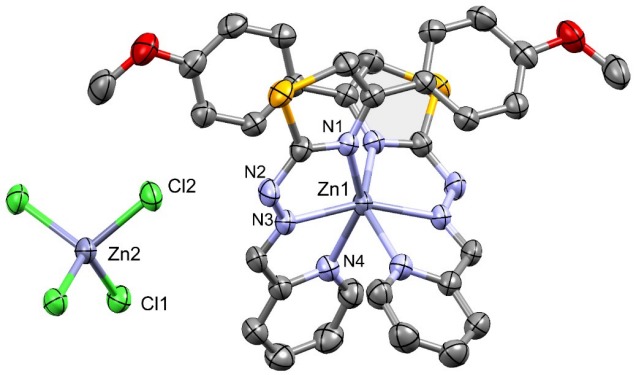

Fig. 1. ORTEP[38] drawing of complex **2-Cl-Se**. Displacement ellipsoids are given in 50 % probability level. Hydrogen atoms are omitted for clarity.

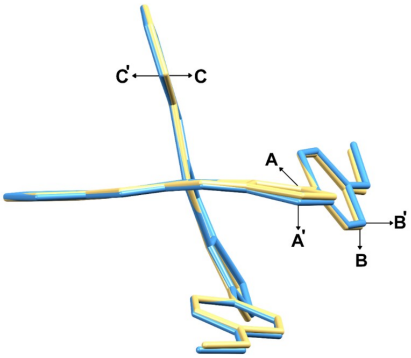

Fig. 2. Overlay of the complex cations of **2-Cl-Se** (yellow) and **2-Cl** (blue). Notation of aromatic rings: 1,3-thiazole/selenazole (**A/A'**), methoxyphenyl (**B/B'**) and pyridine (**C/C'**).

Crystal structure and Hirshfeld surface analysis

A comparative study of intermolecular interactions in isostructural **2-Cl** and **2-Cl-Se** by combined crystal packing and Hirshfeld surface analysis provides valuable insight into key structural differences between them. The contributions of intermolecular interactions in **2-Cl-Se** are represented in the 2D pseudosymmetric plot by red circles (Fig. 3) and quantified and compared to the sulfur isostere in Table I. The analysis of surface area included in intermolecular interactions shows that both crystal packings are based predominantly on classical and non-classical hydrogen interactions which account for 52.8 (**2-Cl-Se**) and

52.9 % (**2-Cl**) of all interactions. The orientations of adjacent cations and anions are in such a position that π–π stacking and anion–π interactions occur (8.5 in **2-Cl-Se** and 7.9 % in **2-Cl**). Hydrophobic interactions are slightly represented in **2-Cl-Se**, which is a consequence of the isosteric replacement of sulfur by selenium atom and is caused by the higher polarizability of selenium atom. The remaining contacts in the case of both complexes are H–H contacts.

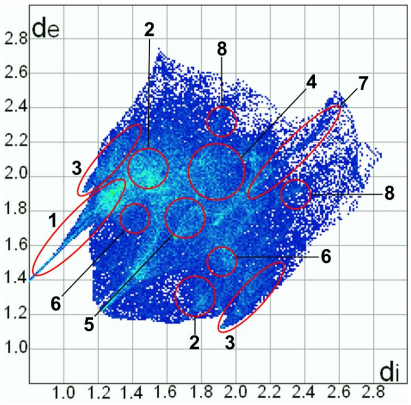

Fig. 3. 2D pseudosymmetric plot of intermolecular interactions in **2-Cl-Se**. Numbered regions correspond to contacts shown in Table I.

TABLE I. Relative contribution of the Hirshfeld surface to individual intermolecular interactions (H···H contacts are disregarded) in the crystal structure of **2-Cl-Se** and **2-Cl**

Complex	Label of interaction							
	1	2	3	4	5	6	7	8
	Interaction type							
	H···Cl	H···C	H···Se(S)	H···O	C···C	H···N	Se(S)···Cl	C···O
2-Cl-Se	19.0	18.1	9.7	4.9	3.6	1.1	2.2	2.7
2-Cl[4]	18.8	18.8	9.3	5.2	3.4	0.8	1.7	2.8

On the Hirshfeld surface most common H···Cl interactions are observed as red patches (Fig. 4A). The complex cation is a double donor in classical (N2––H2A···Cl2, d = 2.287 Å, i = 1–x, y, 1/2–z) and non-classical (C11–H11···Cl1^{i}, d = 2.744 Å; i = 1–x, y, 1/2–z) hydrogen interactions with the tetrachloridezincate(II) anion, which results in the formation of a 1D chain parallel to the *a*-crystallographic axis (Fig. 4B). A higher level of assembly is based on the linking of 1D chains by interactions marked with orange circles on Hirshfeld surface (Fig. 4C). By non-classical C14–H14···Cl2^{ii} interactions (d = 2.932 Å; ii = 1/2–x, 1.5–y, 1–z), the chains are connected in a 2D "pleated" layer parallel to the *ac*-crystallographic plane (Fig. 4D). The remaining interactions are responsible for stacking of 2D layers into the final 3D crystal structure (Fig. 4E). Hydrophobic C–H···π and π···π stacking interactions with a total contribution of 21.7 %

participate of the existence of 3D packing through C10–H10B··· $\pi_{pyridin}$ ^{iii} (d = = 3.956 Å; *iii* = x, 1–y, 1/2+z) and $\pi_{methoxyphenyl}$···$\pi_{pyridine}$^{iv} (d = 3.461 Å; *iv* = = –1/2–x, –1/2+y, 1/2–z).

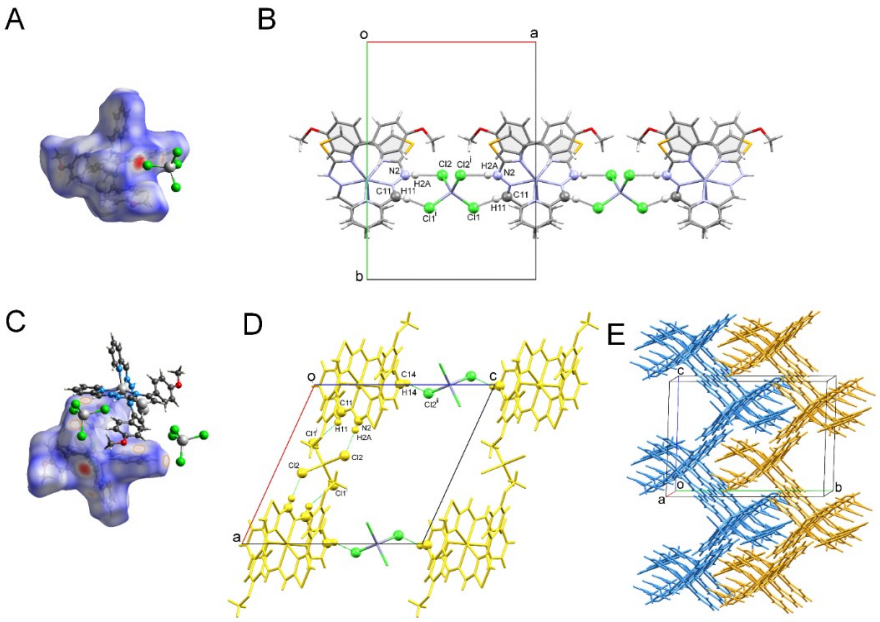

Fig. 4. Hirshfeld d_{norm} surface for **2-Cl-Se** with neighboring tetrachloridozincate(II) anion responsible for formation of 1D chain (A); 1D chain formed parallel to the *a*-crystallographic axis (B); Hirshfeld d_{norm} surface with neighboring species responsible for the formation of 2D and 3D crystal packing (C); Part of a 2D "pleated" layer formed due to the connection of 1D chains (yellow, D). The resulting 3D crystal packing as a result of stacking 2D layers (blue and ochre, E).

Analysis of intermolecular interactions by generating full interaction maps (FIM) using Mercury[38] also provides insight into geometrical analysis of intermolecular interactions grouping them into (non)classical and hydrophobic (aromatic) interactions. Fig. 5A shows a 3D map of the highest probability of finding interactions between certain functional groups, wrapped around the molecule. The most common regions are colored red and blue which implies a significant influence of classical and non-classical hydrogen interactions in the crystal packing of **2-Cl-Se**. The presence of ocher colored regions indicating the existence of aromatic interactions, which are the smallest part of FIM. Fig. 5B shows a hotspots which represent the positions of highest local density for each contour surface colored with the same colors as the corresponding part of the 3D surface. Arrangement of donor and acceptor functional groups is in good correlation with

the surface area included in intermolecular interactions obtained by Hirshfeld surface analysis.

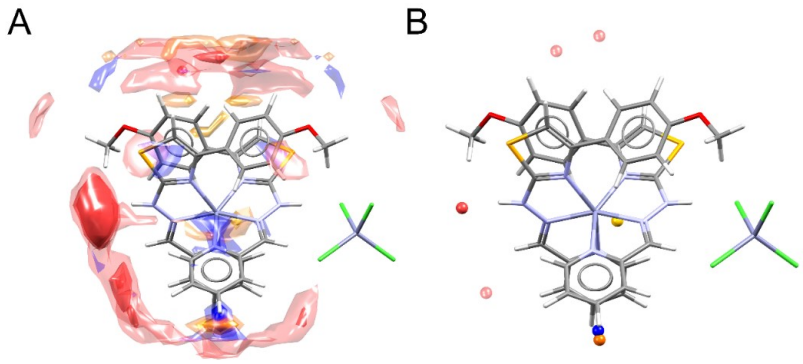

Fig. 5. Contour surface colored red (hydrogen bond acceptors), blue (hydrogen bond donors) and ocher (interactions which includes aromatic part of molecules) (A); the positions of highest local density for each contour surface showed as hotspots (B) around **2-Cl-Se**.

Energy distribution of intermolecular interactions

The use of B3LYP functional[43-46] and DGDZVP basis set[47,48] in investigations of molecular crystals based on metal coordination compounds, organic salts and solvates, as well as open shell molecules (radicals), provide a sufficiently good relative ratio of computing time and quality of obtained results.[49] The energy models in CrystalExplorer21[41] are calibrated and include optimum scale factors for B3LYP functional[49] (Table II). In the crystal structures of isosteres, there is the same trend in energy values. The nature of stabilizing interactions is predominantly electrostatic, with a significantly smaller contribution of polarization and dispersion components (Table II). Interactions in crystal structure of **2-Cl**[4] (Table S-III, Supplementary material) are realized at shorter distances (0.1–0.3 Å), thus attractive interactions are stronger (1–6 kJ mol^{-1}) than those in **2-Cl-Se**. The repulsive interactions are also more pronounced in **2-Cl**, while the polarization and dispersion components differ in the interval of 1–3 kJ mol^{-1}. The crystal packing energy represented as the sum of *E*_tot values is –1330.7 and –1322.0 kJ mol^{-1} for **2-Cl-Se** and **2-Cl**, respectively, thus the crystal packing energy of selenium based isostere is more stable by –8.7 kJ mol^{-1}. This difference comes from isosteric replacement of the sulfur by the selenium atom and arises from the nature of the selenium atom.

In order to visualize intermolecular interaction energies, using the calculated interaction energies in Table II the energy framework was calculated (Fig. 6). Since **2-Cl-Se** and **2-Cl** crystallize in the same space group, topology of the energies that stabilize and destabilize the crystal packing is complex but the same

pattern is observed for both isosteres.[4] The strongest interactions are realized in 3D, but mostly along the *a*-crystallographic axis while the repulsive interactions are located along the *b* and *c*-crystallographic axes. The calculated pattern confirms three-dimensional crystal packing based on geometrical parameters (*vide supra*).

TABLE II. Interaction pair energies in the crystal structure of **2-Cl-Se** based on the B3LYP/ /DGDZVP energy model; *E*_tot represents the sum of individual components with scaling factors (*k*_ele = 1.057; *k*_pol = 0.740; *k*_dis = 0.871; *k*_rep = 0.618), while the individual components are not scaled

R / Å	Energy component				
	*E*_ele	*E*_pol	*E*_dis	*E*_rep	*E*_tot
7.39	547.4	–72.0	–119.2	114.5	492.4
11.80	550.9	–51.3	–15.9	3.4	532.7
11.79	480.4	–43.0	–30.7	19.9	461.6
8.37	–622.6	–76.0	–11.7	17.1	–714.1
9.90	–632.4	–65.8	–11.1	15.6	–717.3
14.43	407.1	–21.5	–11.3	0.0	404.7
7.53	–858.7	–162.3	–28.9	102.8	–989.6
7.18	–662.0	–130.4	–26.1	29.2	–801.1

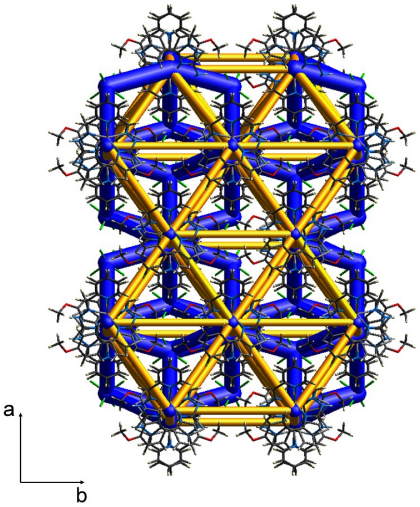

Fig. 6. Diagram of the energy framework of the total energies for the supercell (2×2×2) of the **2-Cl-Se**. The figure shows cylinders of the same scale (blue cylinders represent total energy, while yellow cylinders represent destabilizing energy).

CONCLUSION

The synthesis, structural characterization (spectroscopic and SCXRD), crystallographic and DFT analysis of crystal packing and intermolecular interactions of a new octahedral Zn(II) complex with a ligand from the pyridine-based 1,3--selenazolyl hydrazone class was performed. The two ligands are coordinated in

the neutral form by chelate *NNN*-tridentate forming a complex cation, while the anion is $[ZnCl_4]^{2-}$. The results of a comparative crystallographic study showed that novel complex crystallize in the same space group and has the same topology of intermolecular interactions as its sulfur isostere. However, due to nature of selenium, the crystal packing energy of Se-based isostere is higher by –8.7 kJ mol^{-1}. Hirshfeld surface analysis showed that the interactions involving the Se atom are more prevalent than the analogous ones in the S-based isostere which confirms additional contribution of the Se atom to the stabilization of the crystal packing.

SUPPLEMENTARY MATERIAL

Additional data and information are available electronically at the pages of journal website: https://www.shd-pub.org.rs/index.php/JSCS/article/view/12573, or from the corresponding author on request. CCDC 2269543-2269546.

Acknowledgement. The authors gratefully acknowledge financial support from the Ministry of Science, Technological Development and Innovation of Republic of Serbia, contract numbers 451-03-47/2023-01/200168, 451-03-47/2023-01/200288 and 451-03-47/2023-01/ /200116.

И З В О Д

Zn(II) КОМПЛЕКС СА 1,3-СЕЛЕНАЗОЛИЛ-ХИДРАЗОНОМ НА БАЗИ ПИРИДИНА: СИНТЕЗА, СТРУКТУРНА КАРАКТЕРИЗАЦИЈА И DFT СТУДИЈА

ЈОВАНА Б. АРАШКОВ[1], ПРЕДРАГ Г. РИСТИЋ[1], ALEKSANDAR VIŠNJEVAC[2], АНДРЕЈ Љ. МИЛИВОЈАЦ[3], ДРАГАНА М. МИТИЋ[3], НЕНАД Р. ФИЛИПОВИЋ[4] и ТАМАРА Р. ТОДОРОВИЋ[1]

[1]Универзитет у Београду – Хемијски факултет, Студентски трг 12–16, 11000 Београд, [2]Division of Physical Chemistry, Institute Ruđer Bošković, Bijenička cesta 54, Zagreb 10000, Croatia, [3]Иновациони центар Хемијског факултета, Универзитет у Београду, Студентски трг 12–16, 11000 Београд и [4]Универзитет у Београду – Пољопривредни факултет, Немањина 6, 11000 Београд

Октаедарски комплекс Zn(II) са лигандом из класе 1,3-селеназолил-хидразона на бази пиридина је синтетисан и окарактерисан IC и NMR спектроскопијом и дифракцијом X-зрака са монокристала. Чистоћа комплекса је потврђена елементалном анализом. Два лиганда су координована у неутралном NNN-тридентатном облику формирајући комплексни катјон, док је позитивно наелектрисање неутрализано помоћу $[ZnCl_4]^{2-}$. Комплекс кристалише у моноклиничној C2/*c* просторној групи при чему се атоми Zn(II) налазе у специјалном положају. Карактеристике кристалног паковања новог комплекса су анализиране употребом Хиршфелдових површина, конструкцијом 2Д псеудосиметричних графикона и употребом DFT квантномеханичких прорачуна при чему су добијени резултати упоређени са резултатима анализе претходно објављеног изоструктурног комплекса на бази сумпора. Идентификоване су кључне разлике у структурама које произилазе из изостерне замене атома сумпора атомом селена.

(Примљено 31. августа, ревидирано 25. септембра, прихваћено 13. октобра 2023)

REFERENCES

1. Y. Su, I. Cockerill, Y. Wang, Y. X. Qin, L. Chang, Y. Zheng, D. Zhu, *Trends Biotechnol.* **37** (2019) 428 (https://doi.org/10.1016/j.tibtech.2018.10.009)

2. T. Zhang, X. Li, Y. Qiu, P. Su, W. Xu, H. Zhong, H. Zhang, *J. Catal.* **357** (2018) 154 (https://doi.org/10.1016/j.jcat.2017.11.003)
3. D. Drozd, K. Szczubiałka, Ł. Łapok, M. Skiba, H. Patel, S. M. Gorun, M. Nowakowska, *Appl. Catal., B* **125** (2012) 35 (https://doi.org/10.1016/j.apcatb.2012.05.021)
4. J. B. Araškov, A. Višnjevac, J. Popović, V. Blagojević, H. S. Fernandes, S. F. Sousa, I. Novaković, J. M. Padrón, B. B. Holló, M. Monge, M. Rodríguez-Castillo, J. M. López--De-Luzuriaga, N. R. Filipović, T. R. Todorović, *CrystEngComm* **24** (2022) 5194 (https://doi.org/10.1039/d2ce00443g)
5. Z. Li, A. Dellali, J. Malik, M. Motevalli, R. M. Nix, T. Olukoya, Y. Peng, H. Ye, W. P. Gillin, I. Hernández, P. B. Wyatt, *Inorg. Chem.* **52** (2013) 1379 (https://doi.org/10.1021/ic302063u)
6. S. D. Han, N. N. Rajput, X. Qu, B. Pan, M. He, M. S. Ferrandon, C. Liao, K. A. Persson, A. K. Burrell, *ACS Appl. Mater. Interfaces* **8** (2016) 3021 (https://doi.org/10.1021/acsami.5b10024)
7. C. R. Groom, I. J. Bruno, M. P. Lightfoot, S. C. Ward, *Acta Crystallogr., B* **72** (2016) 171 (https://doi.org/10.1107/S2052520616003954)
8. P. Ristić, V. Blagojević, G. Janjić, M. Rodić, P. Vulić, M. Donnard, M. Gulea, A. Chylewska, M. Makowski, T. Todorović, N. Filipović, *Cryst. Growth Des.* **20** (2020) 3018 (https://doi.org/10.1021/acs.cgd.9b01661)
9. N. J. Williams, W. Gan, J. H. Reibenspies, R. D. Hancock, *Inorg. Chem.* **48** (2009) 1407 (https://doi.org/10.1021/ic801403s)
10. Z. Xun-Zhong, F. An-Sheng, Z. Fu-Ran, L. Min-Cheng, L. Yan-Zhi, M. Meng, L. Yu, *Bioinorg. Chem. Appl.* **2020** (2020) 1 (https://doi.org/10.1155/2020/8852470)
11. X. Zou, Y. Liao, C. Yang, A. Feng, X. Xu, H. Jiang, Y. Li, *J. Coord. Chem.* **74** (2021) 1009 (https://doi.org/10.1080/00958972.2020.1869952)
12. J. B. Araškov, M. Nikolić, S. Armaković, S. Armaković, M. Rodić, A. Višnjevac, J. M. Padrón, T. R. Todorović, N. R. Filipović, *J. Mol. Struct.* **1240** (2021) 130512 (https://doi.org/10.1016/j.molstruc.2021.130512)
13. L. K. Durgeswari, R. K. Ganta, Y. L. N. Murthy, *Russ. J. Org. Chem.* **57** (2021) 1552 (https://doi.org/10.1134/s1070428021090232)
14. A. A. Alfi, A. Alharbi, J. Qurban, M. M. Abualnaja, H. M. Abumelha, F. A. Saad, N. M. El-Metwaly, *J. Mol. Struct.* **1267** (2022) 133582 (https://doi.org/10.1016/j.molstruc.2022.133582)
15. V. A. Adole, R. A. More, B. S. Jagdale, T. B. Pawar, S. S. Chobe, *ChemistrySelect* **5** (2020) 2778 (https://doi.org/10.1002/slct.201904609)
16. S. Abu-Melha, *Pigment Resin Technol.* **48** (2019) 375 (https://doi.org/10.1108/PRT-09-2018-0102)
17. G. S. Masaret, *ChemistrySelect* **6** (2021) 974 (https://doi.org/10.1002/slct.202004304)
18. M. S. Shah, M. M. Rahman, M. D. Islam, A. Al-Macktuf, J. U. Ahmed, H. Nishino, M. A. Haque, *J. Mol. Struct.* **1248** (2022) 131465 (https://doi.org/10.1016/j.molstruc.2021.131465)
19. O. A. El-Khouly, M. A. Henen, M. A. A. El-Sayed, M. I. Shabaan, S. M. El-Messery, *Bioorganic Med. Chem.* **31** (2021) 115976 (https://doi.org/10.1016/j.bmc.2020.115976)
20. R. M. Kassab, S. M. Gomha, S. A. Al-Hussain, A. S. Abo Dena, M. M. Abdel-Aziz, M. E. A. Zaki, Z. A. Muhammad, *Arab. J. Chem.* **14** (2021) 103396 (https://doi.org/10.1016/j.arabjc.2021.103396)
21. S. Abu-Melha, *Arab. J. Chem.* **15** (2022) 103898 (https://doi.org/10.1016/j.arabjc.2022.103898)

22. A. Y. Alzahrani, Y. A. Ammar, M. Abu-Elghait, M. A. Salem, M. A. Assiri, T. E. Ali, A. Ragab, *Bioorg. Chem.* **119** (2022) 105571 (https://doi.org/10.1016/j.bioorg.2021.105571)
23. A. Pricopie, I. Ionuţ, G. Marc, A. Arseniu, L. Vlase, A. Grozav, L. Găină, D. C. Vodnar, A. Pîrnău, B. Tiperciuc, O. Oniga, *Molecules* **24** (2019) 3435 (https://doi.org/10.3390/molecules24193435)
24. N. J. C. Oliveira, I. N. S. Teixeira, P. O. Fernandes, G. C. Veríssimo, A. D. Valério, C. P. de S. Moreira, T. R. Freitas, A. C. V. Fonseca, A. de P. Sabino, S. Johann, V. G. Maltarollo, R. B. de Oliveira, *J. Mol. Struct.* **1267** (2022) (https://doi.org/10.1016/j.molstruc.2022.133573)
25. R. Gondru, S. Kanugala, S. Raj, C. Ganesh Kumar, M. Pasupuleti, J. Banothu, R. Bavantula, *Bioorganic Med. Chem. Lett.* **33** (2021) 127746 (https://doi.org/10.1016/j.bmcl.2020.127746)
26. S. Mor, S. Sindhu, S. Nagoria, M. Khatri, P. Garg, H. Sandhu, A. Kumar, *J. Heterocycl. Chem.* **56** (2019) 1622 (https://doi.org/10.1002/jhet.3548)
27. M. R. Shaaban, T. A. Farghaly, A. M. R. Alsaedi, *Polycycl. Aromat. Compd.* **42** (2022) 2521 (https://doi.org/10.1080/10406638.2020.1837887)
28. A. Pricopie, M. Focşan, I. Ionuţ, G. Marc, L. Vlase, L. Găină, D. C. Vodnar, E. Simon, G. Barta, A. Pîrnău, O. Oniga, *Molecules* **25** (2020) 1079 (https://doi.org/10.3390/molecules25051079)
29. S. S. Jadav, V. N. Badavath, R. Ganesan, N. M. Ganta, D. Besson, V. Jayaprakash, *Anti--Infective Agents* **18** (2018) 101 (https://doi.org/10.2174/2211352516666181016122537)
30. M. V. de O. Cardoso, G. B. de Oliveira Filho, L. R. P. de Siqueira, J. W. P. Espíndola, E. B. da Silva, A. P. de O. Mendes, V. R. A. Pereira, M. C. A. B. de Castro, R. S. Ferreira, F. S. Villela, F. M. R. da Costa, C. S. Meira, D. R. M. Moreira, M. B. P. Soares, A. C. L. Leite, *Eur. J. Med. Chem.* **180** (2019) 191 (https://doi.org/10.1016/j.ejmech.2019.07.018)
31. A. Višnjevac, J. B. Araškov, M. Nikolić, Ž. Bojić-Trbojević, A. Pirković, D. Dekanski, D. Mitić, V. Blagojević, N. R. Filipović, T. R. Todorović, *J. Mol. Struct.* **1281** (2023) 135193 (https://doi.org/10.1016/j.molstruc.2023.135193)
32. D. Radomska, R. Czarnomysy, D. Radomski, A. Bielawska, K. Bielawski, *Nutrients* **13** (2021) 1 (https://doi.org/10.3390/nu13051649)
33. D. Radomska, R. Czarnomysy, D. Radomski, K. Bielawski, *Int. J. Mol. Sci.* **22** (2021) 1 (https://doi.org/10.3390/ijms22031009)
34. N. R. Filipović, H. Elshaflu, S. Grubišić, L. S. Jovanović, M. Rodić, I. Novaković, A. Malešević, I. S. Djordjević, H. Li, N. Šojić, A. Marinković, T. R. Todorović, *Dalt. Trans.* **46** (2017) 2910 (https://doi.org/10.1039/c6dt04785h)
35. Agilent Technologies UK Ltd., *CrysAlisPro Software system*, 2014 (n.d.)
36. G. M. Sheldrick, *Acta Crystallogr., C* **71** (2015) 3 (https://doi.org/10.1107/S2053229614024218)
37. A. L. Spek, *Acta Crystallogr., D* **65** (2009) 148 (https://doi.org/10.1107/S090744490804362X)
38. C. F. MacRae, I. Sovago, S. J. Cottrell, P. T. A. Galek, P. McCabe, E. Pidcock, M. Platings, G. P. Shields, J. S. Stevens, M. Towler, P. A. Wood, *J. Appl. Crystallogr.* **53** (2020) 226 (https://doi.org/10.1107/S1600576719014092)
39. L. J. Farrugia, *J. Appl. Crystallogr.* **45** (2012) 849 (https://doi.org/10.1107/S0021889812029111)
40. O. V. Dolomanov, L. J. Bourhis, R. J. Gildea, J. A. K. Howard, H. Puschmann, *J. Appl. Crystallogr.* **42** (2009) 339 (https://doi.org/10.1107/S0021889808042726)

41. P. R. Spackman, M. J. Turner, J. J. McKinnon, S. K. Wolff, D. J. Grimwood, D. Jayatilaka, M. A. Spackman, *J. Appl. Crystallogr.* **54** (2021) 1006 (https://doi.org/10.1107/S1600576721002910)
42. *Gaussian 09, Revision A.02*, Gaussian, Inc., Wallingford, CT, 2009
43. T. Lecklider, *EE Eval. Eng.* **50** (2011) 36 (https://go.gale.com/ps/i.do?p=AONE&u=anon~9e9d6b50&id=GALE|A272486022&v=2.1&it=r&sid=googleScholar&asid=467f45d4)
44. A. D. Becke, *J. Chem. Phys.* **104** (1996) 1040 (https://doi.org/10.1063/1.470829)
45. A. D. Becke, *J. Chem. Phys.* **96** (1992) 2155 (https://doi.org/10.1063/1.462066)
46. A. D. Becke, *J. Chem. Phys.* **98** (1993) 5648 (https://doi.org/10.1063/1.464913)
47. N. Godbout, D. R. Salahub, J. Andzelm, E. Wimmer, *Can. J. Chem*. **70** (1992) 560 (https://doi.org/10.1139/v92-079)
48. C. Sosa, J. Andzelm, B. C. Elkin, E. Wimmer, K. D. Dobbs, D. A. Dixon, *J. Phys. Chem*. **96** (1992) 6630 (https://doi.org/10.1021/j100195a022)
49. C. F. Mackenzie, P. R. Spackman, D. Jayatilaka, M. A. Spackman, *IUCrJ* **4** (2017) 575 (https://doi.org/10.1107/S205225251700848X).

Journal of the Serbian Chemical Society
JSCS@tmf.bg.ac.rs • www.shd.org.rs/JSCS
J. Serb. Chem. Soc. 88 (12) S407–S411 (2023) *Supplementary material*

SUPPLEMENTARY MATERIAL TO

Zn(II) complex with pyridine based 1,3-selenazolyl-hydrazone: Synthesis, structural characterization and DFT study

JOVANA B. ARAŠKOV[1], PREDRAG G. RISTIĆ[1]*, ALEKSANDAR VIŠNJEVAC[2]**, ANDREJ LJ. MILIVOJAC[3], DRAGANA M. MITIĆ[3], NENAD R. FILIPOVIĆ[4] and TAMARA R. TODOROVIĆ[1]

[1]University of Belgrade – Faculty of Chemistry, Studentski trg 12–16, 11000 Belgrade, Serbia, [2]Division of Physical Chemistry, Institute Ruđer Bošković, Bijenička cesta 54, Zagreb 10000, Croatia, [3]Innovation Centre of Faculty of Chemistry, University of Belgrade, Studentski trg 12–16, 11000 Belgrade, Serbia and [4]University of Belgrade – Faculty of Agriculture, Nemanjina 6, 11000 Belgrade, Serbia

J. Serb. Chem. Soc. 88 (12) (2023) 1355–1367

ANALYTICAL AND SPECTRAL DATA

The ligand based on (1,3-selenazol-2-yl)hydrazone. Anal. Calcd. for $C_{32}H_{28}Cl_4N_8O_2Se_2Zn_2$ (Fw = 987.08) (%): C, 38.93; H, 2.86; N, 11.35. Found: C, 39.21; H, 3.09; N, 11.16. Λ_M (1×10^{-3} M, MeOH) = 108.2 Ω^{-1} cm^2 mol^{-1}. IR (ATR, νmax/cm^{-1}): 3099 (m), 2924 (s), 2872 (ms), 2836 (ms), 1621 (ms), 1610 (ms), 1600 (ms), 1546 (m), 1532 (ms), 1499 (s), 1469 (s), 1415 (m), 1355 (ms), 1275 (ms), 1229 (s), 1136 (ms), 1022 (ms), 944 (m), 882 (m), 708 (m), 597 (w), 514 (vw). ^{1}H NMR (DMSO-d_6;400 MHz) δ_H (ppm): 3.75 (s, 3H); 6.93 (d, 2H); 7.33 (dd, 1H); 7.54 (s, 1H); 7.75 (d, 2H), 7.80-7.83 (m, 2H); 8.06 (s, 1H); 8.54 (d, 1H); 12.54 (s, 1H). ^{13}C{1H} NMR (DMSO-d_6;126 MHz) δ_C (ppm): 55.55, 106.26, 114.37, 119.64, 124.13, 127.51, 128.56, 137.24, 142.72, 149.90, 153.58, 159.09, 171.30.

Abbreviations used for IR spectra: s, strong; ms, medium-strong; m, medium; w, weak; vw, very weak.

Table S-I. Crystal data and structure refinement for **2-Cl-Se**

Empirical formula	$C_{32}H_{28}Cl_4N_8O_2Se_2Zn_2$
Formula weight	987.08
Temperature/K	298(2)
Crystal system	monoclinic
Space group	*C2/c*
a/Å	14.4341(3)
b/Å	18.6583(4)
c/Å	14.7422(7)
α/°	90
β/°	114.347(4)

* Corresponding authors. E-mail: (*)predrag@chem.bg.ac.rs, (**)visnevac@irb.hr

γ/°	90
Volume/Å^3	3617.2(2)
Z	4
ρ_{calc}g/cm^3	1.813
μ/mm^{-1}	7.014
F(000)	1952.0
Crystal size/mm^3	0.2 × 0.12 × 0.08
Radiation	CuKα (λ = 1.54184)
2Θ range for data collection/°	8.226 to 151.928
Index ranges	-18 ≤ h ≤ 17, -18 ≤ k ≤ 23, -18 ≤ l ≤ 15
Reflections collected	9475
Independent reflections	3728 [R_{int} = 0.0253, R_{sigma} = 0.0354]
Data/restraints/parameters	3728/0/236
Goodness-of-fit on F^2	1.029
Final R indexes *[I>=2σ (I)]*	R_1 = 0.0318, wR_2 = 0.0837
Final R indexes [all data]	R_1 = 0.0345, wR_2 = 0.0866
Largest diff. peak/hole / e Å^{-3}	0.51/-0.65

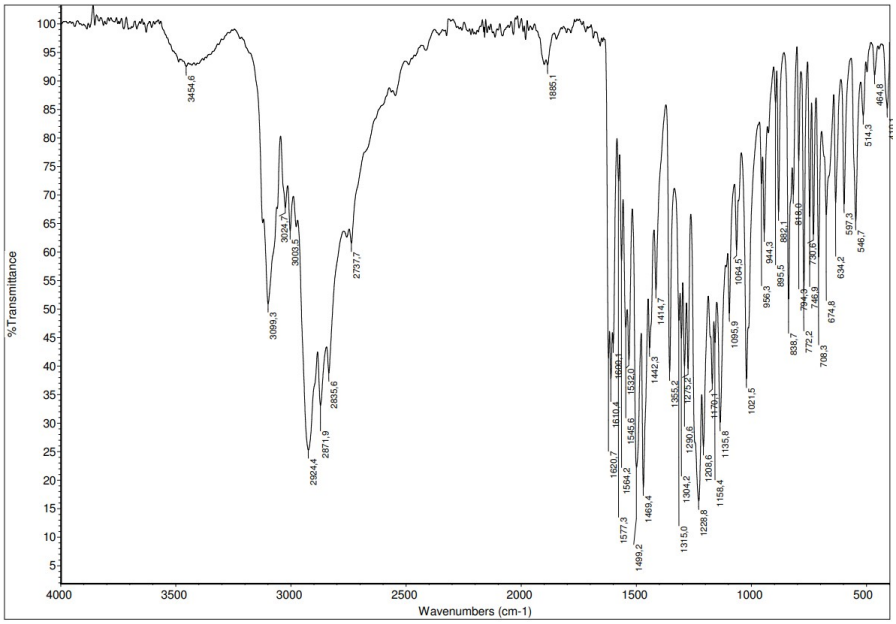

Figure S-1. IR spectrum of **2-Cl-Se**.

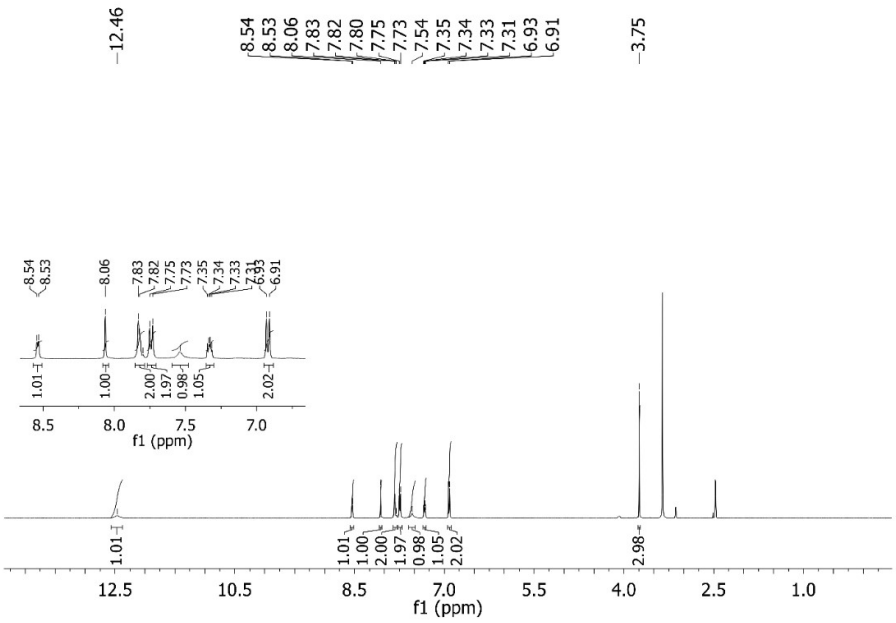

Figure S-2. ^{1}H NMR spectrum of **2-Cl-Se** in DMSO-d_6.

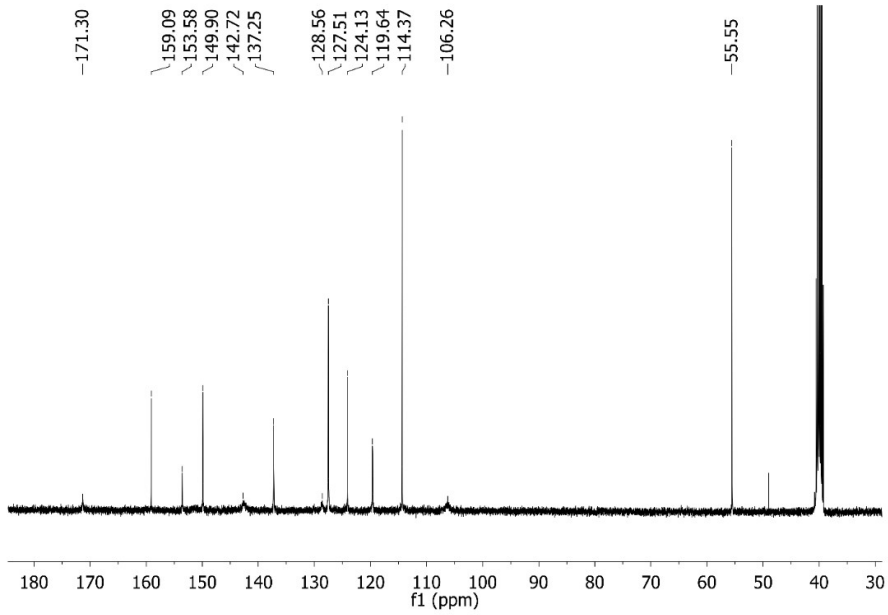

Figure S-3. ^{13}C NMR spectrum of **2-Cl-Se** in DMSO-d_6.

Table S-II. Bond angles for **2-Cl-Se**.

Angle label	Angle / °	Angle label	Angle / °
N1–C1–N2	121.5(2)	C11–N3–N2	123.0(2)
N1–C1–Se1	116.0(2)	C11–N3–Zn1	121.0(2)
N2–C1–Se1	123.0(2)	N2–N3–Zn1	116.0 (1)
C3–C2–Se1	111.80(2)	C12–N4–Zn1	114.0(2)
C2–C3–C4	124.10(2)	C16–N4–C12	117.40(2)
C2–C3–N1	116.50(2)	C16–N4–Zn1	128.0(2)
N1–C3–C4	119.40(2)	C7–O1–C10	116.80(3)
C5–C4–C3	120.40(2)	N1–Zn1–N1^{1}	91.80(1)
C5–C4–C9	118.30(2)	N1^{1}–Zn1–N4^{1}	146.66(7)
C9–C4–C3	121.30(2)	N1–Zn1–N4^{1}	99.39(7)
C6–C5–C4	120.50(3)	N1^{1}–Zn1–N4	99.39(7)
C5–C6–C7	120.70(2)	N1–Zn1–N4	146.66(7)
C6–C7–C8	119.40(2)	N3–Zn1–N1^{1}	122.17(7)
O1–C7–C6	115.80(3)	N3^{1}–Zn1–N1	122.17(7)
O1–C7–C8	124.80(3)	N3–Zn1–N1	74.73(7)
C9–C8–C7	119.50(2)	N3^{1}–Zn1–N1^{1}	74.73(7)
C8–C9–C4	121.50(2)	N3^{1}–Zn1–N3	157.7 (1)
N3–C11–C12	115.80(2)	N3^{1}–Zn1–N4	91.13(7)
C13–C12–C11	121.60(2)	N3^{1}–Zn1–N4^{1}	72.74(7)
N4–C12–C11	115.50(2)	N3–Zn1–N4	72.73(7)
N4–C12–C13	122.90(2)	N3–Zn1–N4^{1}	91.13(7)
C12–C13–C14	118.70(3)	N4^{1}–Zn1–N4	88.4(1)
C15–C14–C13	118.70(3)	Cl1^{2}–Zn2–Cl1	113.66(4)
C14–C15–C16	119.40(3)	Cl1^{2}–Zn2–Cl2	110.57(2)
N4–C16–C15	122.90(3)	Cl1–Zn2–Cl2^{2}	110.56(2)
C1–N1–C3	112.0(2)	Cl1–Zn2–Cl2	106.22(2)
C1–N1–Zn1	113.0(2)	Cl1^{2}–Zn2–Cl2^{2}	106.22(2)
C3–N1–Zn1	133.0(2)	Cl2–Zn2–Cl2^{2}	109.62(4)
N3–N2–C1	114.0(2)	C2–Se1–C1	84.0(2)

Symmetry code: ^{1}-x,+y, ½-z; ^{2}1-x,+y, ½-z

Table S-III. Bond lengths for **2-Cl-Se**.

Bond type	Length / Å	Bond type	Length / Å
C1–N1	1.307(3)	C12–C13	1.382(3)
C1–N2	1.367(3)	C12–N4	1.355(3)
C1–Se1	1.873(2)	C13–C14	1.384(4)
C2–C3	1.349(4)	C14–C15	1.374(5)
C2–Se1	1.867(3)	C15–C16	1.388(4)
C3–C4	1.478(3)	C16–N4	1.329(3)
C3–N1	1.394(3)	N1–Zn1	2.16(2)
C4–C5	1.390(3)	N2–N3	1.355(3)
C4–C9	1.394(3)	N3–Zn1	2.14(2)
C5–C6	1.383(4)	N4–Zn1	2.250(2)
C6–C7	1.387(4)	Cl1–Zn2	2.275(6)
C7–C8	1.389(4)	Cl2–Zn2	2.303(7)
C7–O1	1.363(3)	Zn1–N1^{1}	2.16(2)

C8–C9	1.385(3)	Zn1–N3[1]	2.14(2)
C10–O1	1.432(5)	Zn1–N4[1]	2.250(2)
C11–C12	1.461(4)	Zn2–Cl1[2]	2.275(6)
C11–N3	1.275(3)	Zn2–Cl2[2]	2.303(7)

Symmetry code: [1]-x,+y,½-z; [2]1-x,+y,½-z

Table S-IV. Interaction pair energies in the crystal structure of **2-Cl** based on the B3LYP/ DGDZVP energy model*

R (Å)	Interaction energy, kJ mol^{-1}				
	*E*_ele	*E*_pol	*E*_dis	*E*_rep	*E*_tot
11,25	574,4	–58,5	–18,0	4,0	550,9
7,34	548,4	–76,5	–123,8	127,8	494,3
11,73	481,2	–43,1	–32,5	24,5	463,7
8,27	–618,0	–72,6	–10,0	13,1	–707,7
7,36	–667,3	–132,3	–27,1	35,4	–805,2
7,45	–862,4	–163,1	–30,7	103,5	–995,2
9,60	–648,4	–70,3	–12,6	22,0	–734,8
14,41	408,1	–21,4	–12,5	11,9	412,0

*E_tot represents the sum of individual components with scaling factors (*k*_ele = 1.057; *k*_pol = 0.740; *k*_dis = 0.871; *k*_rep = 0.618), while the individual components are not scaled.

Journal of the Serbian Chemical Society
JSCS@tmf.bg.ac.rs • www.shd.org.rs/JSCS
J. Serb. Chem. Soc. *88* (12) 1369–1376 (2023)

Contents of Volume 88

NUMBER 1

NUMBER 3

NUMBER 5

NUMBER 6

NUMBER 9

NUMBER 10

NUMBER 12
Special Issue dedicated to Academician Vukadin M. Leovac on the occasion of his 80th birthday

Journal of the Serbian Chemical Society
JSCS-info@shd.org.rs • www.shd.org.rs/JSCS
J. Serb. Chem. Soc. *88* (12) 1377–1382 (2023)

Author Index

Subject Index of Vol. **88** and List of Referees in 2023 are given in the electronic form at the Internet address of the Journal of the Serbian Chemical Society: http://www.shd.org.rs/JSCS

End of Volume 88.

Journal of the Serbian Chemical Society
JSCS-info@shd.org.rs • www.shd.org.rs/JSCS
Volume *88* (2023)

Subject index

Journal of the Serbian Chemical Society
JSCS-info@shd.org.rs • www.shd.org.rs/JSCS
Volume *88* (2023)

2023 List of Referees

Editorial Board of the Journal is grateful to the following referees for reviewing the manuscripts during 2023:

Nadica Abazović, *Institute of Nuclear Sciences Vinča, Belgrade, Serbia*
Heba Abdel-Mohsen, *Department of Chemistry of Natural and Microbial Products, Division of Pharmaceutical and Drug Industries Research, National Research Centre, Dokki, Cairo, Egypt*
Aly Abdou, *Chemistry Department, Faculty of Science, Sohag University, Sohag, Egypt*
Salam Ahmed Abed, *University of Kerbala, Kerbala, Iraq*
Biljana Abramović, *Faculty of Science, University of Novi Sad, Serbia*
Gamal El-Din Abuo-Rahma, *Department of Medicinal Chemistry, Faculty of Pharmacy, Minia University, Minia, Egypt*
Milica Aćimović, *Institute of Field and Vegetable Crops, Novi Sad, Serbia*
Oluwasesan Adegoke, *Leverhulme Research Centre for Forensic Science, University of Dundee, United Kingdom*
Esvet Akbas, *Van YuzuncuYil University, Department of Chemistry, Van, Türkiye*
Vesna Alar, *Faculty of Mechanical Engineering and Naval Architecture, University of Zagreb, Croatia*
Ivana Aleksić, *Institute of Molecular Genetics and Genetic Engineering, University of Belgrade, Serbia*
Luma Ahmed Mohammed Ali, *Department of Chemistry, College of Science, University of Babylon, Babylon, Iraq*
Ratna Surya Alwi, *Department of Chemical Engineering, Fajar University, South Sulawesi 90231, Indonesia*
Tina P. Andrejević, *University of Kragujevac, Faculty of Science, Department of Chemistry, Kragujevac, Serbia*
Deana Andrić, *Faculty of Chemistry, University of Belgrade, Serbia*
Boban Anđelković, *Faculty of Chemistry, Department of Organic Chemistry, University of Belgrade, Serbia*
Tina P. Andrejević, *Department of Chemistry, Faculty of Science, University of Kragujevac, Serbia*
Jasmina Anojčić, *Faculty of Science, University of Novi Sad, Serbia*
Vesna Antić, *Faculty of Agriculture, University of Belgrade, Serbia*
Ozgur Arar, *Department of Chemistry, Ege University, İzmir, Türkiye*
Sanja Aramaković, *Faculty of Sciences, Department of chemistry, Biochemistry and Environmental protection, University of Novi Sad, Serbia*Mehdi Asadi, *Department of Chemistry, University of Tabriz, Tabriz, Iran*
Roberta Ascrizzi, *Department of Pharmacy, University of Pisa, Pisa, Italy*
Marcel Ausloos, *School of Business, University of Leicester, Brookfield, Leicester, United Kingdom*
Gazel Burcu Aydin, *Trakya University, Faculty of Science, Department of Biology, Edirne, Türkiye*
Jelena Bajat, *Faculty of Technology and Metallurgy, University of Belgrade, Serbia*

Jelena Dodić, *Faculty of Technology, Department of Biotechnology and Pharmaceutical Engineering, University of Novi Sad, Serbia*
Biljana Dojnov, *Institute of Chemistry, Technology and Metallurgy, University of Belgrade, Serbia*
Miloš Dubovina, *Faculty of Sciences, University of Novi Sad, Serbia*
Christophe Dunand, *Laboratoire de Recherche en Sciences Végétales, Université de Toulouse, CNRS, UPS, Toulouse, France*
Branko Dunjić, *Faculty of Technology and Metallurgy, University of Belgrade, Serbia*
Yaraslau Dzichenka*, Institute of Bioorganic Chemistry NASB, Minsk, Belarus*
Veljko R. Đokić, *IC of Faculty of Technology and Metallurgy, University of Belgrade, Serbia*
Iris Đorđević, *Faculty of Veterinary Medicine, University of Belgrade, Serbia*
Ivana Đorđević, *Institute of Chemistry, Technology and Metallurgy, University of Belgrade, Serbia*
Marija Đošić, *Institute for Technology of Nuclear and Other Mineral Raw Materials, Belgrade, Serbia*
Maja Đukić, *University of Kragujevac, Faculty of Science, Kragujevac, Serbia*
Miloš I. Đuran, *Department of Chemistry, Faculty of Science, University of Kragujevac, Serbia*
Jelena Đuriš, *Faculty of Pharmacy, University of Belgrade, Serbia*
Mihal Đuriš, *Institute of Chemistry, Technology and Metallurgy, University of Belgrade, Serbia*
Zdravko Džambaski, *Institute of Chemistry, Technology and Metallurgy - Department of Chemistry, University of Belgrade, Serbia*
Predrag Džodić, *Department of Pharmacy, Faculty of Medicine, University of Niš, Serbia*
Mohammed I. El-Gamal, *Department of Medicinal Chemistry, Faculty of Pharmacy, University of Mansoura, Egypt*
Dina Elnaggar, *Applied Organic Chemistry Department, National Research Centre, Dokki, Giza, Egypt*
İlker Erdem, *Abdullah Gül University (AGU), Faculty of Engineering, Department of Nanotechnology Engineering, Kayseri, Türkiye*
Olivera Erić-Cekić, *The University of Kragujevac, Faculty of Mechanical and Civil Engineering in Kraljevo, Serbia*
Mihajlo Etinski, *Faculty of Physical Chemistry, University of Belgrade, Serbia*
Zahra Fakhri, *Department of Physical Chemistry, Faculty of Chemistry, Razi University, Kermanshah, Iran*
Fatih İslamoğlu, *Recep Tayyip Erdoğan University, Faculty of Science and Art, Department of Chemistry, Türkiye*
Izabela Fecka, *Department of Pharmacognosy and Herbal Medicines, Faculty of Pharmacy, Wroclaw Medical University, Wroclaw, Poland*
Eder Carlos Ferreira de Souza, *Universidade Estadual Paulista (UNESP), Instituto de Química, Brasil*
Evgeny Filatov, *Nikolaev Institute of Inorganic Chemistry, Siberian Branch, Russian Academy of Sciences, Novosibirsk, Russia*
Suzana Filipović, *Institute of Technical Sciences of SASA, Belgrade, Serbia*
Gordana Đ. Gajica, *Faculty of Chemistry, University of Belgrade, Serbia*
Georgiy A. Gamov, *State University of Chemistry and Technology, Ivanovo, Russia*
Li Gao, *Precision Medical Center Laboratory, The First Affiliated Hospital, Wenzhou Medical University, Wenzhou, PR China*
Neda Gavarić, *Department of Pharmacy, Faculty of Medical Sciences, University of Novi Sad, Serbia*
Marija Gavrović-Jankulović, *Faculty of Chemistry, University of Belgrade, Serbia*
Jahanbakhsh Ghasemi, *University of Tehran, Iran*

Milka Jadranin, *Institute of Chemistry, Technology and Metallurgy, University of Belgrade, Serbia*
Goran Janjić, *Institute of Chemistry, Technology and Metallurgy, University of Belgrade, Serbia*
Ivona Janković-Častvan, *Faculty of Technology and Metallurgy, University of Belgrade, Serbia*
Nenad Janković, *Department of Chemistry, Faculty of Science, University of Kragujevac, Serbia*
Verica Jevtić, *Department of Chemistry, University of Kragujevac, Serbia*
Xueyang Jiang, *Department of Natural Medicinal Chemistry, China Pharmaceutical University, Nanjing, China*
Kristina Joksimović, *Institute of Chemistry, Technology and Metallurgy, University of Belgrade, Serbia*
Igor Jordanov, *Faculty of Technology and Metallurgy, University of Ss Cyril and Methodius, Skopje, Republic of North Macedonia*
Ana Maria Josceanu, *University Politehnica of Bucharest, Department of Analytical Chemistry and Environmental Engineering, Bucharest, Romania*
Vesna Jovanović, *Faculty of Chemistry, University of Belgrade, Serbia*
Sofija Jovanović Stojanov, *Department of Neurobiology University of Belgrade, Institute for Biological Research "Siniša Stanković", National Institute of the Republic of Serbia, Serbia*
Ivan Juranić, *Faculty of Chemistry, University of Belgrade, Serbia*
Karolina Kafarska, *Institute of General and Ecological Chemistry, Lodz University of Technology, Poland*
Goran Kaluđerović, *Department of Bioorganic Chemistry, Leibniz-Institute of Plant Biochemistry, Halle (Saale), Germany*
Alexander Karamanov, *Institute of Physical Chemistry, Bulgarian Academy of Sciences, Sofia, Bulgaria*
Milica Kašanin-Grubin, *Institute of Chemistry, Technology and Metallurgy, University of Belgrade, Serbia*
Krisztián Kertész, *Centre for Energy Research, Institute of Technical Physics and Materials Science, Budapest, Hungary*
Ramachandra Kini, *Department of Studies in Biotechnology, University of Mysore, Manasagangotri, Mysore, Karnataka, India*
Gergana Kirova, *Faculty of Pharmacy, Medical University of Plovdiv, Bulgaria*
Aleksandra Cvetanović Kljakić, *Institute of Chemical Industry of Forestry Products, Chinese Academy of Forestry, Nanjing, China*
Željko Knez, *Faculty of Chemistry and Chemical Technology, University of Maribor, Slovenia*
Andraž Kocjan, *Department for Nanostructured Materials, Jožef Stefan Institute, Ljubljana, Slovenia*
Lukasz Komsta, *Department of Medicinal Chemistry, Medical University of Lublin, Poland*
Branko Kordić, *Faculty of Sciences, University of Novi Sad, Novi Sad*
Tatjana Kop, *Institute of Chemistry, Technology and Metallurgy - Department of Chemistry, University of Belgrade, Serbia*
Stjepan Kovačević, *Department of Polytechnic, Faculty of Science, University of Split, Split, Croatia*
Jelena Kotur-Stevuljević, *Faculty of Pharmacy, University of Belgrade, Serbia*
Hülya Koyuncu, *Bursa Technical University, Faculty of Engineering and Natural Sciences, Chemical Engineering Department, Bursa, Türkiye*
Sanja Krstić, *Institute of Pharmaceutical Sciences, University of Graz, Austria*
Vesna Krstić, *Mining and Metallurgy Institute Bor, Serbia*
Olga Krutova, *Ivanovo State University of Chemistry and Technology, Russia*

Chandrasekhar Masta, *Vignan Institute of Technology and Science, Yadadri, Bhuvanagiri, Telangana, India*
Emilio Mateev, *Department of Pharmaceutical Chemistry, Faculty of Pharmacy, Medical University, Sofia, Bulgaria*
Pavle Mašković, *University of Kragujevac, Faculty of Agronomy, Department of Chemistry, Kragujevac, Serbia*
Višnja Mihajlović, *Technical Faculty "Mihajlo Pupin", University of Novi Sad, Zrenjanin, Serbia*
Daniel Mijailović, *Innovation Center of Faculty of Technology and Metallurgy, University of Belgrade, Sebia*
Svetislav Mijatović, *Faculty of Physics, University of Belgrade, Serbia*
Dušan Mijin, *Faculty of Technology and Metallurgy, University of Belgrade, Serbia*
Vesna Milanović, *Faculty of Chemistry, University of Belgrade, Serbia*
Nemanja Miletić, *Faculty of Agronomy, University of Kragujevac, Čačak, Serbia*
Dragana Milić, *Faculty of Chemistry, University of Belgrade, Serbia*
Miomir Miljković, *University of Niš, Faculty of Civil Engineering and Architecture, Serbia*
Maja Milojević-Rakić, *Faculty of Physical Chemistry, University of Belgrade, Serbia*
Nenad Milosavić, *Department of Medicine, Columbia University, New York, USA*
Nataša Milošević, *Institute for Pharmacology, Medical Faculty, University of Novi Sad, Serbia*
Branislav Milovanović, *University of Belgrade-Faculty of Physical Chemistry, Serbia*
Djenana Miodragovic, *Chemistry of Life Processes Institute, Northwestern University, Evanston, IL, USA*
Aleksandra Mitrović, *Faculty of Chemistry, University of Belgrade, Serbia*
Liviu Mitu, *University of Pitesti, Pitesti, Romania*
Salwa Mohamed, *Applied Organic Chemistry Department, National Research Centre, Dokki, Giza, Egypt*
Ljiljana Mojović, *Faculty of Technology and Metallurgy, University of Belgrade, Serbia*
Milan Momčilović, *Vinča Institute of Nuclear Sciences, Belgrade, Serbia*
Reda Ben Mrid, *Institute of Biological Sciences (ISSB-P), Mohammed VI Polytechnic University (UM6P), Ben-Guerir, Morocco*
Draginja Mrvoš Sermek, *Faculty of Science, University of Zagreb, Croatia*
Shaik Md Mayeem, *KRK Government Degree College, Addanki, Bapatla Distrct, AndhraPradesh, India*
Monica Nardi, *Dipartimento di Scienze della Salute, Università Magna Græcia, Catanzaro, Italy*
Bojana Nedić Vasiljević, *Faculty of Physical Chemistry, University of Belgrade, Serbia*
Olgica Nedić, *Institute for the Application of Nuclear Energy, University of Belgrade, Serbia*
Aleksandra Nešić, *Faculty of Technology and Metallurgy, University of Belgrade, Serbia*
Ludwig Niewoehner, *Forensic Science Institute Wiesbaden, Federal Criminal Police Germany, Germany*
Bogdan Nikolić, *The Institute for Plant Protection and Environment, Belgrade, Serbia*
Katarina Nikolić, *Faculty of Chemistry, University of Belgrade, Serbia*
Vesna Nikolić, *Faculty of Technology, University of Niš, Leskovac, Serbia*
Branislava Nikolovski, *Faculty of Technology, University of Novi Sad, Serbia*
Innocent Nkurikiyimfura, *Physics Department, School of Science, College of Science and technology, University of Rwanda, Kigali, Rwanda*
Jasmina Novaković, *Apotex Inc, Toronto, Ontario, Canada*
Irena Novaković, *Institute of Chemistry, Technology and Metallurgy, University of Belgrade, Serbia*

Marko Popović, *School of Life Sciences Weihenstephan, Technische Universität München, Germany*
Miljana Popović, *Faculty of Technology and Metallurgy, University of Belgrade, Serbia*
Mira Popović, *Department of Chemistry, Biochemistry and Environmental Protection Faculty of Sciences, University of Novi Sad, Serbia*
Marija Popović-Nikolić, *Faculty of Pharmacy University of Belgrade, Serbia*
Mirjana Popsavin, *Faculty of Sciences, University of Kragujevac, Serbia*
Velimir Popsavin, *Faculty of Science, University of Novi Sad, Serbia*
Mihalj Poša, *Department of Pharmacy, Faculty of Medicine, University of Novi Sad, Serbia*
Umesh Prasad, *Arizona State University, USA*
Kamatchi Pravinkumar, *St. Joseph's College of Engineering, Department of Mechanical Engineering, Chennai, India*
Katarina Putica, *Innovation Center of Faculty of Chemistry, Belgrade, Serbia*
Vladislav Rac, *Faculty of Agriculture, University of Belgrade, Zemun, Serbia*
Mirjana Radenković, *Vinča Institute of Nuclear Sciences, University of Belgrade, Serbia*
Bojana Radojković, *Institute of Chemistry, Technology and Metallurgy, University of Belgrade, Serbia*
Mirjana Radomirović, *Faculty of Chemistry, University of Belgrade, Serbia*
Nataša Radosavljević-Stevanović, *National Criminalistic-Technical Centre, Ministry of Internal Affairs of the Republic of Serbia, Belgrade, Serbia*
Lidija Radovanović, *Innovation Center of Faculty of Technology and Metallurgy, Serbia*
Milan Radovanović, *Tehnical Faculty in Bor, University of Belgrade, Bor, Serbia*
Magadalena Radović, *University of Belgrade-Institute of Nuclear Sciences Vinča, Belgrade*
Olga Radulović, *Department of Plant Physiology, Institute for Biological Research Siniša Stanković, University of Belgrade, Serbia*
Abhay Raj, *Environmental Microbiology Laboratory, Environmental Toxicology Group,CSIR-Indian Institute of Toxicology Research (CSIR-IITR), Vishvigyan Bhawan, Lucknow, Uttar Pradesh, India*
Vesna Rakić, *Faculty of Agriculture, University of Belgrade, Serbia*
Jon Rainier, *Department of Chemistry, University of Utah, Salt Lake City, Utah, USA*
Snežana Rajković, *Faculty of Science, Department of Chemistry, University of Kragujevac, Serbia*
Shashi Vivek Ranga, *Gujarat Technological University, Chandkheda, Ahmedabad, Gujarat, India*
Vesna Rastija, *Department of Chemistry, University of Osijek, Croatia*
Kumaresan Rathinam, *Department of Physics, Govt. Arts College Coimbatore, Tamil Nadu, India*
Slavica Ražić, *Faculty of Pharmacy, University of Belgrade, Serbia*
Dubravka Relić, *Faculty of Chemistry, University of Belgrade, Serbia*
Yanfei Ren, *Qingdao University, Qingdao, Shandong, China*
Ali Riahi-Madvar, *Department of Biotechnology, Institute of Science and High Technology and Environmental Sciences, Graduate University of Advanced Technology, Kerman, Iran*
Marija Ristić, *University of Kragujevac, Faculty of Science, Kragujevac, Serbia*
Predrag Ristić, *Faculty of Chemistry, University of Belgrade, Serbia*
Milena Rmandić, *University of Belgrade, Faculty of Pharmacy, Serbia*
Dragana Robajac, *Institute for the Application of Nuclear Energy, University of Belgrade, Serbia*
Dušica Rodić, *Faculty of Sciences, University of Novi Sad, Serbia*
Marko Rodić, *Faculty of Sciences, University of Novi Sad, Serbia*
Jelena Rogan, *Faculty of Technology and Metallurgy, University of Belgrade, Serbia*
Tamara Rončević, *Faculty of Sciences, University of Novi Sad, Serbia*

Milan Stojanović, *Department of Systems Biology, Columbia University Department of Systems Biology, Irving Cancer Research Center, New York, USA*
Evica Stojiljković, *Faculty of Occupational Safety, Univeristy of Niš, Serbia*
Venkatesan Subramanian, *Central Leather Research Institute, Adyar Chennai, India*
Suma Sudarsan, *Sree Narayana College, Chempazhanthy, India*
Jasmina Sulejmanović, *Faculty of Natural Sciences and Mathematics, Sarajevo, Bosnia & Herzegovina*
Claudiu T. Supuran, *University of Florence, Neurofarba Department, Polo Scientifico, Sesto Fiorentino, Firenze, Italy*
Ljiljana Suručić, *Faculty of Medicine, University of Banja Luka, Bosnia and Herzegovina*
Michal Swieca, *Department of Biochemistry and Food Chemistry, Faculty of Food Science and Biotechnology, University of Life Sciences, Lublin, Poland*
Aleksandra Šajnović, *Institute of Chemistry, Technology and Metallurgy, Department of Chemistry, University of Belgrade, Serbia*
Zoran Šaponjić, *Vinča Institute of Nuclear Sciences, Belgrade, Serbia*
Slobodan Šerbanović, *Faculty of Technology and Metallurgy, University of Belgrade, Serbia*
Biljana Šmit, *Faculty of Science, University of Kragujevac, Serbia*
Bogdan Šolaja, *Faculty of Chemistry, University of Belgrade, Serbia*
Tatjana Šolević Knudsen, *Institute of Chemistry, Technology and Metallurgy, University of Belgrade, Serbia*
Olja Šovljanski, *University of Novi Sad, Faculty of Technology Novi Sad, Novi Sad, Serbia*
Vladimir Šukalović, *Institute of Chemistry, Technology and Metallurgy - Department of Chemistry, University of Belgrade, Serbia*
Arezoo Tahan, *Semnan Branch, Islamic Azad University, Semnan, Iran*
Akhilesh K Tamrakar, *Biochemistry & Structural Biology Division, CSIR-Central Drug Research Institute, Lucknow, India*
Bo Tang, *School of Pharmacy, Nantong University, Jiangsu Province, China*
Gordana Tasić, *Faculty of Pharmacy, University of Belgrade, Serbia*
Visa Tasic, *Mining and Metallurgy Institute Bor, Serbia*
Renjith Thomas, *St Berchmans College, Changanassery, Kerala, India*
Pinnu Thriveni, *Department of Chemistry, Vikrama Simhapuri University, Nellore, India*
Nina Todorović, *Institute of Chemistry, Technology and Metallurgy, Department of Chemistry, University of Belgrade, Serbia*
Tamara Todorović, *Faculty of Chemistry, University of Belgrade, Serbia*
Zoran Todorović, *Faculty of Technology University of Niš, Serbia*
Lavinia Tofan, *Gheorghe Asachi Technical University of Iaşi, Romania*
Biljana Tomašević, *Faculty of Chemistry, University of Belgrade, Serbia*
Zorica Tomičić, *Institute of Food Technology in Novi Sad, Novi Sad, Serbia*
Jelena Tričković, *Department of Chemistry, Biochemistry and Environmental Science, Faculty of Sciences, University of Novi Sad, Serbia*
Milena Trmčić, *Innovation Center of Faculty of Chemistry, University of Belgrade, Serbia*
Turgay Tunç, *Ahi Evran Üniversitesi, Department of Chemistry, Kirşehir, Tyrley*
Amac Fatih Tuyun, *Department of Chemistry, Faculty of Science, Istanbul University, Fatih, Istanbul, Türkiye*
Olga Tzakou, *Section of Pharmacognosy and Natural Product Chemistry, Department of Pharmacy, National and Kapodistrian University of Athens, Greece*

Ljiljana Živković, *Vinča Institute of Nuclear Sciences, Belgrade, Serbia*
Irena Žižović, *Faculty of Technology and Metallurgy, University of Belgrade, Serbia*
Fabio Zobi, *University of Fribourg, Department of Chemistry, Fribourg, Switzerland*
Jovana Zvicer, *Faculty of Technology and Metallurgy, University of Belgrade, Serbia*